

istituto nazionale di fisica nucleare
laboratori nazionali di Frascati

2000 ANNUAL REPORT



Cover: (from top, clockwise) KLOE drift chamber; FINUDA tracking in its mechanical support structure; DEAR cryogenic setup on DAΦNE's interaction region; NAUTILUS gravitational wave antenna.

Cover artwork by C. Federici

istituto nazionale di fisica nucleare
laboratori nazionali di Frascati

2000

ANNUAL REPORT

LNF-01/025 (IR)
26 October 2001

Editor
S. Bianco

Technical Editor
L. Invidia

Published by
SIS-Pubblicazioni
P.O.Box 13 – I-00044 Frascati (Italy)

Available at [/www.lnf.infn.it/](http://www.lnf.infn.it/)

Paolo Laurelli
LNF Director

Lucia Votano
Head, Research Division

Sergio Bertolucci
Head, Accelerator Division

LNF Scientific Coordinators

Maria Curatolo
Particle Physics

Alessandro Marini
Astroparticle Physics

Valeria Muccifora
Nuclear Physics

Stefano Bellucci
Theory and Phenomenology

Francesco Celani
Techn. and Interdisciplinary Research

CONTENTS

FOREWORD	1
DAΦNE	3
Particle Physics	17
ALEPH	17
ATLAS	25
BABAR	32
CDF	40
E831-FOCUS	45
KLOE	49
Astroparticle Physics	63
ICARUS	63
MACRO	66
OPERA	72
ROG	74
VIRGO	80
WIZARD	84
Nuclear Physics	89
AIACE	89
DEAR	96
DIRAC	103
FINUDA	107
GRAAL	115
HERMES	119
Theory and Phenomenology	129
LF-11	129
LF-21	133
OG-21	140
PI-11	142
PI-31	143
Technological and Interdisciplinary Research	145
DOSIME2	145
FREEDOM	147
GEDI	151
ICMAG2	152
MIVEDE	154
MUST	156

NEMO5	158
OBD	159
PIAP2	160
PLAMIC	162
POLYX	163
SFERA	164
SI-EYE2	165
Progetti Speciali	167
CTF3	167
DAΦNE-L	169
GILDA	177
TTF	179
List of Internal Reports	185
Glossary	191

FOREWORD

THE FRASCATI NATIONAL LABORATORIES

Paolo Laurelli
Director

The *Laboratori Nazionali di Frascati* (LNF) is the largest national laboratory of the Italian *Istituto Nazionale di Fisica Nucleare* (INFN) with more than 320 among researchers, technicians, engineers, and administrative personnel working in it.

The LNF research activities, while covering all the five fields of the INFN – elementary particles, astroparticles, nuclear physics, theory, technological and interdisciplinary research, are centred around the DAΦNE facility with its experiments KLOE, DEAR, FINUDA, and the synchrotron light source DΦNE-LIGHT.

During 2000, DAΦNE, the most luminous e^+e^- ϕ -factory collider in operation, after important modifications on the injection kickers at the beginning of the year, reached the best peak luminosity of about $2 \cdot 10^{29} \text{ cm}^{-2}\text{s}^{-1}$ per bunch with typically 45 bunches. Most importantly, such luminosity was accompanied by a tolerable level of background for KLOE operation. In 2.5 months of data-taking mode, interleaved with machine development periods, KLOE received 24 pb^{-1} and was able to produce its first preliminary results in hadronic physics. DEAR was allocated two weeks in December and further reduced the signal-to-background ratio by reinforcing shielding around the detector and by optimising optical functions and beam trajectory in the IR.

During scheduled shutdowns, FINUDA completed cable installation and accomplished hook-up of the cryo line and energization of the superconducting solenoid. DAΦNE-LIGHT, the synchrotron radiation facility, completed installation of beamlines down to the experimental hall: in December both the x-ray and the UV beamlines were connected to the storage ring and on December 11th the two x-ray beams were observed.

The panorama of activities employing LNF facilities is completed by NAUTILUS, the gravitational wave antenna which, along with the EXPLORER antenna at CERN, constitutes the ROG project. During 2000, NAUTILUS, in continuous data taking mode, achieved first observation of antenna excitation due to the passage of cosmic rays, as well as a component of several anomalously large amplitude signals (up to about 100 TeV).

Particle, astroparticle and nuclear physics projects at laboratories abroad (such as CERN, FERMILAB, SLAC, HERA, TJNAF) with relevant contributions from Frascati groups include experiments that finished data taking and are in data analysis mode (ALEPH, E831-FOCUS, DIRAC, MACRO), experiments in construction (ATLAS, OPERA, VIRGO), experiments in data-taking (BABAR, AIACE, GRAAL, HERMES) and others which will shortly be so (CDF) and experiments in test-run mode (ICARUS, WIZARD).

A small but powerful theory group is traditionally present in the Laboratory. Its main activity, connected to the physics of KLOE, is the phenomenology of particle interactions at colliders. Other minority, high-quality projects include field theory in low-dimensional systems, gravity theory, fermionic systems and lattice, and nuclear theory.

Finally, numerous, highly specialised projects focus on technological applications and detector developments: medical physics (DOSIME2, OBD, SI-EYE2), earth sciences (GEDI), detector R&D (MIVEDE, MUST, NEMO, PIAP-2, POLYX, PLAMIC) and accelerator science (SFERA, CTF, GILDA, TTF-TESLA).

LNF has been recognized as a Large Scale Facility by the EU, and has been assigned a three-year contract in the TARI framework. Many researchers from various EU countries already joined the Laboratory to participate in the ongoing activities.

I would like to thank all the personnel of the Laboratory, which with their skillness and professionalism made possible the success of this global effort. My thanks go to all the people who contributed to the realization of this report, in particular to Dr. Stefano Bianco, for the accurate editing of the whole document.

DAΦNE

D. Alesini, G. Benedetti (Dott.), S. Bertolucci (Resp.), C. Biscari, R. Boni
M. Boscolo, A. Clozza, G. Delle Monache, S. Di Mitri (Dott.), G. Di Pirro, A. Drago
A. Gallo, A. Ghigo, S. Guiducci, F. Marcellini, G. Mazzitelli, C. Milardi, L. Pellegrino
M. Preger, R. Ricci, C. Sanelli, F. Sgemma, F. Sannibale, M. Serio, A. Stecchi
A. Stella, C. Vaccarezza, M. Vescovi, M. Zobov

1 Introduction

The first phase of the realization of DAΦNE, the new double ring electron-positron collider of the Frascati National Laboratory was completed on Sunday, March 1st, 1998, when the first interactions between the two beams circulating in the two rings of the machine were observed. From that moment on the main task of the LNF Accelerator Division staff members, who have designed and built the facility, has been the improvement of its performance which, after the installation of the KLOE detector during the first three months of 1999, allowed to observe the production of the first Φ resonances and its CP violating decays.

DAΦNE has been therefore the first "electron-positron factory" in operation. With this name we call the storage rings for electrons and positrons delivering a high rate of mesons for high resolution experiments requiring an extremely large number of events. In order to reach such high rates, the factories are designed to work at the energies of the meson resonances, where the production cross section peaks. Examples of such resonances are the Φ near 1 GeV, the J/ψ around 3 GeV and the Y near 10 GeV, which decay into mesons containing the "strange", "charm" and "beauty" quarks respectively. However, it is not sufficient to exploit the high cross section to obtain the required production rate: it is also necessary that the collider luminosity (the number of events per unit time of the reaction under investigation divided by its cross section weighted by the acceptance of the detector) is very high, between one and two orders of magnitude larger than that obtained in the conventional colliders with a single ring where electrons and positrons run on the same orbit in opposite directions.

DAΦNE is the heart of a system consisting of a double ring collider, a linear accelerator (LINAC) an intermediate damping ring to make injection easier and faster and 180 m of transfer lines connecting these machines. The geometry of this accelerator complex has been designed to reuse the buildings hosting ADONE (the 3 GeV center of mass electron-positron collider in operation at LNF from 1969 to 1993) and its injector, a LINAC used both to refill the collider and to perform nuclear physics experiments. The layout of DAΦNE and its injector inside these buildings is shown in the following Fig. 1.

The reason why a double ring collider can deliver a much larger luminosity than a single ring one is the following: in an electron-positron storage ring both beams consist of a number N of short "bunches". Since in a single ring the bunches, due to the invariance of the Lorentz force in the absence of electric fields with respect to particles of opposite charge and velocity, follow the same trajectory, they cross in $2N$ points. The maximum obtainable luminosity is limited by the electromagnetic beam-beam interaction. The effects of this interaction can be reduced with a very strong focussing (called "low- β ") at the points where the beams cross, obtained by means of quadrupole doublets or triplets in the interaction region (IR). These magnetic structures require space and excite chromatic aberrations which must be corrected elsewhere in the ring. It is clear

that in a small machine like DAΦNE only two of these regions can be realized, and therefore only a single electron bunch and a single positron one could be stored in a single ring. A larger number of bunches could be stored only if more low- β points would be available, twice the number of bunches stored in each beam.

This limitation does not hold for a double ring collider, consisting in two separate rings crossing in two low- β points. The number of bunches that can be stored in such a collider is limited only by the geometry of the IR's.

In DAΦNE the trajectories followed by the two beams cross at the interaction point (IP) at an angle of 1.5 degrees in the horizontal plane. A positron bunch leaving the IP after crossing an electron one will reach the following electron bunch at a distance of half the longitudinal separation between bunches from the IP. However, due to the horizontal angle between the trajectories of the two beams, the distance in the horizontal direction between the two bunches is equal to the horizontal angle times half the longitudinal distance between the bunches in the beam. The beam-beam interaction can be harmful to beam stability even if the distance in the horizontal direction between bunches of opposite charge is of the order of few bunch widths at points where the β function is high and this sets a lower limit on the bunch longitudinal separation and therefore on the number of bunches which can be stored in the collider. For DAΦNE the minimum separation is 80 cm, and the maximum number of bunches to be stored in each ring is 120. This number determines the frequency of the radiofrequency cavity which replaces at each turn the energy lost in synchrotron radiation, which must be 120 times the revolution frequency. The luminosity of the collider can therefore be up to 120 times larger than that obtainable in a single ring with the same size and optical functions.

Crossing at an angle could in principle be a limitation to the maximum single bunch luminosity. In order to make the beam-beam interaction less sensitive to this parameter and similar to the case of single ring colliders where the bunches cross head-on, the shape of the bunches at the IP is made very flat (typical r.m.s. sizes are 30 mm in the longitudinal direction, 2 mm in the horizontal and 0,02 mm in the vertical one).

Of course the double ring scheme with many bunches has also important drawbacks: the total current in the ring reaches extremely high values (5 A in the DAΦNE design) and the high power emitted as synchrotron radiation (≈ 50 KW) needs to be absorbed by a complicated structure of vacuum chambers and pumping systems in order to reach the very low residual gas pressure levels necessary to avoid beam loss. In addition, the number of possible oscillation modes of the beam increases with the number of bunches, calling for sophisticated bunch-to-bunch feed-back systems.

Somebody may ask why such a simple solution to improve the luminosity of electron-positron colliders has not been adopted in the past: the answer is that two machines of this kind has been built (DORIS at DESY and DCI at LAL-Orsay) but they were not able to reach a good performance. The reasons why this happened are now well understood and the new machines have been designed taking into account this experience. In addition to DAΦNE, two other colliders at the energy of the Y resonance (PEPII at SLAC and KEK-B in Japan) have been realized with the double ring scheme and are presently in operation.

The structure of the collider is shown schematically in Figure 2: both rings lay in the same horizontal plane and each one consists of a long external arc and a short internal one. Starting from the IP the two beams travel together inside a common vacuum chamber and their distance increases until it becomes ≈ 12 cm at the level of the magnetic separators called "splitters" (SPL). These are special magnets with two regions of opposite field which deflect the two beams in opposite directions, allowing them to reach the separate vacuum chambers of the long and short arcs. Each arc consists of two "almost achromatic" bends (deflecting the beam by 81 degrees in the short arc and 99 degrees in the long one) similar to those frequently used in synchrotron radiation sources, with a long straight section in between. Each bend consists of two dipoles, three quadrupoles, two

sextupoles and a wiggler. This structure is used for the first time in an electron-positron collider and it has been designed for the particular requirements of DAΦNE: the amount of synchrotron radiation power emitted in the wigglers is the same as in the bending magnets and the wigglers can be used to change the transverse size of the beams. The increase of emitted power doubles the damping rates for betatron and synchrotron oscillations, thus making the beam dynamics more stable, while the possibility of changing the beam sizes makes the beam-beam interaction parameters more flexible.

The straight section in the long arc houses the pulsed magnets used to store into the rings the bunches coming from the injection system, while in the short arc straight there are the radiofrequency cavity and the equipment for the feed-back systems which are used to damp longitudinal and transverse instabilities.

The most delicate part of the whole structure are however the IR's. The collider can host two experiments, even if up to now only one at a time can get useful luminosity. Three detectors have been realized, KLOE, DEAR and FINUDA. The first two have been installed in the two IP's, while the third is being assembled in its pit inside the DAΦNE hall and will take data in the near future in the IR now occupied by DEAR. The detectors of KLOE and FINUDA are surrounded by large superconducting solenoid magnets for the momentum analysis of the decay particles and their magnetic fields represent a strong perturbation on the beam dynamics. This perturbation tends to induce an effect called "beam coupling", consisting in the transfer of the betatron oscillations from the horizontal plane to the vertical one. If the coupling is not properly corrected, it would give a significant increase of the vertical beam size and a corresponding reduction of luminosity. For this reason a superconducting solenoid magnet with half the field integral of the detector one and of opposite direction is placed near each splitter in such a way that the overall field integral in the IR's vanishes.

However, this is not sufficient to obtain full compensation of the beam coupling induced by the main solenoids. In the case of KLOE the low- β at the IP is realized by means of two quadrupole triplets (indicated as PMQ in Figure 2). Due to the flat shape of the beam at the IP, the low- β is realized only in the vertical plane. The quadrupole cannot be of the conventional electromagnetic type for two reasons: the first is that the iron of the yoke would degrade the flatness of the magnetic field in the detector and the second is that the overall transverse size of a conventional quadrupole is at least twice its useful aperture. Therefore quadrupoles realized with permanent magnets have been built, which exhibit a surprisingly good field quality, very small transverse size and are fully transparent to external fields. The region of space around the IP occupied by machine elements, which is unavailable for the detection of decay particles by the experiment consists in two cones with the vertex at the IP and a half aperture of only 9 degrees. In order to obtain a good compensation of the above mentioned coupling effects induced by the solenoids, these quadrupoles are rotated around their longitudinal axis by angles between 10 and 20 degrees and are provided with actuators to finely adjust their position and rotation. If one takes into account the fact that the whole structure (shown in Figure 3) is completely embedded inside the KLOE detector, it is easy to imagine how complicate is this realization from the engineering point of view.

The structure of the FINUDA IR is quite similar. Since its superconducting solenoid magnet has half the length (but twice the field) of the KLOE one, the low- β focusing at the IP is obtained by means of two permanent magnet quadrupole doublets inside the detector and completed with two other conventional doublets outside. The DEAR experiment, which is presently installed on the IR opposite to KLOE, does not need magnetic field and therefore only conventional quadrupoles are used. Two synchrotron radiation lines, one from a bending dipole and the other from the wiggler have also been realized by the DAΦNE-LIGHT group. The DAΦNE hall is shown in Figure 4.

The vacuum chambers of the arcs have been designed to stand the high level of radiation

power emitted by the beams (up to 50 KW per ring): they consist of 10 m long aluminum structures built in a single piece: its cross section exhibits a central region around the beam and two external ones, called the antechambers, connected to the central one by means of a narrow slot. In this way the synchrotron radiation hits the vacuum chamber walls far from the beam and the desorbed gas particles can be easily pumped away. The chambers contain water cooled copper absorbers placed where the radiation flux is maximum: each absorber has a sputter ion pump below and a titanium sublimation pump above.

The single cell copper radiofrequency cavities, one in each ring, are capable of running at 250 KV and are designed with particular care to avoid high order modes which could induce longitudinal instabilities in the particular multibunch structure of the beams. This is obtained by means of external waveguides terminated on 50Ω loads, as shown in Figure 5. A sophisticated longitudinal feedback has however been built to maintain a reasonable safety margin on the threshold of multi-bunch instabilities. The system is based on the digital signal processing technique and acts on each single bunch individually. Additional feedback systems on the vertical betatron motion have been also realized following the observation of coherent instabilities during the collider operation.

The correct superposition of the beams at the IP is of course of critical importance for the luminosity of the ring. For this reason, 46 beam position monitors are available in each ring and 31 small dipoles can be used to steer the beam and correct orbit distortions caused by alignment errors or wrong currents in the magnetic elements by means of sophisticated software procedures implemented in the Control System of the collider. Additional beam diagnostics are two synchrotron radiation outputs, from which the transverse and longitudinal size of the beam can be measured, total beam current monitors and strip-line pickups delivering the charge of each bunch.

The DAΦNE Control System is based on a three level architecture, where the third level consists of a large number of CPU's placed along the rings and the power supply halls. These CPU's perform all kinds of control tasks on the corresponding devices and are linked by means of a mailbox system (the second level) to the computers in the Control Room, where high-level procedures allow to control and tune all machine and beam parameters. A luminosity monitor based on single beam-beam bremsstrahlung, delivering a fast response to machine parameter changes is also used to optimize the collider performance, while the absolute value of the luminosity is directly measured by the experiments. The original system is all based on MacIntosh computers.

In a low energy electron-positron collider, such as DAΦNE, the lifetime of the stored current is mainly limited by the Touschek effect, namely the particle loss due to the scattering of the particles inside the bunches. In the present operating conditions it is of the order of half an hour. It is therefore necessary to have a powerful injection system, capable of refilling the beam without dumping the already stored one. In addition, flexibility of operation requires that any bunch pattern can be stored among the 120 available buckets. The injection system of DAΦNE is therefore designed to deliver a large rate of particles in a single bunch at the working energy of the collider. It consists of a linear accelerator (LINAC, see Figure 1) with a total accelerating voltage of 800 MV. In the first section, electrons are accelerated to 250 MeV before hitting a tungsten target (called positron converter) where positrons in a single bunch at the working energy of the collider. It consists of a linear accelerator (LINAC, see Figure 1) with a total accelerating voltage of 800 MV. In the first section, electrons are accelerated to 250 MeV before hitting a tungsten target (called positron converter) where positrons are generated by bremsstrahlung and pair production with an efficiency of $\approx 1\%$. The positrons exit from the target with an energy of few MeV and are then accelerated by the second section of the LINAC to their final energy of ≈ 0.51 GeV. The positrons are then driven along a transfer line and injected into a small storage ring, called Accumulator (see Figure 1 again), at a frequency of 25 Hz. Up to 19 positron pulses are stacked into a single bucket of the Accumulator, then injection stops and the bunch damps down to its equilibrium beam size

and energy spread, which are much smaller than the LINAC ones. Damping takes ≈ 0.1 seconds and then the beam is extracted from the Accumulator and injected into the positron main ring at an overall repetition rate of 1 Hz. A powerful and flexible timing system allows the storage of any desired bunch pattern in the collider. In the electron mode, the converter is extracted from the LINAC and electrons are directly accelerated to 0.51 GeV and injected into the Accumulator in the opposite direction with respect to positron operation. They are then extracted like in the positron case and injected into the electron main ring through the second transfer line.

The Accumulator has been introduced for the following reasons. The first is that the LINAC can deliver pulses of 10 ns with a charge of ≈ 1 nC. Since the design charge of the main ring at the maximum luminosity is $1.5 \mu\text{C}$ and the longitudinal acceptance of the main rings is only 2 ns, the number of pulses necessary to fill the ring is of the order of 104. In order to avoid saturation it is therefore necessary that at each injection pulse a fraction smaller than 10^{-4} of the already stored beam is lost, and this is not easy to achieve. The Accumulator instead can work with a lower frequency RF cavity and therefore with a larger longitudinal acceptance. In this way the full charge coming from the LINAC can be stored. The number of pulses into the Accumulator is only 19, and after damping the whole charge stacked into an Accumulator bunch can be stored into the main ring. In this way a single main ring bucket can be filled with only one pulse from the Accumulator, reducing to 120 the number of injection pulses into each main ring. As an additional benefit, the transverse beam size and energy spread of the beam coming from the Accumulator are at least one order of magnitude smaller than those of the LINAC beam, and this strongly reduces the aperture requirements of the main ring and, as a consequence, the overall cost of the collider.

2 DAΦNE history

The construction of DAΦNE was approved by INFN in June 1990. The engineering design started in spring 1991, based on the assumption of using the buildings of ADONE, which of course needed some important modifications to house the new facility. ADONE was shut down at the end of April 1993 and the DAΦNE hall was ready for installation in January 1996.

Commissioning of the injection system started in January 1996, with the first electron beam acceleration. In June the first electron beam was stored in the Accumulator, while in July also positrons were available from the LINAC. The rings were completed and under vacuum in August 1997: the first electron beam was stored in DAΦNE in October and the positron one in November. The first collisions were detected in March 1998: the machine was running in a commissioning configuration, called "DAY-ONE" without any magnetic detector. The low- β at the IP's was obtained by a symmetric arrangement of seven quadrupoles, with the central one sitting on the IP. A luminosity of $1.6 \times 10^{30} \text{cm}^{-2} \text{s}^{-1}$ in the single bunch mode was reached in November with stored currents of ≈ 20 mA, and a first attempt of multibunch operation with 13 bunches in each beam yielded a luminosity of $\approx 10^{31} \text{cm}^{-2} \text{s}^{-1}$.

In the first months of 1999 the KLOE detector was installed and commissioning in the new configuration with the strong solenoid, superconducting compensators and permanent magnet quadrupole triples was resumed in April, with particular care dedicated to coupling correction. The vertical beam size was minimized by tuning the main solenoid field, the compensator currents and the excitation of skew quadrupole correctors around the ring. The result was better than design (the vertical emittance was reduced to less than 1% of the horizontal one). However the single bunch luminosity was less than $2 \times 10^{29} \text{cm}^{-2} \text{s}^{-1}$, much smaller than what obtained in the "DAY-ONE" configuration.

At the end of the year a period of approximately one month was dedicated to KLOE operation: working with stored currents of $300 \div 400$ mA in $30 \div 40$ bunches, with peak luminosity in the range of $5 \times 10^{30} \text{cm}^{-2} \text{s}^{-1}$ and beam lifetime of the order of one hour, $\approx 2.5 \text{pb}^{-1}$ were delivered to the

experiment.

3 Year 2000 activity

Some important modifications on the injection kickers required a long shut-down of DAΦNE in January and February. Collider operation was resumed in March, with machine time mainly dedicated to machine development. Some important improvements in the performance of the collider were obtained: total currents in excess of 1 A were separately stored in both rings, the coupling was further reduced to less than 0.5% and the single bunch luminosity reached $5 \cdot 10^{29} \text{cm}^{-2} \text{s}^{-1}$ by carefully adjusting collision parameters. In multibunch mode the maximum luminosity was $10^{31} \text{cm}^{-2} \text{s}^{-1}$ with 30 bunches and 0.35 A per beam.

The collider was dedicated to data collection by KLOE for the whole month of July and an integrated luminosity of $\approx 4 \text{pb}^{-1}$ was delivered to the experiment. However, data collection was affected by high rates of beam induced backgrounds and short luminosity lifetime (typically half an hour). Injection had to be performed frequently with data acquisition stopped because of unacceptable background rate which tripped the KLOE drift chamber, leading to poor average luminosity.

At the beginning of September two weeks of machine operation were dedicated to DEAR: this experiment is particularly sensitive to the signal to background ratio, which was found to be larger by two orders of magnitude than the minimum required to start the experiment. By changing the optical functions near the IR's, improving closed orbit correction and optimizing the position of four couples of scrapers placed upstream the IR's, it was possible to decrease the background rate by a factor 5.

The following period, from mid-September to the end of November, was shared (at typically 50% each) between KLOE data taking and machine development dedicated at improving the background situation and the average luminosity. The first important result of this work was that the beam losses during injection were reduced to a level which allowed injecting without switching off the KLOE drift chamber, inhibiting data acquisition only for 50 ms at each injection pulse. In this way, in spite of the short beam lifetime, the average luminosity can be kept close to the maximum one by frequently refilling the stored beams to the maximum current allowed by the beam-beam interaction.

Typical operation for KLOE data taking at the end of the year was performed with $45 \div 48$ bunches. The filling pattern interleaved one empty bucket with a full one, with a $\approx 20\%$ gap to avoid ion trapping by the electron beam. Currents per bunch were ≈ 15 mA in the positron beam and 12 mA in the electron one, limited by the beam-beam interaction. The best peak luminosity was $1.8 \times 10^{29} \text{cm}^{-2} \text{s}^{-1}$ with total currents of ≈ 0.75 A and ≈ 0.55 A respectively. The luminosity per bunch is therefore $\approx 30\%$ less than that obtained in the single bunch mode, due to non perfectly uniform filling and parasitic crossing effects. The collider was running with the beams separated vertically in the DEAR IR.

In 2.5 months of operation, interleaved with machine development, 24pb^{-1} were delivered to KLOE. Figure 6 shows the integrated and peak luminosity per day during the periods of data taking. The former, although with significant fluctuations between different days because of variable beam time dedicated at machine development, increases significantly with time while the latter exhibits a smoother improvement. This may be attributed to the fact that during this period of data taking no major breakthroughs were obtained in the single bunch luminosity, but at the same time there has been a steady increase of the overall efficiency in multibunch operation due to refinements in beam dynamics control and fine tuning of machine parameters.

The last two weeks of December were dedicated to DEAR: by reinforcing the shielding around the detector and further optimizing the optical functions and beam trajectory in the IR, another

factor 4 was gained in the signal-to-background ratio. An absolute luminosity monitor based on the detection of charged kaons from the decay of the Φ resonance was brought into operation. A trial to run the collider with the beams crossing in KLOE and DEAR at the same time was also attempted, but led to a substantial reduction in luminosity.

The operation and improvement of DAΦNE has been the main task of the Accelerator Division in year 2000, with deep involvement of both its research and technical staff during machine development and data taking shifts. However some other important activities can be mentioned.

As already described before, one of the problems connected with the operation of DAΦNE is the short lifetime of the beam, dominated by the Touschek effect. Its cross section is inversely proportional to the volume of the bunches, and therefore the lifetime can be increased by modifying the bunch length by means of an additional RF cavity working at zero phase at an harmonic of the main cavity frequency. The design and prototyping of a third harmonic cavity has been realized in the RF laboratory, and installation of such systems on both rings is foreseen during the long shutdown for FINUDA roll-in.

The superconducting solenoid of FINUDA has been installed inside its pit in the DAΦNE hall, connected to its power supply, cooled and tested. A series of magnetic measurements, needed both by the experiment to establish the field map and by the machine to demonstrate the compatibility with machine optics requirements, has been performed.

During the machine development shifts dedicated to coupling correction, it was realized that changing the sign of the current in the skew quadrupoles in the ring directly from the Control Room could greatly improve the efficiency of operation. It was therefore decided to change the present power supplies with manual switches for the polarity, which are installed inside the DAΦNE hall, with new bipolar ones. These new power supplies have been specified and ordered from industry.

The power transformers for the 1.5 MVA power supplies of the wigglers, which caused some failures with consequent machine down-time, have been modified.

The longitudinal feedback system has been improved by increasing the power of the final amplifiers from 250 W to 750 W, while new digital/analog multimode feedback systems on the vertical coherent instabilities have been implemented on both rings.

The transverse sizes of the beam are continuously monitored with of an optical system which extracts the synchrotron radiation from a bending magnet by means of a water cooled mirror inside the arc vacuum chamber. The image of the beam is then focused on a CCD camera mounted on top of the magnet. The same light output can be used to measure the longitudinal size of the beam with a streak camera. However, the latter is a rather complicate system which cannot be easily remote controlled. For this reason a new optical system has been completed, which drives the synchrotron radiation light beam outside the DAΦNE hall through a couple of holes in the wall to a small laboratory placed near the DEAR-FINUDA counting room. In the new synchrotron radiation laboratory it is possible to optimize beam focusing and magnification to the needs of any beam size measurement.

The first level of the Control System, which was previously based on MacIntosh computers, has been changed to a new one, consisting of a SUN unit with a large number of terminals in the Control Room. The new system runs a UNIX operating system, while the second and third levels are still operating with MacIntosh subsystems. Important modifications to the Control Room have also been done to cope with the new structure of the Control System.

A system of 6 couples of scrapers to trap lost particles from the beam before hitting the detectors has been implemented in order to decrease the background rates in the experiments. Four of them are placed upstream the IR's and reduce the horizontal aperture, screening the experiments mainly from Touschek scattered particles. The other two are moved in the vertical direction and are planned to trap particles scattered by the atoms of the residual gas. These systems have been equipped with stepping motors and can be remotely controlled from the Control Room.

A system of beam loss monitors based on solid state detectors has also been realized, which can be used to find where beam losses occur with the stored beam or during injection. Also this system is connected to the Control System and can be used in real time.

4 List of Publications

1. S. Guiducci: "e⁺e⁻ Factories: PEP-II, KEKB, DAΦNE", Proceedings of Frontier Detectors for Frontier Physics, 8th Pisa Meeting on Advanced Detectors - 21-27 May 2000, Isola d'Elba, p.1.
2. A. Gallo *et al.*: "Design Status of a High Harmonic RF System for DAΦNE", European Particle Accelerator Conf. EPAC2000, 26-30 June 2000, Wien, Austria, p. 1495.
3. M. Zobov, for the DAΦNE Commissioning Team: "Status Report on DAΦNE Performance", European Particle Accelerator Conference EPAC2000, 26-30 June 2000, Wien, Austria, p.43.
4. C. Biscari, A. Ghigo, F. Marcellini, C. Sanelli, F. Sannibale, M. Serio, F. Sgamma, G. Vignola, M. Zobov, R. Corsini, T.E. D'Amico, L. Groening, G. Guignard: "CTF3: Design of Driving Beam Combiner Ring", European Particle Accelerator Conference EPAC2000, 26-30 June 2000, Wien, Austria, p.450.
5. A. Gallo *et al.*: "Studies on the RF Deflectors for CTF3", European Particle Accelerator Conference EPAC2000, 26-30 June 2000, Wien, Austria, p.465.
6. G. Di Pirro *et al.*: "Data Handling Tools at DAΦNE", European Particle Accelerator Conference EPAC2000, 26-30 June 2000, Wien, Austria, p.1862.
7. C. Milardi *et al.*: "Optics Measurements in DAΦNE", European Particle Accelerator Conference EPAC2000, 26-30 June 2000, Wien, Austria, p.1051.
8. G. Di Pirro *et al.*: "The Evolution and Status of the DAΦNE Control System", European Particle Accelerator Conference EPAC2000, 26-30 June 2000, Wien, Austria, p.1868.
9. F. Sannibale *et al.*: "Beam Measurements for Luminosity Optimisation in DAΦNE", European Particle Accelerator Conference EPAC2000, 26-30 June 2000, Wien, Austria, p. 312.
10. A. Ghigo *et al.*: "HOM Damping in the DAΦNE Injection Kickers", European Particle Accelerator Conference EPAC2000, 26-30 June 2000, Wien, Austria, p. 1145.

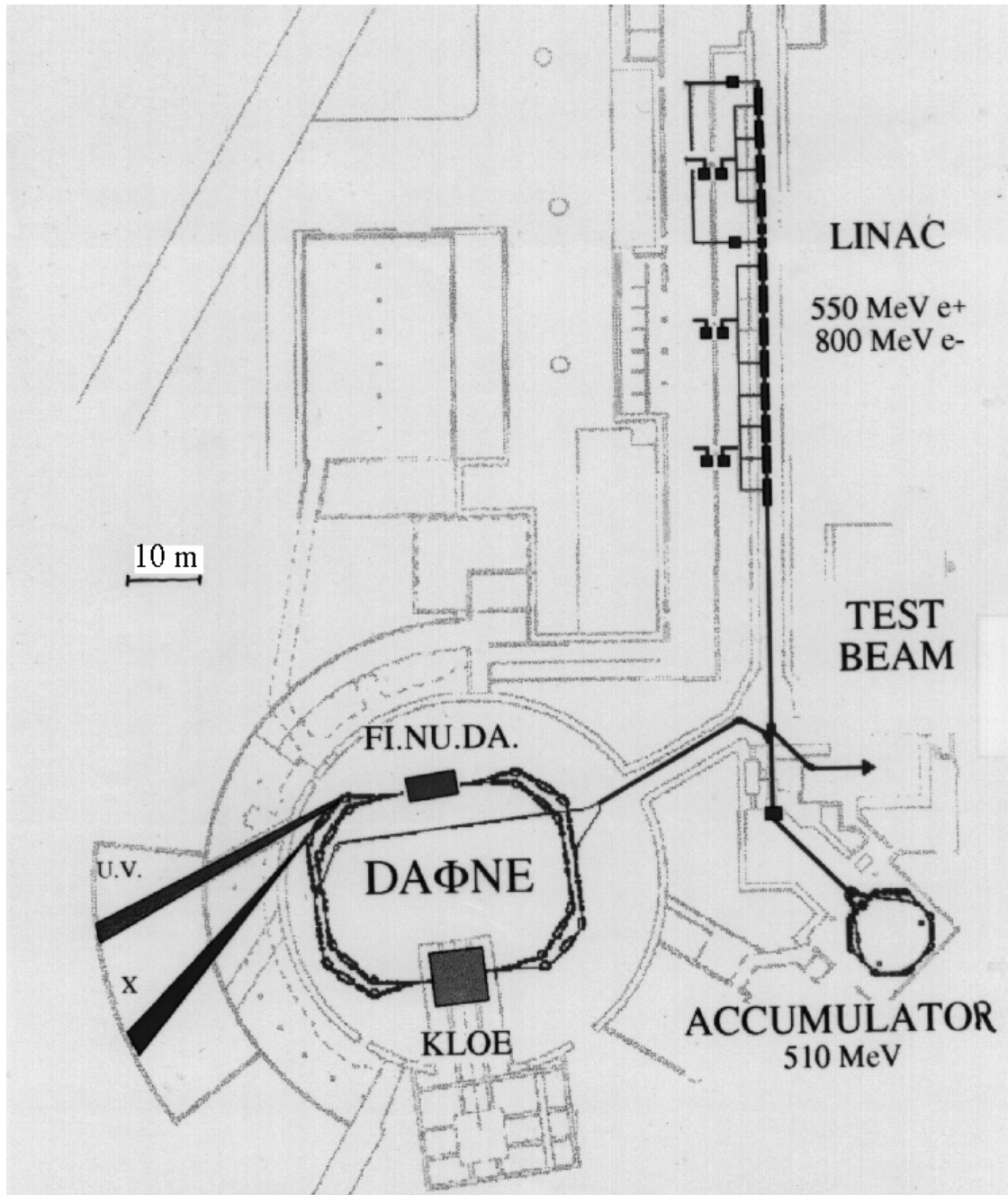


Figure 1 – The layout of the DAΦNE accelerator complex inside its buildings.

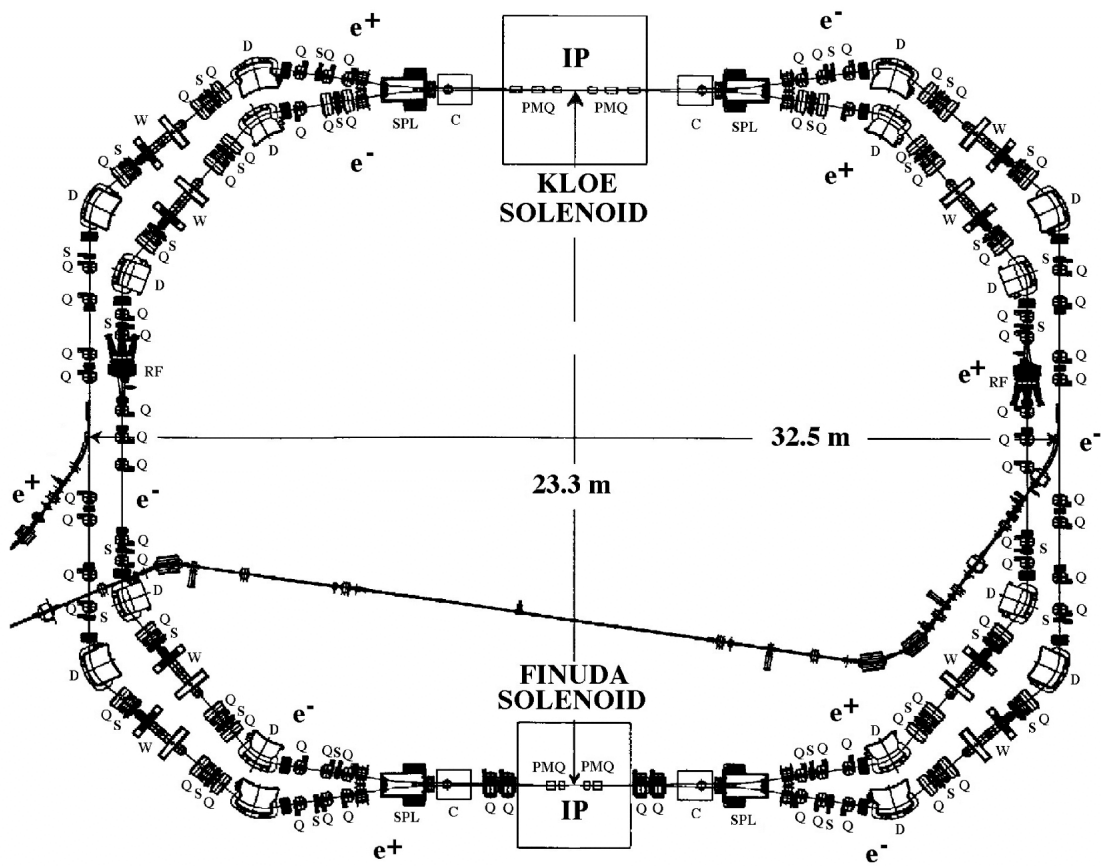


Figure 2 – Schematic layout of the DAΦNE double ring collider (IP = interaction point, PMQ = permanent magnet quadrupole, SPL = splitter magnet, Q = quadrupole, S = sextupole, D = dipole, RF = radiofrequency cavity, W = wiggler magnet, C = solenoid compensator).

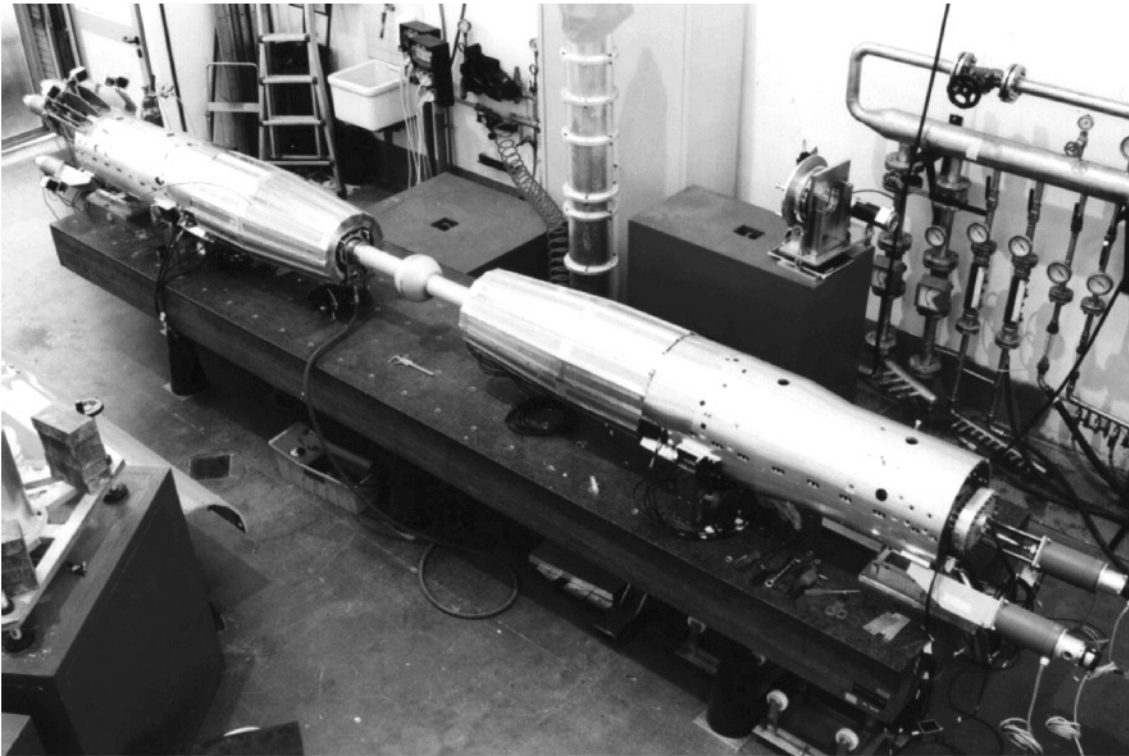


Figure 3 – *The KLOE interaction region on its assembly bench.*



Figure 4 – *Fish-eye view of the DAΦNE hall. The picture shows one half of the collider*

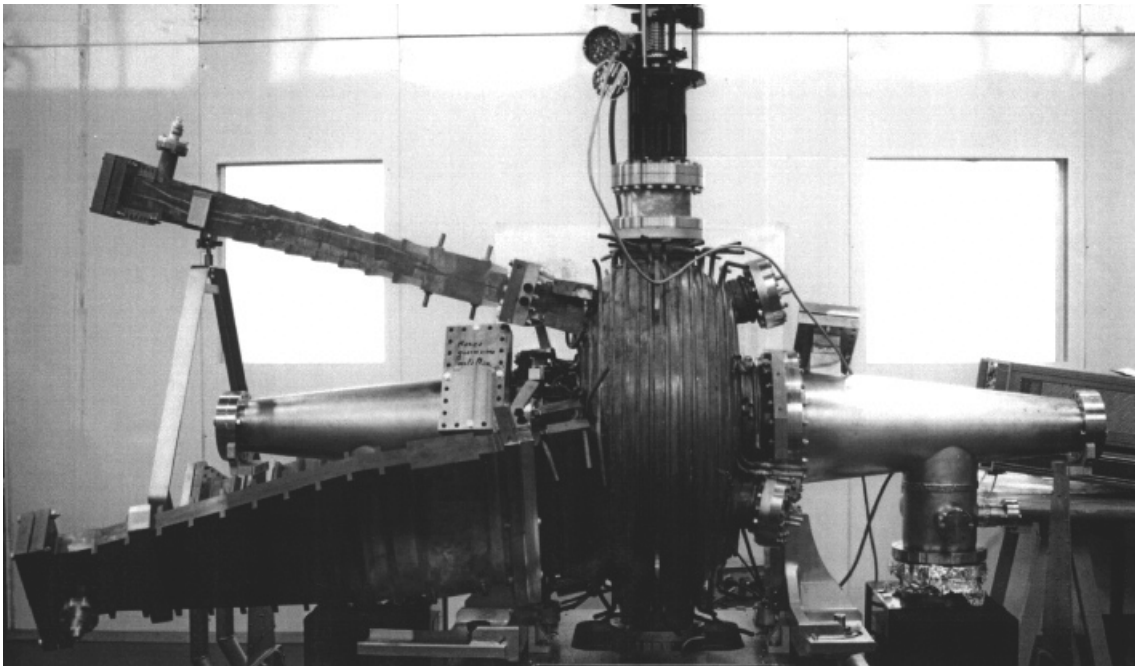


Figure 5 – *The radiofrequency cavity with high order mode dampers.*

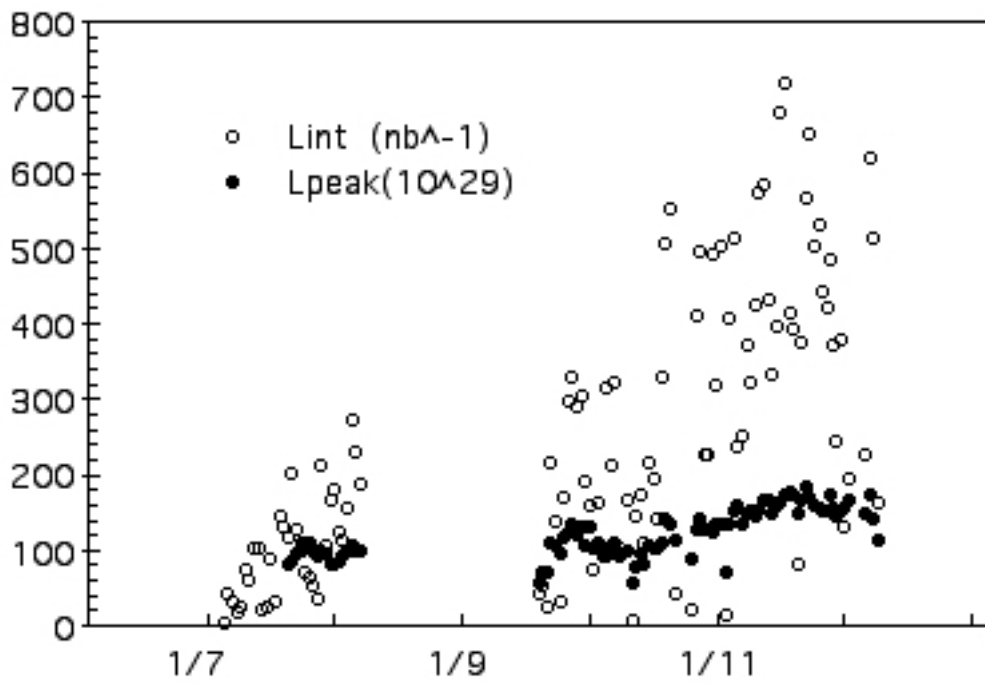


Figure 6 – Peak luminosity during KLOE runs (full dots, in units of $10^{29} \text{cm}^{-2} \text{s}^{-1}$) and integrated luminosity (empty dots, inverse nanobarns) per day.

ALEPH

A. Antonelli, M. Antonelli, G. Bencivenni, G. Bologna (Ass.) , F. Bossi
P. Campana, G. Capon (Resp.), M. Carletti (Tecn.), V. Chiarella, P. Laurelli
G. Mannocchi (Ass.), F. Murtas, G. P. Murtas (Ass.), L. Passalacqua, M. Pepe-Altarelli

1 Introduction

The year 2000 has been the final one for data taking at Lep.

The insertion of the last superconducting RF cavities has allowed LEP to reach its maximum c.m. energy; most of the luminosity was delivered at 206 and 207 GeV, with a record of 210 GeV for a very short time. The total delivered luminosity was 233 pb^{-1} .

To achieve the best sensitivity in the Higgs search the machine was operated in a special mode (miniramp strategy) going toward the end of each fill to the maximum possible energy with only one RF cavity in reserve .

Experiments started operation in mid april, then following the Aleph evidence for the Higgs signal the Cern management agreeded to delay the end of Lep operation (initially foreseen beginning of September) up to November 1st.

The machine operation was smooth and the Aleph detector efficiency was very high, close to 100 %. The Frascati group participated to the data taking and assured the operation and maintenance of the hadron calorimeter and the muon chambers. At the end of the data taking the detector dismantling started; the full dismantling will take about 9 months; the dismantling of the hadronic calorimeter and muon chambers is under Frascati responsibility.

New physics results have been produced both from the final analysis of the full Z sample as well from the new data collected at the highest Lep energy; the Frascati group gave valuable contributions to some specific topics in physics analysis.

In the following only a selection of the main physics results is presented.

2 Electroweak Physics

The final value for the b quark production forward-backward asymmetry ¹⁾ has been evaluated using the full Z sample (~ 4 millions of events) :

$$A_{FB}^b = 10.09 \pm 0.27(stat) \pm 0.12(syst)\%$$

corresponding to a value of the effective weak mixing angle of:

$$\sin^2\theta_W = 0.23193 \pm 0.00056$$

The energy dependence of the asymmetry is shown in fig. 1

Equally the final value for the tau lepton polarization ²⁾ has been measured - see fig. 2 - yielding (assuming tau - electron universality) :

$$A_e = A_\tau = 0.1474 \pm 0.0045$$

to which corresponds

$$\sin^2\theta_W = 0.23147 \pm 0.00057$$

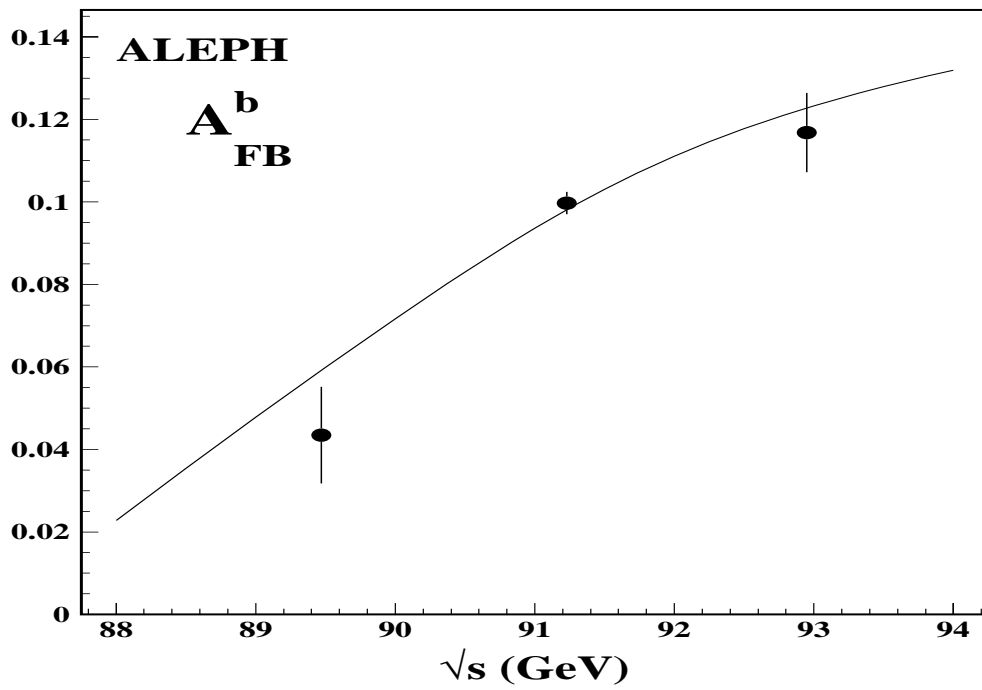


Figure 1: *Energy dependence of the b quark forw/backw asymmetry.*

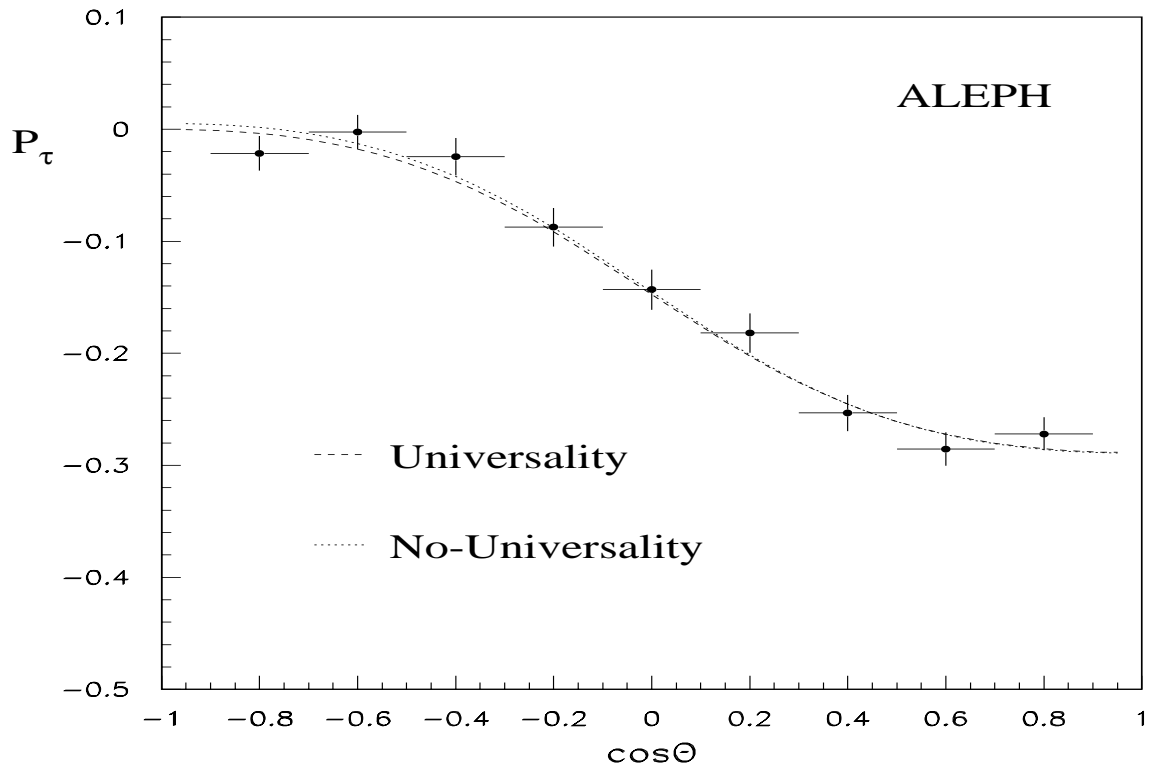


Figure 2: *Angular dependence of the tau polarization.*

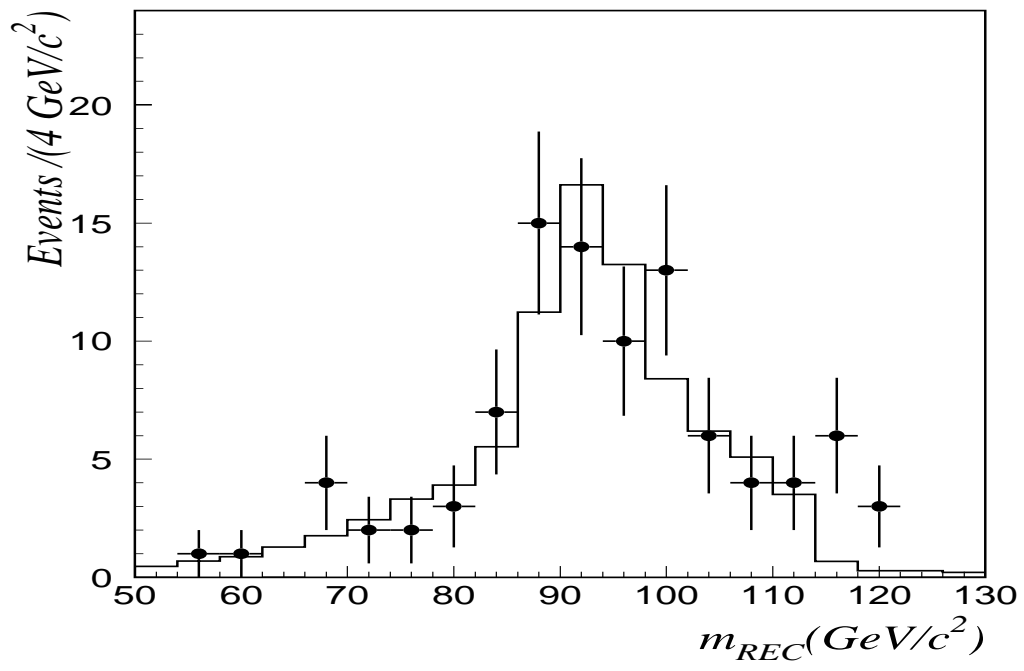


Figure 3: *Distribution of reconstructed Higgs mass.*

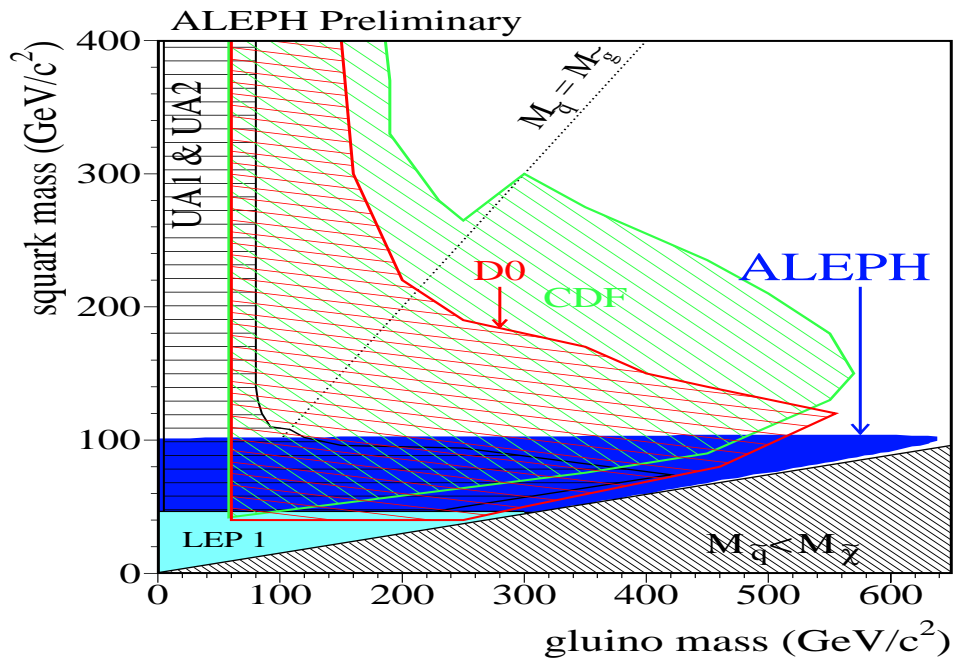


Figure 4: Excluded regions at 95 % C.L. in the gluino - squark mass plane; together with results from hadron colliders.

The test of the triple gauge-boson couplings ³⁾ have been made at mean centre-of-mass energies of 183 GeV and 189 GeV.

The deviation of the couplings from the Standard Model values $:\Delta g_1^Z, \Delta K_\gamma$ and λ_γ , are measured using W-pair events, single-W production and single-gamma production.

The 95 % confidence level intervals for the above quantities are:

$$-0.087 < \Delta g_1^Z < 0.141$$

$$-0.200 < \Delta K_\gamma < 0.258$$

$$-0.062 < \lambda_\gamma < 0.147.$$

A measurement of the Michel parameters ⁴⁾ and the average ν_τ helicity in τ lepton decays has also been made. The Michel parameters ρ_l , ξ_l , $(\xi\delta)_l$ ($l = e, \mu$), and η_μ are determined for the leptonic decays, and the chirality parameters ξ_π , ξ_ρ , and ξ_{a_1} for the hadronic final states. Under the assumptions of $e - \mu$ universality and $\xi_\pi = \xi_\rho = \xi_{a_1}$, the values $\rho_l = 0.742 \pm 0.016$, $\eta_l = 0.012 \pm 0.026$, $(\xi\delta)_l = 0.776 \pm 0.051$, $\xi_l = 0.986 \pm 0.074$, and $\xi_h = 0.992 \pm 0.011$ are obtained. No significant deviation is observed from the Standard Model assumption of the V - A structure of the charged weak interaction.

3 B Physics

The decay $B^0 \rightarrow J/\Psi K_S^0$ is reconstructed with $J/\Psi \rightarrow e^+e^-$ or $\mu^+\mu^-$ and $K_S^0 \rightarrow \pi^+\pi^-$. From the full ALEPH dataset at LEP1 of about 4 million hadronic Z decays, 23 candidates are selected with an estimated purity of 71 %. They are used to measure the CP asymmetry ⁵⁾ of this decay, given by $\sin 2\beta$ in the Standard Model, with the result :

$$\sin 2\beta = 0.84 \pm_{-1.04}^{0.82} \pm 0.16$$

A measurement of the inclusive semileptonic branching ratios ⁶⁾ of b hadrons produced in Z decay has been performed using four million hadronic events collected by the ALEPH detector from 1991 to 1995. Electrons and muons are selected opposite to b-tagged hemispheres. Two different methods are explored to distinguish the contributions from direct $b \rightarrow l$ and cascade $b \rightarrow c \rightarrow l$ decays to the total lepton yield. One is based on the lepton transverse momentum spectrum, the other makes use of the correlation between the charge of the lepton and charge estimators built from tracks in the opposite hemisphere of the event. The latter method reduces the dependence on the modelling of semileptonic b decays. The results obtained by averaging the two techniques are

$$BR(b \rightarrow l) = 0.1070 \pm 0.0010 \pm 0.0023 \pm 0.0026$$

$$BR(b \rightarrow c \rightarrow l) = 0.0818 \pm 0.0015 \pm 0.0022 \pm_{0.0014}^{0.0022}$$

where the last error represents the uncertainty due to the theoretical model.

4 Susy searches

Searches for pair production of squarks, sleptons, charginos and neutralinos ⁷⁾ have been performed with the data collected by the ALEPH detector at LEP at centre-of-mass energies from 188.6 to 201.6 GeV. No evidence for any such signals is observed in a total integrated luminosity of about

410 pb^{-1} . The negative results of the searches are translated into exclusion domains in the space of the relevant MSSM parameters, which improve significantly on the constraints set previously. Under the assumptions of gaugino and sfermion mass unification, these results allow a 95 % C.L. lower limit of $37 GeV/c^2$ to be set on the mass of the lightest neutralino for any $\tan\beta$ and sfermion mass. Additional constraints in the MSSM parameter space are derived from the negative results of ALEPH searches for supersymmetric Higgs bosons. The results have been also interpreted in the framework of minimal supergravity.

5 Higgs search

The Standard Model Higgs has been searched for through the so-called Higgs-strahlung process i.e. $e^+e^- \rightarrow H Z$, looking at the topologies where the Higgs decays into b quarks pairs (here enters the b-tag signature from the silicon vertex detector) while all Z decays are used (lepton pairs, neutrino pairs, quarks pairs) in the data sample collected at centre-of-mass energies up to 209 GeV.

The search was performed using both a neural network based stream and a cut based stream. Both analysis show a 3σ excess ⁸⁾ beyond the background expectation, which is largely due to candidate events selected in the four jet analyses at centre of mass energies greater then 206 GeV.

The observation is consistent (see fig. 3) with the production of a Higgs boson with a mass near 114 GeV.

Reprocessing the most significant candidates using the final calibration and varying the background estimates within the systematic uncertainties has shown that the results are stable.

Clearly more data would have been needed to determine if these observations are due to a statistical fluctuation or are the first evidence of direct production of the Higgs boson.

The same data can be used to put a lower limit on the Higgs mass of 111 GeV with a confidence level of 95 %.

6 Contributions from the Frascati group

6.1 Search for single top production

Single top production ⁹⁾ via flavour changing neutral currents in the reactions $e^+e^- \rightarrow tc$ or $e^+e^- \rightarrow tu$ is searched for in 214 pb^{-1} of data collected at centre-of-mass energies in the range between 204 and 208 GeV. In total, 24 events are selected in the data to be compared with 20.1 expected from Standard Model backgrounds. No deviation from the Standard Model expectation is observed . Upper limits at 95% CL on single top production cross sections at $\sqrt{s} = 204 - 208$ GeV are derived. A model dependent limit on the branching ratio $BR(t \rightarrow Zc + Zu) < 14\%$ is obtained combining all centre-of-mass energies, including the data collected at lower centre-of-mass energies, and assuming $m_{top} = 174 GeV/c^2$ and $BR(t \rightarrow \gamma c + \gamma u) = 0$.

6.2 Searches for sleptons and squarks

Data collected at centre-of-mass energies from 203 GeV to 208 GeV by corresponding to an integrated luminosity of 217 pb^{-1} , are analysed in a search for squarks pair production ¹⁰⁾ .

According to new theoretical ideas the 4-body decay of the stop quark could be competitive or even dominant respect the 2-body decay depending on the MSSM parameters. Therefore a modified version of the generator has been used to simulate this channel.

The signal has been looked for in various final state configurations and in each of these the number of candidates is consistent with the background level expected from Standard Model processes. For the 4-body decay a mass limit of 72 GeV is obtained. In the other channels the previous Aleph limits are improved by 3-7 GeV.

The negative results of the searches are translated into exclusion domains (see fig. 4) in the MSSM framework.

7 List of Publications

References show the papers quoted in the text, while the full list of Aleph papers can be found on the Aleph Web page.

References

1. Aleph collab., CERN EP/2001-050 (Submitted to Eur. Phys. Jou. C)
2. Aleph collab., Eur. Phys. Jou. **C20**, 401 (2001).
3. Aleph collab., Eur. Phys. Jou. **C21**, 423 (2001).
4. Aleph collab., CERN EP/2001-035 (Submitted to Eur. Phys. Jou. C)
5. Aleph collab., Physics Letters **B492** , 259 (2000)
6. Aleph collab., CERN EP/2001-057 (Submitted to Eur. Phys. Jou. C)
7. Aleph collab., Physics Letters **B499** , 67 (2001)
8. Aleph collab., Physics Letters **B495** , 1 (2000)
9. Aleph collab., Contributed paper to LP01 and EPS HEP 2001
10. Aleph collab., Contributed paper to LP01 and EPS HEP 2001

ATLAS

H. Bilokon, V. Chiarella, M. Curatolo, B. Dulach, B. Esposito (Resp.)
G. Felici, M.L. Ferrer, G. Maccarrone, G. Nicoletti, E. Pace, M. Pepe
G. Pileggi (Tecn.), B. Ponzio (Tecn.), V. Russo (Tecn.), M.C. Spitalieri (Bors.)

1 Introduction

The Atlas experiment at the Large Hadron Collider (LHC) is one of the two general purpose experiments. The physics goal of the experiment is to discover and/or investigate all the expected interesting processes and to reveal possible new physics signals. The energy and the luminosity of the LHC machine open new energy frontiers to the experimentation. In order to fully exploit the very rich physics potential of the LHC, a very powerful detector of unprecedented size, complexity, granularity, performances, is needed. The design and the construction of the detector is shared by a world-wide collaboration of unprecedented size.

The Frascati group is involved in the design and the construction of the muon precision tracking chambers. The muon detection and precise measurement is one of the most important tools to identify and study the most interesting physics channels at LHC. For this reason, special emphasis has been given in the Atlas detector to the muon detection, by designing a muon spectrometer capable of extremely precise muon measurement ($\delta p/p \sim 10\%$ at $p=1$ TeV) and achieving such a performance in stand-alone mode. The design is based on super-conducting air core toroids, instrumented with high precision chambers. The precision chambers have to provide a $50 \mu\text{m}$ sagitta measurement over a very large area (5000 m^2). For this purpose, chambers made of an assembly of high pressure drift tubes, called MDT (Monitored Drift Tube) chambers, have been designed and are being built by the Atlas Collaboration.

The Frascati group has given important contributions to the design and development of the MDT chambers ¹⁾ and has taken the responsibility of building all the MDT chambers of the middle station, in between the barrel toroid coils, that are called BML (Barrel Middle Large) chambers. The commitment of the Frascati group is to build 94 chambers 3.6 m long and from 1.2 to 1.7 m wide, which consist of ~ 30000 tubes). The design of the detector has been accompanied by the design of largely automated production and QA/QC facilities, which allow to perform the series production and to control the quality of the production. Also in this field, important contributions have been given to the project by the Frascati group ²⁾.

The activity of the group in the year 2000 has been devoted to the completion of the production facilities. The construction procedures and facilities have been tested by the construction and test of the Module0 chamber.

The work done and the results obtained are the object of this report and are illustrated in the following sections, after a brief description of the MDT detector.

2 The Atlas-MDT tracking chambers

The MDT chambers are the detector developed by the Atlas Collaboration for large area precision tracking. In order to comply with the specifications required, high pressure drift tubes, achieving an average position resolution of $80 \mu\text{m}$, are used as base element, and two multi-layers of 3 or 4 layers of tubes are assembled on the two sides of a support structure by a gluing technique. The final chamber must achieve a $20 \mu\text{m}$ rms precision in the wire positioning. This is achieved by a construction method proposed and developed by the Frascati group, based on the use of a granite

table equipped with high precision jiggling tools used to keep the tubes in position before applying the glue and during the glue curing time.

The construction process of the detector consists of various phases. The main activity lines are:

- wiring of the tubes,
- QA/QC of the tubes (test of the wire tension, gas tightness, dark current),
- assembly of the chamber,
- equipment of the chamber (with gas system and electronics),
- test of the chamber,
- storage of the chamber and/or transportation of the chamber to Cern.

Construction and test stations and specific tools are necessary to accomplish the work.

The Frascati group has designed and built a fully automated wiring machine and computer operated test stations for the wire tension, gas leak and HV test.

3 Activity in the year 2000

All the construction and test facilities have been completed and installed in the clean room by the end of the year 1999, but the final optimization had still to be done.

The first part of the year 2000 has been dedicated to the final performance test and fine tuning of the facilities. Then the module 0 has been built and checked. Following that further optimization of the production facilities has been done.

3.1 Tube wiring automate

The wiring automate performs in a fully automated way, under computer control, all the operations needed to wire the tubes:

- threading of the wire through the tube (3.6 m long) by an air flow,
- threading of the wire through the end-plugs by air flow and vacuum suction,
- insertion of the end-plugs in the tube,
- cutting of the wire,
- swaging of the tube on the end-plugs by 200 bar air pressure,
- pretensioning and tensioning of the wire at the desired tension by a system based on a step motor and a force sensor,
- crimping of the wire pins by means of pneumatic pliers.

The manual operations to be performed by an operator are limited to the loading in the machine “reservoirs” of a batch of tubes, end-plugs and a wire bobbin.

A computer program controls all the operations of the machine leading to the production of wired tubes from the bare components. The complexity of the machine has required a long careful tuning work.

A photograph of the wiring automate is shown in Fig.1.



Figure 1: *The MDT tube wiring automate.*

3.2 Tube QA/QC

Another complex system, of a different nature, is the leak and HV test station. In order to achieve the required chamber performance, the MDT tubes must comply with tight specifications, i.e. gas leak $< 10^{-8}$ bar·l/s, dark current < 7 nA. It is therefore mandatory to perform a quality check of every tube to make sure that the tubes to be assembled in the chambers are within the specifications, rejecting the ones out of the range of tolerance.

The leak rate is delicate and time consuming. The leak test station performs the leak test with a spectrometer He-detector and is fully automated under computer control, by means of a complex system of electro-valves and pumps, in addition to the He-detector. The optimisation of the procedure and the program has required careful studies.

The HV test is performed in the same station by applying HV to the tubes and measuring the current. The program operates suitable conditioning cycles of the tubes in the case larger currents than allowed are drawn.

Another quality check to be performed on the tubes is the measurement of the wire tension. This is done by measuring with an electrostatic method the wire resonance frequency. The measuring system is operated under computer control.

3.3 MDT chamber assembly

The chamber assembly jig, mounted on the granite table, is the fundament of the mechanical precision of the chamber ($< 20 \mu\text{m}$ rms on the wire position). That is obtained by designing and building precise mechanical components of the jig, aligning them very precisely on the granite table, and carefully checking their position on the table.

Auxiliary systems are also needed to

- handle the chamber on the jig,
- compensate the bending due to its weight,
- hold the tubes on the jig by vacuum suction,
- distribute the glue on the tubes.

3.4 Module 0 and measurement results

The test of the series production procedures and facilities was performed by constructing the module 0, i.e. a chamber, in all respects, identical to the series chambers, to be carefully tested to establish the readiness of the production facilities.

The large amount of work required to setup all the production facilities was completed by may, and then the production of the tubes for the module 0 started. The results of QA/QC tests for the tubes of the module 0 are shown in Fig.2. The module 0 was built in July.

In July, also the “site review” took place. An Atlas committee is charged of checking on the status of readiness of the MDT construction centres. The site review was successfully passed by the Frascati group.

A photograph of the module 0 chamber in the frame used for the transportation from Frascati to Cern, is shown in Fig. 3.

The verification of the module 0 compliance with the specifications was done by measuring the 2D wire coordinates by an X-ray tomograph. The chamber was sent in august to Cern, where it underwent the X-ray tomography. The results showed that the wire position precision was better than $20 \mu\text{m}$ rms, as required by the Atlas specifications. This confirmed the correct

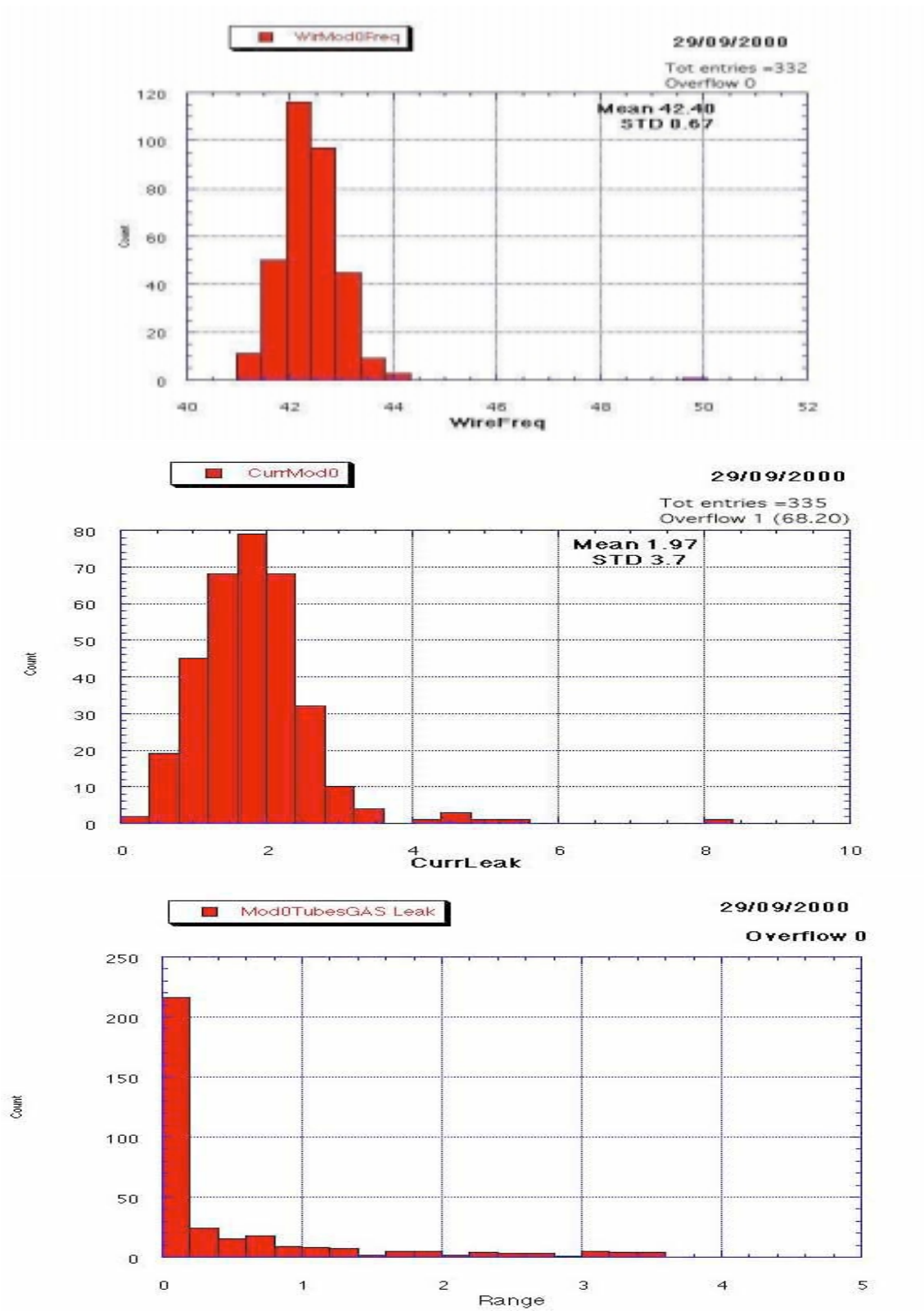


Figure 2: Results of the QA/QC measurements for the tubes assembled in the MDT BML module 0.



Figure 3: *The MDT BML module 0 in its storage/transport frame, before being shipped to Cern for the X-ray tomograph measurement.*

design, realization and operation of the production facilities and the adequateness of the production procedures and tools to achieve the required specifications.

Once the basic performances were verified, before passing from the module 0 construction to the production phase, it was necessary to assure an adequate smoothness and reliability of the machines and of the operations. Therefore toward the end of the year 2000 a program of work started to further adjust the machines and further optimise the software.

The group devoted a particular intense work to the wiring machine, which had exhibited, during the module 0 tube construction, some operation failures from time to time.

4 Activity program

The plan of activity in the year 2001 is basically to start the series production. This will have a first learning phase, with the production proceeding at a moderate rate, in order to allow for some further improvements of the facilities, finalized to easy and make most reliable the production work.

By the end of the year 2001 it is expected to reach the full speed production of 2.5 chambers per month.

References

1. H. Bilokon *et al*, ATL-MUON-95-081;
P. Benvenuto *et al*, ATL-MUON-97-152;

A. Ackermann *et al*, ATL-MUON-97-153;
S. Cerioni *et al*, ATL-MUON-99-007.
2. P. Benvenuto *et al*, ATL-MUON-98-200;
A. Balla *et al*, ATL-MUON-98-26 .

BaBar

F. Anulli (Dott.), R. Baldini Ferroli, A. Calcaterra, L. Daniello(Tecn.), R. de Sangro
D. Falciari (Bors. P.D.), G. Finocchiaro, G. Fuga (Tecn.), P. Patteri, I. Peruzzi (Resp.)
M. Piccolo, Y. Xie (Bors.), A. Zallo

1 Introduction

BaBar is the experiment running at the SLAC asymmetric B -factory PEP-II; the physics program is centered on, but not limited to, the study of the CP violation effects in the decay of neutral B mesons. The B system is the best suited to study CP violation because the expected effects are large, should appear in many final states and, most importantly, can be directly related to the Standard Model parameters. The large data sample now being collected will also allow significant advances in a large number of topics in B , charm and top quark physics.

2 Activity

PEP-II is a two-ring e^+e^- storage ring, colliding 9 GeV electrons with 3.1 GeV positrons, energies chosen to maximize the production of B mesons. The c.m. energy corresponds to the mass of the $Y(4S)$ resonance which decays 50% in B^+B^- , 50% in $B^0\bar{B}^0$. The energy asymmetry is necessary in order to boost the B mesons momentum, so that the decay length can be measured with the accuracy needed to prove the CP violation effects. The machine commissioning ended on schedule, and data taking started in October 1999. After an engineering run in 1999, a first year of data taking followed in the year 2000. The total recorded luminosity up to Dec 31st 2000 has reached $24fb^{-1}$ (fig. 1). The design peak luminosity, $3 \times 10^{33} \text{ cm}^{-2} \text{ sec}^{-1}$, has been reached. The plans for an upgrade to 10^{34} and beyond are being actively addressed. The BaBar Collaboration includes more than 500 physicists, with contributions from 72 Institutions in 9 countries in North America, Europe, and Asia. Approximately half of the group are physicists from U.S. Universities and Laboratories, with the largest foreign contribution coming from Italy, with 12 INFN Institutions and approximately 85 people.

The BaBar detector has been designed primarily for CP studies, but it will also serve well for the other physics objectives of the experiment. A schematic view is shown in fig. 2. The asymmetry of the beam energies is reflected in the detector design: the apparatus is centered 37 cm ahead of the collision point, along the direction of the high-energy beam, to increase forward acceptance. All services are placed on the opposite side of the detector, in order to minimize multiple scattering in the forward direction. The momentum of the charged tracks is obtained from the curvature in a solenoidal field of 1.5 T and is measured in a low mass Drift Chamber. Different species of hadrons are identified in the DIRC, a dedicated device of a novel kind, based on the detection of Čerenkov light. Excellent photon detection and electron identification is provided by a CsI crystals electromagnetic calorimeter.

Muons and neutral hadrons are identified in the iron magnet's yoke, where a total thickness of 65 cm of Fe plates has been segmented in 18 slabs of graded thickness (from 2 to 10 cm) and instrumented with Resistive Plate Counters. This system, made of a 6-sided barrel, 2 endcaps and a double cylindrical layer inside the magnet coil, is called Instrumented Flux Return, or IFR. The final ingredient in the CP asymmetry measurements, the distance between the two decay vertices, is measured by a state of the art vertex detector, with five layers of double sided silicon strips.

BaBar has published a number of measurements obtained with the $50 fb^{-1}$ recorded in the first 2 years of data taking; these include time-dependent CP -violating asymmetries, proportional

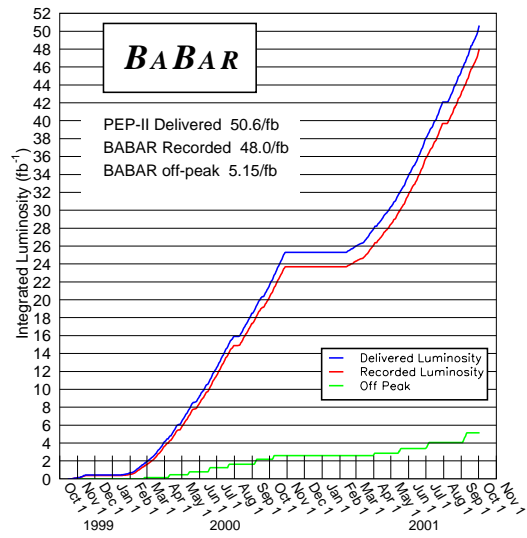


Figure 1: *Integrated Luminosity from June 1999 to October 31st, 2001; the blue line indicates luminosity delivered by PEP-II, the red one luminosity recorded by BaBar .*

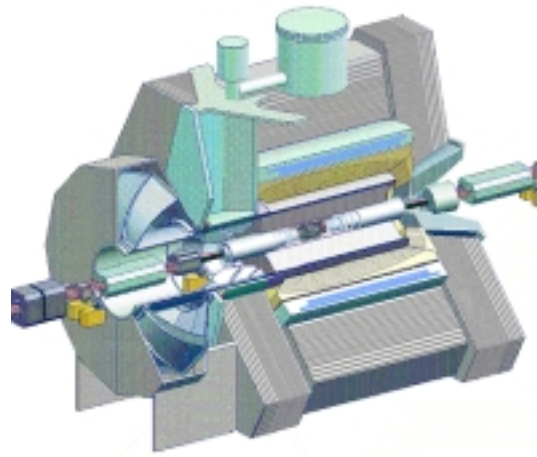


Figure 2: *The BaBar Detector.*



Figure 3: *The LNF testing facility at the RPC factory.*

to $\sin(2\beta)$ in the Standard Model; the value measured by BaBar for $\sin(2\beta)$, $(0.59 \pm 0.14(stat.) \pm 0.05(syst.))$, establishes CP violation in the B^0 meson system. Other important BaBar results include measurements of B meson lifetimes and branching fractions .

The Frascati group has played a major role in the design of the IFR, construction, testing and operation of the RPC's. The system consists of 330 RPC chambers equipped with a two dimensional readout on external aluminum strips etched on a plastic support foil. Each chamber is made of 3 RPC modules in the central region and two RPCs in the doors, for a total of approximately 800 modules (total surface 2000 m^2).

The modules are operated in limited streamer regime; the gas used is a mixture containing approximately 60% Argon, 36% Freon 134a (1,1,1,2 tetrafluoroethane) and 4% isobutane. This choice satisfies the security requirements for flammability and does not contain environment damaging Freon. The mixture is drawn from a 760-liter mixing tank which is filled on demand by the combined flow from three mass-flow controllers, each adjusted to provide the desired fraction of the corresponding component gas. Samples are extracted from the mixing tank periodically and analyzed to verify the correct mixture.

During the year 2000, a strong R&D program has been pursued in several Institutions, including Frascati, to understand the mechanism of the efficiency loss appeared after the overheating of summer 1999, and find operating conditions to alleviate and possibly solve the problem. After the decision to replace all chambers in the Forward Endcap, the Frascati group has taken the responsibility to build a test setup at the RPC factory (fig. 3). This facility, that is now operational, has the capability to read out cosmic rays passing a stack of 10 finished IFR chambers; the expected impact point on each one being predicted by two additional trigger chambers, 2-dimensional efficiency maps will be obtained for all chambers before shipping to SLAC. This is the first time that a full-size testing Lab has been installed on the site of a commercial firm, *i.e.* at a non-INFN, and non-High Energy Physics, location.

The ability of the IFR for identifying muons was not seriously affected by the loss in efficiency of the RPCs, thanks to the large number of layers and the redundancy of information. Different values of the cut on the likelihood ratio of the muon and pion hypotheses give different levels of muon efficiency and pion misidentification probability, which are used in different analysis according to the needed level of purity. Examples of muon efficiency as a function of momentum obtained with control samples of $\mu^+ \mu^- e^+ e^-$ and using respectively looser and tighter cuts are shown in fig. 4.

After the commissioning of the detector, the Frascati group has contributed, together with other Institutions, to its maintenance and running; specific responsibilities include the HV and LV distribution systems, the database maintenance, the IFR software validation and releases. In

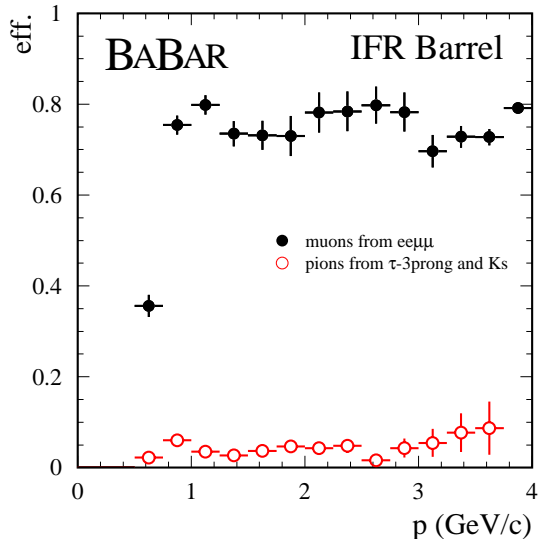


Figure 4: *Muon ID in BaBar with the IFR.*

the software sector, the biggest part of our contribution has regarded writing and optimizing the code dedicated to find and identify “Neutral Hadron” interactions. K_L and other neutral hadrons interact in the iron of the IFR producing one or more clusters of hits in the RPC’s. Monte Carlo simulations predict that about 64% of K_L from the most interesting physics channels produce at least 1 cluster with 2 or more layers hit. The main goal of these studies is the measurement of the CP asymmetry in the decay $B^0 \rightarrow J/\psi K_L$: this channel produces an event sample comparable to that of the “gold-plated” $B^0 \rightarrow J/\psi K_S$ and contributes convincing evidence for any observed CP asymmetry since K_L and K_S have opposite CP eigenvalues and asymmetries.

The signal reconstruction is obtained by first considering all the clusters that are not associated with any charged track. These three dimensional (3D) clusters are reconstructed separately in the 6 barrel sextants, the cylindrical RPC and the top, middle and bottom sections of the end-caps, starting from the strip hits in the various layers. Each single 3D cluster is characterized by its position, which is given by the center of gravity of all the strips it is made of, and by other information that is stored with it, like the number of hit layers, number of strips hit, etc. Since the IFR segmentation does not provide a sufficient sampling of the energy deposition of the hadrons, no measurement of the energy of the incident particle is obtained.

Since a significant fraction of K_L initiate their shower in the electromagnetic calorimeter before reaching the cylindrical RPC and IFR, a degradation of the resolution on the direction is observed unless one includes the information from the calorimeter. This is done by associating to each neutral hadron a calorimeter cluster if their directions are sufficiently close in space. In this case we require that the probability of the χ^2 of the match be $\leq 1\%$. For neutral hadrons that have a calorimeter cluster associated to them, the direction is computed using the position of the calorimeter cluster.

In fig. 5 we show the angular resolution obtained from Monte Carlo $J/\psi K_L$ events showing a clear improvement when the calorimeter information is used (bottom) or not used (top) to determine the K_L flight direction. In fig. 6 we show for real data the distribution of the $\Delta\varphi$ between the missing momentum in all inclusive J/ψ events and the direction of the Neutral Hadron. The peak at zero shows that indeed part of the missing momentum is accounted for by the Neutral Hadron.

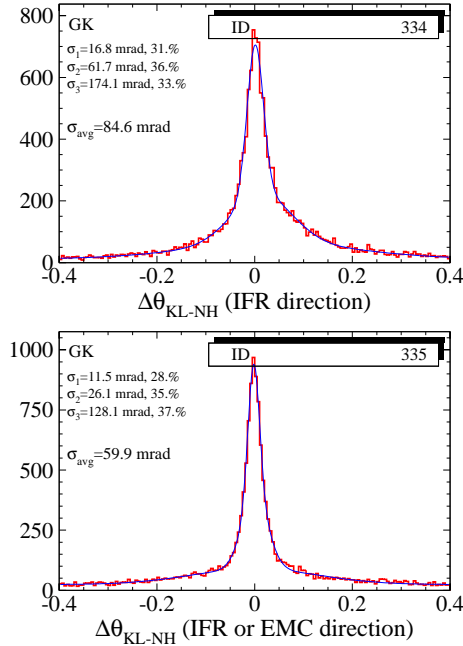


Figure 5: *Neutral hadron angular resolution.*

The detailed Monte Carlo study initiated in September 2000 to optimize the reconstruction of neutral hadrons in the IFR for the detection of K_L from the $B \rightarrow J/\psi K_L$ decay was completed, and the results have been summarized in an extensive document .

The analysis method for reconstructing the final state $J/\psi K_L$ relies on the measurement of the K_L direction, coupled with the kinematics constraints; these are sufficient to eliminate most of the combinatorial background for $J/\psi K_L$ candidates. The J/ψ is reconstructed in the dilepton final states and a momentum in the $Y(4S)$ c.m. frame in the 1.4 to 2.0 GeV/c range is required. The K_L direction is taken from the J/ψ vertex to the centroid of the neutral hadron cluster. Control samples used to check the K_L efficiency obtained by Monte Carlo have been proposed by the Frascati group and include the inclusive J/ψ decays and the process $e^+e^- \rightarrow \phi\gamma$. The result obtained on the $J/\psi K_L$ signal is shown in fig. 7. The inclusion of the K_L channel reduces the error on $\sin(2\beta)$ by $\approx 10\%$.

Two new analyses have recently been started inside the Frascati group.

The first one is the study of the CP violating decay $B \rightarrow \chi_{c1} K_L$, whose expected branching ratio is $3.7 \cdot 10^{-4}$. This channel will provide another measurement of $\sin(2\beta)$ which can be combined with all the others to improve the overall statistical error on the measurement of this important Standard Model parameter. The measurement is more difficult than in the $J/\psi K_L$ final state case because the χ_c is reconstructed via its decay into a J/ψ and a photon. This introduces an additional efficiency factor with some increase in the background. This work is in its preliminary stage of Monte Carlo evaluation of the signal and background.

The other analysis recently started inside the Frascati group is the measurement of the sign of $\cos(2\beta)$ using the interference between $B^0 \rightarrow J/\psi K^0$ and $B^0 \rightarrow J/\psi \bar{K}^0$.

It has already been emphasized that the sign of $\cos(2\beta)$, possibly obtained in a model independent way, is needed to get β . In fact, $\sin(2\beta) \sim 0.6$ is consistent with both $\beta \sim 18^\circ$ and

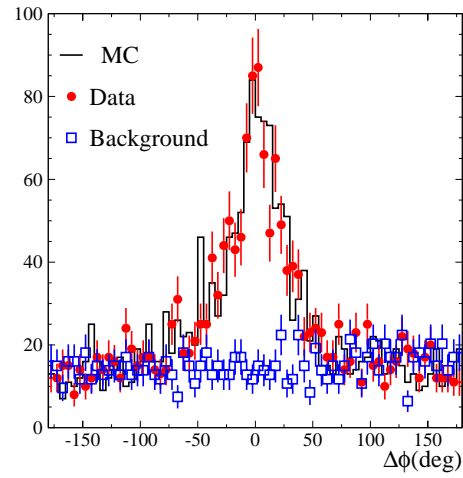


Figure 6: *Between neutral hadron and missing momentum.*

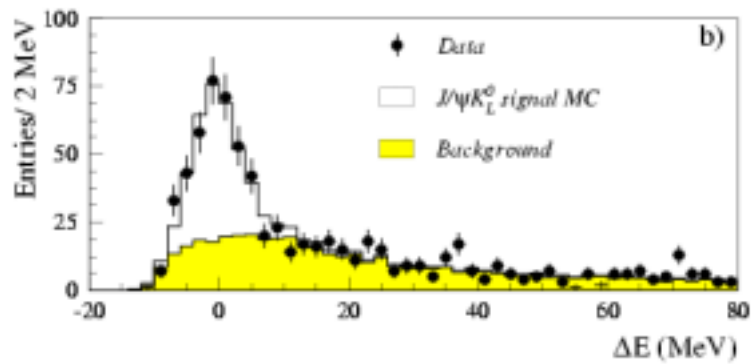


Figure 7: *Results on the $J/\psi K_L$ signal.*

$\beta \sim 72^\circ$, that is with two quite different CP violation scenarios. It has been proposed to identify the processes $B^0 \rightarrow J/\psi K^0$ and $B^0 \rightarrow J/\psi \bar{K}^0$ looking for cascade mixing in K semileptonic decay or K_S^0 regeneration. By means of these processes it is possible to detect a $K_S - K_L$ interference and to have access to a model independent measurement of the sign of $\cos(2\beta)$.

An additional way for identifying these processes has been proposed and is being pursued by us, namely looking for inelastic interactions with definite strangeness on the inner part of BaBar (beam pipe, SVT and DCH inner wall). Reconstruction of a $\Lambda \rightarrow p\pi^-$ decay or identification of a K^- would tag negative strangeness (therefore a \bar{K}^0), while the K^0 would be signalled by a K^+ . In both cases the detected particles would be produced by the interaction of a neutral particle in the BaBar inner part. In principle it is not needed, for the measurement of $\text{sign}(\cos(2\beta))$, that the efficiency for detecting positive and negative strangeness are well known. It turns out that the fraction of interaction length in this region is small, but not vanishing, and there are chances to get a ~ 2 standard deviations measurement of $\text{sign}(\cos(2\beta))$ collecting $\sim 100\text{fb}^{-1}$.

References

1. H. Kang *et al.* [SLD Collaboration], SLAC-PUB-8687.
2. K. Abe *et al.* [SLD Collaboration], arXiv:hep-ex/0012043.
3. B. Aubert *et al.* [BABAR Collaboration], arXiv:hep-ex/0012042.
4. K. Abe *et al.* [SLD Collaboration], arXiv:hep-ex/0011041.
5. C. J. Lin *et al.* [SLD Collaboration], arXiv:hep-ex/0011040.
6. A. W. Weidemann *et al.*, SLAC-PUB-8689 *Contributed to 4th Rencontres du Vietnam: International Conference on Physics at Extreme Energies (Particle Physics and Astrophysics), Hanoi, Vietnam, 19-25 Jul 2000.*
7. P. N. Burrows *et al.* [SLD Collaboration], arXiv:hep-ex/0011002.
8. K. Abe *et al.* [SLD Collaboration], Nucl. Phys. Proc. Suppl. **93** (2001) 126.
9. K. Abe *et al.* [SLD Collaboration], Phys. Rev. Lett. **86** (2001) 1162 [arXiv:hep-ex/0010015].
10. M. Iwasaki *et al.* [The SLD Collaboration], arXiv:hep-ex/0010003.
11. K. Abe *et al.* [SLD Collaboration], arXiv:hep-ex/0009064.
12. K. Abe *et al.* [SLD Collaboration], Phys. Rev. D **63** (2001) 032005 [arXiv:hep-ex/0009035].
13. K. Abe *et al.* [SLD Collaboration], SLAC-PUB-8504 *Contributed to 30th International Conference on High-Energy Physics (ICHEP 2000), Osaka, Japan, 27 Jul - 2 Aug 2000.*
14. B. Aubert *et al.* [BABAR Collaboration], arXiv:hep-ex/0008060.
15. B. Aubert *et al.* [BABAR Collaboration], arXiv:hep-ex/0008059.
16. B. Aubert *et al.* [BABAR Collaboration], arXiv:hep-ex/0008058.
17. B. Aubert *et al.* [BABAR Collaboration], arXiv:hep-ex/0008057.
18. B. Aubert *et al.* [BABAR Collaboration], arXiv:hep-ex/0008056.
19. B. Aubert *et al.* [BABAR Collaboration], arXiv:hep-ex/0008055.

20. B. Aubert *et al.* [BABAR Collaboration], arXiv:hep-ex/0008054.
21. B. Aubert *et al.* [BABAR Collaboration], arXiv:hep-ex/0008053.
22. B. Aubert *et al.* [BABAR Collaboration], decays,” arXiv:hep-ex/0008052.
23. B. Aubert *et al.* [BABAR Collaboration], arXiv:hep-ex/0008051.
24. B. Aubert *et al.* [BABAR Collaboration], arXiv:hep-ex/0008050.
25. B. Aubert *et al.* [BABAR Collaboration], arXiv:hep-ex/0008049.
26. B. Aubert *et al.* [BABAR Collaboration], arXiv:hep-ex/0008048.
27. K. Abe *et al.* [SLD Collaboration], SLAC-PUB-8542 *Talk given at the 30th International Conference on High-Energy Physics (ICHEP 2000), Osaka, Japan, 27 Jul - 2 Aug 2000.*
28. M. Kalelkar *et al.* [SLD Collaboration], Nucl. Phys. Proc. Suppl. **96** (2001) 31 [arXiv:hep-ex/0008032].
29. K. Abe *et al.* [SLD Collaboration], Phys. Rev. Lett. **86** (2001) 962 [arXiv:hep-ex/0007051].
30. K. Abe *et al.* [SLD Collaboration], Phys. Rev. Lett. **85** (2000) 5059 [arXiv:hep-ex/0006019].
31. T. R. Wright *et al.*, SLAC-PUB-8449 *Invited talk at 35th Rencontres de Moriond: Electroweak Interactions and Unified Theories, Les Arcs, France, 11-18 Mar 2000.*
32. K. Abe *et al.* [SLD Collaboration], arXiv:hep-ex/0005001.
33. K. Abe *et al.* [SLD Collaboration], Phys. Rev. Lett. **84** (2000) 5945 [arXiv:hep-ex/0004026].

CDF

M. Cordelli, S. Dell’Agnello, P. Giromini (Resp.), F. Happacher (Ass.), S. Miscetti, A. Sansoni

1 Introduction

The CDF experiment at the Fermilab TeVatron Collider has collected data until the spring of year 1996 integrating a luminosity of about 120 pb^{-1} .

The TeVatron, with the new Main Ring, has been upgraded to achieve a $p\bar{p}$ collision energy up to 2 TeV in the centre of mass system and to increase the instantaneous luminosity delivered to the experiments up to $2 \times 10^{32} \text{ cm}^{-2}\text{sec}^{-1}$. During the Run IIa (officially begun in march of this year and that will be lasting until 2004) we expect to integrate 2 fb^{-1} of data.

The CDF group of the Frascati laboratory was historically responsible of the construction and maintenance of the central hadronic calorimeter during Run I operations; the lead-scintillator based calorimeter in the central region has been retained for Run II operations having worked satisfactory in Run I.

The central calorimeters have worked properly for ten years and their commissioning played an important role in driving the commissioning and tuning of the new sub-detectors of CDF. At the end of 2001 central calorimeter will be ready to acquire data with the required quality for the first physics publications in the summer 2002.

The Frascati group is involved in the fulfillment of the detector upgrades necessary to keep the calorimeter working with the higher instantaneous luminosity and the shorter bunch crossing time interval that is now of 132 nsec , during Run I it was of $3.5 \text{ }\mu\text{sec}$.

Furthermore, the group is still active in Run I data analysis playing an important role in the measurement of the top production cross section and in a detailed analysis of the heavy flavor quarks content of the $W + \text{jets}$ sample. This analysis resulted in the observation of an excess of events with heavy flavor quarks undergoing semileptonic decays with an anomalous behaviour with respect to the known Standard Model processes. Both this works have been published on PRD.

2 Run II activities

The increase of the luminosity together with the shortening of the time interval between two adjacent bunch crossings required an upgrade of the CDF detector. CDF essential components, like the central tracking chamber, the silicon secondary vertex detector and the forward regions of the calorimeter needed to be built *ex novo*. The central electromagnetic and hadronic calorimeters are the only devices, with the muon chambers, that are still working properly in the new Run after substantial modifications. The main change is the renewal of all the Front-End electronics and in the integration time of charge signals that has to be completed within the 132 nsec window of the new machine clock.

The Frascati group had also designed and built the new fast discriminator for the TDC’s of the hadronic calorimetry. During year 2000 and 2001 the boards have been built, their thresholds have been set on a test-stand and then installed on the detector’s crates.

To analyze collisions data the group developed software packages, integrated in the official CDF standard (that uses C++ and AC++). Preliminary studies of the timing behaviour of the hadronic calorimeter have been carried on in order to test the discriminators and TDC functionality. The debugging of the installation and the verification of the thresholds (see Fig. 1) have been pursued through the analysis of the first “engineering” collisions runs acquired by CDF since april

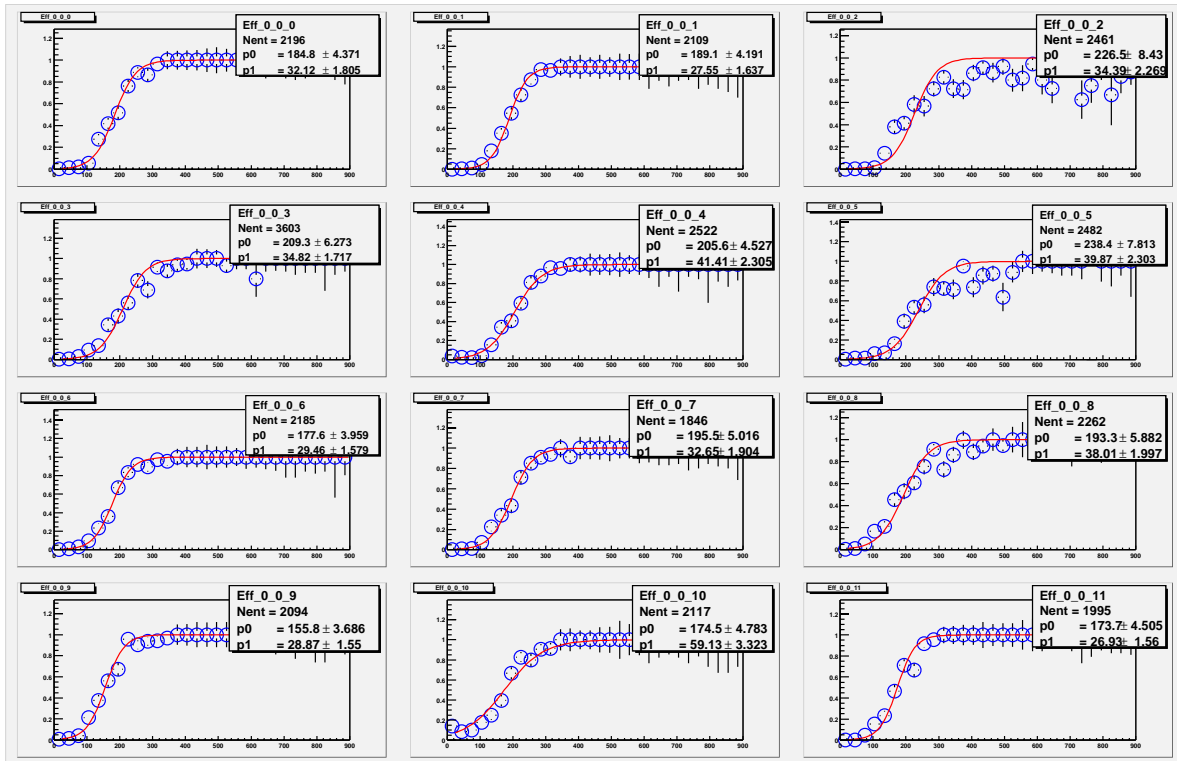


Figure 1: *Distributions of typical efficiency curves for few TDC channels of CHA.*

2001. Moreover, the dependence of the timing on pulse-height (see Fig. 2) has been studied and parametrized. This correction has then been applied to all channels.

The timing distribution for a large sample of collisions is shown in Fig. 3. A narrow peak around the expected collision time is observed together with other structures coming from other buckets and a flat distribution probably due to cosmics. To test the behaviour of the resolution vs energy we report in Fig. 4 the distribution of timing with an applied cutoff in energy (0.6,0.9,1.2,1.5 GeV); the resolution improves as expected. Work is in progress to incorporate also the correction due to the longitudinal shower development.

The calibration of the energy scale is also responsibility of the LNF group. A lot of effort has been devoted to re-install the monitoring of the photomultipliers' gains through the N₂Laser and to set the energy scale of each tower by running the Cs¹³⁷ sources. Many optical fibers, used to funnel the light to each photocathode, have been replaced or repaired and the system has been fully integrated in the new DAQ/Monitoring chain. Also, all 48 driving-motors for the sources of the EndWall calorimeters have been replaced. While the Laser is useful to quickly test the functionality of all channels and the downloading of the ADC gains in the Front-End boards, the sources re-establish the absolute energy scale.

We had also re-integrated the software to set and monitor the high voltages in the new standard of the CDF SlowControl.

3 Run I data analysis

The commitment of the group for the analysis of Run I consists in the study of “quarkonia” states for heavy quarks which has brought to a publication on the charmonium and on a detailed study of the production cross-section of t-tbar pairs in the lepton+Jets channel. For this last analysis, the requirement of “tags” based on the location of the secondary vertex has been used in order

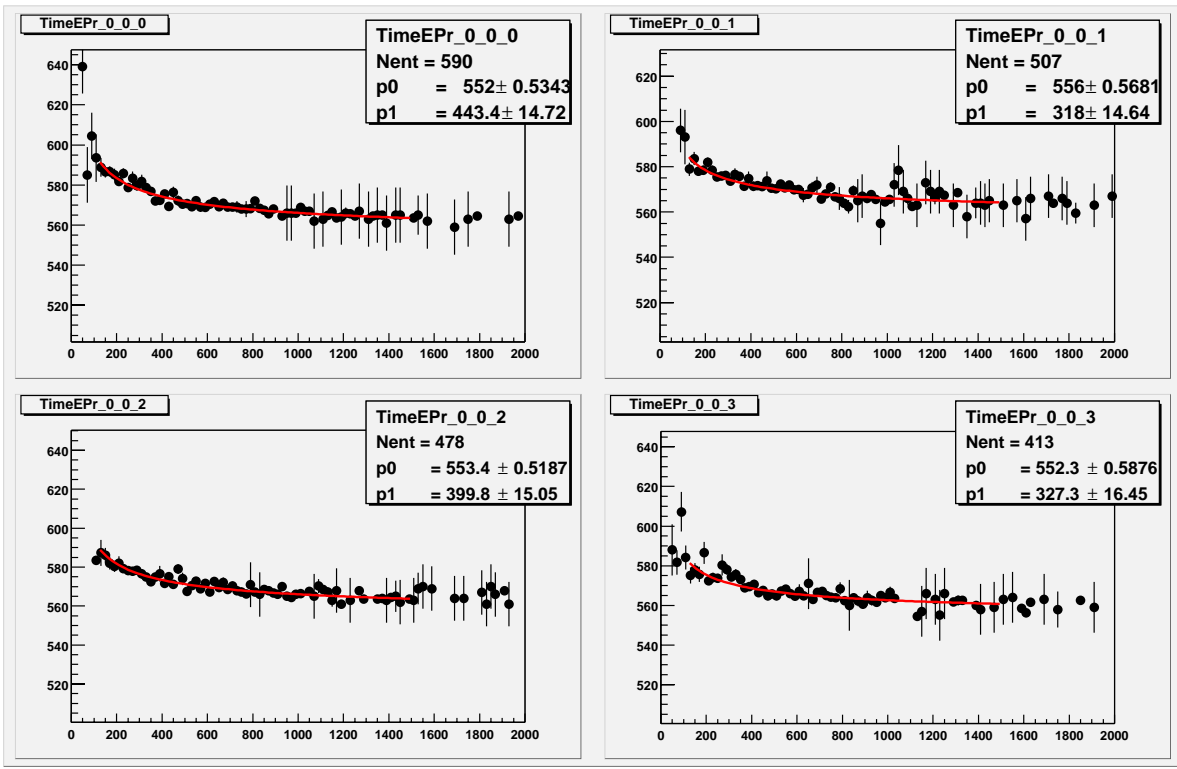


Figure 2: *Timing dependence on pulse height (ADC counts).*

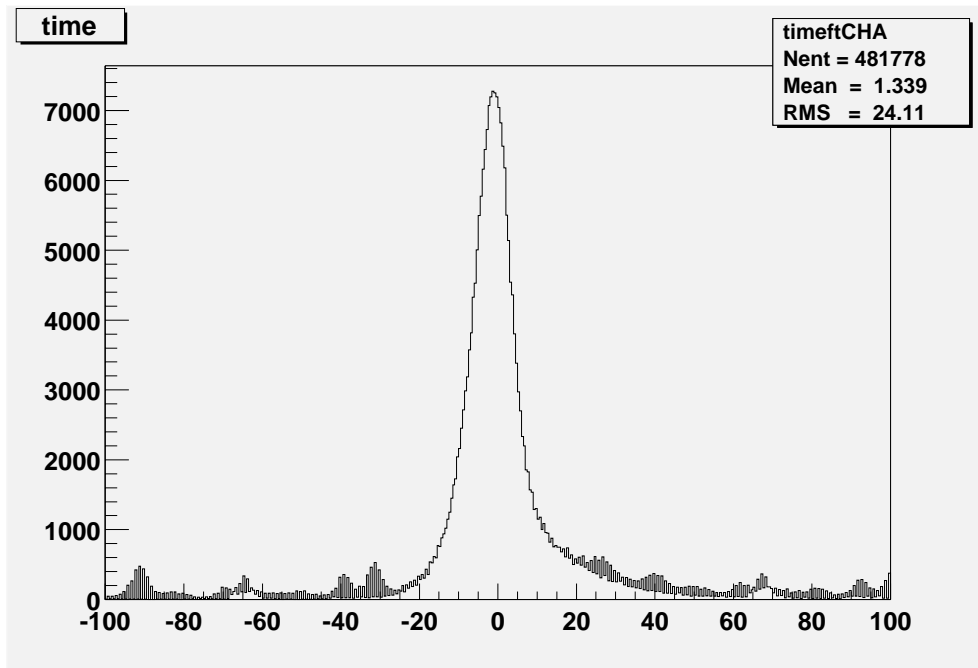


Figure 3: *t_0 's distribution for the central hadronic calorimeter.*

to identify the hadronic-jets coming from b-quarks decay. The yield of the number of events as a function of the jet multiplicity is reported in Fig. 5 for the whole statistics of Run I; the value of the derived cross-section is also shown.

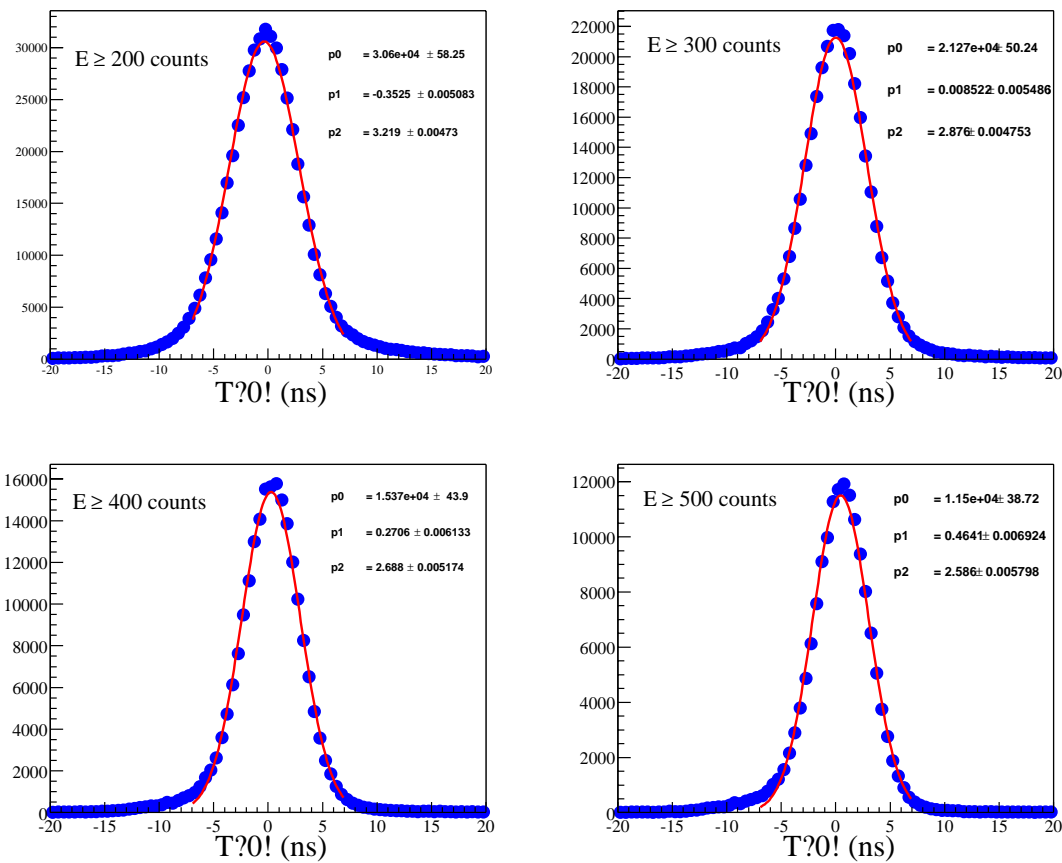


Figure 4: t_0 's distribution for the central hadronic calorimeter after slewing corrections showed in function of the energy deposition in the tower.

In the W+2,3 jets topology, we observed an excess of events with characteristics far from the expected Standard Model predictions. The main difference consisting on having tagged b-jets undergoing semileptonic decays with an anomalous rate. Anyhow, the observed effect represents a deviation from Standard Model ranging between $4.1 \div 4.8$ sigma.

Events with similar behaviour have been searched for in samples of low-Pt leptons. The analysis is still under way.

List of Publications 2000

1. The CDF Collaboration (T.Affolder et al.): "SEARCH FOR COLOR SINGLET TECHNICOLOR PARTICLES IN $p\bar{p}$ COLLISIONS AT $\sqrt{S} = 1.8$ TEV", Phys. Rev. Letters Vol 84 (2000) pag. 1110 \div 1115;
2. The CDF Collaboration (T.Affolder et al.): "SEARCH FOR NEW PARTICLES DECAYING TO $t\bar{t}$ IN $p\bar{p}$ COLLISIONS AT $\sqrt{S} = 1.8$ TEV", Phys. Rev. Letters Vol. 85 (2000) pag. 2062 \div 2067;
3. The CDF Collaboration (T.Affolder et al.): "DIFFRACTIVE DIJETS WITH A LEADING ANTI-PROTON IN $p\bar{p}$ COLLISIONS AT $\sqrt{S} = 1.8$ TEV", Phys. Rev. Letters Vol. 84 (2000) pag. 5043 \div 5048;
4. The CDF Collaboration (T.Affolder et al.): "LIMITS ON GRAVITINO PRODUCTION AND NEW PROCESSES WITH LARGE MISSING TRANSVERSE ENERGY IN $p\bar{p}$ COLLISIONS AT $\sqrt{S} = 1.8$ TEV", Phys. Rev. Letters Vol. 85 (2000) pag. 1378 \div 1383;

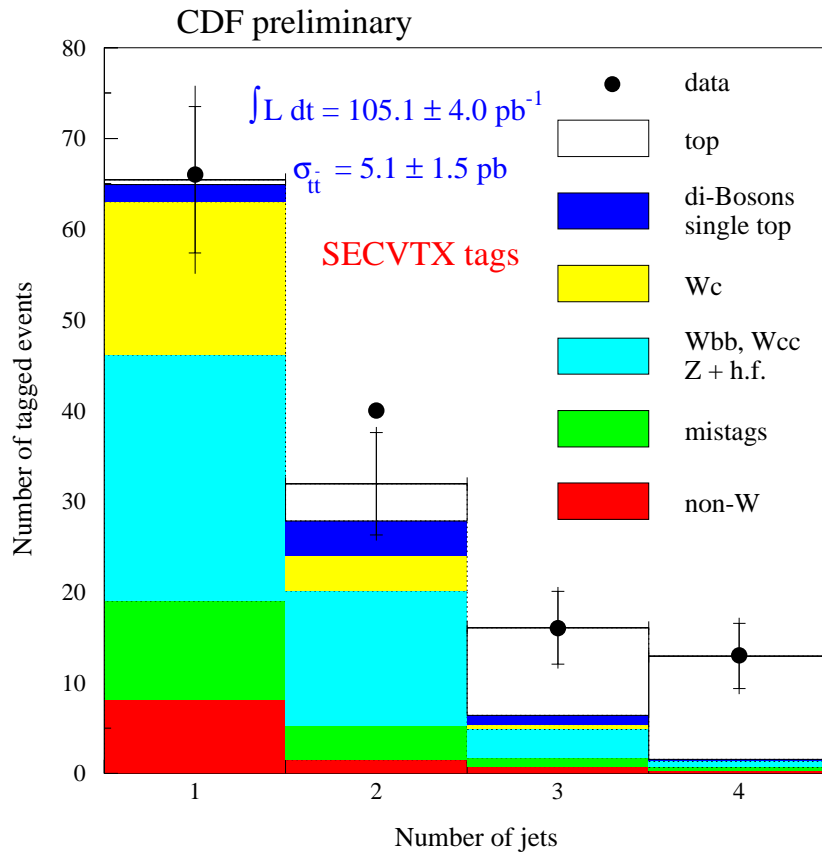


Figure 5: *Number of SECVTX tags in $W + jets$ events*

5. The CDF Collaboration (T.Affolder et al.): “SEARCH FOR SECOND AND THIRD GENERATION LEPTOQUARKS INCLUDING PRODUCTION VIA TECHNICOLOR INTERACTIONS IN $p\bar{p}$ COLLISIONS AT $\sqrt{S} = 1.8$ TEV. Phys. Rev. Letters Vol. 85 (2000) pag. 2056 ÷ 2061;
6. The CDF Collaboration (T.Affolder et al.): “DIRECT MEASUREMENT OF THE W BOSON WIDTH IN $p\bar{p}$ COLLISIONS AT $\sqrt{S} = 1.8$ TEV.” Phys. Rev. Letters Vol. 85 (2000) pag. 3347 ÷ 3352;
7. The CDF Collaboration (T.Affolder et al.): “MEASUREMENT OF J/PSI AND PSI(2S) POLARIZATION IN $p\bar{p}$ COLLISIONS AT $\sqrt{S} = 1.8$ TEV.” Phys. Rev. Letters Vol. 85 (2000) pag. 2886 ÷ 2891;
8. The CDF Collaboration (T.Affolder et al.): “DIJET PRODUCTION BY DOUBLE POMERON EXCHANGE AT THE FERMILAB TEVATRON.” Phys. Rev. Letters Vol. 85 (2000) pag. 4215 ÷ 4220;

E831 FOCUS

R. Baldini-Ferrolì, S. Bianco (Resp. Naz.), F.L. Fabbri, M. Giardoni, A. Zallo

FOCUS ¹⁾ (Experiment 831 at Fermilab, www-focus.fnal.gov) studies photoproduction and decays of charm mesons and baryons at Fermilab. In FOCUS, a forward multi-particle spectrometer is used to measure the interactions of high energy photons on a segmented BeO target. The FOCUS detector is a large aperture, fixed-target spectrometer with excellent vertexing, particle identification, and reconstruction capabilities for photons and π^0 's. FOCUS is a considerably upgraded version of a previous experiment, E687, and it amply surpassed the goal of collecting ten times the E687 sample of fully reconstructed charm decays, i.e. a sample of over 1 million fully reconstructed charm particles in the three major decay modes: $D^0 \rightarrow K^-\pi^+$, $K^-\pi^+\pi^-\pi^+$ and $D^+ \rightarrow K^-\pi^+\pi^+$. The FOCUS Italian groups (Milano, Pavia and Frascati) hold full responsibility for the μ -strip detector, the Hadron calorimetry, and the Outer em calorimetry ¹⁾ respectively, and coordinate about half of the software-related projects. The Frascati group also coordinates the calorimetry working group, and is responsible for the first level selection process in physics analyses utilizing em calorimetry.

1 Activity during year 2000

During year 2000, most of the efforts were devoted to the optimization of monte-carlo simulation codes. Highlights results included lifetimes and $D^0\bar{D}^0$ mixing, hadronic meson decays, baryon spectroscopy and decays, excited charm meson spectroscopy and diffractive physics.

During 2000, the Frascati group contributed in completing second and third level event selection processes (*skims*) for the ongoing analyses, presented results at numerous conferences, and finalized studies on excited charm mesons, and light quark spectroscopy. Members of the FOCUS Frascati group have served as members in International Advisory Committees of CALOR, PIC and HQ2K conferences.

1.1 Excited charm meson spectroscopy results

With the high-statistics, high-mass resolution experiments such as FOCUS attaining maturity, emphasis has been shifted from the ground state (0^- and 1^-) $c\bar{q}$ mesons and ($1/2^+$ and $3/2^+$) cqq baryons to the orbitally- and, only very recently, radially-excited states¹. A consistent theoretical framework for the spectrum of heavy-light mesons is given by the ideas of Heavy Quark Symmetry (HQS), later generalized by Heavy Quark Effective Theory in the QCD framework. The basic idea (mediated from the JJ coupling in atomic physics) is that in the limit of infinite heavy quark mass: a) the much heavier quark does not contribute to the orbital degrees of freedom, which are completely defined by the light quark(s) only; and b) properties are independent of heavy quark flavor. Heavy Quark Symmetry provides explicit predictions on the spectrum of excited charmed states. In the limit of infinite heavy quark mass, the spin of the heavy quark \mathbf{S}_Q decouples from the light quark degrees of freedom (spin \mathbf{s}_q and orbital \mathbf{L}), with \mathbf{S}_Q and $\mathbf{j}_q \equiv \mathbf{s}_q + \mathbf{L}$ the conserved quantum numbers. Predicted excited states are formed by combining \mathbf{S}_Q and \mathbf{j}_q . For $L = 1$ we have $j_q = 1/2$ and $j_q = 3/2$ which, combined with S_Q , provide prediction for two $j_q = 1/2$ ($J=0,1$) states, and two $j_q = 3/2$ ($J=1,2$) states. These four states are named respectively D_0^* , $D_1(j_q = 1/2)$, $D_1(j_q = 3/2)$ and D_2^* . Finally, parity and angular momentum conservation favor

¹In the past, these excited states were called generically and improperly D^{**} .

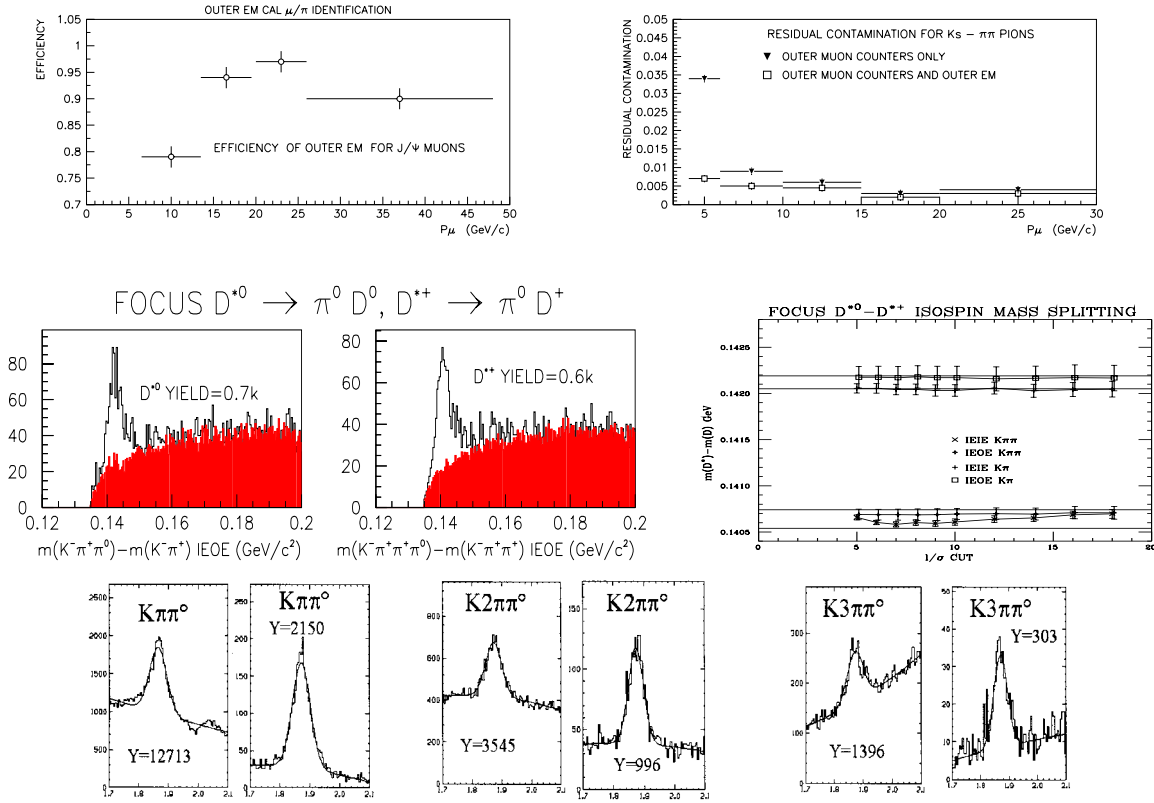


Figure 1: *FOCUS* preliminary results on a fraction of the dataset. From top to bottom: efficiency on muons from $J/\psi \rightarrow \mu^+\mu^-$ and rejection of pions from $K_s \rightarrow \pi^+\pi^-$; D^{*0} and D^{*+} decays with π^0 in the final state, and comparison of the precision attainable on the isospin mass splittings compared to world average, as functions of detached vertex significance l/σ ; several decays of D^+ and D^0 mesons with π^0 in the final state, with a selection of preliminary background-reducing cuts.

the ($j_q = 1/2$) states to decay to the ground states mainly via S-wave transitions (broad width), while ($j_q = 3/2$) states would decay via D-wave (narrow width). While the narrow states are well established, the evidence for the broad states (both in the c -quark and in the b -quark sector) is much less stringent.

The analysis efforts in 2000 were focussed on the precision measurement of masses and widths of established excited states. The study of the $D\pi$ mass spectrum provided new preliminary values of the masses and widths for the D_2^* meson (Tab. 1). The $D\pi$ mass spectrum (once subtracted the background, the D_2^* signal, and the expected feed-downs) shows an excess of events centered around $2420 \text{ MeV}/c^2$ and about $185 \text{ MeV}/c^2$ wide. The observed excess could be reminiscent of the broad D_0^* predicted by HQS and never observed sofar, or of a feed-down from another broad state such as the $D_1(j_q = 1/2)$, possibly interfering. Work is in progress to verify such hypothesis.

1.2 Light quarks physics results

A somewhat unexpected stream of projects coming from FOCUS and E687 data is the diffractive photoproduction of light quarks. By means of a dedicated trigger, FOCUS has collected a very significant sample of diffractive events, thus starting studies of interest in hadronic physics and predictions of χ QCD. A study begun in 1999 was concluded in 2000, which looked for structures in the 6π invariant mass spectrum, coming from the interference of a new narrow resonance just above the $N\bar{N}$ threshold with the phasespace, or possibly with known resonances such as ρ' , etc. (Fig.3).

Table 1: Preliminary measurements of masses and widths for narrow structures in $D^+\pi^-$ and $D^0\pi^+$ invariant mass spectra.

	Mass MeV/c^2	Width MeV/c^2
D_2^{*0}	$2463.5 \pm 1.5 \pm 1.5$	$30.5 \pm 1.9 \pm 3.8$
PDG2000	2458.9 ± 2.0	23 ± 5
D_2^{*+}	$2468.2 \pm 1.5 \pm 1.4$	$28.6 \pm 1.3 \pm 3.8$
PDG2000	2459 ± 4	25^{+8}_{-7}

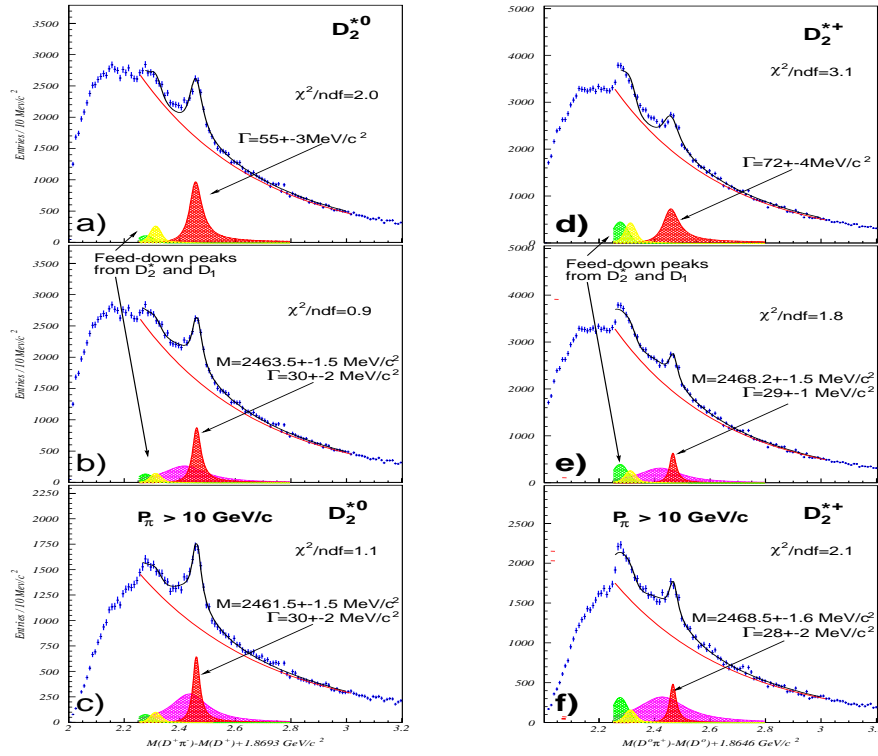


Figure 2: The $D^+\pi^-$ ($D^0\pi^+$) mass spectra is shown in insets a, b, c (d, e, f). Insets c, f show the effect of a soft pion momentum cut.

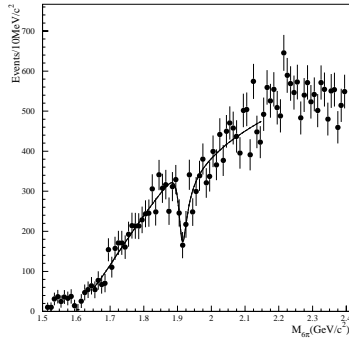


Figure 3: Acceptance-corrected distribution of $3\pi^+3\pi^-$ invariant mass for diffractive events. The mass resolution has been unfolded. Curve is Breit-Wigner resonance coherently summed to Jacob-Slanski background parametrization.

2 Outlook

The activity in 2001 will be focussed in finalizing the excited charm meson masses and widths measurements, as well as in searching for radial excitations. In the light quark sector, we plan to seek confirmation of the six pion structure found out of a larger data sample, and to study f_0 production and $\eta - \eta'$ mixing from our diffractive sample.

3 List of publications in 2000

1. J. M. Link *et al.* [FOCUS Collaboration], “A study of the decay $D^0 \rightarrow K^+\pi^-$ ” accepted by Phys. Rev. Lett. [hep-ex/0012048].
2. J. M. Link *et al.* [FOCUS Collaboration], “Search for CP violation in D^0 and D^+ decays,” Phys. Lett. B **491** (2000) 232 [hep-ex/0005037].
3. J. M. Link *et al.* [FOCUS Collaboration], “Measurements of the $\Sigma_c^0 \Sigma_c^{++}$ mass splittings,” Phys. Lett. B **488** (2000) 218 [hep-ex/0005011].
4. J. M. Link *et al.* [FOCUS Collaboration], “A measurement of lifetime differences in the neutral D meson system,” Phys. Lett. B **485** (2000) 62 [hep-ex/0004034].
5. S. Sarwar *et al.* [FOCUS Collaboration], “Preliminary results on charmed meson spectroscopy,” hep-ex/0011072, DPF2000 Columbus, Ohio.
6. F. L. Fabbri *et al.* [FOCUS Collaboration], “Results on charmed meson spectroscopy from FOCUS,” hep-ex/0011044, ICHEP2000, Osaka, Japan.
7. S. Bianco *et al.* [FOCUS Collaboration], “New FOCUS results on charm mixing and CP violation,” CPCConf2000 Ferrara, Italy, hep-ex/0011055.

References

1. The E687 spectrometer is described in P. L. Frabetti *et al.* (E687 Coll.), Nucl. Instrum. Meth. **A320**, 519 (1992). The E687 Outer em calorimeter is described in S. Bianco *et al.*, hep-ex/9912066.

KLOE

A. Antonelli, M. Antonelli (Ass.ric.), G. Bencivenni, S. Bertolucci (Resp.), F. Bossi, P. Campana, G. Capon, P. Ciambrone (Bors.), P. De Simone, S. Dell’Agnello, A. Denig (Bors.CEE), G. Felici, M. L. Ferrer, G. Finocchiaro, C. Forti, A. Franceschi, S. Giovannella (Dott.), G. Lanfranchi, J. Lee-Franzini (art.23), W. Mei (art.23), S. Miscetti, M. Moulson (Bors.), F. Murtas, A. Nedosekin (art.23), L. Passalacqua, V. Patera, P. Santangelo, A. Sciubba, I. Sfiligoi (Bors.), P. Valente (Bors.)

The KLOE-LNF Technical Staff:

M. Anelli, A. Balla, E. Capitolo, M. Carletti,
G. Corradi, U. Denni, G. Fortugno, M.A. Frani, G. Paoluzzi,
G. Papalino, M. Santoni, A. Saputi, A. Rutili

1 Physics at DAΦNE

DAΦNE is a double annular e^+e^- collider on the ϕ resonance $\sqrt{s} = 1020$ MeV which has been designed for a peak luminosity of $5 \cdot 10^{32} \text{cm}^{-2}\text{s}^{-1}$ ¹). The $\phi(1020)$ vector meson is predominantly decaying into kaon pairs, where the decay into the neutral pair $K^0\bar{K}^0$ (i.e. $K_S K_L$) is of special interest, since it opens the possibility to study CP violation. The collinear production of the monochromatic ¹ $K_S K_L$ pair allows one to tag one of the kaons (with defined direction and identity) when the partner kaon had been identified.

In table 1 the main ϕ decays are summarized, together with the event yield at design luminosity in one “technical” year (10^7s) of data taking. One notes that DAΦNE is not only a “factory” for kaon pairs but produces also at huge statistics ρ ’s, η ’s and the rare ϕ decays into $\eta'(958)$, $f_0(980)$ and $a_0(980)$. The physics program of KLOE is therefore complementary and goes beyond the study of symmetry violations (CP, CPT test) ²). It covers - among many other studies - the analysis of kaon form factors, the investigation of rare ϕ decays, as well as the measurement of the hadronic cross section below the ϕ mass.

¹momenta: $\vec{p}_S = -\vec{p}_L$ with $|\vec{p}_{S,L}| = 110 \text{MeV}/c$; mean decay path: $\tau_S = 0.6 \text{ cm}$, $\tau_L = 340 \text{ cm}$

Table 1: $\phi(1020)$ Decays

ϕ decay	BR [%]	Events/year
K^+K^-	49.5	$9.8 \cdot 10^{10}$
$K^0\bar{K}^0$	34.4	$6.9 \cdot 10^{10}$
$\rho\pi, \pi^+\pi^-\pi^0$	15.5	$3.0 \cdot 10^{10}$
$\eta\gamma$	1.3	$2.6 \cdot 10^8$
$f_0\gamma, a_0\gamma, \eta'\gamma$	$\approx 10^{-2} \dots 10^{-4}$	$\approx 2 \cdot 10^6 \dots 2 \cdot 10^8$

1.1 Measurement of ϵ'/ϵ

The KLOE detector is designed primarily with the goal of measuring the direct CP violation in K^0 decays with a sensitivity of $\approx 10^{-4}$ in $\Re(\epsilon'/\epsilon)$ ². The measurement of ϵ' has a long history, yielding in a first round of experiments (*NA31*, CERN and *E731*, FNAL) with contradictory results which only recently have been converging better (*NA48*, CERN³) and *KTeV*, FNAL⁴). The world average of the two experiments $\Re(\epsilon'/\epsilon) = (2.1 \pm 0.5) \cdot 10^{-3}$ ⁵) indicates a value off 0 and therefore rules out the *superweak* postulate for the violation of the CP symmetry.

Double Ratio

KLOE will measure $\Re(\epsilon'/\epsilon)$ with a different experimental setup (collinear kaon pair production) than the CERN and FNAL experiments and hence with systematic errors from completely different sources. The double ratio R is the standard quantity measured to obtain $\Re(\epsilon'/\epsilon)$:

$$R = \frac{BR(K_L \rightarrow \pi^+\pi^-)/BR(K_S \rightarrow \pi^+\pi^-)}{BR(K_L \rightarrow \pi^0\pi^0)/BR(K_S \rightarrow \pi^0\pi^0)} = 1 + 6 \cdot \Re(\epsilon'/\epsilon). \quad (1)$$

The experimental goal is the measurement of the branching ratios $BR_{L,S;+-,00}$ of K_S and K_L into the $\pi^+\pi^-$ and $\pi^0\pi^0$ final state:

$$BR_{L,S;+-,00} = \frac{N_{L,S;+-,00}^{Obs} - N_{L,S;+-,00}^{Bkg}}{N_{KK} \cdot \epsilon_{L,S}^{Tag} \cdot \epsilon_{L,S;+-,00}^{Rec} \cdot \int \int_{FV} I(\vec{x}) \cdot G(\vec{x} - \vec{x}') d\vec{x} d\vec{x}'}, \quad (2)$$

where the total number of kaon pairs N_{KK} and the tagging efficiency $\epsilon_{L,S}^{Tag}$ drop out in the double ratio, while the reconstruction efficiency $\epsilon_{L,S;+-,00}^{Rec}$ has to be known at the 10^{-4} level. The decay intensity $I(\vec{x})$ is convoluted with the detector resolution $G(\vec{x} - \vec{x}')$ and requires an alignment of the fiducial volume (FV) with a precision of few millimeters. An important issue is the separation of the CP violating decays $K_L \rightarrow 2\pi$ from the CP conserving K_L decays ($K_L \rightarrow 3\pi$ and $K_L \rightarrow \pi l \nu_l, l = e, \mu$). The required background rejection is of the order 10^4 to 10^5 (depending on the signal channel) and makes use of the high resolution drift chamber and the hermetic electromagnetic calorimeter of KLOE (see next chapter).

Kaon Interferometry

At DAΦNE a novel phenomenon can be studied for the first time: interference patterns which arise due to the existence of two amplitudes in the initial quantum state of the neutral kaon system being produced in the ϕ decay with charge parity $C = -1$:

$$|i\rangle = \frac{1}{\sqrt{2}}(|K_L, \vec{p}\rangle|K_S, -\vec{p}\rangle - |K_L, -\vec{p}\rangle|K_S, \vec{p}\rangle) \quad (3)$$

The decay intensity I for the decay of the two kaons into the final states f_1 and f_2 is expressed in the following as a function of the time difference $\Delta t = t_1 - t_2$, where t_1 and t_2 are the individual decay times. The amplitude ratios $\eta_i = \langle f_i | K_L \rangle / \langle f_i | K_S \rangle$ contain the relevant parameters which describe CP violation ($\Delta m = m_L - m_S$):

$$I(f_1, f_2; \Delta t) = |\langle f_1 | K_S \rangle \langle f_2 | K_S \rangle|^2 \cdot [|\eta_1|^2 e^{-\Gamma_L \cdot \Delta t} + |\eta_2|^2 e^{-\Gamma_S \cdot \Delta t} - 2|\eta_1||\eta_2| e^{-\Gamma \cdot \Delta t/2} \cdot \cos(\Delta m \Delta t + \Delta \varphi)] \quad (4)$$

One can thus perform a whole spectrum of “kaon-interferometry” experiments⁶) with KLOE by measuring the above decay intensity distributions for different final states f_1, f_2 . In total, one can determine the full set of parameters describing the system³. As an example the decay pattern for

²A statistical error of $1 \cdot 10^{-4}$ can be achieved in ≈ 2 years of data taking at design luminosity.

³also under the assumption of CPT - non-invariance or under a violation of the $\Delta S = \Delta Q$ rule.

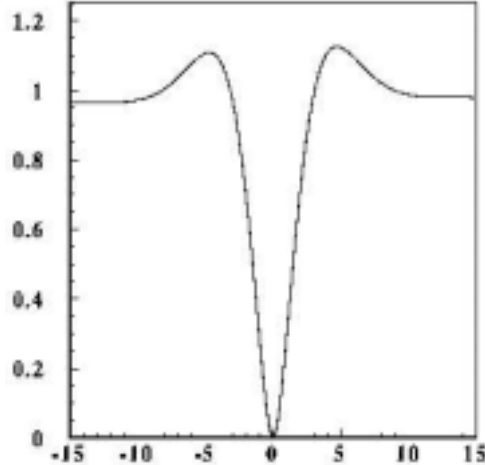


Figure 1: *Decay intensity (a.u.) as a function of $\Delta t/\tau_S$ for the neutral kaon pair decaying into $f_1 = \pi^+\pi^-$, $f_2 = \pi^0\pi^0$. The measurement of this interference patterns allows to extract ϵ'/ϵ .*

$f_1 = \pi^+\pi^-$ and $f_2 = \pi^0\pi^0$ is displayed in figure 1. Small asymmetries in the counting rate for large Δt and for $\Delta t \leq 5\tau_S$ are a measure of $\Re(\epsilon'/\epsilon)$ and of $\Im(\epsilon'/\epsilon)$ respectively. A good experimental vertex resolution for the charged and neutral decays is required to perform such an analysis.

1.2 Hadronic Physics

One of the first physics results of KLOE were obtained from the analyses of the radiative decays of the ϕ into the *scalar mesons* $f_0(980)$ and $a_0(980)$ ⁷⁾. The nature of these narrow states is unclear. Several models have been proposed which try to explain the total width (≈ 50 MeV) and the small $\gamma\gamma$ coupling (≤ 0.6 keV for f_0 , ≈ 0.2 keV for a_0) which is very different from the $q\bar{q}$ expectation. At present the alternative models range from a four quark state $q\bar{q}q\bar{q}$ hypothesis to a kaonic molecule $K\bar{K}$ or models with a large strangeness or even gluonic content (see also in these proceedings ⁸⁾ and references in ⁷⁾). The several models are predicting different branching ratios for the decays $\phi \rightarrow f_0\gamma$, $\phi \rightarrow a_0\gamma$, between $\approx 10^{-4}$ down to $\approx 10^{-6}$. A precise measurement of these decays can hence give a definite answer on the structure of the states.

The reason for studying ϕ radiative decays into the *pseudoscalars* η and η' is twofold. While the measurement of the $BR(\phi \rightarrow \eta'\gamma)$ can help to probe a large strangeness content of the η' , the measurement of the ratio $R_\phi = BR(\phi \rightarrow \eta'\gamma)/BR(\phi \rightarrow \eta\gamma)$ allows one to extract the $\eta - \eta'$ mixing angle ϑ_P ⁹⁾ for which no precise data exist (see also in these proceedings ¹⁰⁾).

In this paper we also present the results of an analysis of the reaction $\phi \rightarrow \pi^+\pi^-\pi^0$, where this final state can be reached either from the direct decay of the ϕ or via the ρ decay ($\phi \rightarrow \rho^\pm\pi^\mp, \rho^0\pi^0$).

Finally we will present a project which aims to measure the hadronic cross section using Initial State Radiation (ISR) events $e^+e^- \rightarrow \gamma\gamma^* \rightarrow \gamma \text{ hadrons}$. The “radiative return” allows us to get a measurement of the hadronic cross section in the Q^2 invariant mass range $2m_\pi^2 \leq Q^2 \leq 1\text{GeV}^2$, even when DAΦNE is operating at a fixed center of mass energy $\sqrt{s} = m_\phi$. The precise knowledge of the hadronic cross section - especially at low energies - is of great interest for an improvement of the theoretical error of the muon anomaly a_μ and for the fine structure constant α_{em} at the Z^0 pole. The hadronic contributions of these fundamental quantities cannot be calculated in the framework of perturbative QCD and are rather obtained through dispersion integrals using as

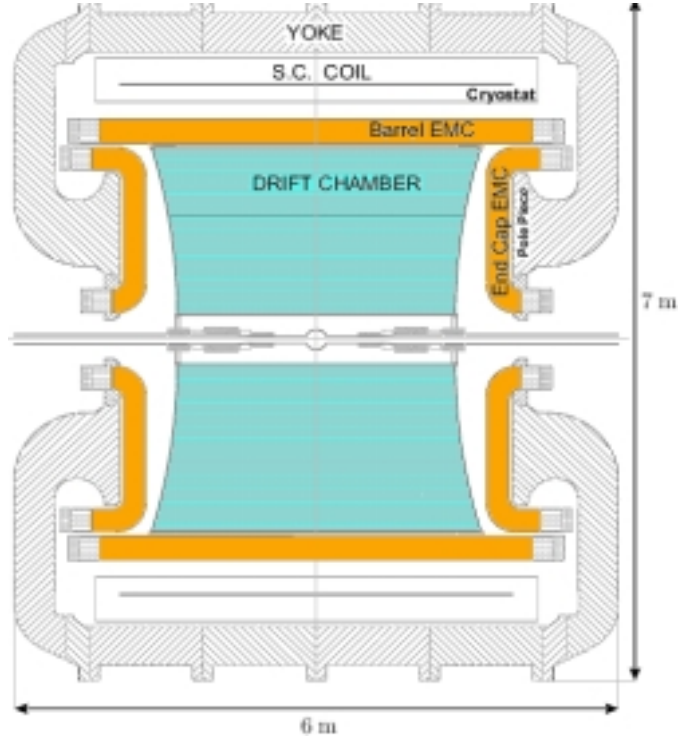


Figure 2: *Side view of the KLOE detector*

input experimental cross section data ¹¹⁾.

2 The KLOE Detector

KLOE ¹²⁾ ¹³⁾ ¹⁴⁾ (see figure 2.) is a typical e^+e^- general purpose detector with solenoid geometry, consisting of a very large helium based *drift chamber* (DC), surrounded by an *electromagnetic calorimeter* (EmC) and a superconducting magnet (0.6 T). The EmC consists of a barrel part and two endcap parts which are surrounding the cylindrical DC; a 98% hermetic coverage of the solid angle is achieved. The beam pipe around the interaction point (I.P.) has a spherical shape (10 cm radius, 500 μm thickness) which allows all K_S 's to decay within this volume ($16K_S$ lifetimes). The DAΦNE beams are collimated close to the I.P. with a set of six permanent quadrupoles which are instrumented with two KLOE tile calorimeters (lead-scintillating tiles). This instrumentation helps to reject γ 's which hit the quadrupoles. The detector acceptance is therefore increased, especially the discrimination of the CP violating decay $K_L \rightarrow \pi^+\pi^-$ from $K_L \rightarrow \pi^+\pi^-\pi^0$.

2.1 Electromagnetic Calorimeter

The EmC has been constructed for a precise detection of low energetic photons (down to ≈ 20 MeV). It has to discriminate $K_L \rightarrow 2\pi^0$ from $K_L \rightarrow 3\pi^0$ decays and to measure the $K_{S,L}$ neutral decay vertex with an accuracy of a few mm . Moreover the calorimeter serves as a fast, unbiased first level trigger. In order to fulfill these requirements, a detector has been constructed in which a matrix of scintillating fibres is embedded in lead. This construction results in an excellent timing

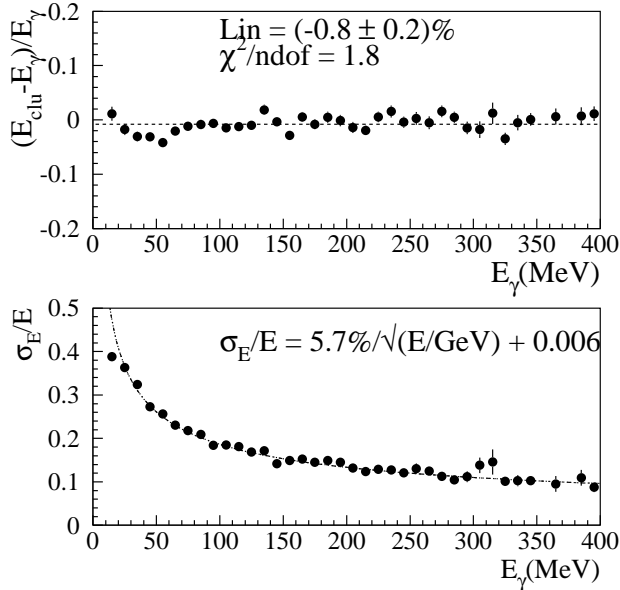


Figure 3: Energy residuals and resolution of the EmC measured with radiative Bhabha events

and very good energy resolution (design values: $\sigma_E/E = 5\%/\sqrt{E(GeV)}$, $\sigma_t = 70ps/\sqrt{E(GeV)}$) with high detection efficiency.

The calorimeter energy calibration is performed using cosmic rays to equalize the cell response, plus Bhabha and $e^+e^- \rightarrow \gamma\gamma$ events to refine the equalization and to set the absolute energy scale. The linearity and the resolution as a function of energy are measured with radiative Bhabha events $e^+e^- \rightarrow e^+e^-\gamma$, where the photon energy is determined by the missing momentum (measured in the DC with the two charged tracks). The linearity is better than 1% over the full energy range (20 – 400 MeV); the energy resolution is found to be $\sigma_E/E = 5.7\%/\sqrt{E(GeV)}$ as can be seen in figure 3. The absolute energy calibration is checked by reconstructing the two-photon invariant mass for $\phi \rightarrow \pi^+\pi^-\pi^0$ events. We find a mass of $134.5MeV/c^2$ ($\sigma = 14.7MeV/c^2$) which is in good agreement with m_{π^0} .

After time equalization with cosmic rays, the time resolution as a function of energy is deduced from radiative Bhabha and ϕ radiative events: $\sigma_t = 54ps/\sqrt{E(GeV)} + 147ns$. Such a good timing performance translates to a neutral vertex resolution (measured with $K_L \rightarrow \pi^+\pi^-\pi^0$ events) of about 1.6 cm.

2.2 Cylindrical Drift Chamber

The KLOE drift chamber ¹⁵⁾ has been designed to optimize the detection and reconstruction of the charged K_S and K_L decays, aiming at a precise determination of the decay vertex ($\approx 1mm$) and a very high momentum resolution of the low momenta tracks⁴. The mean decay path of the K_L is 340 cm; therefore the decay vertices are far from the I.P.. Thus, the chamber dimension, the drift cell shapes, the choice of magnetic field and gas mixture had to be optimized for these demanding requirements. The need for a very large fiducial volume led to a cylindrical drift chamber with 2 m

⁴The momenta of the K_L decays have a spectrum between $\approx 150MeV/c$ and $270 MeV/c$

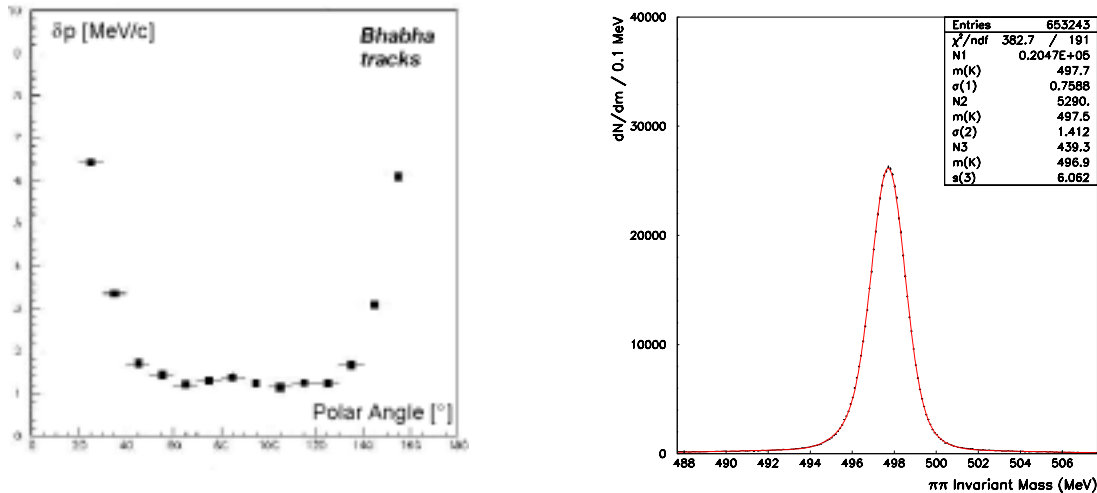


Figure 4: *KLOE* drift chamber performance: In the left plot the momentum resolution for Bhabha events is drawn as a function of the polar angle of the tracks. The right plot shows the K_S invariant mass for $K_S \rightarrow \pi^+\pi^-$ and illustrates the excellent momentum resolution of the DC.

radius and 3.3 m length. The isotropy of the decay products led us to a full stereo geometry of the drift cells which ensures the highest uniformity in filling the sensitive volume. Multiple scattering and photon conversion in the chamber walls are kept under control by employing low Z material (carbon fibre) in the chamber structure and the use of a low mass Helium based gas mixture (90% Helium, 10% Isobutane; $X_0 = 900$ m). The 12582 cells of the chamber are arranged in 58 circular layers. In order to improve the acceptance for the K_S decays, the inner 12 layers consist of $2 \times 2 \text{ cm}^2$ cells while the outer layers are made of $3 \times 3 \text{ cm}^2$ cells. Consecutive layers have stereo angles of opposite sign, with the stereo angles increasing with radius in order to achieve similar cell shapes all over the chamber (stereo angles from 60 mrad to 150 mrad).

Due to the peculiar cell geometry and the drift properties of the Helium based gas mixture, which is not saturated, the calibration of the space-to-time-relation of the DC is important and is done using cosmic ray events. The cell response gives a resolution of $\approx 150 \mu\text{m}$ over most of the drift distance. The momentum resolution for Bhabha events (see figure 4, left) is found to be better than the design value: $\sigma_{p_\perp}/p_\perp \leq 0.4\%$. The very good DC performance is illustrated also in figure 4 (right) where the invariant mass plot of $K_S \rightarrow \pi^+\pi^-$ is shown: $\sigma \approx 1 \text{ MeV}/c^2$.

2.3 Trigger and DAQ

The *KLOE* trigger ¹⁶⁾ is designed to have a high (and almost equal) efficiency for the CP violating K_L decays and to downscale the rates from Bhabhas (≈ 20 kHz), cosmic rays and machine background in order to keep the total DAQ rate below 10 kHz. The first stage (T1) of this 2-level-trigger provides a start to the FEE of the EmC, while the second stage (T2) serves as a validation trigger which stops the readout of the DC TDC's. T1 and T2 are based on the energy and topology of the deposits in the EmC and on the number of hits in the DC.

The DAQ system ¹⁷⁾ handles 23000 FEE channels on an expected 2.5 kHz ϕ decay rate and ≈ 5 kHz properly downscaled background rate. The signal digitization occurs in $2 \mu\text{s}$ and the bandwidth is 50 MByte/s (at 5 kByte/event). The DAQ system has been fully tested at the design

rates.

3 First Data Taking of KLOE

The first stable data taking of KLOE took place in December 1999. The collected integrated luminosity in 2000 is $\int \mathcal{L} dt = 30 pb^{-1}$, corresponding to about 100 million ϕ decays with a peak luminosity $\geq 2 \cdot 10^{31} cm^{-2} s^{-1}$. The 2000 data has been used for the study and calibration of the detector performance (as discussed in the previous chapter), for the preliminary investigation of the systematics for the $\Re(\epsilon'/\epsilon)$ measurement (this chapter) and for the analysis of the radiative decays of the ϕ for which the results will be presented in more detail in the following chapter.

Tagging Strategies

The K_L can be tagged by a clearly identified $K_S \rightarrow \pi^+\pi^-$ event, for which the selection is a charged vertex with 2 tracks of opposite sign reconstructed close to the I.P. ($r \leq 6cm$, $|z| \leq 8cm$) and an invariant mass between 400 and $600 MeV/c^2$. The K_L tagging efficiency is found to be 72%; the background contamination is less than 1% (mainly $\phi \rightarrow K^+K^-$). An important check for the systematics of the K_S sample (and hence for the K_L tagging) is the measurement of the K_S lifetime which is possible by looking at the spatial difference between the secondary vertex $K_S \rightarrow \pi^+\pi^-$ and the e^+e^- primary vertex (luminous region). The measured K_S mean decay path is found to be in agreement with the expectation: $\lambda_S = (5.78 \pm 0.1) \text{ mm}$ [18] [5].

A possibility to tag K_S 's, is given by K_L particles which did not decay within the DC and are stopped in the EmC making a hadronic interaction (“ K_L crash”). The excellent time resolution of the EmC is used to look for a neutral cluster within a velocity interval $0.195 \leq \beta \leq 0.245$ and with a cluster energy $E_{cluster} \geq 100 \text{ MeV}$. The K_S tagging efficiency (percentage of identified K_S 's via the K_L crash method) is 31%.

Fiducial Volume

An important issue for the measurement of the double ratio R is the control of the alignment of the K_L fiducial volume ($30cm \leq r \leq 150cm$, $|z| \leq 125 \text{ cm}$). Since the vertex resolution for the $K_L \rightarrow \pi^+\pi^-$ and $K_L \rightarrow \pi^0\pi^0$ decay differs, a systematic error is introduced which is in the order of $\delta R = 4 \cdot 10^{-4}$ when the boundary of the fiducial volumes are shifted by $\delta r_{FV} = 5mm$. A control of the alignment is given by events with a reconstructable charged *and* neutral vertex, like e.g. $K_L \rightarrow \pi^+\pi^-\pi^0$. For those decays the residuals between the reconstructed charged ($\pi^+\pi^-$) and neutral ($\pi^0 \rightarrow \gamma\gamma$) vertices have been measured and were found to be below few millimeters.

Selection of $K_L \rightarrow \pi^+\pi^-$ events

The selection of the CP violating channel $K_L \rightarrow \pi^+\pi^-$ is based on the very good momentum resolution of the KLOE DC. In figure 5 (left) the two dimensional plane “missing momentum”⁵ vs. missing mass” is shown for charged K_L decays in which the K_L had been tagged before by $K_S \rightarrow \pi^+\pi^-$. The charged decay $K_L \rightarrow \pi^+\pi^-\pi^0$ and the semileptonic channels $K_L \rightarrow \pi\mu\nu_\mu$ and $K_L \rightarrow \pi e\nu_e$ are nicely separated from each other. Applying a loose cut ($p_{miss} \leq 10 MeV/c$, $|M_{miss}^2| \leq (70 MeV/c^2)^2$), the first CP violating events could be identified for which the mass distribution is shown in figure 5 (right).

⁵the missing momentum is evaluated in the pion mass hypothesis from the two charged tracks

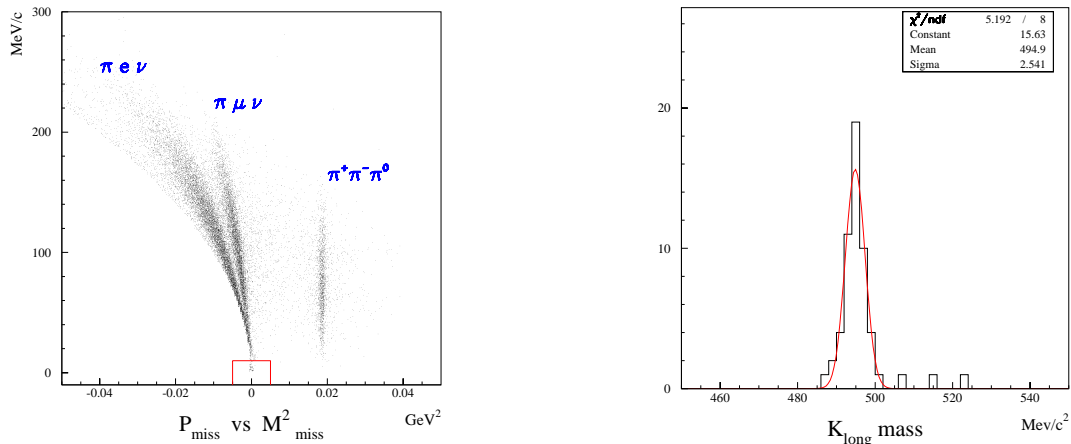


Figure 5: The CP violating events $K_L \rightarrow \pi^+\pi^-$ can be selected in the two dimensional plane missing momentum vs. missing mass at $p_{miss} = 0, M_{miss}^2 = 0$ (left plot). The mass distribution for the selected events (box, left) are shown in the right plot.

4 Hadronic Physics at KLOE

In this chapter we will report on the first KLOE physics results which were obtained in the analysis of the radiative decays of the ϕ and the decay $\phi \rightarrow \pi^+\pi^-\pi^0$ (1999 data set ⁶). The statistical errors for the BR measurements are already comparable to the precision obtained at the Novosibirsk VEPP-2M collider (see ⁷) and references there).

4.1 Radiative ϕ decays

4.1.1 $\phi \rightarrow f_0\gamma$ with $f_0 \rightarrow \pi^+\pi^-$

The signature for this decay are two charged tracks from the I.P. and a prompt photon. Two other processes lead to the same $\pi^+\pi^-\gamma$ final state: Initial State Radiation (ISR) in which the photon is emitted by the incoming e^- or e^+ and Final State Radiation (FSR) in which the γ is emitted by one of the pions. The latter process gives rise to an interference with the signal for which the sign of the interference term is still unknown.

The selected $\pi^+\pi^-\gamma$ sample is hugely contaminated with radiative Bhabhas; a maximum likelihood method for an efficient $\pi - e$ separation has therefore been developed. For the identification of the signal $f_0 \rightarrow \pi^+\pi^-$, the Q^2 spectrum of the pion pair is used. In the region $Q^2 < 0.84\text{GeV}^2$ - where only ISR and FSR contribute to the final state - the experimental spectrum has been fitted with the theoretical event generator ²²) and then extrapolated into the signal region ($Q^2 > 0.84\text{GeV}^2$). An excess of (35 ± 160) events is found which has been used to set an upper limit on the branching ratio: $BR(\phi \rightarrow f_0\gamma \rightarrow \pi^+\pi^-\gamma) < 1.64 \cdot 10^{-4}$ at 90% CL. In figure 6 the measured Q^2 spectrum is compared with the MC simulation (ISR and FSR only); both of them are in good agreement over the whole Q^2 range.

⁶The results are preliminary. A complete analysis of the systematic effects as well as the analysis of the year 2000 data is going on. At present (Oct. 2000) the collected integrated luminosity *per week* is considerably higher than the full 1999 data set for which results are presented here.

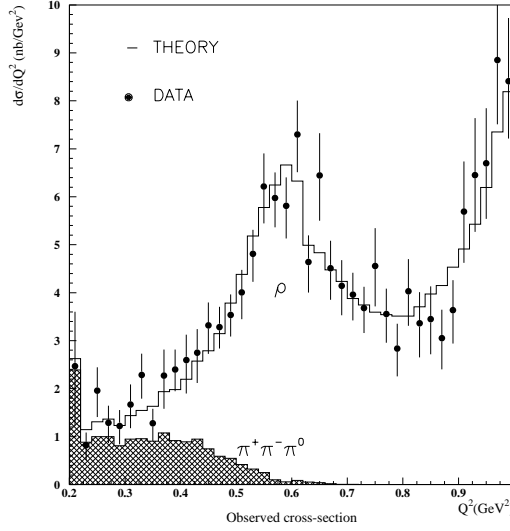


Figure 6: *Experimental cross section as a function of Q^2 for $\pi^+\pi^-\gamma$ events ($45^\circ \leq \Theta \leq 135^\circ$ for $\Theta_\pi, \Theta_\gamma$). The data is compared with the MC simulation under the assumption of pure ISR and FSR. At the given statistical resolution no signal $f_0 \rightarrow \pi^+\pi^-$ can be seen.*

4.1.2 $\phi \rightarrow f_0\gamma$ with $f_0 \rightarrow \pi^0\pi^0$

The signature for the neutral decay of the $f_0(980)$ are 5 prompt photons in the EmC and no charged particle tracks in the DC. The main background comes from the non-resonant reaction $e^+e^- \rightarrow \omega\pi^0$ ($S/B = 0.5$); other background processes are $\phi \rightarrow \rho\pi^0$ and $\phi \rightarrow a_0\gamma \rightarrow \eta\pi^0\gamma$ with only photons in the final state. A two-step kinematic fit (with and without mass constraints) and suitable topological cuts are applied to reduce the background. The final detection efficiency is $\approx 40\%$. In a data sample of $1.8pb^{-1}$ (307 ± 18) $\pi^0\pi^0\gamma$ events have been selected; the expected background rate (estimated from Monte Carlo) is (112 ± 11) . We find the following branching ratio for the neutral decay of the f_0 : $BR(\phi \rightarrow f_0\gamma \rightarrow \pi^0\pi^0\gamma) = (0.80 \pm 0.09_{stat} \pm 0.06_{syst}) \cdot 10^{-4}$. The same data sample has been used to select $\omega\pi^0$ events. Therefore different topological cuts have been applied resulting in (529 ± 23) accepted events at a background contamination of (93 ± 10) (estimated by Monte Carlo); we find the cross section at the ϕ mass for this process as: $\sigma_{e^+e^- \rightarrow \omega\pi} = (0.67 \pm 0.04_{stat} \pm 0.05_{syst})nb$.

4.1.3 $\phi \rightarrow a_0\gamma$ with $a_0 \rightarrow \eta\pi^0 \rightarrow 4\gamma$ ($\eta \rightarrow \gamma\gamma$)

Events are selected with a signature of 5 prompt photons and the absence of a charged track in the detector. The main background process is the decay discussed in the previous subchapter $\phi \rightarrow f_0\gamma \rightarrow 5\gamma$ ($S/B = 0.1$) and $\phi \rightarrow \eta\gamma$ ($\eta \rightarrow \pi^0\pi^0$). A constrained kinematic fit and topological cuts are applied to reduce this background. There have been (74 ± 9) $\eta\pi^0\gamma$ events selected (23% detection efficiency) with a background of (21 ± 6) events (MC estimate), corresponding to a branching ratio $BR(\phi \rightarrow a_0\gamma \rightarrow \omega\pi^0\gamma) = (0.77 \pm 0.15_{stat} \pm 0.10_{syst}) \cdot 10^{-4}$.

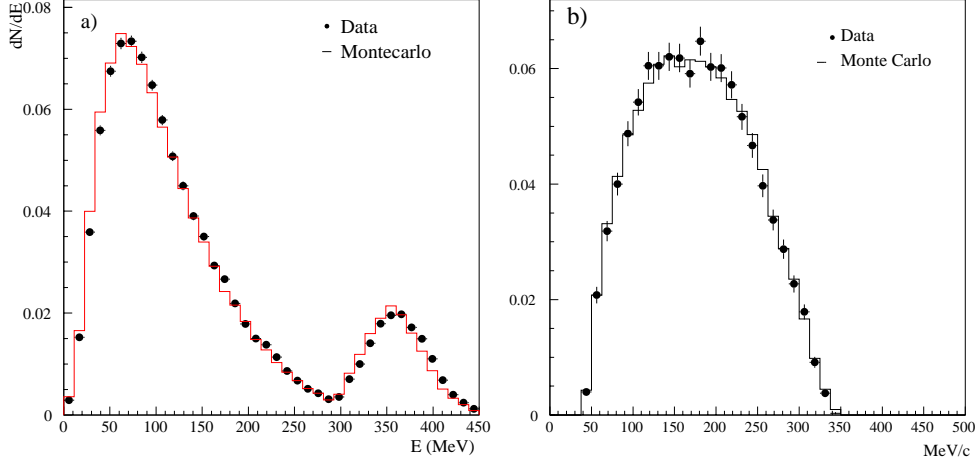


Figure 7: Comparison Data - Monte Carlo for the $\phi \rightarrow \eta\gamma$ sample: photon energy spectrum in 7γ events (left plot); charged pions momentum spectrum in $\pi^+\pi^-3\gamma$ events (right).

4.1.4 $\phi \rightarrow \eta\gamma, \phi \rightarrow \eta'\gamma$

We are studying four processes, giving rise to two different final states:

$$\phi \rightarrow \eta(\eta')\gamma \rightarrow \pi^+\pi^-\pi^0(\pi^+\pi^-\eta)\gamma \rightarrow \pi^+\pi^-3\gamma$$

and

$$\phi \rightarrow \eta(\eta')\gamma \rightarrow \pi^0\pi^0\pi^0(\pi^0\pi^0\eta)\gamma \rightarrow 7\gamma$$

We use both decay chains to construct separately the ratio $R_\phi = BR(\phi \rightarrow \eta'\gamma)/BR(\phi \rightarrow \eta\gamma)$ in which most of the selection efficiencies (e.g. trigger efficiency) and all the normalisation efficiencies (luminosity, ϕ cross section) cancel.

The $\phi \rightarrow \eta\gamma$ is the main background for the rare corresponding $\phi \rightarrow \eta'\gamma$ decay (see Table 1), but - since the η decay can be selected almost background free on a simple topological basis - they constitute also an important control channel for testing the systematics. Comparison between data and Monte Carlo (see figure 7) show a very good agreement for the η channel.

The event selection is based on a first level kinematic fit with mass constraints, followed by a selection which uses the χ^2 probability for the hypotheses of an event to be either $\eta\gamma$ or $\eta'\gamma$ like. After this procedure we are left with (21 ± 4.6) η' events in the $\pi^+\pi^-3\gamma$ final state and with $6_{-2.2}^{+3.3}$ in the 7γ final state with less than one expected background event at 90% CL. This is the first observation of the $\phi \rightarrow \eta'\gamma \rightarrow 7\gamma$ decay chain. Using the number of selected η and η' events, the efficiencies evaluated by Monte Carlo and the intermediate states BR's as given by PDG ⁵⁾ we evaluate the ratio $R_\phi = (7.1 \pm 1.6_{stat} \pm 0.3_{syst}) \cdot 10^{-3}$ or $BR(\phi \rightarrow \eta'\gamma) = (8.9 \pm 2_{stat} \pm 0.6_{syst}) \cdot 10^{-5}$. This result has the same level of accuracy as the current world average. Using a formula proposed by Bramon ¹⁹⁾ we can use this value of R_ϕ to extract the $\eta - \eta'$ mixing angle: $\vartheta_P \simeq -19^\circ$. The value of the $BR(\phi \rightarrow \eta'\gamma)$ disfavors models with large gluonium admixtures of the η' .

4.2 $\phi \rightarrow \pi^+\pi^-\pi^0$

$\pi^+\pi^-\pi^0$ events are selected requiring a prompt vertex with two opposite sign tracks in the DC and two prompt photons in the EmC. Cuts on the opening angle of the tracks and on the two photons are applied for background subtraction. The data has been analyzed by means of Dalitz

Parameter	Fit result	PDG result
$M(\rho_0)$ (MeV)	776.1 ± 1.0	776.0 ± 0.9
ΔM (MeV)	-0.5 ± 0.7	0.1 ± 0.9
$\Gamma(\rho)$ (MeV)	145.6 ± 2.2	150.9 ± 2.0
$A(\text{direct term})/A(\rho\pi)$	0.10 ± 0.01	$-0.15 \div 0.11$
$\text{phase}(\text{direct term})-\text{phase}(\rho\pi)$	$(114 \pm 12)^\circ$	

Table 2: Results of the fit to the $\pi^+\pi^-\pi^0$ Dalitz plot compared with the PDG values.

plots. The Dalitz plot (binned in 8×8 MeV squares and corrected for the efficiency) is fitted to a model of $\pi^+\pi^-\pi^0$ production including the following terms:

- $A_{\rho\pi}$ is the $\rho\pi$ amplitude given by the sum of the three ρ states, each described by a Gounaris-Sakurai parametrization. Free parameters are the ρ masses and the width;
- A_{direct} is the direct term contribution given by a complex number. The modulus is normalized in such a way that a value equal to 1 corresponds to a direct term equal to the $\rho\pi$ term.
- $A_{\omega\pi}$ is the $\omega\pi$ term, where mass and width of the ω are fixed to the PDG values, and only a complex amplitude (modulus and phase) is left free.

The fitting function is then given by: $f(X, Y) = |\vec{p}^+ \times \vec{p}^-|^2 \cdot |\mathbf{A}_{\rho\pi} + \mathbf{A}_{\text{direct}} + \mathbf{A}_{\omega\pi}|^2$ (X and Y are two Dalitz variables). In Table 2 the results of the fit are shown and compared with PDG values.

First, we observe a sizeable direct term (about 10 % of the $\rho\pi$ amplitude) with a phase respect to $\rho\pi$ not too far from 90° . We remark that this is the first observation of this decay. Second we find values of the ρ line-shape parameters which are in agreement with PDG ⁵⁾ numbers. Furthermore the mass difference between the neutral and the charged ρ 's is compatible with 0; hence no isospin violation is observed.

4.3 Measurement of the hadronic cross section

At KLOE we plan to perform a high precision measurement of the hadronic cross section below the ϕ mass *using ISR events: $e^+e^- \rightarrow \gamma\gamma^* \rightarrow \gamma \text{ hadrons}$* ^{20) 21)}. This measurement can significantly reduce the theoretical error of a_μ and $\alpha_{em}(m_Z^2)$ (see motivation in chapter 1). We are concentrating on the measurement of the hadronic cross section for the reaction $e^+e^- \rightarrow \rho\gamma \rightarrow \pi^+\pi^-\gamma$ as a function of Q^2 ($\pi\pi$ invariant mass) which allows us to extract the cross section of the dominating hadronic process at low energies: $\sigma(e^+e^- \rightarrow \pi^+\pi^-)$ ⁷⁾. We would like to stress that the method to use ISR events (while DAΦNE is operating at a fixed beam energy) is a complementary approach to the conventional energy scan. In the case of the ISR method, many systematic effects (e.g. luminosity, beam energy measurement) enter only *once*, while they have to be determined for *each* energy step in the case of a variable beam energy.

An important issue for this measurement is the suppression of FSR. Monte Carlo simulations ²²⁾ showed that a restriction of the photon polar angle ($10^\circ \leq \Theta_\gamma \leq 40^\circ$) and energy ($E_\gamma \geq 50$ MeV) suppresses FSR below 1%.

From a data sample of $1.8pb^{-1}$ we selected $\pi^+\pi^-\gamma$ events like described in section 4.1.1 (search

⁷⁾The $\pi^+\pi^-\gamma$ cross section is enhanced due to the coupling of the virtual photon to the ρ in the case of ISR: $e^+e^- \rightarrow \gamma^*\gamma \rightarrow \rho\gamma \rightarrow \pi^+\pi^-\gamma$

for $f_0 \rightarrow \pi^+\pi^-$) and we reduced the huge radiative Bhabha contamination (maximum likelihood method). We find a good agreement of the experimental Q^2 distribution with the Monte Carlo simulation, proving that the experimental techniques (detector performance, selection criteria) and the theoretical description are good. The final goal to reduce δa_μ^{hadr} to $\approx 1.5 \cdot 10^{-10}$ in the energy range below the ϕ resonance (the main contribution coming from the $\pi^+\pi^-$ cross section) requires an integrated luminosity of $\approx 100pb^{-1}$.

5 Prospects for year 2001

The KLOE detector expects to take data in 2001 and collect an integrated luminosity of $\approx 200pb^{-1}$. These data will be used for a preliminary check of systematics for the determination of the CP direct violation parameter and to measure the majority of the non CP physics quantity. The milestone is also to maintain KLOE at the high level of efficiency as in year 2000.

6 Talks by LNF authors in year 2000

- I. Sfiligoi, Data Handling in KLOE, Computing in High Energy and Nuclear Physics (CHEP 2000), Padova, Italy
- S. Giovannella, Frascati, Observation of the $\phi \rightarrow \pi^0 \pi^0 \gamma$ decay at KLOE, X EURO-DAPHNE Collaboration Meeting - Granada, Spain
- G. Lanfranchi, Frascati, Search for $\phi \rightarrow \eta \pi^0 \gamma$, $\eta \rightarrow 3\pi^0$ decay with the KLOE detector at DAPHNE, X EURO-DAPHNE Collaboration Meeting - Granada, Spain
- G. Capon, Frascati, Physics programs and initial data at Daphne, Orsay
- L. Passalacqua, Frascati, Phi factories, XXVIII International Meeting on Fundamental Physics, Sanlucar de Barrameda, Cadiz, Spain
- M. Moulson, Frascati, The KLOE Experiment at DAFNE, Seminar at Brookhaven National Lab, Upton, NY USA
- S. Miscetti, Frascati, First performances of the KLOE e.m. calorimeter at DAFNE, La Biodola, Elba
- P. Valente, Frascati, The KLOE drift chamber, La Biodola, Elba
- P. De Simone, Frascati, KLOE at DAFNE, CIPANP 2000, Quebec City, Canada
- F. Bossi, Frascati, KLOE first results, Intern. Conference on CP violation in Ferrara
- I. Sfiligoi, Frascati, KID, KLOE Integrated Dataflow, VII Int. Workshop on Advanced Computing and Analysis Techniques in Physics Research, Fermilab
- C. Bloise, Frascati, KLOE first results, Heavy Quark at fixed target, Rio de Janeiro
- A. Denig, Frascati, KLOE: Status and first Results, Stara Lesna, High Tatra Mountains (Slovakia)
- P. Campana, Frascati, KLOE status and first results, Seminar at DESY

7 KLOE papers in year 2000

- KLOE Collaboration, NOVEL DAQ and Trigger Methods for the KLOE experiment, hep-ex/0006039
- KLOE Collaboration, KLOE first results on hadronic physics, hep-ex/0006036
- KLOE Collaboration, First results from $\phi \rightarrow K_L K_S$ decays with the KLOE, hep-ex/0006035
- KLOE Collaboration, The KLOE experiment at DAFNE, Nucl. Phys. A 663 (2000) 1103
- KLOE Collaboration, The KLOE experiment at DAFNE, Proc. of Chiral Dynamics 2000, Newport News (Virginia)
- KLOE Collaboration, KLOE at DAFNE, Proc. of CIPANP 2000, Quebec City, Canada
- KLOE Collaboration, Calibration and reconstruction performances of the KLOE e.m. calorimeter,

Proc.IX int. conf. on calorimetry in part. phys. Annecy, Oct 9-14
C. Avanzini et al., Test of a small prototype of the KLOE drift chamber in a magnetic field, Nucl. Inst. Meth. A449 (2000) pp. 237-247

References

1. C.Milardi: *Proc. DAΦNE'99 Frascati Physics Series XVI* (1999) 75;
2. J.Lee-Franzini: **The Second DAΦNE Physics Handbook** (1995) 761;
3. The NA48 Collaboration: *Phys. Lett. B* **465** (1999) 335;
4. The KTeV Collaboration: *Phys. Rev. Lett.* **83** (1998) 22;
5. The Particle Data Group: *Europ. Phys. Jour.* **C 15** (2000) 1;
6. C.D.Buchanan et al.: *Phys. Rev. D* **45** (1992) 4088;
7. The KLOE collaboration: *KLOE first Results on Hadronic Physics: Proc. XXXth Int. Conf. on High Energy Physics, Osaka, Japan* (2000) ;
8. R. Escribano: *these proceedings* (2000) ;
9. J.L.Rosner: *Phys. Rev. D* **27** (1983) 1101;
10. A. Bramon: *these proceedings* (2000) ;
11. S.Eidelman, F.Jegerlehner: *Z.f.Physik C* **67** (1995) 585;
12. The KLOE collaboration: *A Gen. Purp. Detect. for DAΦNE LNF-92/019* (1992) ;
13. The KLOE collaboration: *The KLOE Detet.; Techn. Prop. LNF-93/002* (1993) ;
14. The KLOE collaboration: *Novel DAQ and Trigger Methods for the KLOE Experiment: Proc. XXXth Int. Conf. on High Energy Physics, Osaka, Japan* (2000) ;
15. The KLOE collaboration: *The KLOE Drift Chamber LNF-94/028* (1993) ;
16. The KLOE collaboration: *The KLOE Trigger System LNF-96/043* (1996) ;
17. The KLOE collaboration: *The KLOE Data Acquisition System LNF-95/014* (1995) ;
18. The KLOE collaboration: *First Results from $\phi \rightarrow K_L K_S$ Decays with the KLOE Detector: Proc. XXXth Int. Conf. on High Energy Physics, Osaka, Japan* (2000) ;
19. A.Bramon: *Europ. Phys. Jour.* **C 7** (1999) 271;
20. S.Spagnolo: *Europ. Phys. Jour.* **C 6** (1999) 637;
21. A.Denig: *Proc. DAΦNE'99 Frascati Physics Series XVI* (1999) 569;
22. S.Binner et al.: *Phys. Lett. B* **459** (1999) 279;

ICARUS

P. Picchi (Resp.), M. Santoni (Tecn.)

1 Introduction.

During the year 2000 the activity of the LNF group in the framework of the ICARUS project was devoted to *R&D* on aspects of the detector not yet fully defined. We developed those activities in parallel with the industrialization phase of the T600 module which took successfully pace in Pavia.

We studied the problem of the trigger and the absolute time determination of the events in the in the ICARUS LAr-TPC. The most natural way is to exploit the prompt signal due to scintillation light in liquid Argon.

2 Successful tests of scintillation light (128 nm) in liquid Argon.

This test was performed with a MgF_2 window and PM in vacuum. Figures illustrate the results showing a stopping muon (Figure 1) used in this study. The double light pulse, from muon and electron from muon decay (Figure 2), and a precision measurement of the muon lifetime (Figure 3) as a cross check that all systematics are well understood. This measurement took about 2 months of data taking and required the analysis of 100,000 events.

3 Further tests of scintillation light in liquid argon.

Being practically impossible to find commercial large Photomultiplier with MgF_2 windows, sensitive to 128 nm light which work at liquid argon temperature, during the year 2000 we purchased some PM (10" EMI 1864) which works at liquid argon temperature (87K). This kind of tube is not sensitive to 128 nm light so wave shifting is necessary.

We tried various ways to deposit a wave shifter that could stand the thermal contractions due to the LAr temperature. A spray of aspirin on a MgF_2 layer did not work because it was found that aspirin dissolves very easily in liquid argon. This was verified with a study under a microscope of the window, before and after operating the PM. Care was taken in this study to avoid Cerenkov light, by having the PM looking down onto the liquid argon volume.

More test were performed with P-terphenyl as wave shifter. A first MgF_2 layer was deposited on the PM to provide a structure holding on firmly to the glass. The P-terphenyl is evaporated on the MgF_2 layer. Then, a protective MgF_2 layer is added to avoid washing out of the P-terphenyl by liquid argon.

Mechanically the system seemed to behave in a very stable way when confronted with fast temperature gradients. Not so satisfactory results were reached concerning the behaviour in liquid Argon (poor stability in time and low quantum efficiency).

A new set of PM was purchased early 2001 with a sand-blasted window which proved thøbe very effective to mechanically hold the wave shifter in tests dove in Pavia.

We developed a new method to deposit the wave shifter: first it is diluted in a chemical solvent, then the solution is sprayed on the PM window; when the solvent evaporates the wave-shifter is effectively trapped in the sand-blasted surface of the PM window. We tried this PM in liquid Argon obtaining enough quantum efficiency ($\simeq 8\%$) and good stability in time (several months with no changes).



Figure 1: *Picture of a stopping μ^+ event, showing the decay into a positron. This type of event gives a characteristic double light pulse, one associated with the incoming muon, the other, on average $2.2\mu\text{s}$ later, associated with the decay into e^+ . Both the charge collection and the charge induction views are showed here. Note the visible time delay between the muon stopping point and the electron starting point.*

We are now performing a test were we use two PM's to trigger the LAr-TPN by means of the scintillation light. This should provide coincidences that could allow complex trigger-patterns with high efficiency. We will test this layout to obtain a cleaner sample of stopping muon. The large size of the EMI tubes, will allow for a larger data rate, which will make it possible to study rapidly small systematics of the method. This *R&D* programme will therefore continue through the year 2001.

References

1. F. Arneodo *et al*, Nucl. Inst. and Meth. **A449**, 36 (2000).
2. F. Arneodo *et al*, Nucl. Inst. and Meth. **A449**, 42 (2000).
3. F. Arneodo *et al*, Nucl. Inst. and Meth. **A449**, 147 (2000).
4. F. Arneodo *et al*, Nucl. Inst. and Meth. **A455**, 376 (2000).

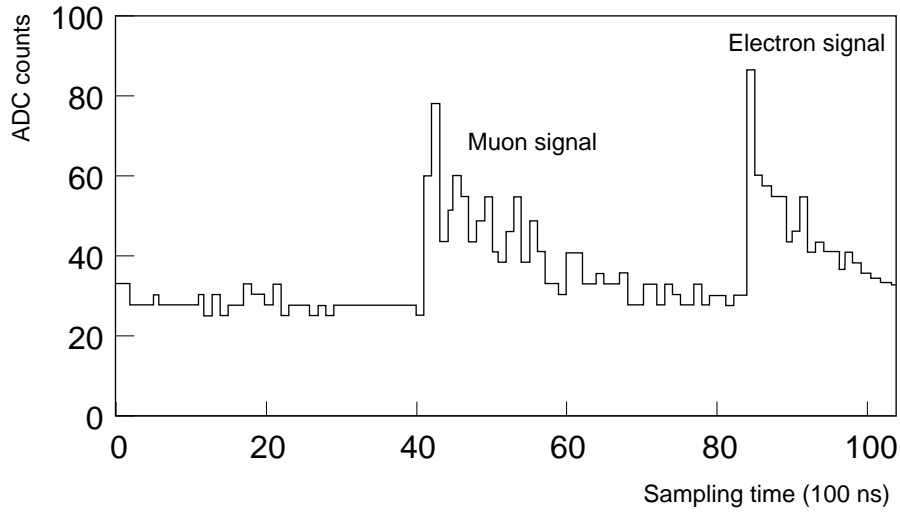


Figure 2: *Flash ADC output showing the double pulse structure characteristic of a stopping muon in the liquid argon, decaying about 2 μ s later into a positron.*

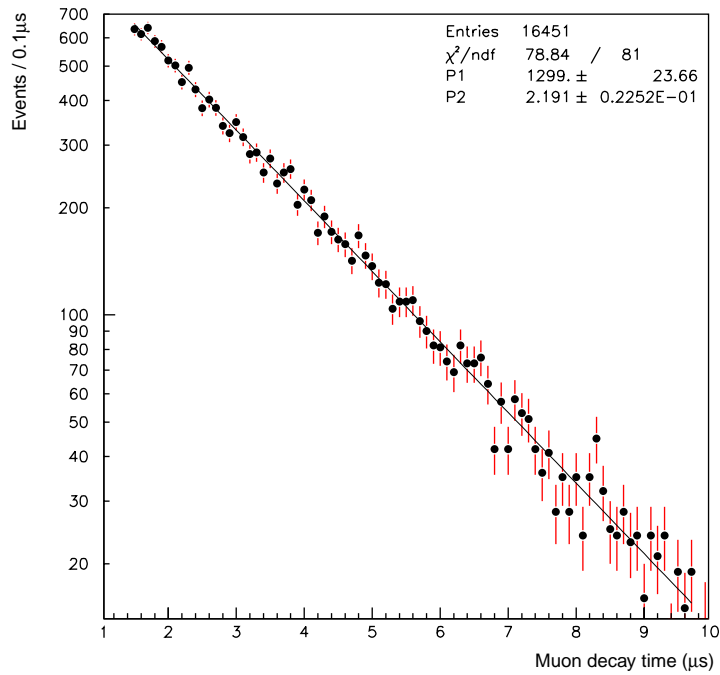


Figure 3: *Measurement of the muon lifetime, from light information in an ICARUS 50 litre prototype chamber ($t_{1/2} = 2.191 \pm 0.025 \mu$ s). For the first time this measurement could be made in an experiment without background.*

MACRO

G. Battistoni (Ass.), H. Bilokon, C. Bloise, M. Carboni, V. Chiarella
C. Forti, E. Iarocci (Ass.), A. Marini, A. Mengucci(Tecn.), V. Patera (Ass.)
F. Ronga, A. Sciubba (Ass.), M. Spinetti (Resp. Naz.)

Collaboration with: University of Boston, Caltech, Drexel, Indiana, Michigan and Texas A&M, Infn Sections of Bari, Bologna, Lecce, Napoli, Pisa, Roma, Torino, LNGS, University of L'Aquila and University of Oudja.

1 Introduction

MACRO (Monopole, Astrophysics, and Cosmic Ray Observatory) is a large area underground detector optimized to search for the supermassive magnetic monopoles predicted by Grand Unified Theories (GUTs).

The detector allows to perform also observations relevant to particle physics, astrophysics, and cosmic ray physics. These include different studies of the high energy underground muon flux relevant to primary cosmic ray composition and origin, search for low energy gravitational collapse neutrinos, high energy neutrino astronomy and study of atmospheric neutrinos.

In order to provide redundant and complementary particle identification for rare events like monopoles, MACRO employs three different detector types: liquid scintillation counters, gas filled limited streamer tubes, and Lexan/CR39 nuclear track-etch detectors. The active components (the scintillators and the streamer tubes) measure particle tracks with resolutions of $\sim 0.2^\circ$ in angle, ~ 1 cm in position, ~ 0.5 ns in time of flight and ~ 6 MeV in energy loss (for muons). The passive nuclear track detector provides additional information for heavy ionizing particles.

The MACRO detector has dimensions $76.6 \times 12 \times 9.3$ m³, divided longitudinally in six supermodules and horizontally in a lower part (4.8 m high, with absorbers interleaved between tracking planes) and in an upper part (4.5 m high). The total acceptance for isotropic flux is about 104 m⁻² sr⁻¹. The MACRO detector started in February 1989 taking data with one supermodule, has been fully implemented in August 1995 and since then it is running in its final configuration. In December 2000, the data taking was completed. Hereafter are reported some results reached in the years 1999-2000.

2 Magnetic monopoles

GUT monopoles are normally expected to have relatively low velocities: around $10^{-4}c$ if gravitationally bound to the solar system, $10^{-3}c$ if bound to the galaxy and greater than $10^{-2}c$ for extragalactic origin. Therefore MACRO has been designed to identify monopole in the whole β range.

Since 1989 up to December 2000 data have been collected in different detector configurations. Several limits on monopole flux have been derived independently with the three detectors and with various analysis techniques. The limit for relativistic monopoles has been particularly improved intensifying the track-etch development. These limits have been combined all together taking properly into account time and spatial overlapping. The obtained limit is:

$$1.8 \div 2.6 \cdot 10^{-16} \text{cm}^{-2} \text{sr}^{-1} \text{s}^{-1} \quad \text{for} \quad 10^{-4} < \beta < 1$$

In the whole β range, the obtained limit is particularly important, being well below the Parker bound ($\sim 10^{-15} \text{cm}^{-2} \text{sr}^{-1} \text{s}^{-1}$) as deduced from the survival of the galactic magnetic field.

Moreover in the β range $10^{-4} < \beta < 10^{-2}$ is the best limit in the literature. This limit also means that a monopole contribution to dark matter cannot be larger than about 20%.

3 Atmospheric neutrinos

In this field, the results obtained concern the update of statistics up to December 2000 for the standard analysis and the addition of new analysis for extracting more relevant experimental informations from data. In general the whole results obtained by Macro indicate that the anomaly observed in 1993 on the atmospheric neutrino flux (presented at Taup 1993) has the most probable interpretation in a $\nu_\mu - \nu_\tau$ oscillation. Results are based on three event categories:

1. events with through-upgoing muons induced by neutrino interactions in the rock below the detector ($E_{median} \approx 40$ GeV, 863 events) identified through the time of flight between 2-3 scintillator layers (rejection factor about 10^{-7});
2. events induced by neutrino interactions in the lower and dense part of the detector (about 3.5 Kton) with an upgoing muon identified through the time of flight between the upper 2 scintillator layers ($E_{median} \approx 5$ GeV, 154 events);
3. events with muons stopping in the lower and dense part of the detector induced both by upgoing neutrinos interacting in the rock below the detector (about 50%) and by downgoing neutrinos interacting in the lower and dense part of the detector (about 50%); these events are selected through topological cuts ($E_{median} \approx 4$ GeV, 262 events).

From the events of the first category the angular distribution of the atmospheric neutrino flux has been derived as a function of the zenith angle (see Fig. 1). This result has to be compared with the MC predictions based on the Bartol flux calculations. The theoretical uncertainty on this flux is $\pm 17\%$, slightly dependent on the angle. In Fig. 1 the simulated flux is shown with and without a $\nu_\mu - \nu_\tau$ oscillation effect: respectively, the probabilities to be the right interpretation are 66% and 0.2%. The best gives the following parameters:

$$\Delta m^2 = 2.5 \cdot 10^{-3} \text{ eV}^2; \quad \sin^2 2\theta = 1.$$

Coherently with these parameters and with the involved neutrino energies, the angular distribution of the second event categories shows a uniform deficit of about 50%. The distribution of the third event category shows a uniform deficit: being this category a mixture of upgoing and downgoing neutrinos the deficit must be only about 3/4 of the full flux. More precisely, the observed deficits on the three event category are the following:

1. $R_1 = 0.721 \pm 0.026$ (*stat*) ± 0.043 (*syst*) ± 0.123 (*theor*)
2. $R_2 = 0.54 \pm 0.04$ (*stat*) ± 0.06 (*syst*) ± 0.14 (*theor*)
3. $R_3 = 0.70 \pm 0.04$ (*stat*) ± 0.07 (*syst*) ± 0.18 (*theor*)

to be compared, in presence of oscillations using the above quoted parameters, with:

1. $R'_1 = 0.73$
2. $R'_2 = 0.59$
3. $R'_3 = 0.75$

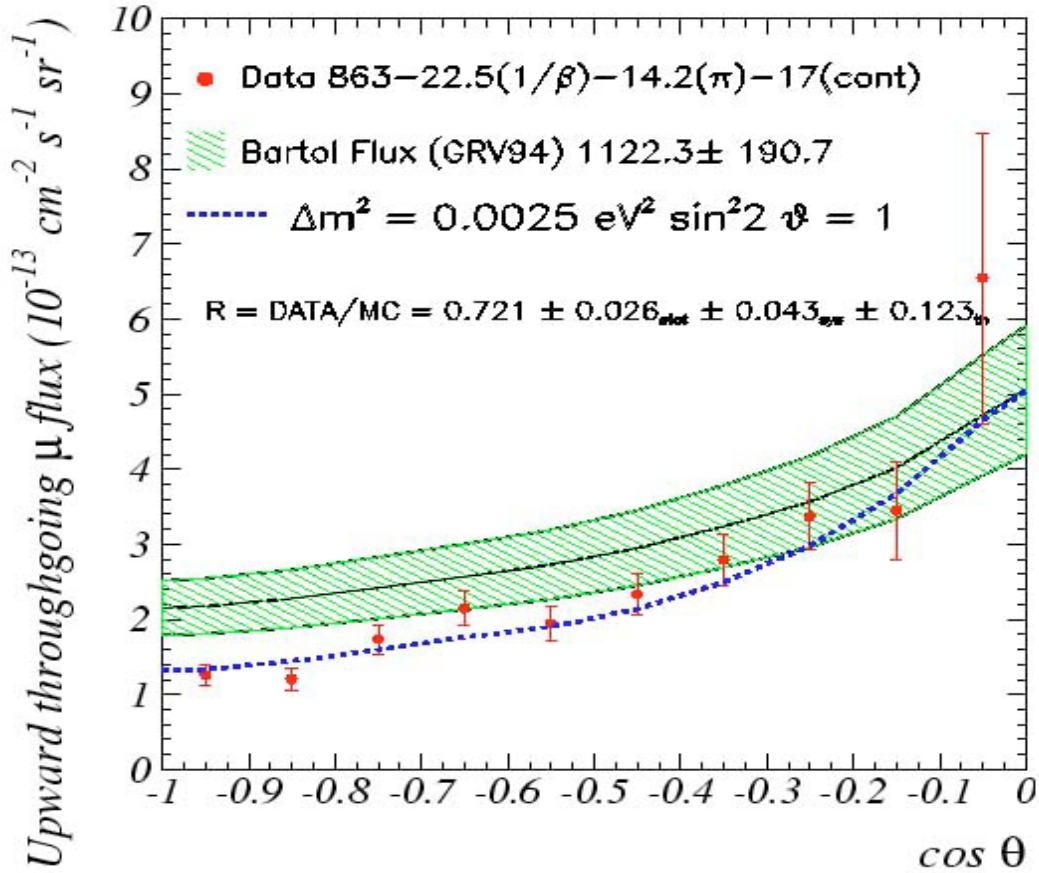


Figure 1: Zenith angle distribution of upgoing muon events. Data (full dots) are compared with the expected atmospheric neutrino flux without the effects of oscillations (continuous line) and with the effects of oscillations (dashed line). The dashed area represents the theoretical uncertainty on the expectations, slightly dependent with the angle.

Moreover, another sign of the internal coherence of these results is to look to the ratio between the two ratios of points 2) and 3). In this case, most of the theoretical uncertainties are cancelled. The measured value of this ratio is $R=0.59 \pm 0.060$ (stat) to be compared with 0.59 ± 0.046 expected in presence of oscillations and with $R=0.76 \pm 0.059$ expected without oscillations. This last value has a 2% probability of agreement with the data. The angular distribution of this double ratio is shown in Fig. 2.

The internal coherence between all these results gives a good support to the oscillation hypothesis.

Another important result has been achieved comparing the data with the $\nu_\mu - \nu_\tau$ and a $\nu_\mu - \nu_{\text{sterile}}$ oscillation schemes. The second scheme implies a "matter effect" which deforms the angular distribution of Fig. 1. As a consequence, the expected distribution has the probability reduced from 66% to 8%.

To improve the discrimination power between the two hypothesis, another parameter has been analysed. This parameter is the ratio between the events collected around the vertical ($\cos \theta <$

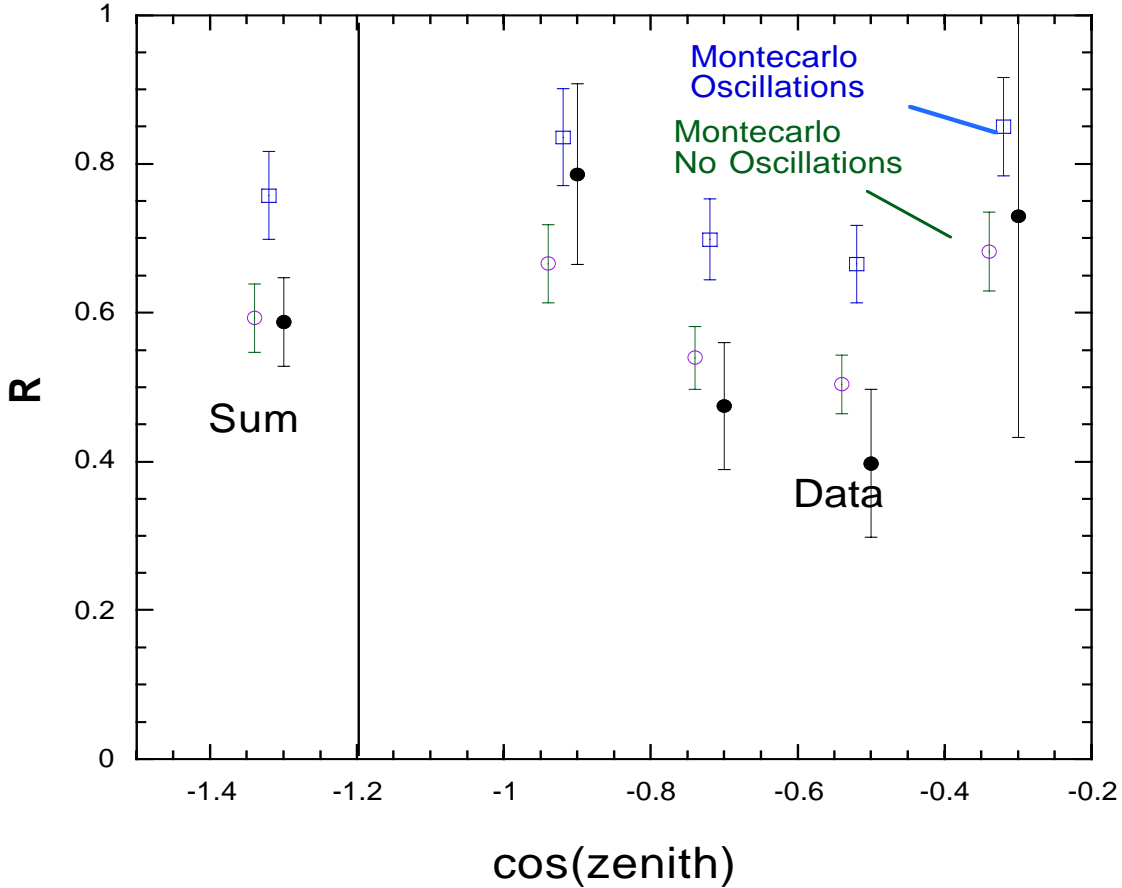


Figure 2: Zenith angle distribution of the double ratio between R_2 and R_3 . Data (full dots) are compared with the expected atmospheric neutrino flux without the effects of oscillations (open circle) and with the effects of oscillations (open square).

-0.7) and that collected around the horizontal ($\cos\theta < -0.4$). The ratio is reported in Fig. 3 as function of the Δm^2 . The agreement for the $\nu_\mu - \nu_\tau$ scheme has a probability of 9.4%, while for the $\nu_\mu - \nu_{sterile}$ scheme the probability is reduced down to 0.06%.

4 Search for neutrinos from stellar collapses

A stellar gravitational collapse should result in the emission of a 5-15 MeV electron antineutrino burst of about 10 sec duration. This antineutrino burst, interacting with the 560 tons of liquid scintillator of MACRO, is detected as a positron burst. The live time for observation has been kept close to 97%. Up to now no burst has been detected integrating about 8.5 years of observation of our galaxy (about 30% of the mean life for a collapse per galaxy).

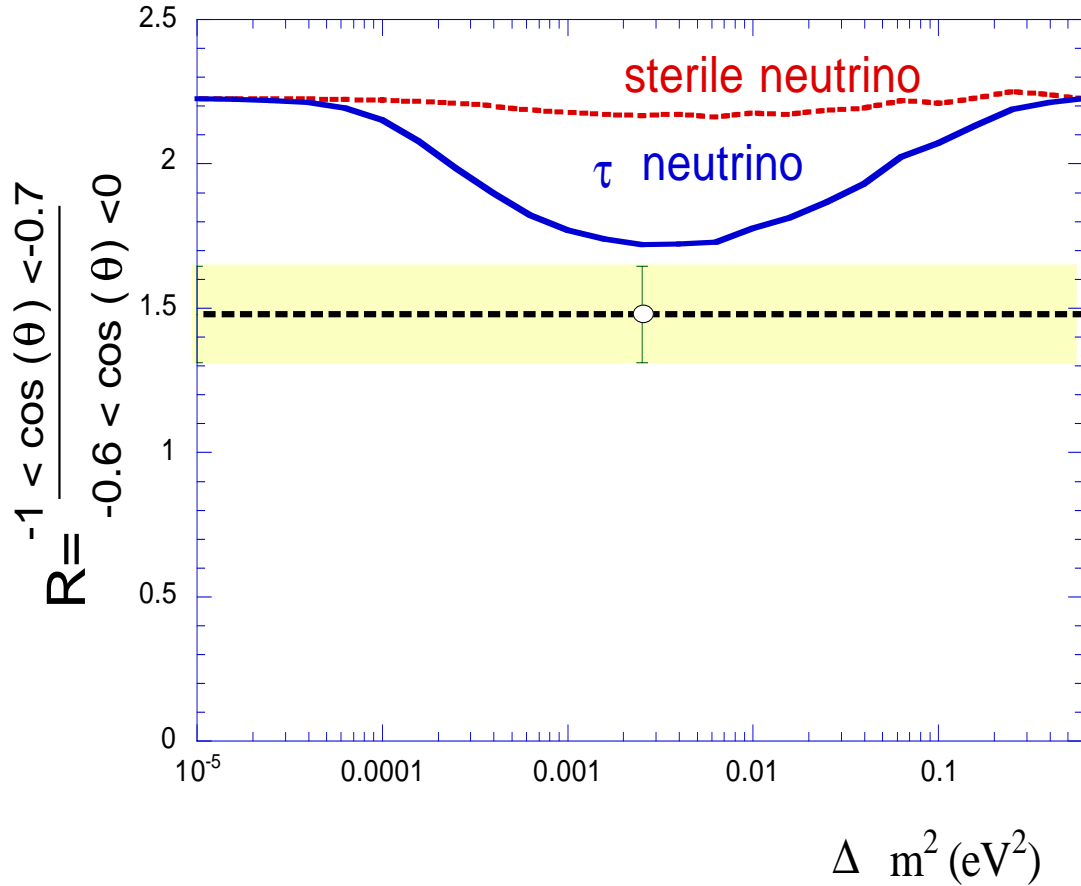


Figure 3: Ratio between the events collected around the vertical ($\cos \theta \lesssim -0.7$) and that collected around the horizontal ($\cos \theta \lesssim -0.6$) as function of Δm^2 .

5 Indirect search for WIMPs

WIMPs (Weakly Interacting Massive Particles) are candidate for being part of the dark matter inside the galaxies. These particles, hitting celestial bodies like Sun or Earth, slow down remaining trapped by gravity in their centers. So an accumulation forms during the time inside the celestial bodies. If the density grows enough, WIMPs and anti-WIMPs could annihilate in these celestial bodies producing neutrinos of GeV or TeV energy, in small angular windows around their centers. These neutrinos are detected through the yield of up-throughgoing muons. An upper limit on this yield can be translated through appropriate models in a limit on WIMP density in the galaxy. These limits have been published by Macro.

6 Publication on referenced Journals

1. MACRO Collaboration, M.Ambrosio *et al.*, Nuclearite Search with the MACRO Detector at Gran Sasso, Eur. Phys. Jour. C1453 (2000).

2. MACRO Collaboration, M.Ambrosio *et al.*, Low Energy Atmospheric Muon Neutrinos in MACRO, Phys Lett **B478**,5 (2000).
3. MACRO Collaboration, M.Ambrosio *et al.* A Search for Lightly Ionizing Particles with the MACRO Detector, Phys Rev. **D62**,052003 (2000).
4. MACRO Collaboration, M.Ambrosio *et al.* Neutrino Astronomy with the MACRO Detector, Astrophys.J. **546**1038 (2001).
5. MACRO Collaboration, M.Ambrosio *et al.*, Matter Effects in Upward-Going Muons and Sterile Neutrino Oscillation, Phys. Lett. **B517**,59 (2001).
6. MACRO Collaboration, M. Ambrosio *et al.* The MACRO Detector at Gran Sasso, Accepted for publication on NIM A.

OPERA

B. Dulach, A. Franceschi, A. Mengucci (Tecn.), M. Spinetti (Resp.),
M. Ventura (Tecn.), L. Votano

1 The experiment

The aim of the OPERA experiment ¹⁾ is the observation of $\nu_\mu \rightarrow \nu_\tau$ oscillations in the parameter region indicated by Super-Kamiokande as the explanation of the zenith dependence of the atmospheric neutrino deficit. OPERA is a long baseline experiment to be located at the Gran Sasso Laboratory in the CNGS neutrino beam from the CERN SPS. The detector design is based on a massive lead/nuclear emulsion target. Nuclear emulsions are used as high resolution tracking devices, for the direct observation of the decay of the τ leptons produced in ν_τ charged current interactions. Electronic detectors locate the events in the emulsions. They are made up of extruded plastic scintillator strips read out by wavelength-shifting fibers coupled with photodetectors at both ends. Magnetised iron spectrometers measure charge and momentum of muons. Each spectrometer consists of a dipolar magnet made of two iron walls interleaved by pairs of precision trackers. The particle trajectories are measured by these trackers, consisting of vertical drift tube planes. Resistive Plate Chambers (RPC) with inclined strips, called XPC, are combined with the precision trackers to provide unambiguous track reconstruction in space. Moreover, planes of RPC's (Inner Tracker) are inserted between the magnet iron plates. They allow a coarse tracking inside the magnet to identify muons and ease track matching between the precision trackers. They also provide a measurement of the tail of the hadronic energy leaking from the target and of the range of muons which stop in the iron. The discovery potential of OPERA originates from the observation of a ν_τ signal with very low background level. The direct observation of $\nu_\mu \rightarrow \nu_\tau$ appearance will constitute a milestone in the study of neutrino oscillations. Opera is an international collaboration (Belgium, China, Croatia, France, Germany, Israel, Italy, Japan, Russia, Switzerland, and Turkey) and the INFN groups involved are Bari, Bologna, LNF (Frascati), LNGS (Gran Sasso), Naples, Padova, Rome and Salerno.

2 Activities in Frascati

The Frascati group is responsible for the design and construction of the dipolar magnet. It also shares responsibility with CERN and INFN Padova for the construction and installation of the bakelite RPC planes (Inner Tracker). Finally, Frascati and Naples designed and prototyped the wall support structure housing the lead/emulsion bricks and will take care of the overall support structure of the experiment in Gran Sasso.

2.1 Magnets

A full scale prototype of part of the dipole magnet has been constructed in Frascati ²⁾. It consists of two vertical walls of rectangular cross section and of top and bottom flux return path. The walls are made up of four iron layers (5 cm thick) interleaved with 2 cm of space allocated for the housing of RPC. Each iron layer is made up of two plates $50 \times 1250 \times 8200$ mm². The final OPERA spectrometer will have the same structure but consists of seven plates instead of two (overall length 8750 mm) and 12 layers instead of 4. Studies have been made in order to understand its mechanical construction, and the performance of the final magnets, as well as to measure and monitor the magnetic field. Four driving coils have been installed. One of these is a prototype of the final coil

to be used in Gran Sasso. The magnetisation has been measured using additional pick-up coils and Hall probes. The agreement with simulation of the measurements of the magnetic field in the bulk of the spectrometer is at the level of a few percent. These results permit the optimisation of the coil design in order to reach the best performance in terms of magnetic field. The procedure for the construction of the OPERA magnets has started at the beginning of 2001. The tender for the iron slabs has been concluded and the contract has been assigned. The design of the final apparatus for current and temperature monitoring and the setup of the acquisition system for the pick-up coil will be studied during 2001. Installation in Gran Sasso will start in summer 2002.

2.2 Wall support structure

The wall support structure is made of thin stainless steel vertical bands welded to light horizontal trays where the bricks are positioned with a precision of one millimeter. Using high resistance stainless steel bands of 0.8 mm thickness, the structure weight is less than 0.4% of the total target weight. This design limits as much as possible neutrino interactions in the target area outside of the bricks themselves, ensures easy and quick removal of bricks from lateral sides and permits a minimum separation between bricks in transverse and longitudinal directions. The structure is suspended through rods and joints from the general support structure and tensioned from the bottom through a spring system. The structure design has been accomplished and the whole system including suspensions and tensioning system checked against the effect of earthquakes in the general support structure frame. After many destructive tests on the critical welding points, the stainless steel band material has been chosen and the welding procedure established. One prototype (full height and 1 m wide) has been assembled at the Frascati Laboratory, suspended and loaded with dummy bricks. The expected positioning precision has been achieved. Long term mechanical stability tests are underway. A second prototype (full width and 1 m high) is under construction and will be equipped with a more compact tensioning system. This prototype will be used for the brick manipulator tests.

2.3 Inner trackers

The design of the Resistive Plate Chambers (RPC) inserted in the magnets has been studied and measurements have been performed. RPC prototypes have been tested at CERN, Frascati, Gran Sasso and Padova, as well as at the T9 test beam from the CERN PS. Efficiencies as well as spatial and time resolutions have been studied as a function of various parameters (high voltage, gas mixtures, etc.). Also some physical parameters of the streamer processes have been measured, like the streamer charge as function of the primary ionization and the dead zone around a streamer. The knowledge of these parameters permits a full Montecarlo simulation of the RPC both for tracking and for calorimetry. Sixteen full scale prototypes are under construction. These chambers will be tested, in particular to check their performance around the 6 cm diameter holes which house the bolts of the magnet. A full scale tool for the installation will be developed in Padova. Its 9 meters length allows the installation of a whole row of RPC's in one go. Such prototype tool will be used in Frascati starting from November 2001 with the full scale RPCs, to control and check all the different phases of the installation procedure.

References

1. M. Guler *et al.*, OPERA proposal, CERN/SPSC 2000-028, SPSC/P318, LNGS P25/2000
2. M. Guler *et al.*, Status report of the OPERA experiment, CERN/SPSC 2001-025, SPSC/M668, LNGS-EXP 30/2001 Add. 1/01

ROG

S. D'Antonio (Bors), D. Babusci, F. Campolungo (Tecn.), V. Fafone
G. Giordano, M. Iannarelli (Tecn.), R. Lenci (Tecn.), A. Marini, G. Modestino
G. Pizzella (Ass.), L. Quintieri (Bors.), F. Ronga (Resp.), E. Turri (Tecn.), L. Votano
collaboration with L'Aquila, Roma 1 La Sapienza, Roma 2 Tor Vergata

1 Introduction

The ROG (Roma Onde Gravitazionali) group is operating currently two cryogenic gravitational wave bar detectors: Explorer (at CERN) and Nautilus (in Frascati). The main goal of this search is the direct detection of the gravitational waves that could be emitted by astrophysical sources (Supernova, Coalescent Binaries. ecc.). Such detection could be of enormous interest for general relativity and for astrophysics.

Cryogenic resonant-mass detectors were conceived in the '70s with the aim of improving the sensitivity of room temperature Weber detectors by many orders of magnitude, by reducing the temperature of the bar to or below helium temperature (4.2 K) and employing superconducting electronic devices in the readout system.

The principle of operation of resonant-mass detectors is based on the assumption that any vibrational mode of a resonant body that has a mass quadrupole moment, such as the fundamental longitudinal mode of a cylindrical antenna, can be excited by a gravitational wave with non zero energy spectral density at the mode eigenfrequency. The mechanical oscillation induced in the antenna by interaction with the G.W. is transformed into an electrical signal by a motion or strain transducer and then amplified by an electrical amplifier. Unavoidably, Brownian motion noise associated with dissipation in the antenna and the transducer, and electronic noise from the amplifier, limit the sensitivity of the detector.

The sum at the output of the contributions due to the Brownian noise and to the electronic noise gives the total detector noise. This can be referred to the input of the detector (as if it was a GW spectral density) and is usually indicated as $S_h(f)$. This function has a resonant behaviour and can be characterized by its value at the detector resonance frequency f_0 and by its half height width. $S_h(f_0)$ can be written as:

$$S_h(f_0) = \frac{\pi}{8} \frac{KT}{MQL^2} \frac{1}{f_0^3} \quad (1)$$

where T is the antenna temperature, M is the antenna mass, Q is the quality factor of the mode. The half height width of this function gives the bandwidth of a resonant detector. The bandwidth of a resonant detector depends from the mechanical parameters of the detector and from the characteristic of the electronic amplifier and can be written as:

$$\Delta F = \frac{4f_0}{Q} \frac{T}{T_{eff}} \quad (2)$$

where T_{eff} is the noise temperature when the data are filtered to have the maximum signal to noise ratio in the case of delta like signals (like the one expected from supernova). T_{eff} decreases as the noise temperature of the amplifier decreases and as the transducer efficiency increases.

These relations characterize completely the sensitivity of a resonant-mass detector. For instance, the minimum detectable (SNR=1) GW amplitude for a short burst signal lasting for a time τ_g can be written as :

$$h_0 = \frac{2}{\tau_g} \sqrt{\frac{S_h(f_0)}{2\pi\Delta F}} \quad (3)$$

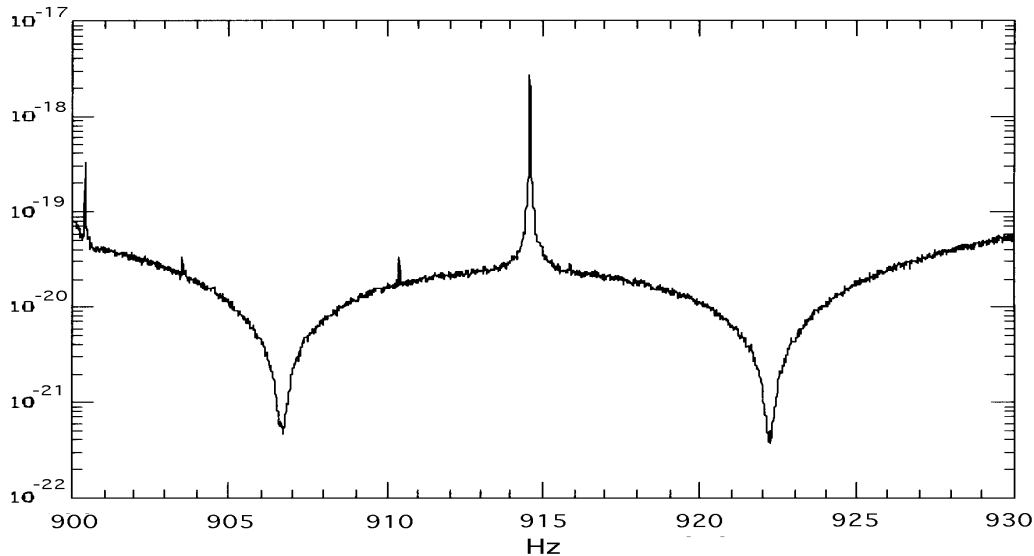


Figure 1: Nautilus strain sensitivity (input noise spectral amplitude in units of $\text{hz}^{-1/2}$). The sensitivity at the two resonances is about $4 \cdot 10^{-22} \text{hz}^{-1/2}$. The spectral amplitude is better than $3 \cdot 10^{-20} \text{Hz}^{-1/2}$ over a band of about 25 hz. The peak at 914.6 hz is a calibration reference signal fed into the dcSQUID amplifier to monitor the gain of the electronics.

We recall also that a resonant bar detector could detect also the stocastical energy density in gravitational wave. The stocastical density respect the one necessary to have a closed universe is given by:

$$\Omega = \frac{4\pi^2}{3H^2} f^3 S_h(f) \quad (4)$$

where H is the Hubble constant.

2 NAUTILUS and EXPLORER

The ultra cryogenic detector NAUTILUS ³⁾ is operating at the Frascati INFN National Laboratory since December 1995. It consists of an Al5056 cylindrical bar, 2300 kg in weight and 3 meters in length, cooled to a temperature of 0.1 K by means of a dilution refrigerator, and equipped with a resonant capacitive transducer and a dcSQUID amplifier. Due to the coupling of two resonators (the antenna and the transducer) the resonant frequency f_0 is split in the two frequencies around 908 and 924 hz. Moreover Nautilus is the only detector in the world equipped with a cosmic ray detector.

Nautilus has undergone, in the first half of 1998, a partial overhaul of its mechanical suspensions and thermal contacts. The results obtained since June 1998 show a considerable improvement in the rejection of non stationary noise and in the sensitivity of the apparatus. We show in Figure 1 the strain sensitivity of the detector, expressed in units of $\text{hz}^{-1/2}$, and in Figure 2 the detector noise temperature over three days in September 1999, the noise temperature of the order of $T_{noise} \simeq 2 \text{ mKelvin}$. This sensitivity allows the detection at $SNR = 1$ of an impulsive gravitational wave (GW) signal of duration 1 ms at amplitudes $h \simeq 4 \cdot 10^{-19}$. We recall that a supernova in

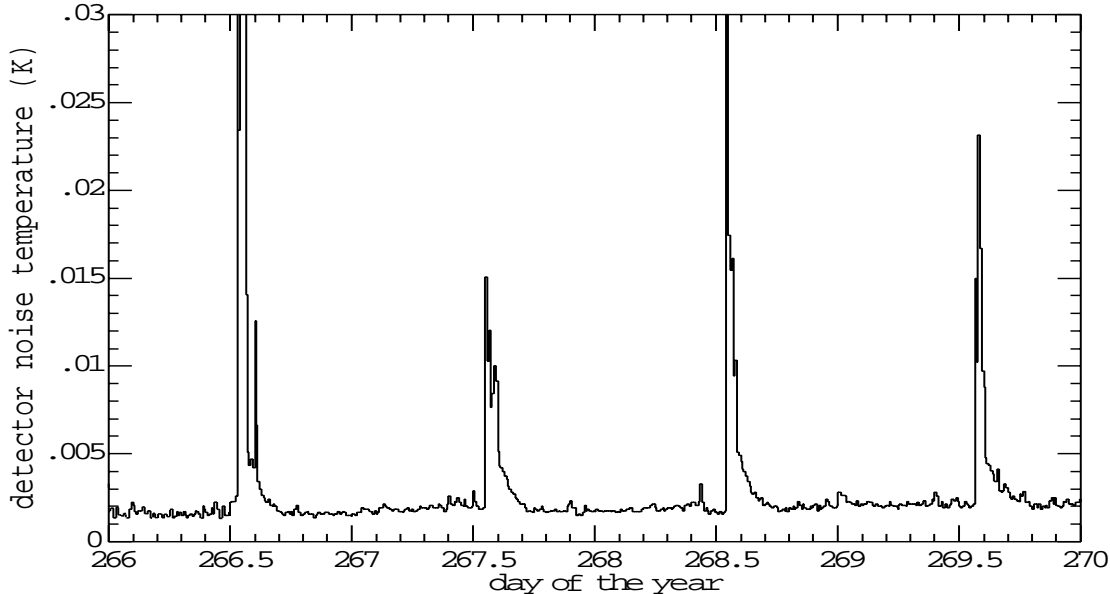


Figure 2: Nautilus noise temperature versus time, averaged every ten minutes, over a period of three days. A noise temperature of 2 mK corresponds to a minimum detectable amplitude h of a GW burst of duration 1 ms $h = 4 \cdot 10^{-19}$. The peaks are due to a daily cryogenic operation.

the Galactic Center should produce gravitational waves having $h \simeq 3 \cdot 10^{-18}$ much bigger than the Nautilus sensitivity.

The Explorer antenna is located in CERN and is very similar to Nautilus, but is cooled only to 2.6 Kelvin. During 1999-2000 major improvements have been done on the suspensions using solutions similar to Nautilus. A new capacitive transducer having a 10μ gap and a commercial Quantum Design D.C. SQUID are now installed in Explorer. Due to the improvement in the fraction of the energy store in the transducer there is a gain in T_{eff} and therefore in the bandwidth (see eq 2). Figure 3 shows some preliminary results. Further improvements are planned on the SQUID.

During 1999-2000 a new data acquisition with a sampling rate of 5Khz and a time precision of the order of a few μsec has been put into operation in Nautilus and Explorer.

There are currently four groups in the world operating 5 bar detectors (EXPLORER, NAUTILUS, ALLEGRO at LSU (USA), AURIGA at the INFN Legnaro National Laboratories, and NIOBE (Australia) The four groups formed the International Gravitational Event Collaboration (IGEC) on July 4th 1997, at CERN, and agreed in a data exchange protocol. The data analysis is presently focused in searching for short GW bursts.

The Frascati group has major responsibilities in the maintenance and running of Nautilus (including the production of liquid helium), in the maintenance and running of the cosmic ray detector, in the development of a new superconductive transformer for the signal readout, in the development of the new 5 khz acquisition and in many items of data analysis.

3 Future

It is assumed now in the gravitational wave resonant detectors community that the next generation of resonant-mass detectors will be of spherical shape. A single sphere is capable of detecting grav-

itational waves from all directions and polarizations and is capable of determining the direction information and tensorial character of the incident wave. A sphere will have a larger mass than the present bars (with the same resonant frequency), translating into an increased cross section and improved sensitivity. Omnidirectionality and source direction finding ability make a spherical detector an unique instrument for gravitational wave astronomy with respect to all present detectors. The measurement of the polarization states and the scalar-tensor discrimination open new possibilities in the study of gravitational physics. Finally, the different features and technology make a spherical detector complementary to an interferometer. It emerges that an observatory composed of both a sphere and an interferometer will have unprecedented sensitivity and signal characterization capabilities. Studies and measurements essential to define a project of a large spherical detector, 40 to 100 tons of mass, cooled to 10 mK have been made in USA, Italy, Netherland and Brasil. The R/D activity of ROG group is related in particular to the cryogenic problems, the suspensions and the effect of the cosmic rays.

4 Main analysis results obtained in 2000-2001

The main analyses using the NAUTILUS and EXPLORER data, just published or in progress, are the following:

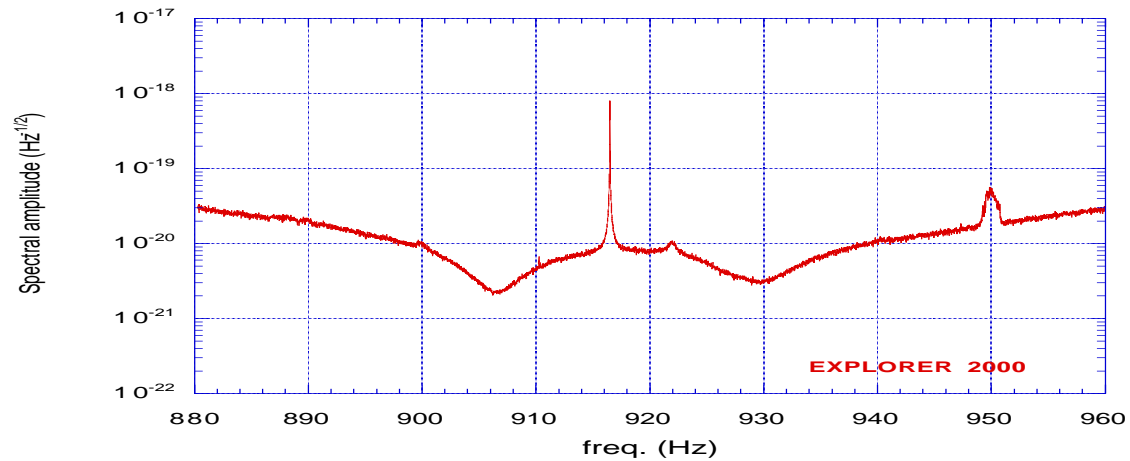


Figure 3: Explorer strain sensitivity with the new trasducer The spectral amplitude is better than $4 \cdot 10^{-21} \text{ Hz}^{-1/2}$ over a band of about 10 hz.

- A search for monochromatic signal. The present sensitivity of NAUTILUS allows the detection at $SNR = 1$ of a continuous GW signal around 1 khz of amplitude $h \simeq 5 \cdot 10^{-26}$ with an observation time of 100 days ⁴⁾.

- Analysis of the 1997-1998 data released under the IGEC (International Gravitational Event Collaboration) protocol is also in progress. The results of the search for coincidence due to short GW bursts among all the five IGEC resonant detectors have be reported to several conferences and now are published Phys Rev. Letters ⁵⁾.

- Search for coincidences between Explorer and Nautilus ⁶⁾

- Studies connected with statistics ⁷⁾, ⁹⁾ and data analysis ⁸⁾

- Search for coincidences with gamma ray bursts.

- Of particular interest is detection of the excitation of NAUTILUS due to the passage of cosmic rays ¹¹⁾. This is the first observation of this effect. Recently ¹²⁾ we have observed

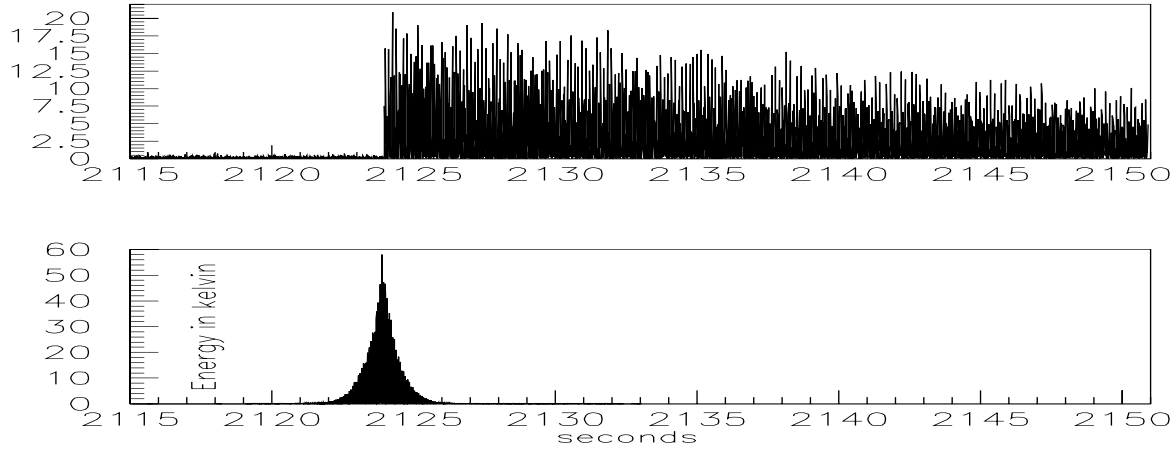


Figure 4: Time behaviour of the largest NAUTILUS event in coincidence with an extensive air shower detected by the cosmic ray detector. The particle density in the extensive air shower is $3500 \text{ particles}/m^2$. In the upper figure we show the NAUTILUS signal (voltage squared) before optimum filtering versus the UT time expressed in seconds, from the preceding midnight. From the decay we evaluate the merit factor of the apparatus, $Q = 1.710^5$. The lower plot shows the data after filtering, in units of Kelvin.

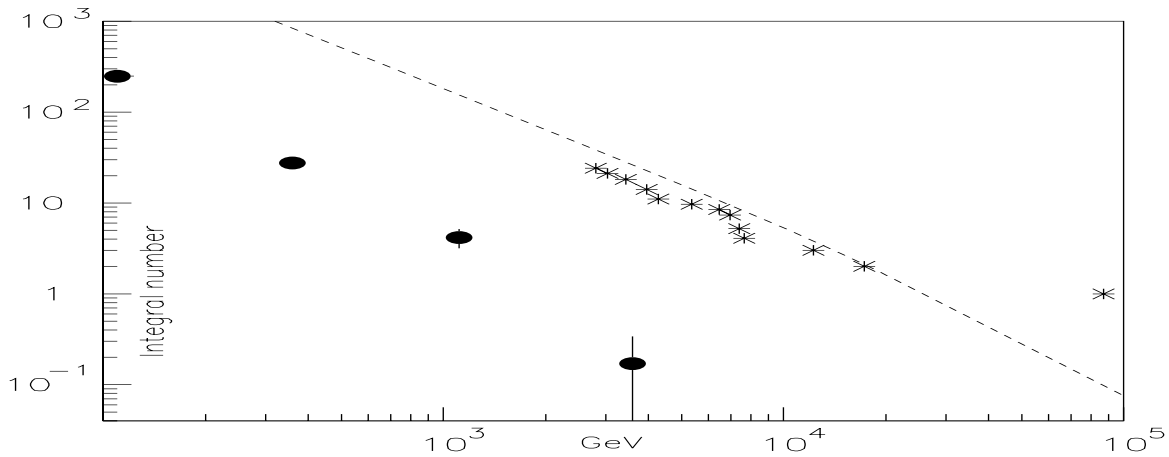


Figure 5: Comparison between the calculations of the number of cosmic rays in coincidence with Nautilus and measurements. The asterisks indicate the integrated number of coincident events versus the energy delivered by the c.r. to the bar, expressed in GeV units, to be compared with the points having error bars, which give the number of events due to hadrons, we expect in the NAUTILUS bar. The dashed line is the experimental integral spectrum for the hadronic component of the showers, for the 83.4 days of observation, obtained by the Cascade experiment ¹²⁾.

several anomalous unexpected signals of large amplitude (up to 60 Kelvin corresponding to 87 TeV). A resonant mass gravitational wave detector used as particle detector has characteristics different from the usual particle detectors, and it could detect new features of cosmic rays. Among several possibilities, one can invoke unexpected behaviour of superconductor Aluminium as particle

detector, producing enhanced signals, the excitation of non-elastic modes with large energy release or anomalies in cosmic rays (for instance, the showers might include exotic particles as nuclearites or Q-balls). After August 2000 NAUTILUS is running at a temperature of 1.1 Kelvin. The Aluminum is not superconductor at this temperature. We have an evidence at 3 standard deviation level that the rate of the anomalous signals is much smaller than the one for superconductor aluminium. We are investigating this interesting effect both experimentally than theoretically.

References

1. G.D. van Albada et al. Measurement of mechanical vibrations excited in aluminum resonators by 0.6 Gev electrons NIKHEF-99-036, Rev. Sci. Instrum. **71**, 1345 (2000)
2. P. Astone et al. Underground spherical gravitational wave detector Nucl. Phys. Proc. Suppl **70**:461-465,1999
3. P. Astone *et al.*, "The gravitational wave detector NAUTILUS operating at $T = 0.1\text{-K}$," Astropart. Phys. **7**, 231 (1997).
4. P. Astone *et al.*, "Search for periodic gravitational wave sources with the Explorer detector," arXiv:gr-qc/0011072. Accepted by Phys Rev D
5. Z. A. Allen *et al.* [International Gravitational Event Collaboration], "First search for gravitational wave bursts with a network of detectors," Phys. Rev. Lett. **85**, 5046 (2000) [arXiv:astro-ph/0007308].
6. P. Astone *et al.*, "Study of coincidences between resonant gravitational wave detectors," Class. Quant. Grav. **18**, 243 (2001) [arXiv:gr-qc/0007055].
7. G. Pizzella, "Workshop on coincidence analysis," Int. J. Mod. Phys. D **9**, 331 (2000).
8. P. Astone, S. D'Antonio and G. Pizzella, Phys. Rev. D **62**, 042001 (2000) [arXiv:gr-qc/0001030].
9. P. Astone and G. Pizzella, "On upper limits for gravitational radiation," arXiv:gr-qc/0001035.
10. G. Modestino and A. Moleti "On the crosscorrelation between Gravitational Wave Detectors for detecting association with Gamma Ray Bursts" Accepted by Phys Rev D
11. P. Astone *et al.*, "Cosmic rays observed by the resonant gravitational wave detector NAUTILUS," Phys. Rev. Lett. **84**, 14 (2000).
12. P. Astone *et al.*, "Energetic cosmic rays observed by the resonant gravitational wave detector NAUTILUS," Phys. Lett. B **499**, 16 (2001) [arXiv:gr-qc/0009066].

VIRGO

D. Babusci, H. Fang (Art.23), G. Giordano (Resp.), M. Iannarelli (Tecn.), E. Turri (Tecn.)

1 Introduction

Virgo is a collaboration between Italy (INFN) and France (CNRS) for the construction of an interferometric detector of gravitational waves (GW). The participating laboratories are: LAPP-Annecy, IPN-Lyon, OCA-Nice, LAL-Orsay and ESPCI-Paris for CNRS and Firenze/Urbino, Frascati, Napoli, Perugia, Pisa, Roma1 for INFN.

The aimed sensitivity (see fig.1) should allow to detect, in the frequency range between a few Hz and a few kHz, GW emitted by coalescing binary compact stars, gravitational collapses, spinning neutron stars, or constituting the stochastic GW background.

Virgo will be a recycled (power enhancement factor $\simeq 50$) Michelson interferometer, having in each arm a 3 km Fabry-Perot cavity with finesse of 50. The interferometer (ITF) will be illuminated by a 25 W Nd:YAG laser ($\lambda = 1.064 \mu\text{m}$), stabilized through a monolithic reference cavity and filtered by a high-finesse triangular mode cleaner of 144 m length.

The optical path will be completely under vacuum and all the optical components will be suspended in vacuum by anti-seismic Super Attenuators able to reduce the seismic noise of more than a factor 10^{12} above a few Hertz.

The construction of Virgo was planned in two main steps: the realization of the central interferometer (CITF) was completed by end 2000, and the realization of the 3 km arms full ITF is foreseen to end within 2002. The CITF consists of all the Virgo final components in the central area, including the 144 m mode cleaner. It will operate as a simple recycled Michelson interferometer where the arm end mirrors will be installed at the place of the input mirrors of the future 3 km Fabry-Perot cavities.

2 Virgo Status of Advancement

All the buildings of the central area are presently finished; they have been occupied and the installation of the apparatus for the Central Interferometer is completed.

The construction of the arm infrastructure (3 km tunnels, intermediate and terminal buildings) has continued and is expected to be completed in early 2001 (see fig.2). All the towers for the Central Interferometer have been installed (see fig. 3); input and detection benches, together with their special suspension elements, are already installed.

3 Activity of the Frascati Group

The Frascati group has the responsibility of the "linear alignment", that is the system providing the informations about the misalignment of the ITF mirrors during the standard operation of Virgo. It will employ 8 quadrant photodiodes (QPHD) placed on the beams emerging from the ITF; demodulating the up-down and left-right differences, the misalignments status will be derived.

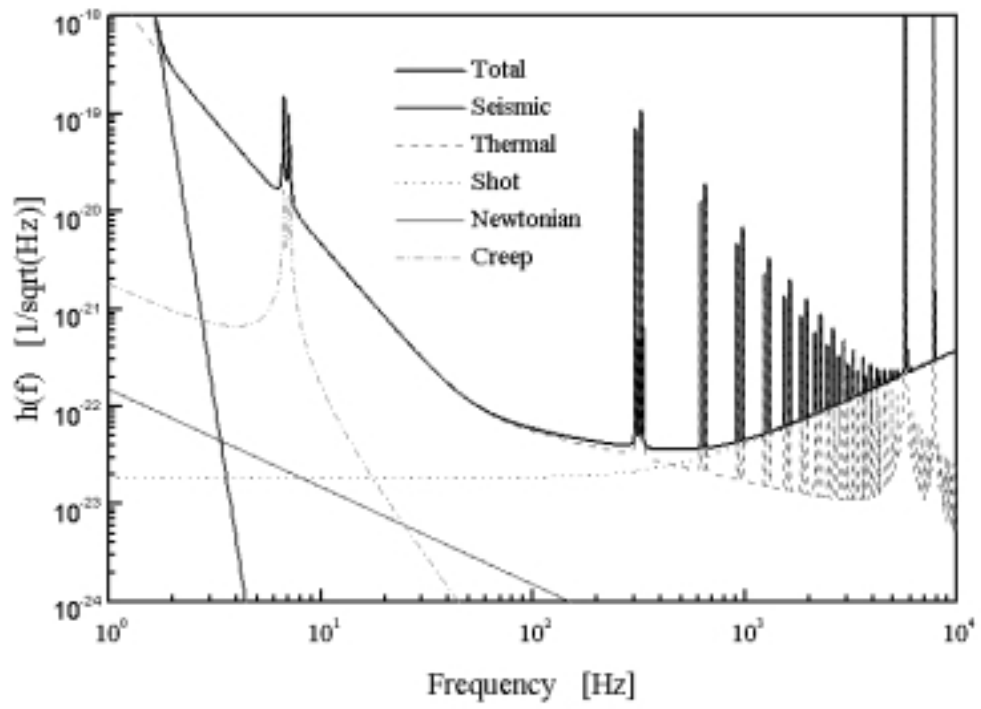


Figure 1: *The Virgo sensitivity curve.*



Figure 2: *Air view of the Virgo Cascina site.*



Figure 3: *The central area towers.*

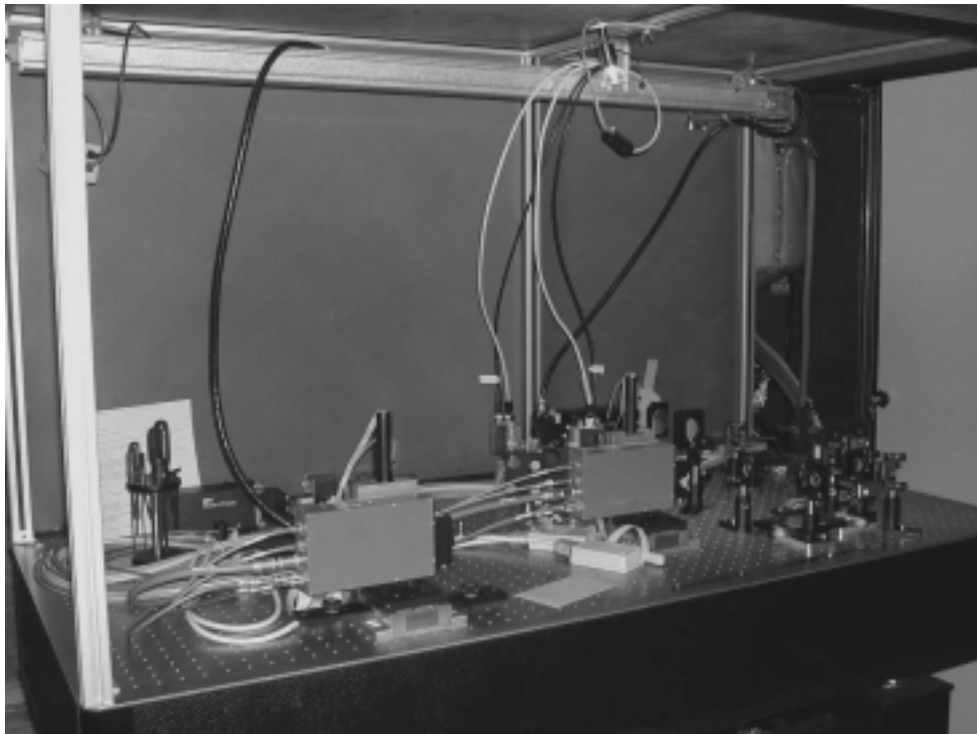


Figure 4: *Assembly on west detectors bench.*

In 2000 we have procured and/or built all the optical and mechanical components for the QPHD assemblies, some of which we already installed on site (see fig.4), and advanced in the realization of the associated electronics.

We also participated to the "Locking Group" activity, namely to the coordination of all the activity necessary to bring into operation the ITF (locking, alignment, controls, software, ...). In this activity, our main contribution was devoted to the study of the procedures for the software treatment of the alignment signals and of the feedback algorithms to be employed.

In 2001 the CITF should become operational, and so our activity will focus both on the participation to the test runs and on the installation of our system. At the same time we will prepare all the modifications and additions required to go forward the full Virgo ITF.

4 List of Publications

1. G. Giordano, A. Serdobolski, *Windows of CITF Terminal Towers*, Virgo note VIR-LIS-FRA-4400-103 (2000).
2. M. Barsuglia, L. Di Fiore, G. Giordano, D. Passuello, *Definition of Band-width and Slope of the Servo-loop for SA Control*, Virgo note VIR-NOT-NAP-1390-143 (2000).
3. D. Babusci, M. Giovannini, *Sensitivity of a Virgo Pair to Relic GW Backgrounds*, Class. Quantum Grav. **17**, 2621 (2000).

WIZARD

S. Bartalucci, G. Basini, F. Bongiorno, L. Marino (Ass.),
G. Mazzenga (Tecn.), M. Ricci (Resp.)

Participant Institutions:

ITALY: INFN Bari, LNF, Firenze, Napoli, Roma2, Trieste;
CNR IROE Firenze;
ASI (Italian Space agency);
Electronic Engineering Department, University of Roma 2 “Tor Vergata”;
RUSSIA: MePhi Moscow;
FIAN Lebedev Moscow;
IOFFE St Petersburg;
TsSKB-Progress Samara;
SWEDEN: KTH Stockholm;
GERMANY: Siegen University;
USA: NASA Goddard Space Flight Center;
New Mexico State University.

1 Experimental Program and Scientific Objectives

The WIZARD experimental program is devoted to the extensive study of cosmic ray spectra (particles, antiparticles, isotopes, abundances and search for antimatter) in several energy ranges achievable through different apparatus on board stratospheric balloons and long duration satellite missions. WIZARD is an International Collaboration between several Universities and Research Institutions from Russia, Sweden, Germany, USA together with the Space Agencies NASA, RKA (Russia), SSC (Sweden), DLR (Germany) and ASI. The experimental activities are carried out through three main programs:

Balloon flights;

Satellite missions NINA-1 and NINA-2;

Satellite mission PAMELA.

We refer to the previous edition of this report for the description of the activities related to the balloon flights and to the two NINA missions.

1.1 The satellite mission PAMELA

PAMELA is a cosmic ray space experiment that will be installed on board a Russian satellite (Resurs-DK1) whose launch is foreseen at the end of 2002 - beginning of 2003. The satellite will fly for at least 3 years in a low altitude, elliptic orbit (300-600 km) with an inclination of 70.4 degrees. The PAMELA telescope consists of a magnetic spectrometer including a permanent magnet coupled to a silicon tracker, a Transition Radiation Detector, an imaging silicon-tungsten calorimeter and a time-of-flight system including anticoincidence counters ¹⁾ ²⁾. A sketch of the PAMELA instrument is shown in fig.1.

The total height of PAMELA is 120 cm, the mass is 440 kg, the power consumption is 385 W and the geometrical factor is 20.5 cm² sr.

The observational objectives of the PAMELA experiment are to measure the spectra of antiprotons, positrons and nuclei in a wide range of energies, to search for antimatter and to study

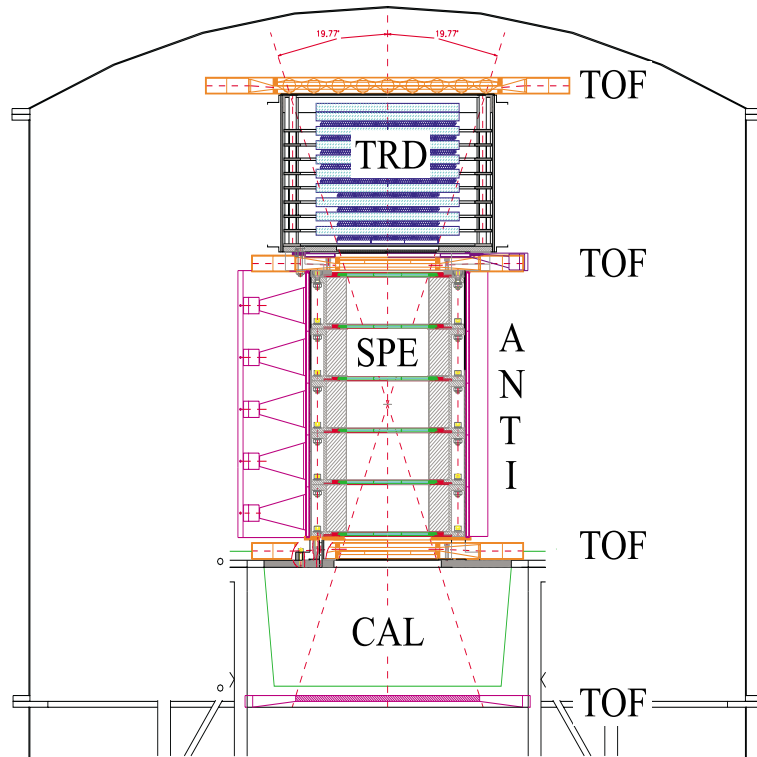


Figure 1: The PAMELA telescope and its main detectors: Transition Radiation Detector (TRD); Permanent Magnet Spectrometer equipped with silicon tracker (SPE); Silicon-Tungsten Calorimeter (CAL). Time Of Flight(TOF) and Anticoincidence (ANTI) systems are also shown.

the cosmic ray fluxes over a portion of the solar cycle. The main observational objectives can be schematically listed as the following:

- a) measurement of the antiproton spectrum in the energy range 80 MeV-190 GeV;
- b) measurement of the positron spectrum in the energy range 50 MeV-270 GeV;
- c) search for antinuclei with a sensitivity of $\sim 3 \times 10^{-8}$ in the \overline{He}/He ratio;
- d) measurement of nuclei spectra (He, Be, C) at energies up to 700 GeV/n;
- e) measurement of the electron spectrum in the energy range 50 MeV-2 TeV.

Moreover, the PAMELA experiment will be able to address the following additional issues:

- a) continuous monitoring of the cosmic rays solar modulation during and after the 23rd maximum of the solar activity;
- b) study of the time and energy distributions of the energetic particles emitted in solar flares;
- c) measurement of the anomalous component of cosmic rays;
- d) study of stationary and disturbed fluxes of high energy particles in the Earth magnetosphere.

Activity in the year 2000 has been carried on the development of the qualification model of the instrument for each detector involved. Calibrations and beam tests have been performed at CERN PS and SPS and specific vibration, thermal and electromagnetic tests have taken place at different european facilities for space qualification. The assembly and integration laboratory, provided with

two clean rooms, has been completed at the INFN Section of Roma 2. Further radiation hardness tests of electronic components have been performed at INFN Laboratori Nazionali Legnaro, at the ENEA Casaccia irradiation facility and at GSI, Darmstadt to verify and characterize such components for radiation tolerance in space. As an example of the performance of PAMELA detectors, in fig.2 is shown the spatial resolution of the silicon tracker during a test at PS-T9 beam with 10 GeV electrons.

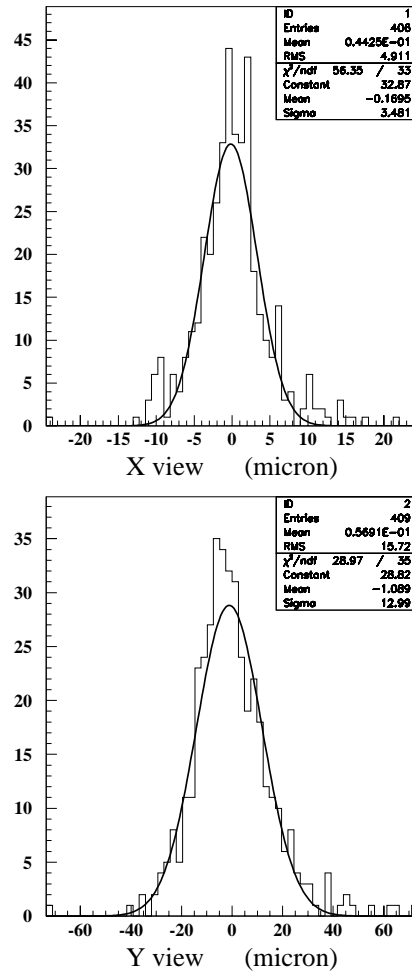


Figure 2: Spatial resolution of the PAMELA silicon tracker with 10 GeV electron beam at CERN PS; x-view is the one subjected to the bending effect of the 0.4 T field of the permanent magnet. A value of less than $3.5\mu\text{m}$ has been achieved in this view.

2 Activity of the LNF group during year 2000

The LNF WIZARD group has been fully involved in all the balloon and satellite programs. During the year 2000 the activity for the PAMELA experiment has been carried on as follows:

Final preparation of the integration laboratory and clean rooms at INFN Roma 2.
Organization of beam test set-up at CERN PS and SPS.
Responsibility of the counting detectors and trigger for beam tests.
Responsibility (shared with the Electronic Engineering Department of the University of Roma 2 “Tor Vergata”) of the radiation hardness beam tests at ENEA Casaccia, INFN-LNS Catania and GSI Darmstadt.
Responsibility of the Mechanical Ground Support Equipment (MGSE) for the assembly and integration of the whole apparatus.

3 Programmed activity of the LNF group during year 2001

Completion of the MGSE and installation in the clean room.
Vibrational tests of PAMELA Dummy model at IABG Company, Munchen (Germany).
Beam tests of qualification model at CERN SPS.
Integration of qualification model with electrical and mechanical Ground Support Equipment in clean room.

4 List of Publications in 2000

“The cosmic-ray electron and positron spectra measured at 1 AU during solar minimum activity”
M.Boezio et al. *Ap. J.* 532, 653 (2000)
“First mass resolved measurement of high-energy cosmic-ray antiprotons” D.Bergstrom et al. *Ap. J.* 534, L177 (2000)
“Measurement of the flux of atmospheric muons with the CAPRICE94 apparatus” M.Boezio et al. *Phys. Rev. D*62, 032007 (2000)
“The cosmic-ray antiproton flux between 3 and 49 GeV” M.Boezio et al. astro-ph/0103513 (accepted by *Astrophysical J.*)

References

1. The PAMELA Collaboration, Proc. XXVI ICRC Salt Lake City, vol.5 p.96 (1999)
2. P. Spillantini for the PAMELA collaboration: “The PAMELA experiment”, Proc. XXVII ICRC Hamburg p. 2215 (2001)

AIACE

H. Avakyan (Ass.), E. De Sanctis (Resp.), M. Mirazita (Ass.),
A. Orlandi (Tecn.), W. Pesci (Tecn.), E. Polli, F. Ronchetti (Dott.),
P. Rossi, A. Viticchiè (Tecn.)

1 Introduction

AIACE stands for Attività Italiana A CEbaf. It is the collaboration of the INFN groups of Frascati and Genova which participate into the physics program carried on with the CLAS detector at the Continuous Electron Beam Accelerator Facility (CEBAF) at the Jefferson Laboratory (JLab), located in Newport News, Virginia (USA). The CEBAF is a superconducting electron accelerator which delivers a low emittance, high resolution, high intensity (up to 200 μA) continuous electron beam of up to 6 GeV energy.

CLAS ¹⁾ is a large acceptance spectrometer based on a toroidal magnetic field, generated by six superconducting coils arranged around the beam line. Each sector is independently instrumented with drift chambers, gas Cerenkov counters, time-of-flight scintillation counters, start counters, and electromagnetic shower calorimeters. The CLAS momentum resolution is about 0.5% in the forward direction and about 1% at large angles. Its high data acquisition rate (3500 Hz) well matches the luminosity of $10^{34}\text{cm}^{-2}\text{s}^{-1}$.

CLAS primary mission is to carry out electro- and photo-production experiments which require the detection of several, only loosely correlated particles in the final hadronic state in situations involving high luminosity. The broad physics program approved by the international Program Advisory Committee of the JLab covers the following fields:

- elementary and nuclear excitations of N^* resonances,
- spin structure functions of the nucleon,
- inclusive electron scattering on nuclei,
- elementary and nuclear hyperon production and decays,
- structure of the few body systems (few quarks or few nucleons),
- nuclear medium effects.

At present, the CLAS collaboration counts 140 physicists from 35 Institutions from seven Countries.

In the period covered by this report the Frascati group has carried out:

- the analysis of data collected in the summer 1999 during the 'g2 run period' for the determination of the deuteron photodisintegration between 0.5 and 3.0 GeV;
- the development of the Quark-Gluon String (QGS) model for the prediction of the deuteron photodisintegration cross section at small momentum transfer.

In addition, the Frascati group has participated to the various CLAS production runs organized by 'run periods' where experiments which share common running conditions take data simultaneously. A huge volume of high quality data from a variety of experiments has been obtained in electro- and photoproduction processes on H, D, Be, and polarised NH_3 and ND_3 . The relevant experiments refer to the measurements of rare radiative decays of the ϕ meson, the neutron magnetic form factor, the polarised structure functions of the proton and deuteron at low to moderate Q^2 , and missing N^* resonances.

2 Deuteron photodisintegration between 0.5 and 3.0 GeV (Experiment E-93-017)

2.1 Physics motivation

The study of high-energy two-body photodisintegration of the deuteron has received a renewed interest in the recent years in the attempt to evidence the quark structure of the nucleus. This because the process is amenable to theoretical calculation and relatively high momentum transfer to the constituents can be achieved at relatively modest photon energies ²⁾. The physics interest deals with how and at what energy the transition takes place from the hadronic picture of the deuteron, which is established in the reactions at low energies (below 1 GeV), to the quark-gluon picture, which is expected to be a correct theory at the energy much higher than 1 GeV, where small distances of the order of 0.2 fm play a role.

A possible signature for the emergence of quark-gluon degrees of freedom would be the observation of the onset of scaling of the cross section. SLAC data ³⁾ above $E_\gamma = 1$ GeV later confirmed and extended by Jlab ⁴⁾ exhibit scaling consistent with a quark gluon picture of deuteron photodisintegration for $E_\gamma \geq 1$ GeV at $\theta_{cm} = 90^\circ$. At forward angles, 36° and 52° , however, scaling is not observed for $E_\gamma \leq 4$ GeV. Recent measurements of the recoil proton polarization for the $d(\vec{\gamma}, \vec{p})n$ reaction at $\theta_{c.m.} = 90^\circ$ show an induced polarisation inconsistent with meson exchange current model prediction and show that the scaling behaviour observed in the $d(\gamma, p)n$ cross sections is not a result of perturbative QCD (pQCD) ⁵⁾. In contrast, very recent results ⁶⁾ for the $\gamma d \rightarrow pn$ differential cross section at forward angles and photon energies up to 5.5 GeV show a behaviour which is consistent with the constituent counting rules also at forward angles, with apparent scaling thresholds at $E_\gamma = 3$ GeV for $\theta_{c.m.} = 37^\circ$ and $E_\gamma = 4$ GeV, for $\theta_{c.m.} = 53^\circ$.

In summary, neglecting the polarization results ⁵⁾ it seems that at high energies, where asymptotic behaviour is expected, the nucleon-nucleon interaction is well described by the scaling behaviour of pQCD; while in the intermediate energy regime, where meson-exchange models fail and pQCD is not yet applicable, non perturbative QCD methods should be considered.

In this context, a few years ago we have derived an expression for the cross section for the reaction $\gamma d \rightarrow pn$ at small momentum transfer t and u in the framework of the QGS model and Regge phenomenology ⁷⁾ (here t, u , and s are the usual Mandelstam variables). In this approach (see next par.) the cross section is a fast decreasing function of the photon energy and t . Its energy behaviour at fixed centre-of-mass angle is complex and cannot be incorporated into a simple power law of energy, in distinction from the quark counting rule which predicts a constant power s^{11} at all angles. The QGS model expression for the cross section reproduces very well the few experimental data at energies between 1.5 and 4.2 GeV at the time available ($E_\gamma \leq 1.8$ GeV). It should work well at sufficiently high energy and small t or u [t or $u \leq 1$ GeV/c²].

The experiment of interest here (experiment E-93-017) intends to measure the differential cross section for the processes $\gamma d \rightarrow pn$ and $\gamma d \rightarrow p\Delta^0$ in the region of small momentum transfers and over the energy range from 0.5 to 3.2 GeV, in order to check the predictions of the Regge phenomenology and the QGS model. ⁸⁾

2.2 Experimental

The data collection was performed during the summer 1999 using the Hall B tagged photon beam ⁹⁾ and CLAS detector ¹⁾. The incident electron beam impinged upon a gold radiator of 10^{-4} radiation lengths. Data were taken at $E_0 = 2.5$ and 3.1 GeV incident electron energies and the photons were tagged in the full range $(0.2-0.95)E_0$. The target cell, a kapton cylinder 4 cm in diameter and 10 cm long, was filled with liquid deuterium at 24 K.

295 M triggers analysed (14% of the total statistic)

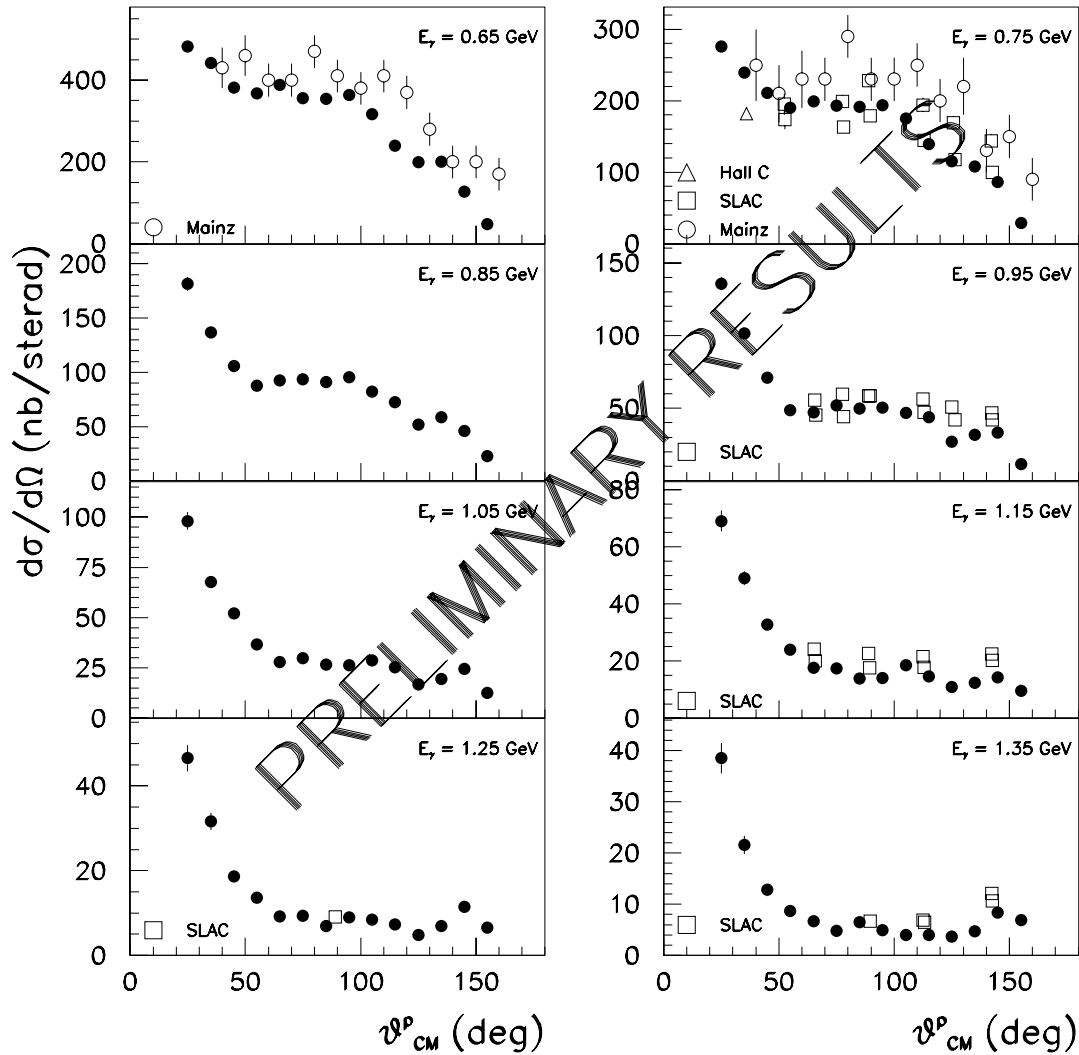


Figure 1: *Differential cross section for the reaction $d(\gamma.p)n$ for photon energies between 0.65 and 1.35 GeV.*

Also a number of calibration data were taken at low intensity which have to allow the determination of photon tagger and the CLAS detector characteristics with great accuracy. The photon flux was determined with the tagging spectrometer and a pair spectrometer located downstream of the target. The efficiency of this pair spectrometer was measured at low intensity ($10^5 \gamma/s$ in the entire bremsstrahlung spectrum) by comparison with a total absorption counter (a lead glass detector of 20 radiation lengths).

Level 1 trigger required a charged particle in the CLAS in coincidence with a signal in the tagger. During data taking at high intensity (about $7 \cdot 10^7$ tagged γ/s), the number of coincidences, true and accidental, between the pair spectrometer and the tagger was recorded by scalers. About 2.5 billions of events have been collected.

At present, about the 14 % of the data have been analysed. Fig. 1 and Fig. 2 show the preliminary results obtained for the the differential cross sections at the given photon energies. The data agree well with previous results available in the literature and cover a broader angular

295 M triggers analysed (14% of the total statistic)

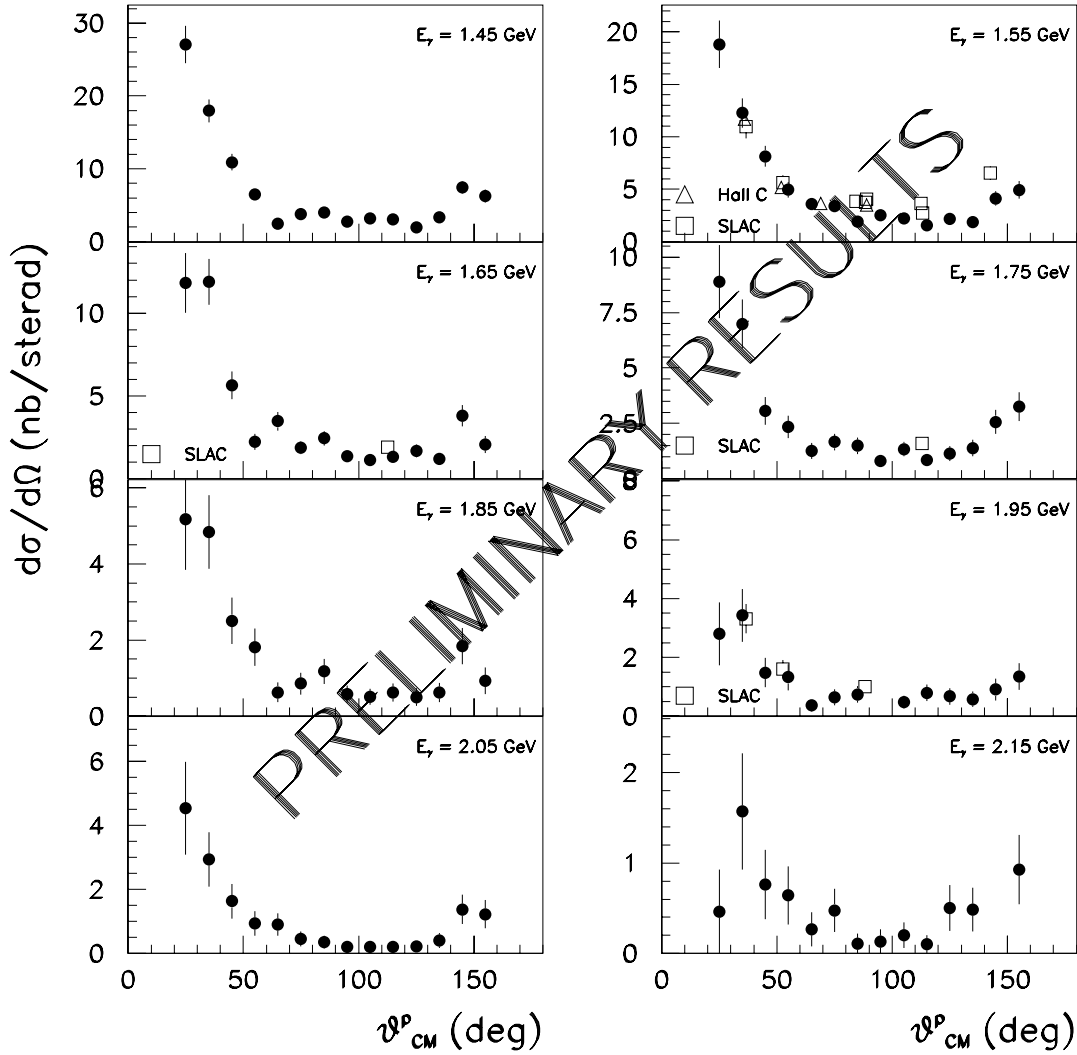


Figure 2: *Differential cross section for the reaction $d(\gamma.p)n$ for photon energies between 1.45 and 2.15 GeV.*

and energy range. This is of paramount importance for stringently constraining the theoretical predictions.

When the whole data set will be analysed, the expected statistical uncertainty in angular bins of about 10° and energy bins of 100 MeV is 0.7 % and 2.5 % (neglecting background) respectively at the lower and higher end of the energy range.

3 Deuteron photodisintegration within the Quark-Gluon Strings model

A few years ago we have applied a non perturbative approach based on the QGS model to the analysis of the angular and energy dependence of the differential cross section for the $\gamma d \rightarrow pn$ reaction in the few-GeV region ⁷⁾. In this approach the amplitude of the reaction is described by the exchange of three valence quarks in the t -channel with any number of gluon exchanges between them. The explicit spin structure of the corresponding 12 helicity amplitudes was not taken into

account and a parameterization corresponding to the differential cross section averaged over the initial and summed over the final helicity states was used. The resulting cross sections is a fast decreasing function of the photon energy and t . At fixed angle and in a limited energy region its energy behaviour can be parameterized as a simple power law with different powers at different angles in distinction from the quark counting rule which predicts a constant power at all angles. This expression, that reproduces reasonably well the experimental data at the time available ($E_\gamma \leq 1.8$ GeV), should works well at sufficiently high energy and small t or u [t or $u \leq 1$ GeV 2].

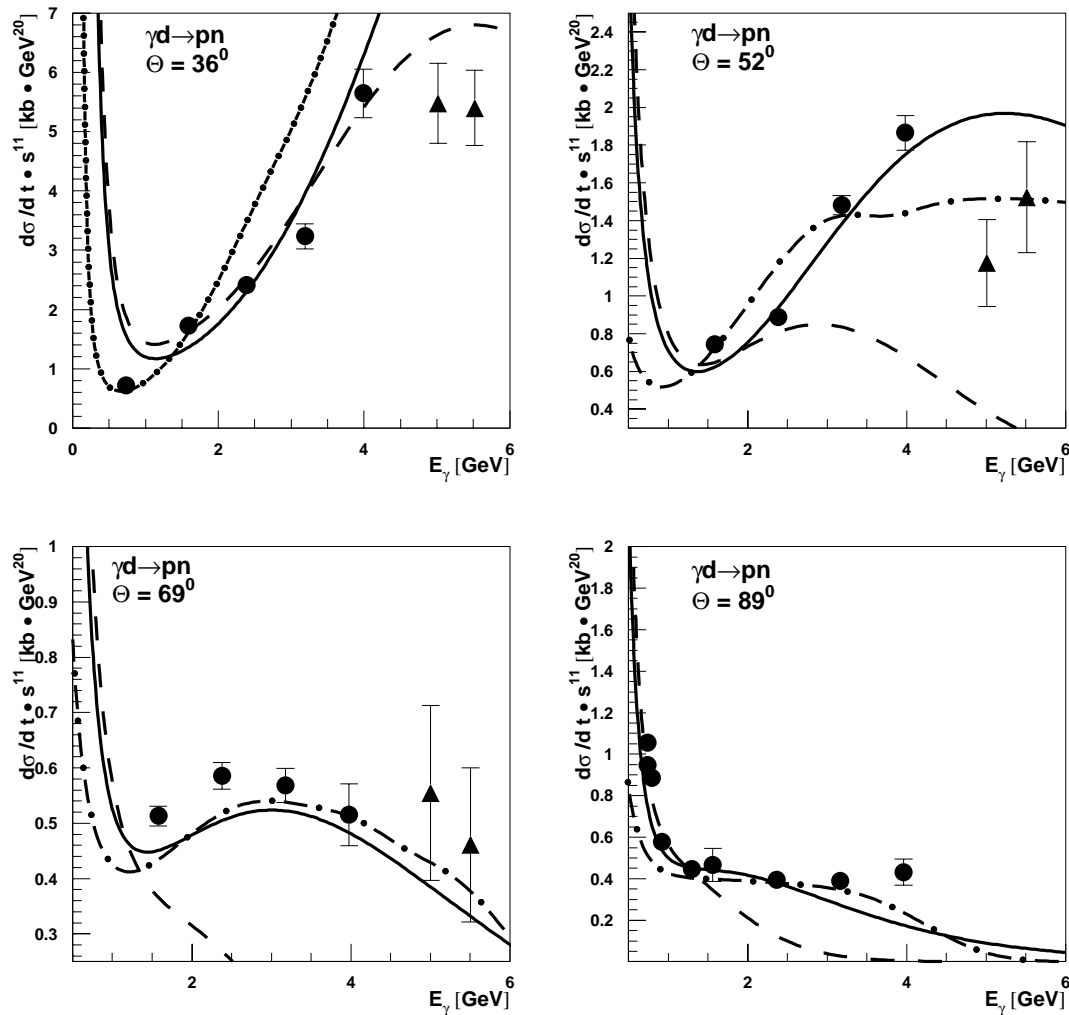


Figure 3: Differential cross section for the reaction $\gamma d \rightarrow pn$ (multiplied by s^{11}) as a function of the photon energy E_γ at different angles in the centre-of-mass frame in comparison to the experimental data from Refs. 4 and 6, The solid, dashed and dash-dotted curves are calculations using the logarithmic, the square root, and a phenomenological Regge trajectory, respectively.

Spin effects and the transversal polarization of the photon lead to a nontrivial angular dependence of the amplitude for the reaction $\gamma d \rightarrow pn$. Then, in the last year we have used an extended approach to the spin effects in QGS model ¹³⁾ as developed in ref. ¹⁴⁾ with respect to the de-

scription of the electromagnetic nucleon form factors F_1 and F_2 . Specifically, we have considered spin dependent hadron (photon)-quark and quark-hadron amplitudes assuming the dominance of those amplitudes that conserve s-channel helicities. The used parameters were fixed partly by previous analysis of data on the reaction $pp \rightarrow d\pi^+$ and partly by the Jlab data on the deuteron photodisintegration at $\theta_{c.m.} = 36^\circ$ ⁴⁾.

In addition, we have paid special attention to the use of nonlinear baryon Regge trajectories. This nonlinearity, which is well supported both by phenomenological evidences ¹⁰⁾ as well as theoretical arguments ^{11, 12)}, is not important for small t , but is very essential in the region of t covered by the experiment E-93-017. We have employed three different forms of nonlinear nucleon Regge trajectories: a phenomenological one, which becomes linear at large t , and two QCD motivated Regge trajectories of the logarithmic and square-root form, which are the limiting cases for a certain class of trajectories allowed in dual models ¹²⁾.

In Fig. 3 it is shown the differential cross section for the reaction (multiplied by s^{11}) as a function of the photon laboratory energy E_γ at the given angles in the center of mass frame in comparison to the experimental data from refs. (4,6). The QGS model with QCD motivated Regge trajectories provides a reasonable description of all the data, the logarithmic Regge trajectory doing better. Then the energy dependence of $d\sigma/dt$ at $\theta_{c.m.} = 36^\circ - 90^\circ$ provides new evidence for a nonlinearity of the Regge trajectory. The QGS model predicts that the $d\sigma/dt$ at fixed c.m. angle decreases faster than any finite power of $1/s$ and at sufficiently large energies the perturbative regime will become dominant. However, at the available s and t , the nonperturbative effects as described by the QGS model are quite important. We have also investigated the angular dependence of the cross section at different energies. This may have a dip at forward angles if the amplitude with a charge-like photon coupling is dominant. By introducing the interference of isovector and isoscalar contributions, we have calculated the forward-backward asymmetry for the cross section. This can be quite pronounced at $E_\gamma = 1.6$ GeV, but is a decreasing function of energy. Clearly, the new data from experiment E-93-017 for small and large angles will be important to check these predictions.

4 List of Publications

1. M. Anghinolfi *et al.*, Response to cosmic rays of the large angle calorimeter of the CLAS detector; Nucl. Instr. and Meth., **A447** (2000) 42.
2. CLAS Collaboration, E. Anciant *et al.*, Photoproduction of $\phi(1020)$ mesons on the proton at large momentum transfer, Phys. Rev. Lett. **85** (2000) 4682.
3. CLAS Collaboration, R. Thompson *et al.*, The $ep \rightarrow e'\eta p$ reaction at and above the $S_{11}(1535)$ baryon resonance, Phys. Rev. Lett. **1** (2001) 1702.
4. CLAS Collaboration, K. Lukashin *et al.*, Exclusive electroproduction of ϕ mesons at 4.2 GeV, Phys. Rev. **C 63** (2001) 065205.
5. V.Yu. Grishina *et al.*, Deuteron photodisintegration within the Quark-Gluon Strings Model and QCD motivated nonlinear Regge trajectories, Eur. Phys. J. A **10** (2001) 355.
6. CLAS Collaboration, S. Stepanyan *et al.*, Observation of exclusive virtual Compton scattering in polarized electron beam asymmetry measurements, Phys. Rev. Lett. **87** (2001) 182002.
7. CLAS Collaboration, S. Barrow *et al.*, Electroproduction of the $\Lambda(1520)$ Hyperon, Phys. Rev. **C** (2001) in print.

8. CLAS Collaboration, M. Battaglieri *et al.*, Photoproduction of ρ_0 Meson on the Proton at large momentum transfer, Phys. Rev. Lett. (2001) in print.

References

1. W. Brooks, for the CLAS Collaboration, Nucl. Phys. A663&664 (2000) 1077.
2. R. Holt, Phys. Rev. C **41** (1990) 2400.
3. S.J. Freedman *et al.* Phys. Rev. C **48** (1993) 1864 and J.E. Belz *et al.* Phys. Rev. Lett. **74** (1995) 646.
4. C. Bochna *et al.*, Phys. Rev. C **41** (1998) 4576.
5. K. Wijesooria *et al.* Phys. Rev. Lett **86** (2001) 2975.
6. E.C. Schulte *et al.*, Phys. Rev. Lett **87** (2001) 102302-1.
7. L.A. Kondratyuk, E. De Sanctis, P. Rossi, *et al.*, Phys. Rev. C **48** (1993) 2491.
8. N. Bianchi *et al.*, CEBAF proposal E-93-017.
9. D.I. Sober *et al.*, Nucl. Instr. and Meth. **A440** (2000) 263.
10. A.E. Inopin, hep-th/0012248.
11. M.M. Brisudová, L. Burakovsky and T. Goldman, Phys. Rev. **D61** (2000) 054013.
12. H. Ito, Prog. Theor. Phys. **84** (1990) 94, and Z.Chikovani, L. Jenkovaszký, F. Paccanoni, Mod. Phys. Lett. **A6** (1991) 1409.
13. V.Yu. Grishina, L.A. Kondratyuk, W. Cassing, A.B. Kaidalov, E. De Sanctis, P. Rossi, Eur. Phys. J. A **10** (2001) 355.
14. A. B. Kaidalov, L.A. Kondratyuk and D. Tevekin, Phys. Atom. Nucl. **63** (2000) 1395.

DEAR

M. Bragadireanu (Ass.), C. Guaraldo (Resp.), M. Iiescu, B. Lauss (Ass.)
V. Lucherini, F. Lucibello (Tecn), C. Petrascu

1 Aim of the DEAR experiment

DEAR (DAΦNE Exotic Atom Research) will observe X rays from kaonic hydrogen and kaonic deuterium, using the “ K^- beam” from the decay of ϕ s produced by DAΦNE. The DEAR setup, shown in Fig. 1, consists of a cryogenic pressurized gaseous target and Charge-Coupled Devices (CCDs) as x-ray detectors.

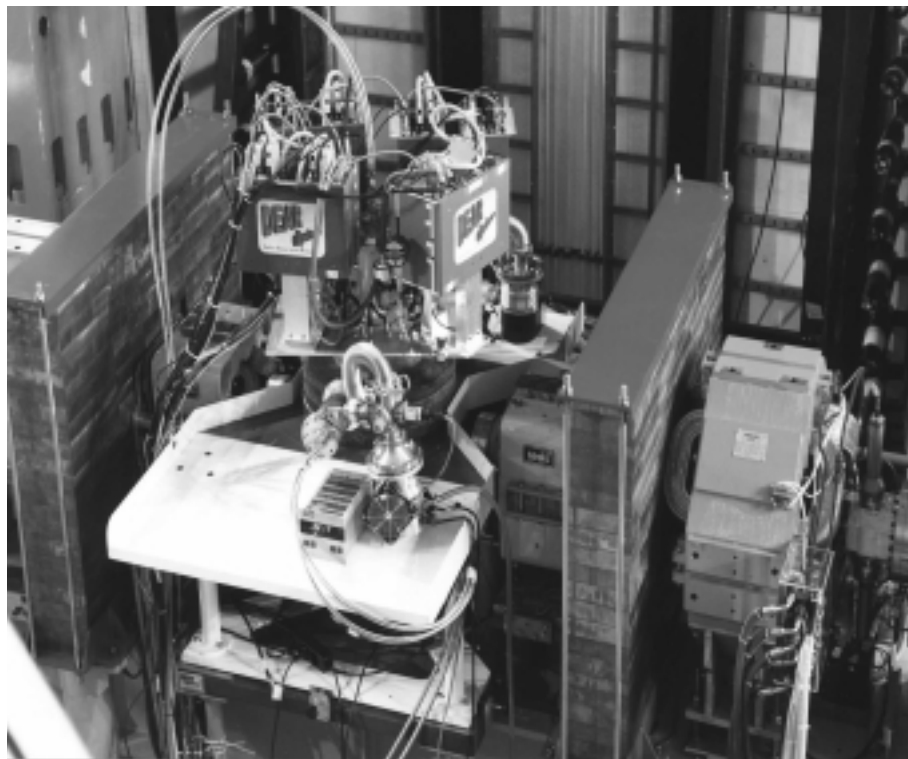


Figure 1: *DEAR cryogenic setup for the measurement of kaonic nitrogen.*

A kaonic atom is formed when a negative kaon enters a target, loses its kinetic energy through ionization and excitation processes of the atoms and molecules of the medium and eventually is captured, replacing the electron, in an excited orbit. Three processes then compete in the deexcitation of the newly formed kaonic atom: dissociation of the surrounding molecules, external Auger transitions and radiative transitions. When a kaon reaches low- n states with small angular momentum, it is absorbed through a strong interaction with the nucleus. The strong interaction causes a shift in the energies of the low-lying levels from their purely electromagnetic values, while the decreased lifetime of the state results in an increase of the observed level width. The shift ϵ

and the width Γ of the $1s$ state of kaonic hydrogen are related in a fairly model-independent way to the real and imaginary parts of the complex S -wave scattering length:

$$\epsilon + \frac{i}{2}\Gamma = 2\alpha^3 \mu_{K-p}^2 a_{K-p} = (412 \text{ eV fm}^{-1}) \cdot a_{K-p} \quad (1)$$

where α is the fine structure constant and μ_{K-p} the reduced mass of the K^-p system. This expression is known as the Deser-Trueman formula. A similar relation applies for the case of kaonic deuterium and the corresponding scattering length a_{K-d} .

DEAR aims a precision measurement of the shift and of the broadening, due to the strong interaction, of the K_α lines of kaonic hydrogen and kaonic deuterium. K^-d will be measured for the first time. In this way, a precise determination of the isospin dependent $\bar{K}N$ scattering lengths will be obtained. This will allow to determine the kaon-nucleon sigma terms. The sigma terms give a direct measurement of chiral symmetry breaking.

Presently, only estimates exist of the KN sigma terms. A measurement of $\bar{K}N$ scattering lengths at a percent level would enable the determination of the KN sigma terms with a precision of about 20% or less, to be compared with the 70% uncertainty of the present estimates.

The sigma terms are also especially important in connection with the strangeness content of the nucleon, that provides the SU(3) description of the nucleon beyond the SU(2) naïve picture. Indeed, the SU(3) structure of the nucleon appears more explicitly in quantities associated with chiral breaking. The strangeness fraction is dependent on both kaon-nucleon and pion-nucleon sigma terms, but is more sensitive to the first one.

1.1 Measurement of kaonic nitrogen

The first stage of the DEAR scientific programme is the measurement of kaonic nitrogen. This because the yields of the transitions in kaonic nitrogen are much higher than in kaonic hydrogen (x25) and therefore a relatively faster observation of exotic atoms is possible.

This stage of the experiment is developed in two phases. The first phase concerns the identification, measurement and possible reduction of the machine background. The check of the DEAR Monte Carlo routines for the background levels predictions is as well performed. In this phase, a setup consisting of a target at NTP, filled by air, is used. As x-ray detectors, 4 CCD-05 are used.

In a second phase, a cryogenic setup is employed with a target filled by cryogenic (120 K) and pressurized (2 bar) nitrogen (equivalent density: $\rho \simeq 5\rho_{NTP}$) and, as detectors, 8 large area CCD-22 and 4 CCD-05. The goal is to optimize the distribution of stopped kaons in order to increase the final yields and to perform the first measurement of the kaonic nitrogen spectrum.

Most of the experimental activities, in laboratory and on the machine, as well as all what concerns simulations, are care of the LNF group. Data taking and analysis are shared among the groups of the collaboration, which include an other INFN group, the Trieste group.

2 Activity in 2000

In the year 2000, the first phase of the kaonic hydrogen measurement has been completed. This phase consisted in studying the machine background and trying to find a strategy to reduce it. An other important objective was to check the DEAR Monte Carlo routines by comparing the calculated background with the measured one.

Most of background measurements were performed in a machine configuration in which the beams were colliding in the KLOE interaction point and split in the DEAR one. In some cases, only one beam was circulating. Two periods with collisions in the DEAR IP occurred as well: in

September and in December 2000. These period allowed to fix the state of the measurement, by evaluating the ratio “predicted signal/measured background”

The study of background in the setup was initially focussed in determining the incoming direction. It turned out a ”bottom origin” of the background: the detectors were essentially hit by the particles entering the target directly from the pipe, through the aperture in the platform and the entrance windows, as well as by particles making showers in the aluminium of the platform. The bottom of the setup was consequently especially considered for the shielding. In particular:

- layers of lead, up to 4 cm, were put below the target cell. The total thickness took obviously into account the reduction of solid angle;
- disk-shaped lead layers were put inside the target;
- all the cylindrical path through the holes in the lead layers, below and inside the target, as well as in the aluminium of the platform, from the beam pipe up to the CCDs, was shielded by polyethylene cylinders. In fact, low energy X rays can be produced inside the “tube” formed by the holes in the lead layers and in the platform by large angle Bremsstrahlung of high energy electrons (positrons) lost by Touschek effect from the circulating beams. This dangerous background can be absorbed by cylinders of polyethylene inserted in all the apertures;
- the cylindrical apertures of the vacuum chambers of the CCDs were as well shielded by polyethylene cylinders. It was in fact checked that the aluminium electronic peak at 1.4 KeV, seen in the x-ray energy spectrum, comes predominantly from the excitation of the aluminium part of the setup which is close to the CCDs, constituting their frame, at the entrance of the vacuum chambers. This frame can therefore be as well a source of Bremsstrahlung X rays, able to reach directly the nearby chips. One can absorb these low nergy X rays by inserting small cylinders of polyethylene at the entrance of the CCDs vacuum chambers.

All these shielding techniques allowed a reduction factor of the background (clusters – multi pixels events – and soft X rays) of about a factor of ten.

In the DEAR runs of December 2000 the signal/ratio was evaluated starting from the Monte Carlo predictions referred to the “fully shielded” setup described above, and by measuring the background when the beams collide in the DEAR IP.

Fig. 2 shows an x-ray energy spectrum taken in the December 2000 runs. The spectrum suffers for poor statistics due to machine problems, however, it is rich of well identified electronic excitations. The more striking feature is the almost complete disappearance of the Al peak at about 1.4 KeV, the dominant peak in all the energy spectra obtained so far. The cut of the aluminium peak is a good check of the hypothesis formulated for shielding the cylindrical aperture of the vacuum chambers of the CCDs.

As a consequence of the suppression of the Al peak, the Si peak coming from the electronic excitation of the silicon atoms of the CCD chips, becomes more apparent – and therefore can eventually be used for calibration – with respect to the small shoulder of the Al peak, as it appeared in all previous spectra.

Another feature of the spectrum is the appearance of lines corresponding to transitions of excited atoms of lead put inside the target. These X rays can reach the CCDs having energies above 10 KeV, but, in principle, could be easily absorbed, as we could check in some tests, by wrapping the lead disks in the target with few hundred microns of aluminium foils. However, these Pb peaks fall in an energy region missing of scientific relevance, therefore their eventual absorption was not taken into consideration.

The more significant information which can be drawn from the spectrum is, obviously, the evaluation of the background at the position of the most easily observable kaonic nitrogen transitions. In the interval $(7.20 \div 8.28)$ keV around the 7.6 keV line corresponding to the $6 \rightarrow 5$ transition of kaonic nitrogen, 921 X rays can be counted. This number corresponds to 153 background events within the 180 eV (FWHM, resolution of the setup) width of the line. Needless to stress that the collected integrated luminosity, 60 nb^{-1} , is by far too low to see any signal. The expected counting rate for the 7.6 keV transition, with the present setup, is 0.05 events per nb^{-1} , which corresponds in this case to 3 good events.

Despite the positive achievement in reducing the DAΦNE background, the signal to background ratio was still far from a realistic (in terms of necessary integrated luminosity) possibility to measure kaonic nitrogen transitions. The actual machine conditions suggested therefore to use the cryogenic setup, already foresaw for the measurement of kaonic hydrogen, also for the measurement of kaonic nitrogen.

The cryogenic setup allows in fact an enhancement both of the signal and of the shielding factor. This is due to a bigger detector solid angle and intrinsic efficiency, to an increased rate of kaonic atoms formation for the higher density of the cryogenic target, and to a better compactness of the setup, which allows a more efficient shielding.

3 Activity in 2001

The activity foreseen in 2001 consists in the final tests in laboratory of the cryogenic setup for the measurement of kaonic nitrogen; in the installation on DAΦNE of the setup; in a first period of data taking dedicated to the optimization of the kaon stopping points distribution, in terms of higher number of transitions, obtained by tuning the kaons degrader; in a second period of data taking with the objective to measure for the first time the kaonic nitrogen spectrum, having optimized the performance both of the machine and of the setup.

The expected increasing of the signal with the cryogenic setup is due, on one side, to the increased density of the gas target (for $T=118\text{K}$ and $P=2$ bar, $\rho \simeq \rho_{NTP}$); on the other side, to the increased number of detectors: 4 CCD-05 and 8 CCD-22, the latter with larger area, higher depletion layer and higher efficiency. The expected increasing in background reduction is obtained acting on many parts of the setup. Firstly, the whole interaction region has been more shielded by reinforcing ($\times 2$ thickness = 200 mm) the lead walls installed on the beam pipe at the two sides of the interaction point. Moreover, the central zone of the aluminium platform was done by pure lead, so reinforcing the “bottom shielding”, against the main flux of background particles. Finally, a special attention was paid to the “internal shielding”, so indicating the shielding of all those parts of the setup which fall within the solid angle seen by the CCDs. The internal shielding regards specifically:

- the cylindrical path through the platform up to the bottom of the vacuum chamber;
- the aluminium frames of the windows of the target cell.

“Golden rule” for the “internal shielding”, learned and applied working with the NTP setup, is the use of sandwich-type structures, made by initial high Z /high density materials, to finish with low Z high materials. Typically, the sequence of layers is lead–aluminium–polyethylene.

4 Publications 2000

4.1 Papers

1. M. Augsburg *et al.*, First measurements at the DAΦNE ϕ -factory with the DEAR experimental setup. Nuclear Instruments and Methods in Physics Research **A** 452 (2000)

306.

2. B. Lauss *et al.* (DEAR Collaboration), The DEAR experiment on DAΦNE, *Acta Physica Polonica B*, Vol.31, No. 10-11 (2000) 2257.
3. V. Lucherini *et al.* (DEAR Collaboration), The DEAR experiment, *Journal of Milan University "Ricerca Scientifica ed Educazione Permanente"*, Supplement N.115, Milan (2000) 375.

4.2 Technical Notes

1. M. Bragadireanu *et al.*, The DEAR Kaon Monitor: results of the first measurements, DEAR Note-IR-16, January 24, 2000.
2. M. Bragadireanu *et al.*, The background measurements with the NTP setup in the first period of collisions in the DEAR interaction region, DEAR Note-IR-17, January 20, 2000.
3. C. Guaraldo *et al.*, Topping-up effect on the background measured in the DEAR interaction region when beams collide in the KLOE interaction point, DEAR Note-IR-18, March 7, 2000.
4. B. Lauss *et al.*, Study of fluorescence excitation, optimal location of calibration foils and x-ray background rates, DEAR Note-IR-19, March 20, 2000.
5. C. Petrascu, DEAR Monte Carlo results for the "16 CCD-22" cryogenic target setup, DEAR Note-IR-20, April 10, 2000.
6. R. King *et al.*, A new CCD command box, DEAR Note-IR-21, May 2, 2000.
7. C. Petrascu, DEAR Monte Carlo results: X-ray signals from different kaonic atoms and different setups, DEAR Note-IR-22, June 14, 2000.
8. B. Lauss *et al.*, Comparison of background measurements in the DEAR interaction region for collisions in KLOE in December 1999 and July 2000, DEAR Note-IR-23, July 21, 2000.
9. M. Iliescu *et al.*, Electron versus positron background measurements in the DEAR interaction region, DEAR Note-IR-24, July 26, 2000.
10. M. Iliescu *et al.*, Check of the background sources with the NTP setup, DEAR Note-IR-25, August 18, 2000.
11. B. Lauss, X-ray rate restriction in charge-coupled devices, DEAR Note-IR-26, August 28, 2000.
12. T. Ishiwatari, Energy spectrum improvement and the effect of minimum ionizing particles on CCDs resulted with a new analysis software, DEAR Note-IR-27, September 7, 2000.
13. T. Ishiwatari, Noise level fluctuations and the reduction of periodic noise occurring in CCD x-ray data, DEAR Note-IR-28, September 19, 2000.
14. G. Beer *et al.*, Report on the run period August-September 2000: NTP setup with CCD detectors, DEAR Note-IR-29, September 25, 2000.
15. G. Beer *et al.*, Report on the run period August-September 2000: Kaon Monitor, DEAR Note-IR-30, October 3, 2000.

16. C. Petrascu, Monte Carlo simulation based on GEANT for the study of the DAΦNE scrapers. Preliminary results, DEAR Note-IR-31, October 30, 2000.
17. C. Petrascu, DEAR Monte Carlo results for the cryogenic target setup filled with nitrogen , DEAR Note-IR-32, November 6, 2000.
18. C. Petrascu, Kaonic nitrogen X rays detection by background subtraction, DEAR Note-IR-33, November 7, 2000.

4.3 Presentations to international conferences

1. C. Guaraldo, The DEAR experiment on DAΦNE, International Conference on Hypernuclear and Strange Particle Physics, Torino, 23-27 October, 2000.
2. C. Curceanu (Petrascu), The DEAR experiment on DAFNE, Workshop on Frontier Tests of Quantum Electrodynamics and Physics of the Vacuum, QED 2000, Trieste, 5-11 October, 2000.
3. V. Lucherini, The DEAR Experiment, 9th International Conference on Nuclear Reaction Mechanisms, Villa Monastero, Varenna (Italy), 5-9 June, 2000.
4. B. Lauss, The DEAR Experiment on DAFNE, MESON 2000 Workshop, Cracow (Poland), 19-23 May, 2000.

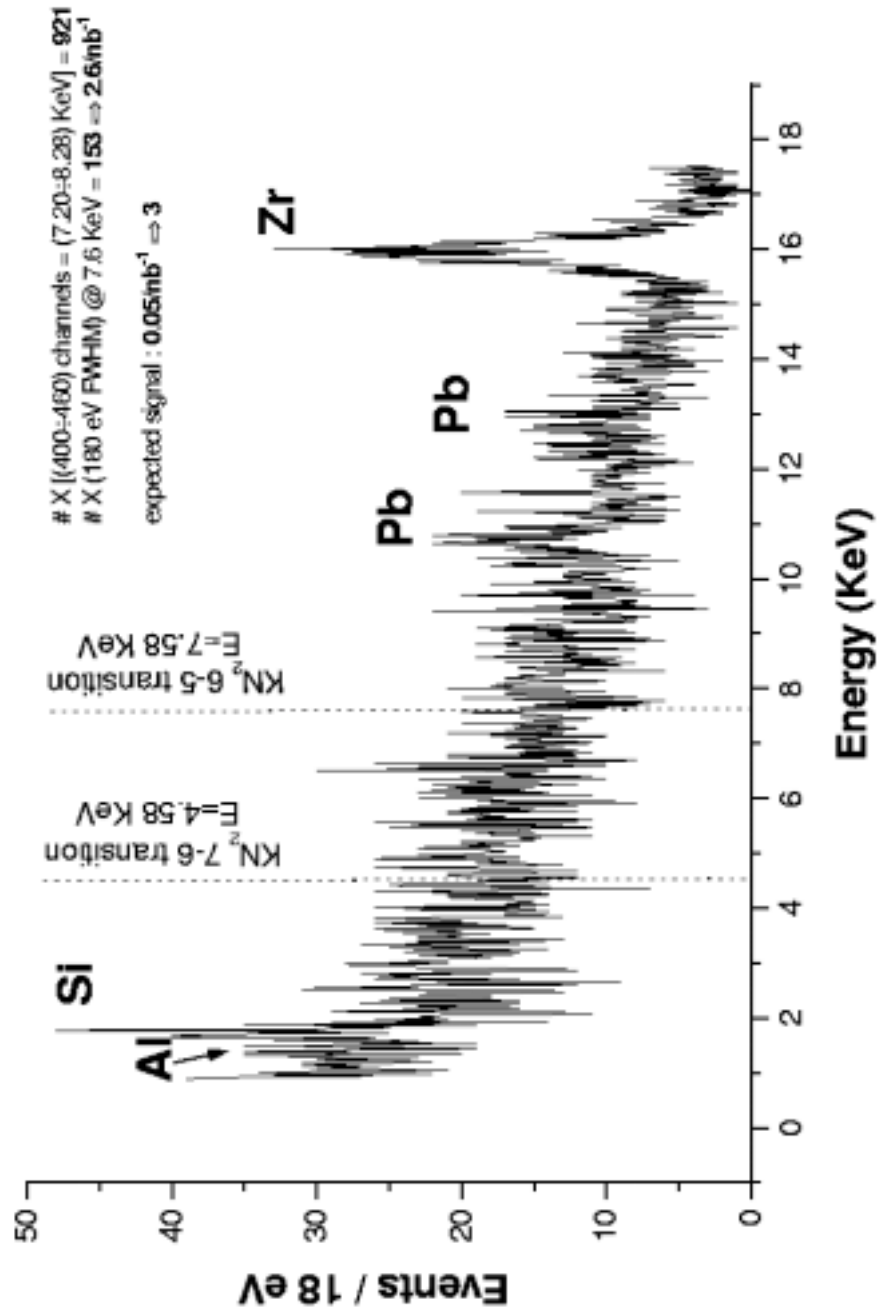


Figure 2: CCD spectrum from December 2000 runs for 60 nb⁻¹ integrated luminosity. Electronic x-ray lines from atomic excitation of the materials of the setup are visible. The positions of the two more easily observable kaonic nitrogen lines are indicated.

DIRAC

P. Gianotti (Resp.), M. Giardoni, C. Guaraldo, M. Iliescu, A. Lanaro (Resp. Naz.),
P. Levi Sandri, V. Lucherini, C. Oana Petrascu

1 Introduction

The DIRAC (Dimeson Relativistic Atomic Complex) Experiment at CERN will submit Chiral Perturbation Theory (ChPT) to a stringent test, by measuring, in a model independent way, the difference between the isoscalar (a_0) and isotensor (a_2) S -wave pion-pion scattering lengths with 5% accuracy. Such determination will be done through a measurement (with 10% accuracy) of the lifetime of Pionic Atoms ($A_{2\pi}$), a weakly bound $\pi^+\pi^-$ system at threshold, produced by proton-nucleus interactions at 24 GeV/c.

The present theoretical estimate of the lifetime of the ground state of the dimeson atom, from calculations performed within the framework of standard ChPT, is $(2.9 \pm 0.1) \cdot 10^{-15} s$ ¹⁾.

The DIRAC experimental apparatus is located at the CERN PS East Hall. It consists of a double arm magnetic spectrometer, consisting of high resolution tracking and particle identification detectors. It is designed to detect with high efficiency charged pion pairs with small relative momentum ($Q < 3 \text{ MeV}/c$), and small opening angle ($\simeq 0.35 \text{ mrad}$). The experiment was approved in 1996, the commissioning was done at the end of 1998 and the apparatus became fully operational in the spring of 1999.

The DIRAC Collaboration includes 83 participants from 19 international Institutes. 14% of the participants are from Italian Institutes (INFN-LNF and Trieste University/INFN). About 25% of leadership roles within the collaboration is granted to INFN members. The yearly budget contribution from INFN to the Experiment amounts to $\sim 20\%$ of the total budget.

The LNF group has contributed to the experiment by providing 2 large threshold Cherenkov counters for e^+e^- identification. The counters use gaseous nitrogen as radiator. Each counter is equipped with 20 mirrors and 10 photomultipliers. The Cherenkov detectors ensure e^+e^- rejection at the trigger level with 99.5% efficiency, and 15 photoelectrons are on average detected in each counter.

2 Experimental activity in 2000

During the early months of 2000, the DIRAC-LNF members have participated to the analysis of the experimental data collected in 1999, devoted mainly to the observation of $A_{2\pi}$. The analysis was performed on a sample of $\sim 150 \cdot 10^6$ triggers, from proton interactions on Ni and Pt targets.

In order to observe $A_{2\pi}$ atoms, the experimental Q -distribution of time-correlated $\pi^+\pi^-$ pairs is compared with the expected distribution of $\pi^+\pi^-$ pairs with (Coulomb) and without (non-Coulomb) final state interaction, namely pairs associated to short (ρ, ω) and long-lived (η, K_s^0) sources, respectively. The latter is computed from the experimental distribution of accidental $\pi^+\pi^-$ pairs, registered simultaneously with the correlated pairs. The two distributions are subtracted one to the other; the difference spectrum should lead to an excess of $\pi^+\pi^-$ pairs at low Q ($\leq 3 \text{ MeV}/c$). This represents the physics signature for $A_{2\pi}$ production. The $\pi^+\pi^-$ pairs in the signal are called *atomic pairs*, as they result from the electromagnetic interaction of $A_{2\pi}$ with the target atoms. The ionization process ($A_{2\pi} \rightarrow \pi^+\pi^-$) competes with the decay of $A_{2\pi}$ into two neutral pions. The latter decay rate is proportional to the square of the difference $a_0 - a_2$, which is known from theory with 1.5% precision ²⁾.

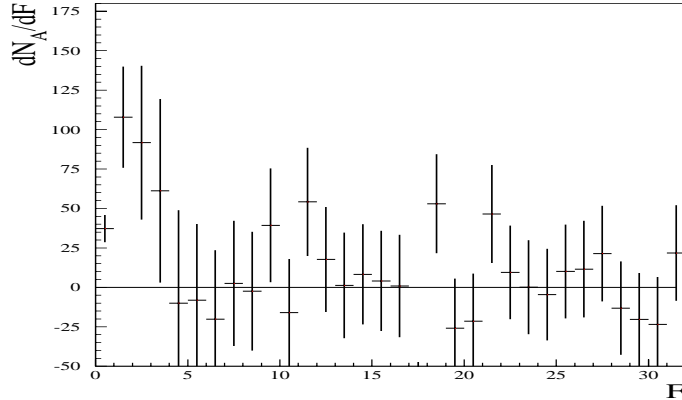


Figure 1: *Signal distribution from 1999 Pt target data. The dimensionless variable F is defined as: $F = \sqrt{\left(\frac{Q_L}{\sigma_{Q_L}}\right)^2 + \left(\frac{Q_X}{\sigma_{Q_X}}\right)^2 + \left(\frac{Q_Y}{\sigma_{Q_Y}}\right)^2}$, where $\sigma_{Q_L} = 0.65 \text{ MeV}/c$, $\sigma_{Q_X} = \sigma_{Q_Y} = 1 \text{ MeV}/c$ are experimental uncertainties.*

The measurement of the fraction of ionized atoms, i.e. the $A_{2\pi}$ ionization probability, yields a value for the $A_{2\pi}$ lifetime and, thus, for the pion-pion scattering lengths. The relation between the atom lifetime and the strong S -wave $\pi\pi$ scattering lengths is ^{1, 3, 4)}:

$$1/\tau = \Gamma_{2\pi^0} = C(a_0 - a_2)^2 |\psi(0)|^2 (1 + \delta_\Gamma) \quad (1)$$

where $\psi(0)$ is the $A_{2\pi}$ wave-function at the origin, a_0 and a_2 are the S -wave $I=0,2$ $\pi\pi$ scattering lengths, δ_Γ is a higher order correction factor to the pionium width Γ .

About 700 atomic pairs have been detected from the analysis of the 1999 Ni and Pt target data. The signal resulting from the analysis of the $\approx 50 \cdot 10^6$ triggers collected with the Pt target is shown in Fig.1. As explained above, the spectrum was obtained by subtracting from the experimental distribution of reconstructed $\pi^+\pi^-$ pairs the expected contributions of Coulomb and non-Coulomb pairs. In the region $Q < 3 \text{ MeV}/c$, $\approx 250 \pm 80$ atomic pairs are detected. At larger Q -values the subtraction procedure shows to be accurate.

The LNF group has been actively contributed to the detectors calibration and offline data reduction. More in general, it has participated to the study of the detectors performance and to the development of the analysis software code, up to the extraction of the final physics signal.

Calibration using particle decay was performed by reconstructing the invariant mass of $p\pi^-$ pairs. Fig.2 shows a well resolved Λ signal, with a standard deviation $\sigma_\Lambda = 0.43 \text{ MeV}/c^2$, which yields the best precision if compared to all previous determinations ⁵⁾.

During the 21 weeks of data taking (from April to November, 2000) the LNF members have participated to the run shifts, taking responsibility for the maintenance and the monitoring of the performances of the Cherenkov and Preshower detectors. In addition, they were coordinating the activity of the team responsible for the offline monitoring of the data quality. Useful contributions to the DAQ and equipment monitoring (slow control) were also provided.

A software simulation of the geometry and physics response of the Cherenkov detectors were made available to the Collaboration, and became part of the full DIRAC Monte Carlo program.

In the 2000 run, more than $1.4 \cdot 10^9$ triggers have been collected, with both Ni and Ti targets. From a preliminary analysis of the Ni data, consisting of $\approx 10^9$ triggers collected in 89 days, more

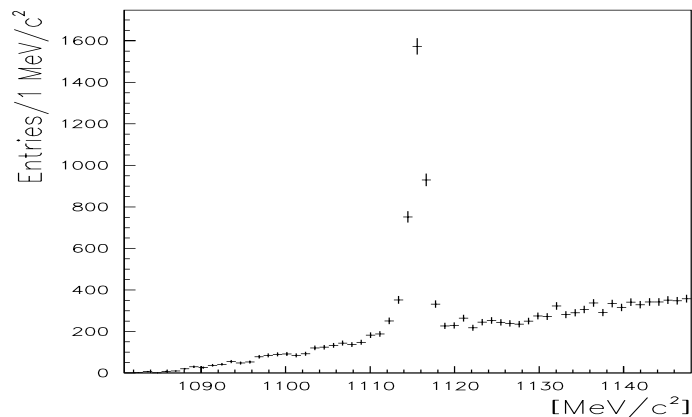


Figure 2: *Invariant mass spectrum of $p\pi^-$ pairs detected by the spectrometer.*

than 2000 atomic pairs have been detected in the low- Q (low- F) region. The $A_{2\pi}$ signal is shown in Fig.3. The LNF group has been involved in this analysis.

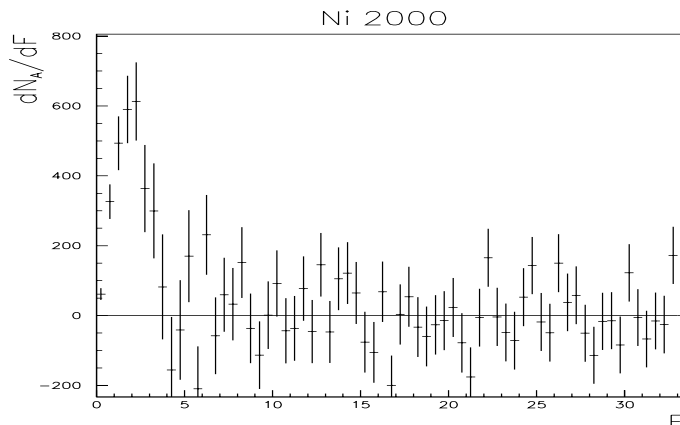


Figure 3: *Signal distribution from Ni 2000 data. The variable F was defined in Fig.1.*

Using the full statistics collected in 2000 the uncertainty on determination of the $A_{2\pi}$ lifetime will be of the order of 30%. The final goal (10% accuracy on $\tau(A_{2\pi})$) is expected by the end of 2002.

In September 2000, the DIRAC Collaboration has submitted to the CERN Scientific Committee (SPSC) an addendum to the present experimental programme ⁶⁾. In the proposal of extension beyond 2002, it is envisaged a more accurate determination of the $\pi\pi$ scattering lengths, to the level of the present theoretical accuracy, and the first observation and lifetime measurement of πK atoms ($A_{\pi K}$), from which to derive a determination of the S -wave pion-kaon scattering lengths ($a_{1/2}, a_{3/2}$). The proposed upgrades to the experimental apparatus are minimal, and con-

cern mainly the particle identification system. Two additional threshold Cherenkov counters filled with heavy gas (Freon 114 or SF₆) will allow K to π discrimination at the trigger level. Moreover, one Aerogel Cherenkov detector is necessary to provide K^+ to p separation.

The LNF group was responsible for the proposal of upgrade of the particle identification system. The technical design of the new detectors and a project feasibility study was performed by the LNF team members. CERN management has not yet approved the new proposal.

3 Planned activity in 2001

DIRAC is granted 6.5 months of running time in the year 2001. Data taking with Ni and Ti targets is foreseen to continue. The combined statistics with the two targets should allow to determine the $A_{2\pi}$ lifetime with 15% accuracy. No major upgrades of the experimental apparatus are envisaged. However, a trigger level exploiting on line reconstruction of tracks in the drift chamber system will be implemented. In addition, shielding against background particles will be improved. The aim is to increase the yield of detectable $A_{2\pi}$ per one proton-nucleus interaction.

Collaborators from LNF will participate to the background study and to the implementation of additional shielding. The participation to the data taking shifts will continue, as well as the involvement in the analysis of collected data.

Concerning the $A_{\pi K}$ proposal, the LNF group is planning a test with a heavy gas radiator (SF₆) in the summer of 2001. The existing Cherenkov counters will be used to investigate the K to π discrimination capability. The goal is to provide a physics signature through the detection of the $\phi(1020) \rightarrow K^+K^-$ decay.

Test samples of Aerogel tiles with very low index of refraction ($n \leq 1.009$) have been requested to manufacturers in Dubna and Novosibirsk (Russia). Delivery is expected in the first half of 2001. Tests are planned in 2002.

4 Publications and reports to Conferences

1. P. Gianotti representing the DIRAC Collaboration:
"Test of chiral perturbation theory with DIRAC at CERN",
contributing talk to Meson 2000 Workshop, 19-23 May 2000, Cracow [Poland], Acta Physica Polonica B Vol.31 N.10-11 (2000) 2571.
2. A. Lanaro representing the DIRAC Collaboration:
"A determination of the S-wave pion-pion scattering lengths from the measurement of the lifetime of ponium",
invited talk to Int. Conf. on High Energy Physics [ICHEP 2000], 27 July - 2 August 2000, Osaka [Japan], Proc. ICHEP 2000, World Scientific Vol.1 (2000) 359.

References

1. A. Gall, J. Gasser, V. Lyubovitskij, A. Rusetsky, Phys. Rev. D **64**, 016008 (2001).
2. G. Colangelo, J. Gasser, H. Leutwyler, Phys. Lett. B **488**, 261 (2000).
3. M. Ivanov, V. Lyubovitskij, E. Lipartia, A. Rusetsky, Phys. Rev. D **58**, 094024 (1998).
4. H. Jallouli and H. Sazdjian, Phys. Rev. D **58**, 014011 (1998).
5. E. Hartouni et al., Phys. Rev. Lett. **72**, 1322 (1994).
6. B. Adeva et al., the DIRAC Collaboration, CERN/SPSC 2000-032, SPSC/P284 Add.2, 17 August 2000.

FINUDA

L. Benussi(Ass. Ric.), S. Bianco, M. Bertani, M.A. Caponero (Ass.), F.L. Fabbri(Resp.),
P. Gianotti, M. Giaroni, V. Lucherini (Resp.), E. Pace, M. Pallotta,
L. Passamonti(Tecn.), D. Pierluigi(Tecn. Art.15), F. Pompili(Bors.), N. Quaiser(Bors.),
A. Russo(Tecn. art.15), S. Sarwar, S. Tomassini(art.23)

1 Introduction

FINUDA (meaning FIsica NUcleare a DAΦNE) is an experimental set up whose aim is the study of hypernuclei formation and decay within the same apparatus. Hypernuclei are nuclei in which a bound nucleon, baryon made of only u (up) and d (down) quarks, is replaced by a hyperon, baryon made also by s (strange) quarks. The added flavour enlarges the basic nucleon-nucleon interactions also to the strange sector: the so changed level scheme of the involved nucleus gives hence information on the modification of the properties of baryon-baryon interaction due to strangeness. High resolution hypernuclear spectroscopy can also, in principle, reveals in a more clearly way a partial deconfinement of quarks in nuclear matter.

The DAΦNE e^+/e^- collider is optimised in *Luminosity* at the *c.m.* energy corresponding to the $\phi(1020)$ meson. The huge number of ϕ s, produced (almost) at rest, decay with a *B.R.* of 0.49 into back-to-back pairs of slow ($127 \text{ MeV}/c$) charged kaons. The K^- s, stopped by a thin target, can hence produce hypernuclei, through the reaction (inside one of the target nuclei):



The levels of the produced hypernucleus can be obtained through an accurate measurement of the momentum of the emitted (*prompt*) π^- . Since the kaons from DAΦNE have a very low and sharp momentum, they can be stopped in very thin targets, allowing unprecedented resolution (0.3pc) to be reached in hypernuclear spectroscopy. Moreover, the subsequent decay of the hypernucleus, both *mesonic* ($p+\pi^-$) and *non-mesonic* (np or nn) can be detected by FINUDA, allowing the simultaneous study of formation and decay of hypernuclei within the same apparatus, a feature never reached in previous experiments. In particular the measurement of the ratio of the two *non-mesonic* decay channels np or nn will allow to obtain the rather elusive information on weak interaction effects between baryons ($\Delta I = 1/2$ rule). The foreseen counting rate for a peak *Luminosity* at DAΦNE of $3 \times 10^{31} \text{ cm}^2 \text{ s}^{-1}$ is 25 produced hypernuclear states per hour, higher of that of existing or planned facilities. In this respect, it should be considered that the top luminosity foreseen for DAΦNE is $10^{32} \text{ cm}^2 \text{ s}^{-1}$. FINUDA is a large acceptance magnetic spectrometer based on a medium sized superconducting solenoid (2.7 m long and 2.4 m diameter), operating at a maximum field of 1.1 T. The inner of the solenoid is equipped with tracking detectors, time-of-flight scintillator barrels and vertex detectors, also embedding a system of multiple targets. The volumes between the tracking detectors are filled with He gas in order to reduce the deterioration of resolution due to multiple scattering effects. A special and complex system of thin windows bags (He bag) is used for this purpose. A sketch of FINUDA spectrometer is shown in fig.1), which also reports the name and type of the different detectors. An extensive description of the FINUDA experiment can be found in 1), 2), and 3).

2 Activity up to January 2001

The FINUDA Collaboration is formed by almost 50 physicists from LNF, several INFN sections and Universities (Torino, Bari, Trieste, Pavia, Brescia) and with the participation of researchers from TRIUMF Laboratory of Vancouver, Canada.

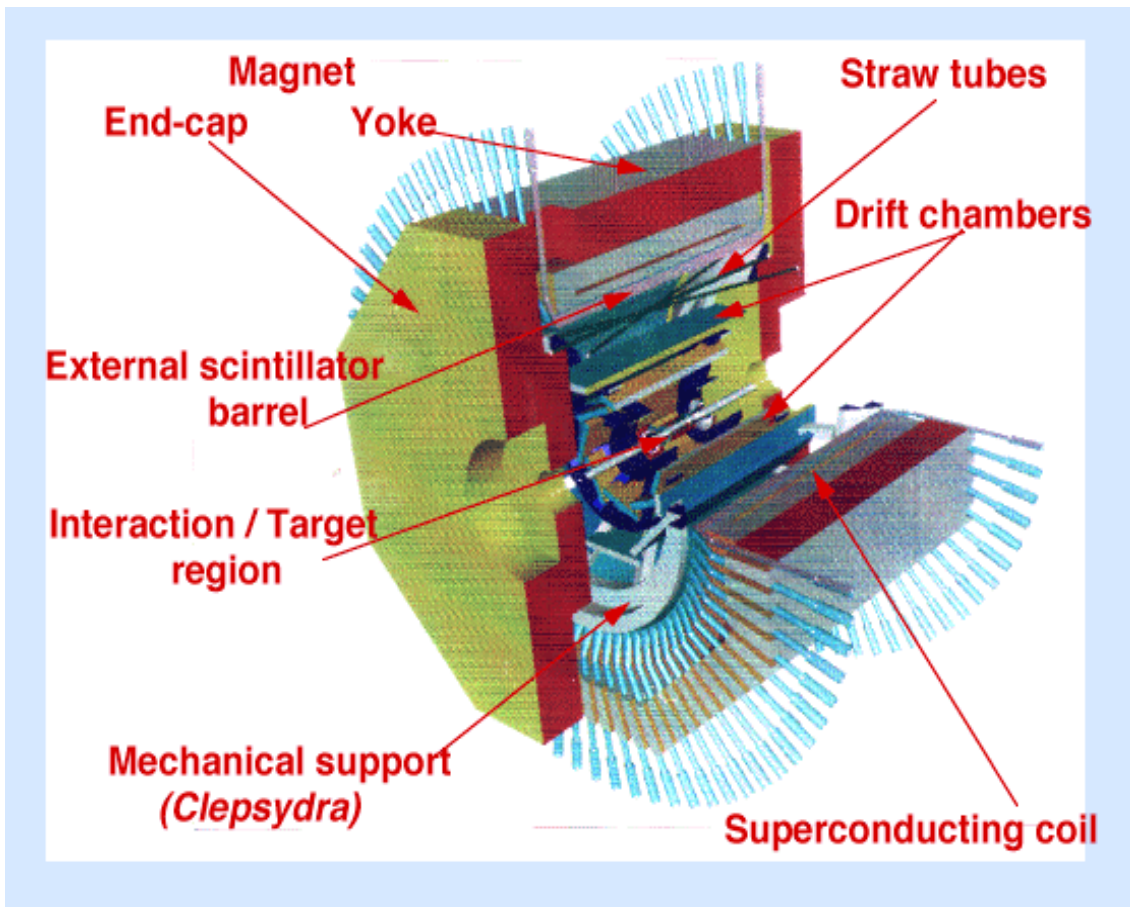


Figure 1: *Three dimensional layout of the FINUDA apparatus.*

The FINUDA-LNF group is charged of different tasks within the Collaboration. It has the full responsibility of the outer tracking detector of the experiment. Moreover, It is involved in the ON-Line activity, Monte Carlo simulation, coordination of the activity at LNF of all the external groups with responsibility of the laboratory ASTRA, of the counting room and pit installations. Finally, the LNF group has been involved in the activity related to the construction, test, mapping of the superconducting solenoid and is involved, together with the D.A. division, in the operation of the magnet.

2.1 Activity on straw tubes: the external FINUDA tracker

The most external tracker of FINUDA is made of long straw tubes. The use of straw tubes was dictated by the well known deterioration of plane drift chamber resolution as the hitting tracks deviate from the normal. The deviation from normal hitting is very relevant in the external region of FINUDA (at about 1.2 m from centre) due to the distance and the high curvature impressed by the strong field (to gain in resolution) to the relatively low momentum pions (270 MeV/c) from hypernuclei formation. The straw tubes with their circular shape obviously overcome this problem. The straw tubes used in FINUDA are made of thin (30μ) aluminized mylar, in order to reduce multiple scattering effects. The overall array consists of 2424 straws, with a diameter of 1.5 cm and a length of 250 cm, each embedding a 30μ thick gold-plated anode wire. The straws are arranged, starting at a radius of 116 cm from the axis of the solenoid, in six layers each with an equal number of straws and are organized in three superlayers. The first superlayer is parallel to z-axis, while the other two are tilted of an angle of $+12.5$ degree and -12.5 degree, respectively, respect to it (stereo straws). All the straws were built at LNF by the local Finuda group, individually tested and mounted in the mechanical structure supporting almost all the detector of the experiment (*Clepsydra*). Also the electronics for the straw (preamplifiers and the double-threshold discriminators) are a project of the local group. Once installed the straw were again tested as a whole during several periods of data taking with cosmic rays in the ASTRA laboratory where the *Clepsydra* was positioned waiting to be moved inside the Finuda magnet in DAΦNE. The performance in resolution of the straw detector turns out very good, showing a radial resolution of 180μ with a gas mixture of Ar-Ethane (50-50). The z resolution obtained with the stereo straw is 500μ . In fig.2) the obtained resolution for the straws is shown.

2.2 Activity on other FINUDA detectors

The other detectors of FINUDA are responsibility of the different external groups of the collaboration. The local group has been, however, also partially involved in several aspects relating to them (from logistic, to technical assistance and support). For this reason a brief description of the activity done on the different FINUDA detectors is here reported too.

2.2.1 *The outer scintillator Barrel: TOFONE*

The TOFONE detector (responsibility of the Bari-INFN section) is made of a barrel of 72 scintillator slabs, 270 cm long and 10 cm thick. The barrel is intended for detection of the prompt π^- from hypernuclei formation and of the charged and neutral nucleons from hypernuclei decay. Each slab has a trapezoidal shape and is seen at both sides by an XP2020 phototube operated outside the magnet. For this reason the coupling scintillator-phototube is made by means of a 90 degree deflector prism coupled, through a conical connection, to a straight cylindrical light guide. Each slab is also equipped with an optical fibre glued in the centre for calibration purposes by means of a laser. This detector is the only one mounted directly on the magnet and not supported by the *Clepsydra*. It is ready and stored in an area of LNF waiting for installation on the magnet.

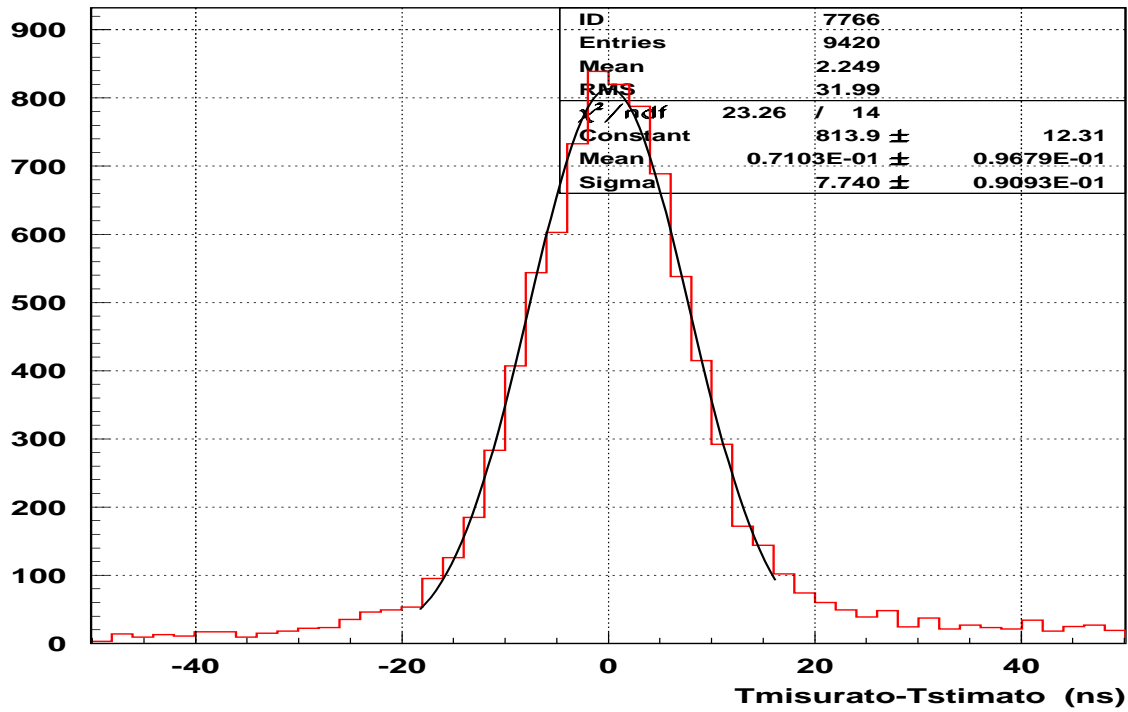


Figure 2: The residual time resolution of the FINUDA straw detector, which, for a drift velocity of $50 \mu/\text{s}$ translates in a spatial resolution of 180μ .

2.2.2 The planar drift chambers

A double layer of planar drift chambers constitutes the detector of the central tracking region of FINUDA. They are responsibility of Torino INFN section and University and, for the manufacturing, of TRIUMF Laboratory. The first layer is located at 30 cm from the solenoid axis, while the second is at a radius of 60 cm from it. Each layer is made of 8 planar, thin windows (6μ), planar drift chambers, operated with a mixture of HE-Isobuthane (70-30). The dimensions of each chamber are (second layer in parenthesis): 123 cm long (187 cm) and 39.6 cm wide (68.6 cm). A $x - y$ resolution of 150μ and of 510μ in z (by charge division) has been experimentally obtained.

2.2.3 The vertex region

The FINUDA vertex region is a complex system of two types of detectors which includes also the eight-fold target system. The mechanical arrangement of the vertex detectors and the automatized installation/removal system of it (*robot*) have seen a heavy participation of the local group.

Starting after the Be pipe (400μ thick, 102 mm diameter), at a distance from it of 10 mm, there is an array of 12 2.3 mm thick 20 cm long scintillator barrel (*Tofino*) whose purpose is to tag the slow back-to-back K^+K^- pairs from ϕ decay at trigger level. Each slab is seen at both sides, through short light guides, by Hybrid Photo-Diodes (HPD), operating inside the 1.1 T magnetic field.

Going outward, after 4 mm from tofino, there is an octagonally-shaped layer (*ISIM*) followed, after 4 mm) by a decagonally-shaped layer (*OSIM*) of double-sided Si microstrips, $300 \mu\text{m}$ thick each, which have each a resolution of $20 \mu\text{m}$ in both z and ϕ coordinates.

The charged kaons are stopped in one of the eight thin targets deposited on the outside surface of the ISIM layer.

2.3 Infrastructures and Installations

FINUDA is a very unconventional nuclear physics experiment, whose *beam* is one of the decay products of a particle produced (almost) at rest by a collider. This fact poses severe constraints on both the hardware, the infrastructures, the installation (in an already working collider), and in the interfacing of the experiment to the accelerator, that are much more demanding than in a conventional nuclear physics experiment performed with an extracted beam on a fixed target. Moreover, the running of the experiment itself has to rely on a smooth operation of all parts of the *facility* (superconducting magnet, detectors, controls) for long period of time, since any access to the machine hall implies the killing of beam to all users. All this aspects, as natural being the host group, had to be handled mainly by the Frascati group and constituted a not negligible part of its activity.

A view of the detectors of FINUDA assembled inside Clepsydra in ASTRA laboratory is shown in fig.3)

3 The magnet

The activities related to the building, the testing, mapping and installation of the FINUDA solenoid have been one of the task of the local group.

The magnetic field map of the magnet needed for the physical purposes of FINUDA has been measured at the factory (ANDALDO) in all the inner volume of the solenoid. The full map of the axial (main z component) and of the radial and tangential (minor) ones has been obtained, by means of the adaptation of an existing mapper furnished by the laboratory of magnetic measurements of CERN. It was verified that, for what concerned the FINUDA physical needs, the

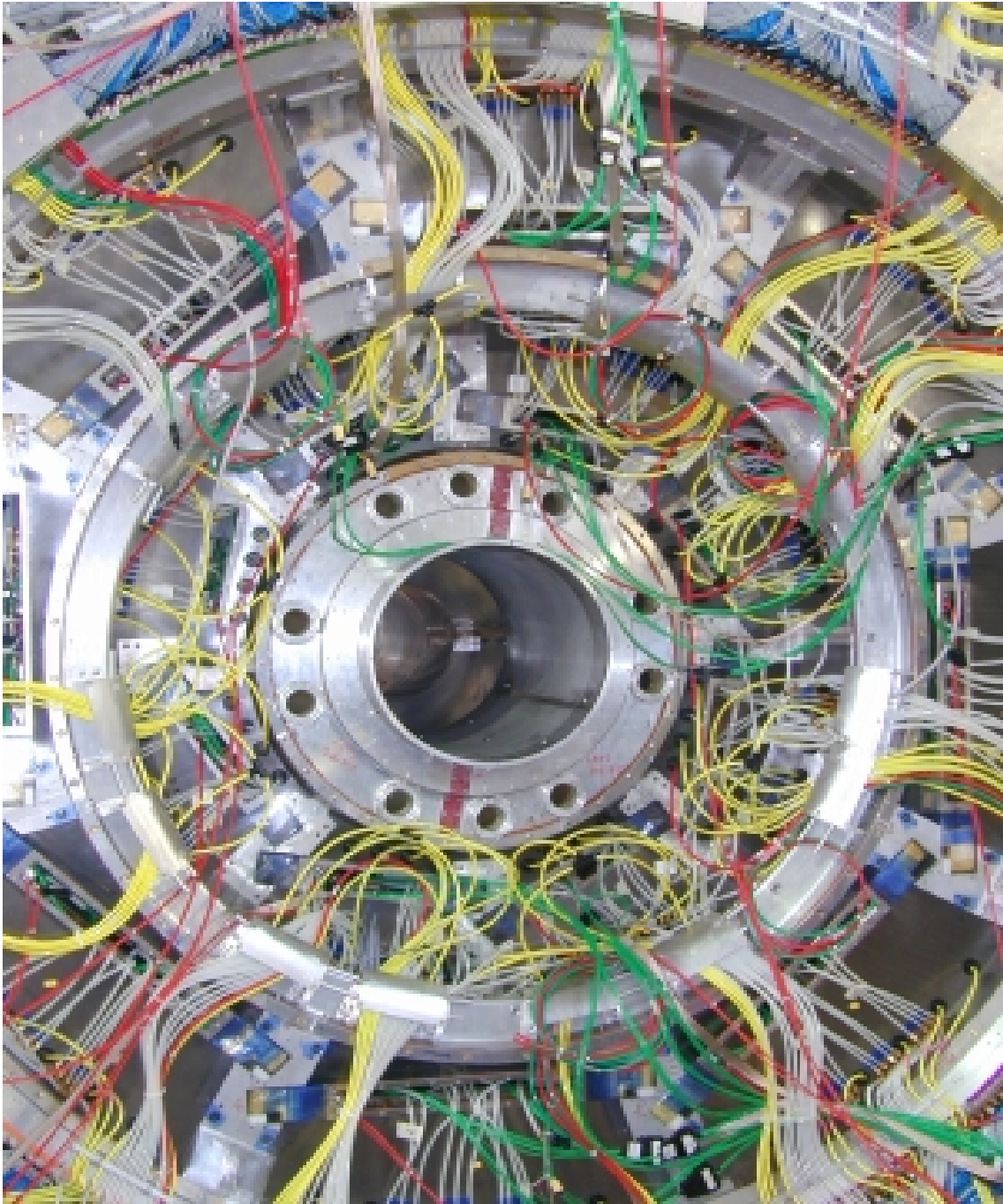


Figure 3: *The FINUDA detectors assembled inside Clepsydra in ASTRA laboratory.*

field omogeneity and uniformity was within the specifications in order to assure the designed resolution in tracking the charged particles from hypernuclei formation.

The FINUDA group was also involved in the preparation of the detailed planning for the transport and the installation of the magnet (iron yoke plus cryostat) inside its pit in the DAΦNE hall. Due to the start of the collider operation when the *go – head* for instalation was given, the previous plan of piece by piece installation of the magnet had to be redrawn in favour of a new plan that foresaw a *one – piece* transport and installation procedure. This procedure, never before done for such high dimensions magnets, was successfully carried out between the end of 1998 and beginning of 1999. Subsequently, the magnet has been connected to the DAΦNE cryo-line, cooled and, at beginning of 2000, energized up to the nominal field.

All this activity was performed during the planned shut-down period of the machine, when access was possible.

During similar other machine shut-down periods of 2000, were found and solved several problems related to vacuum losses on the cryostat and the need to rewrite with an up-to-date software the controls of the magnet.

In the following fig.4 the magnet of FINUDA is shown installed, out beam, in the pit inside DAΦNE.

4 Conclusions

At beginning of 2001 the FINUDA experiment is in the following status. The magnet is installed, in the FINUDA pit, the vacuum leakage problems solved, the new software of the control systems installed and tested. All detectors have tested and are ready for installation. The experiment is ready for the installation campaign scheduled to start from mid 2001, with the aim to be *roll-in ready* for end of summer 2002.

References

1. P. Gianotti *et al*, The FINUDA experiment at DAΦNE, in: Proc. HYP2000 VII International Conference on Hypernuclear and Strange Particle Physics (Torino, October 23-27, 2000).
2. A.Zia *et al*, Nucl. Instr. and Meth. **A461**, 60 (2001).
3. L.Benussi *et al*, Nucl. Instr. and Meth. **A461**, 98 (2001).
4. A.Balla *et al*, Nucl. Instr. and Meth. **A461**, 524 (2001).



Figure 4: *The FINUDA magnet inside the DAΦNE hall.*

GRAAL

O. Bartalini (Dott.) P. Levi Sandri (Resp.)

1 Introduction

Various experiments are presently underway in order to obtain a more precise and complete knowledge of the baryon spectrum. Most of this new generation of measurements make use of high intensity and high polarisation electron and photon beams coupled with large acceptance detectors. The reason for this huge experimental effort is in the still unsatisfactory knowledge of the nucleon excited states. Predicted states are not sufficiently well established, and many properties of the observed states (e.g. coupling constants, branching ratios, helicity amplitudes) are often poorly known. The information contained in the table of baryon resonances ¹⁾ comes almost entirely from partial-wave analyses of pion-nucleon induced reactions. It is therefore necessary to deepen the study of baryon resonances by exploiting the features of the electro-magnetic probe (small coupling constant, easy polarisability of beams) in order to improve our knowledge of resonance properties. Considering the simple case of pseudo-scalar meson photoproduction:

$$\gamma + p \rightarrow PS + nucleon \quad (1)$$

we can see that we have eight possible combination of spin states. The scattering amplitude is thus described by eight matrix elements only four of which are independent, due to rotational invariance and parity considerations.

With these four complex amplitudes, 16 bilinear products can be constructed, corresponding to 16 observables: the differential cross section, three single polarisation observables and twelve double polarisation observables. To completely determine the scattering amplitude, the cross section, the three single polarisation observables and four appropriately chosen double polarisation observables must be measured ²⁾. These observables can be adequately expressed in terms of helicity amplitudes. In that case, the following relations hold ^{3, 4, 5)}:

$$\frac{d\sigma}{d\Omega} \sim H_1^2 + H_2^2 + H_3^2 + H_4^2 \quad (2)$$

$$\Sigma \sim Re(H_1 H_4^* - H_2 H_3^*) \quad (3)$$

$$T \sim Im(H_1 H_2^* - H_3 H_4^*) \quad (4)$$

$$P \sim Re(H_1 H_3^* - H_2 H_4^*) \quad (5)$$

It is clear that the general structure of the scattering amplitude is contained in the differential cross section but its details are more clearly evidenced in the study of polarisation observables, where the interference among the helicity amplitudes can play a fundamental role in revealing more subtle effects ⁷⁾. The necessary experimental tools to perform part of the ambitious program of a full determination of the transition amplitudes are a completely and versatile polarised tagged photon beam, coupled with a large acceptance detector.

2 The Graal Beam and the Lagrange apparatus

The Graal facility provides a polarised and tagged photon beam by the backward Compton scattering of laser light on the high energy electrons circulating in the ESRF storage ring ⁶⁾. Using

the UV line (350 nm) of an Ar-Ion laser we have produced a gamma-ray beam with an energy from 550 to 1470 MeV. Its polarisation is 0.98 at the maximum photon energy and the energy resolution has been measured to be 16 MeV (FWHM). Using the green line of the same laser we have measured the beam polarisation asymmetries and cross sections in the photoproduction of η 8) π^0 and π^+ 9) in the energy region 550-1470 MeV.

The Lagrange detector is formed by a central part surrounding the target and a forward part. Particles leaving the target at angles from 25° to 155° are detected by two cylindrical wire chambers with cathode readout, a barrel made of 32 strips of plastic scintillator parallel to the beam axis, used to determine the $\Delta E/\Delta x$ of charged particles, and the BGO rugby-ball made of 480 crystals of BGO scintillator.

The BGO ball is made of crystals of pyramidal shape with trapezoidal basis which are 21 radiation lengths long (24 cm). This calorimeter has an excellent energy resolution for photons 10), a good response to protons 11) and is very stable in time due to a continuous monitoring and calibration slow control system 12).

Particles moving at angles smaller than 25° encounter two plane wire chambers, (xy and uv) two walls of plastic scintillator bars 3 cm thin located at 3 m from the target point, that provide a measurement of the time-of-flight for charged particles (700 ps FWHM resolution) followed by a shower wall made by a sandwich of four layers of Lead and plastic scintillators 4 cm thick that provides a full coverage of the solid angle for photon detection (with 95 percent efficiency) and a 20 percent efficiency for neutron detection.

Finally, two disks of plastic scintillator separated by a disk of Lead complete the solid angle coverage in the backward direction.

The beam intensity is continuously monitored by a flux monitor, composed by three thin plastic scintillators and by a lead/scintillating fibre detector that measures energy and flux 13).

3 Results

The Graal experiment started data-taking in 1997 after six months of beam and apparatus commissioning during 1996. Two Hydrogen targets were used, respectively three and six cm long. During 1997 the laser green line of 514 nm was used and a tagged photon beam, linearly polarised, was obtained with average intensity of $2 \cdot 10^6 \text{ s}^{-1}$ and energy between 550 and 1100 MeV. In 1998 the laser UV line of 351 nm was used. The corresponding backscattered beam had energy between 550 and 1470 MeV with typical intensity of $1 \cdot 10^6 \text{ s}^{-1}$. The trigger was provided by the coincidence between the tagging counter and the detector trigger. The latter was initially formed only by requesting the total energy collected by the calorimeter to be larger than 160 MeV. Later a charged particles multiplicity trigger was added allowing forward events with small energy release in the calorimeter to be recorded. The rate of the DAQ was typically between 100 and 200 s^{-1} . During data taking, the polarisation of the gamma-ray beam was rotated, approximately every twenty minutes, by rotating the laser beam polarisation. Data were also collected without laser to obtain the contribution of the bremsstrahlung in the residual vacuum of the storage ring. The intensity of the bremsstrahlung beam was typically two orders of magnitude lower, with respect to the Compton beam.

3.1 η photoproduction

Since the isospin of η is $I=0$, the (γ, η) process offers the very attractive opportunity to study N^* resonances in a clean way, being insensitive to the propagation, in the intermediate state, of $I=3/2$ resonances, strongly coupled, exempli gratia, to the pion photoproduction channel. For this reason, the η photoproduction beam asymmetry and cross section were the first experiments analysed at

Graal. The publication of the Σ beam asymmetry for η photoproduction stimulated a number of refinements in the existing theoretical approaches. Li and Saghai¹⁴⁾ investigate the process of η photoproduction within a quark model approach and find that significant contribution from $D_{13}(1520)$, $F_{15}(1680)$ and $P_{13}(1720)$ are required to reproduce the beam asymmetry data. Tiator and collaborators¹⁶⁾ have performed a combined analysis of η photoproduction cross section and asymmetry data. They have confirmed the role of $D_{13}(1520)$ and of $F_{15}(1680)$ and have extracted their ηN branching ratios. N. Mukhopadhyay and N. Mathur¹⁷⁾ have combined cross section¹⁸⁾ and single polarisation observables from Bonn (target asymmetry)²⁰⁾ and from Graal, and by making use of an effective Lagrangian approach have extracted the electro-strong parameters for the $N^*(1520)$ providing a critical test for many QCD inspired hadron models.

The preliminary results of the total η photoproduction cross section show an excellent agreement with the existing Mainz data¹⁸⁾ and the data set is now extended up to 1.1 GeV covering the full region of the $S_{11}(1535)$ resonance. The relevance of these results is discussed by Saghai and Li¹⁹⁾. The increase of the cross section above 1 GeV cannot be reproduced by their chiral constituent quark approach

3.2 Pion photoproduction

Pion photoproduction (π^0 and π^+) is one of the most extensively studied photoreaction and the main source of information on the structure of nucleons and nuclei. For this reason, a huge data base on differential cross section already exists but many of the measurements are not sufficiently accurate. The importance of the Graal contribution in this field lies in the excellent statistical and systematic error that is achieved and in the large energy and angular range covered by asymmetry measurements thus providing a new, consistent data base from 500 to 1500 MeV.

4 Activity in 2000 and conclusions

The Graal experiment started data taking in 1997. It was run for one year with the green laser line giving rise to a photon beam of maximum energy of 1100 MeV and for one year with UV multi-line and the corresponding gamma-ray beam of 1470 MeV maximum energy. Asymmetry data and cross sections have been produced for η , π^0 and π^+ photoproduction channels providing, for these reactions, the most extended and coherent data base available until now.

During the year 2000 the Graal experiment has continued the data taking by using the UV line of the argon laser. The typical intensity was $2 \cdot 10^6 s^{-1}$, a factor two larger than in 1998. The data are now being analysed and show an excellent agreement with previous measurements. A Deuteron target was used in some of the measurements and the possibility of extracting beam asymmetries and cross sections for the photoproduction off neutron has been proved

Beam asymmetries and cross sections for the photoproduction of $2 \pi^0$, ω and η' will soon be extracted from the data collected, and the energy range for η , π^0 and π^+ photoproduction channels is being extended up to 1.5 GeV.

References

1. Particle Data Group, Eur. Phys. Journ. C3 (1998) , 613.
2. W.T. Chiang and F. Tabakin, Phys. Rev. C 55,(1997) 2054.
3. D. Drechsel, O Hanstein, S. Kamalov and L. Tiator, Nucl. Phys A645, (1999), 145.
4. T. Feuster and U. Mosel, Phys. Rev. C59, (1999), 460.

5. B. Saghai and F. Tabakin, Phys. Rev. C55, (1997), 917 and Phys. Rev. C53, (1996), 66 and C. Fasano, F. Tabakin and B. Saghai, Phys. Rev. C46, (1992), 2430.
6. Graal Collaboration, Nucl. Phys. A622, (1997) 110c.
7. R. Arndt *et al.*, Phys. Rev., C42, (1990), 1853.
8. J. Ajaka *et al.*, Phys. Rev. Lett. 81, (1998), 1797.
9. GRAAL Collaboration, Phys. Lett. B, (2000) 15395
10. P. Levi Sandri *et al.* Nucl. Inst. and Meth. in Phys. Research A370, (1996), 396.
11. A. Zucchiatti *et al.*, Nucl. Inst. and Meth. in Phys. Research A321, (1992), 219.
12. F. Ghio *et al.*, Nucl. Inst. and Meth. in Phys. Research A404, (1998), 71.
13. V. Bellini *et al.*, Nucl. Inst. and Meth. in Phys. Research A386, (1997), 254.
14. Z. Li and B. Saghai, Nucl. Phys. A644 (1998) 345.
15. D. Drechsel, O. Hanstein, S.S. Kamalov and L. Tiator, Nucl. Phys. A645, (1999), 145.
16. L. Tiator, D. Drechsel, G. Knöchlein and C. Bennhold, Phys. Rev. n C60, (1999), 035210.
17. N. Mukhopadhyaya and N. Mathur, Phys. Lett. B444, (1998), 7.
18. B. Krusche *et al.*, Phys. Rev. Lett. 75, (1995), 40.
19. B. Saghai and Z. Li, these Proceedings.
20. A. Bock *et al.*, Phys. Rev. Lett. 81, (1998), 534.
21. R. Arndt I. Strakovsky and R. Workman, Phys. Rev., C53, (1996), 430.
22. R. Sdarko and E. Dolly, Nuovo Cimento, 10A, (1972) 10. and G. Knies *et al.*, Phys. Rev. D10, (1974), 2778.
23. P.J. Bussey *et al.*, Nucl. Phys., 32, (1979), 205.

HERMES

M. Albicocco, H. Avagyan (Bors. PD), E. Avetisyan (Bors. PD), N. Bianchi
(Resp. Naz.), G.P. Capitani (Resp.), E. De Sanctis
P. Di Nezza (Ass.), A. Fantoni, D. Hasch (Bors. PD), K. Hovhannisyan (Bors. PD)
V. Muccifora, A. Orlandi (Tecn.), W. Pesci (Tecn.), E. Polli
A.R. Reolon, E. Thomas (Bors. PD), A. Viticchiè (Tecn.)

1 Introduction

HERMES (HERA MEasurement os Spin) is a particle physics experiment located at the DESY research institute in Hamburg, Germany. The main aim of the experiment is to understand the internal spin structure of nucleons. Nucleons (protons and neutrons) are the basic ingredients of the matter and their most important quantum number is the spin $1/2$. Since the nucleon is a composite object which can be described in terms of quarks of different flavours (up, down and strange) in different configurations (valence and sea) and gluons, it is straightforward to understand how important is to study the quark and gluon contributions to the nucleon spin. In 1987 it was found that the spin contribution of the quarks is different compared to the naive expectation at that time. The *spin crisis* was born. HERMES was designed and build to verify this result and to obtain detailed information of the spins of the quarks and gluons in the nucleon. In addition to the original main motivation of the experiment a large number of additional measurement take place with the HERMES apparatus ranging from studies of the hadronic content of the photon to the nuclear effects in fragmentation. HERMES became (after large detector upgrades) a general purpose facility for deep-inelastic scattering off nucleons and nuclei and for diffractive production of vector mesons with polarized unpolarized and nuclear targets. HERMES is an International Collaboration of ~ 200 physicists from 35 Institutes from all over the world. Italy participates with 4 groups from Bari, Ferrara, Frascati and Rome. The Frascati group is responsible for the electromagnetic calorimeter, and is one of the leading group for the physics analysis having provided valuable contributions in inclusive, semi-inclusive and exclusive processes.

2 HERMES detector

The spin structure of the nucleon can be studied through the Deep-Inelastic-Scattering (DIS) of high energy polarized leptons off polarized nucleons and by detecting the scattered lepton and the leptoproduced hadrons. Therefore a polarized beam, a polarized target and a large acceptance spectrometer ¹⁾ are used in the HERMES experiment. The HERMES detector is unique in this field due to the high purity of the internal gas target, to the particle identification capability and to its high luminosity. The beam polarization (up to 60%) was measured using Compton back-scattering of circularly polarized laser light. The Hermes target is a gas target formed by injecting a nuclear-polarized beam of atoms from an atomic beam source into a tubular open-ended storage cell. This technique allows a density 2 orders of magnitude larger than with a free gas jet. The degree of polarization and of the atomic fraction is measured directly in the cell. The spectrometer consists basically of an analysing magnet, tracking devices (originally 4 different sets of chambers), PID detectors (Cerenkov and Electromagnetic Calorimeter) and (originally) two sets of plastic hodoscopes. Timing detector are hodoscopes and Calorimeter. During the years (mainly in 1999) an upgrade of the spectrometer was done with the realization of the two RICH detectors with a double radiator: gas+aerogel (installed in 1998 to replace the Cerenkov) and with the installation of a muon hodoscope for charm physics and a forward quadrupole spectrometer for low Q^2 physics. In 2000 a new target cell of reduced dimension was also introduced. This allowed a doubled gas density. The LNF group designed, build and commissioned the Electromagnetic Calorimeter ^{2, 3)}

and played a major role in the project and in the construction of the two RICH detectors. In Fig.1 the Electromagnetic Calorimeter is shown. In Fig.2 the current setup of the spectrometer is shown.

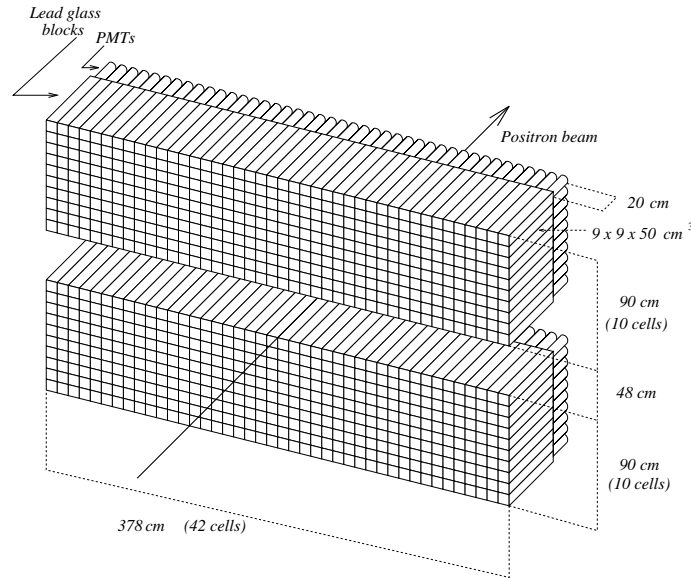


Figure 1: *HERMES Electromagnetic Calorimeter*

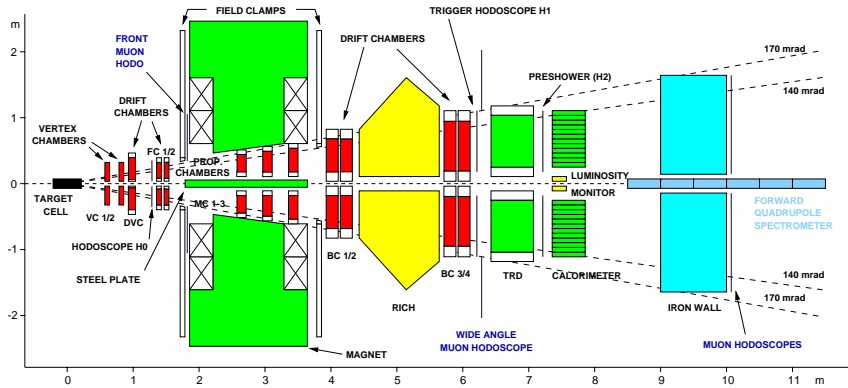


Figure 2: *HERMES spectrometer after 1999*

3 2000 Activity Overview

The 2000 year was devoted to intensive data taking with a total amount of time equivalent to about 11 months; 90% of beam time was used with polarized deuterium target (10 M events!). In 2000 was also introduced a new procedure: the final time (about 1 hour, i.e. 12, 15% of the total acquisition time) of each fill was devoted to high density (up to $10^{16}/cm^{-2}$) targets (H, D, He^4 , N, Ne). The LNF group participated to the data taking, had the duty of the calorimeter maintenance, and contributed heavily to the data analysis (see later).

4 The HERMES Physics

The affordable Physics by HERMES is very broad, from inclusive to semi-inclusive and exclusive electroproduction processes on different targets:

- a) Double (beam and target) polarization:
 - Nucleon spin structure function $g_1^{p,n}$ and sum rules (Bjorken, GDH, ...)
 - Contributions of up (valence and sea), down (valence and sea), strange quarks and gluons to the nucleon spin
- b) Single (beam or target) polarization:
 - Single-spin azimuthal asymmetry and transversity
 - Longitudinal spin transfer to Λ hyperon
 - Exclusive mesons and photons (DVCS) skewed parton distributions
- c) Unpolarized:
 - Flavor asymmetry of the light quark sea
 - Semi-inclusive meson electroproduction and fragmentation functions
- d) Nuclear targets:
 - Exclusive ρ and Φ electroproduction
 - Nuclear effects in F_2 and $R = \sigma_L/\sigma_T$
 - Hadron formation time

In the following some of the more relevant subjects, or ones in which LNF had recently a major role in the analysis, will be described with some more detail.

4.1 Quark polarization from inclusive and semi-inclusive asymmetries.

Inclusive and semi-inclusive double spin asymmetries have been measured by scattering of longitudinally polarized positrons of 27.5 GeV off ^3He and ^1H longitudinally polarized internal gas target. The results of data collected in 95-97 are summarised in Fig. 3. On the left side of Fig. 3, HERMES inclusive asymmetries are compared to SLAC (E143, E154) and CERN (SMC) data, which mean Q^2 is much higher than for HERMES. No Q^2 dependence of A_1 can be seen within the measured range and statistical accuracy. Nucleon spin structure functions g_1 as well as deep inelastic contribution to the generalised Gerasimov-Drell-Hearn integral for the proton and neutron were extracted from these inclusive measurements 4) 5) 6).

One of the main features of HERMES experiment is its unique ability to separate hadrons from scattered lepton with marginal contamination ($< 1\%$). Appropriate kinematic cuts can select hadrons from the current fragmentation region to tag the flavour of the struck quark and therefore provide a flavour decomposition of the quark contribution to the nucleon spin. Semi-inclusive asymmetries $A_1^h(x, Q^2)$ are related to quark polarizations ($\frac{\Delta q(x)}{q(x)}$) by

$$A_1^h(x, Q^2) = \sum_q \frac{e_q^2 q(x) D_q^h(z)}{\sum_{q'} e_{q'}^2 q'(x) D_{q'}^h(z)} \frac{\Delta q(x)}{q(x)} \quad (1)$$

where $q(x)$ are the quark distribution functions and the fragmentation functions $D_q^h(z)$ are related to the probability that a struck quark of flavour q fragments into a hadron of type h . Fig. 4 shows the flavour decomposition of polarized quark distributions 7).

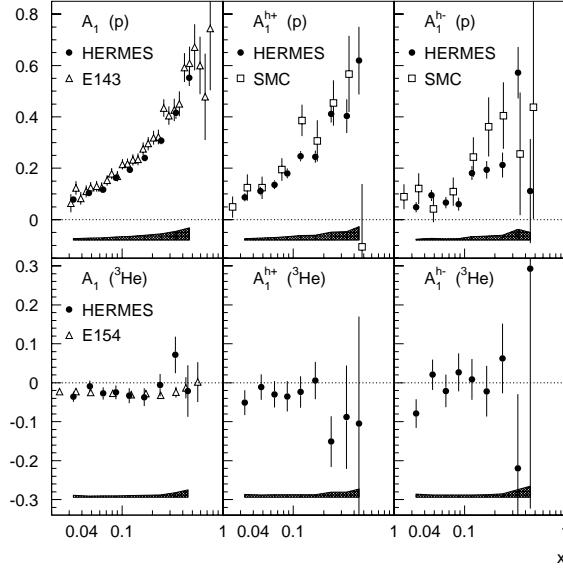


Figure 3: *Inclusive (left) and semi-inclusive double spin asymmetries for positively (center) and negatively (right) charged hadrons on proton (top) and ^3He (bottom). The data points are given for the measured mean Q^2 at each value of x , which is different for each experiment. The bands represent the systematic uncertainties.*

The flavour decomposition arise from a global fit of HERMES inclusive and semi-inclusive asymmetries shown in Fig. 3. The factors relating the measured asymmetries to the quark polarization in equation 1 were computed from unpolarized quark distributions parameterisation and from Monte Carlo simulation based on LUND string fragmentation model. The results show that u quarks polarization is clearly positive while d quarks polarization is negative over the whole x range covered by the experiment. The sea polarization was found to be compatible with zero.

Since the present asymmetries have low sensitivity to the sea polarization because of u quark dominance, the analysis assumed flavour independent sea polarization, namely $\frac{\Delta u_s(x)}{u_s(x)} = \frac{\Delta d_s(x)}{d_s(x)} = \frac{\Delta s(x)}{s(x)} = \frac{\Delta \bar{u}(x)}{\bar{u}(x)} = \frac{\Delta \bar{d}(x)}{\bar{d}(x)} = \frac{\Delta \bar{s}(x)}{\bar{s}(x)}$. The new HERMES Dual-Radiator Ring Imaging Čerenkov Detector (RICH) ⁸⁾ will provide a direct measurement of the sea polarization in near future, through unambiguous identification of all hadrons (pions, protons and kaons) over the whole kinematic range.

4.2 Gluon polarization from high p_T hadron pairs

The quark contribution to nucleon spin is only $\sim 30\%$. The deficit can be explained by a large positive gluon polarization $\Delta G/G$. No measurement of gluon polarization have been performed up to now. The gluon polarization can be indirectly probed through scaling violation of polarized structure function. However, in contrast to the unpolarized case, the $x-Q^2$ range of world polarized DIS data is too limited to constrain ΔG . The first measurement of the gluon polarization have been performed by HERMES by measuring spin asymmetries in photon gluon fusion (PGF) process. The PGF process signature is characterised by two hadrons of opposite charge and high transverse momentum (p_T). In order to maximize the contribution of photon gluon process in the data sample and to include the low Q^2 region which dominates the cross section, the scattered e^+ was not required by the trigger. The semi-inclusive longitudinal cross section asymmetry $A_{||}(p_T^{h^+}, p_T^{h^-})$

for h^\pm pair production measured is close to zero when averaged over the whole p_T range. For the highest p_T accessible, a negative asymmetry is measured ¹²⁾ (see Fig. 5). Averaging over the bins where $p_T^{h^1} > 1.5 \text{ GeV}^2$ and $p_T^{h^2} > 1.0 \text{ GeV}^2$ gives $A_{\parallel} = -0.28 \pm 0.12(\text{stat.}) \pm 0.02(\text{syst.})$. This negative asymmetry is in contrast to the positive asymmetry measured in DIS from proton. This asymmetry is interpreted considering contributions from four different processes: deep inelastic scattering (DIS), vector meson dominance (VMD), LO QCD Compton and PGF. Monte Carlo studies based on PYTHIA ¹¹⁾ model clearly showed that PGF dominates over all other considered processes in the phase space where the negative asymmetry is observed. The asymmetry of QCD Compton process is calculated to be positive whereas the asymmetries of VMD process is assumed to be zero. Within this model, the extracted value for the gluon polarization is $\langle \Delta G/G \rangle = +0.41 \pm 0.18(\text{stat.}) \pm 0.03(\text{syst.})$ at $\langle x_G \rangle = 0.17$. This result is compared at Fig. 5 to several LO QCD fits to world data. The systematic error does not include any model uncertainties from neglected contributions. It is important to stress that any ignored process with zero asymmetry will contribute only as a dilution factor, leading to an increase of value $\langle \Delta G/G \rangle$ extracted but the significance of its deviation from zero will remain the same. An alternative measurement of $\langle \Delta G/G \rangle$ via open and hidden charm asymmetry is currently under study.

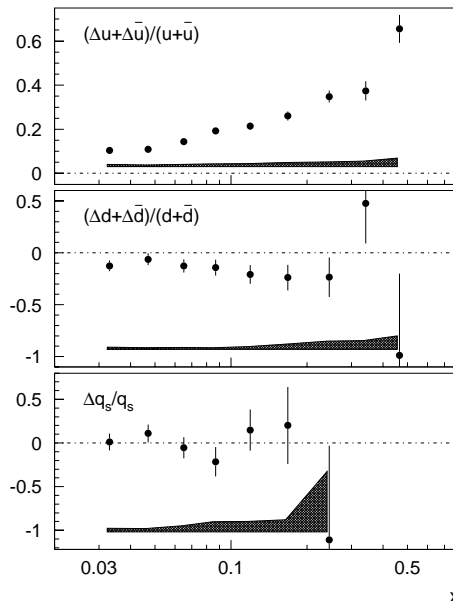


Figure 4: Flavor decomposition of the quark polarization as function of x . The bands represent the systematic uncertainties.

4.3 Single Spin Azimuthal Asymmetries.

The complete twist-2 description of the nucleon requires three sets of structure functions: the unpolarized structure functions, the longitudinal spin distribution functions and the still unmeasured transverse spin distribution functions. A classification of the complete set of distribution functions at the twist-2 and twist-3 levels can be found in ¹³⁾. Transversity distributions are still unmeasured because of their particular chiral-odd nature which implies that they are not directly observable in inclusive lepton scattering experiments. However, transversity distributions are predicted to be measurable in semi-inclusive measurements where only the lepton beam *or* the target are polarized ¹⁴⁾. In the case of semi-inclusive pion production from a longitudinally polarized target, the combination of chiral odd quark spin distribution functions and a fragmentation of the same structure (the Collins chiral-odd time-odd fragmentation function) leads to an asymmetry in

the distribution of the azimuthal angle ϕ of the pion around the virtual photon momentum, with respect to the lepton scattering plane ¹³).

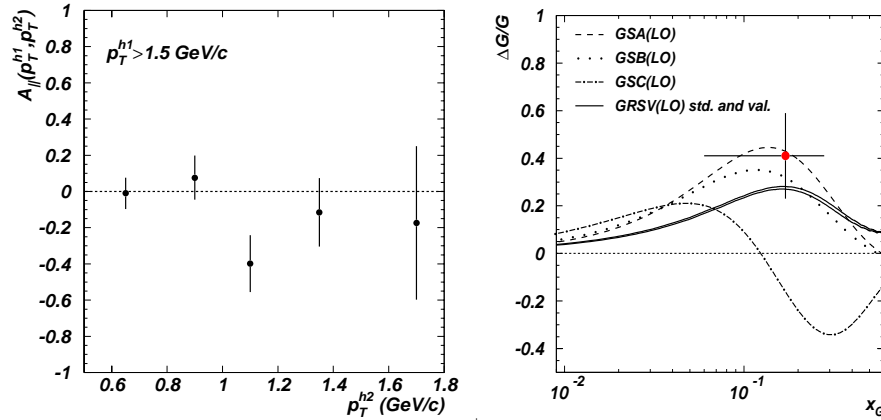


Figure 5: Longitudinal cross section asymmetry $A_{\parallel}(p_T^{h^+}, p_T^{h^-})$ for h^{\pm} pair production (left) and the corresponding extracted value of $\langle \Delta G/G \rangle$ compared with several QCD fits ⁹⁾ ¹⁰⁾ (right). The error bars represent the statistical uncertainty only.

The first measurement of single spin asymmetries for semi-inclusive pion production in DIS as recently been performed by HERMES. The $\sin \phi$ moments of the distribution have been extracted according to

$$\mathcal{A}_{UL}^{\sin \phi} = \frac{\frac{L^+}{L_P^+} \int_0^{2\pi} \sin \phi dN_+ - \frac{L^-}{L_P^-} \int_0^{2\pi} \sin \phi dN_-}{\frac{1}{2} [\int_0^{2\pi} dN_+ + \int_0^{2\pi} dN_-]}$$

where \pm refer to the target spin state, L^{\pm} are the dead-time corrected luminosities, and L_P^{\pm} luminosities weighted by the target polarization. The measured asymmetries for π^+ and π^- are shown on Fig. 6 as function of inclusive variable x and as function of the transverse momentum of pions P_{\perp} ¹⁵). Also shown are preliminary results for π^0 which are in good agreement with π^+ results.

The asymmetries averaged over x and P_{\perp} are

$$\begin{aligned} \pi^+ \mathcal{A}_{UL}^{\sin \phi} &= 0.022 \pm 0.005(stat) \pm 0.003(syst) \\ \pi^- \mathcal{A}_{UL}^{\sin \phi} &= -0.005 \pm 0.008(stat) \pm 0.004(syst). \end{aligned}$$

The difference between π^+ and π^- can be interpreted in term of favoured and unfavoured Collins fragmentation function ¹⁶). The apparent increase of the effect with x suggests that the effect is associated with valence quark contributions. The increase of $\mathcal{A}_{UL}^{\sin \phi}$ for π^+ and π^0 as P_{\perp} increase up to ~ 0.8 GeV can be related to the dominant role of intrinsic quark transverse momentum when P_{\perp} remain below typical hadronic mass scale ¹⁷).

4.4 Other topics 1999-2000

- Azimuthal asymmetries in semi-inclusive hadron electroproduction.
- Spin-dependent cross section for real and virtual photons (see Fig. 7). In particular a first evaluation of the spin-dependent cross section for real photons at high energy was done in the framework of a Regge-inspired model. Results were used to evaluate for the first time

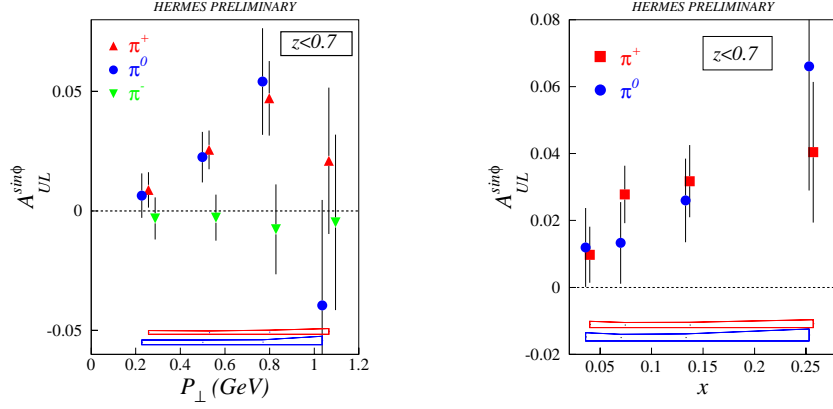


Figure 6: $\mathcal{A}_{UL}^{\sin\phi}$ for π^+ , π^- and π^0 as function of pion transverse momentum (left) and as function of Bjorken x (right). The bands represents the systematic uncertainties.

the high energy contribution to the GDH sum rule and, after 25 years of claiming of a possible violation of this sum rule, it was shown that the sum rule is very likely verified when considering this contribution.

- Preliminary analysis of g_1^D and more precise extraction of the polarized distribution functions with the inclusion of the Deuteron data.
- First measurement of the longitudinal spin transfer to the Λ to study the flavour decomposition of the spin of the Hyperons. There is a preliminary indication that the main contribution of the Λ spin originates from the strange quark.
- Measurement of the angular distribution and of $R = \sigma_L/\sigma_T$ in diffractive electroproduction of ρ^0 meson. Results indicate that the S-Channel-Helicity-Conservation (SCHC) hypothesis is reasonable and are in agreement with calculation based on the Skewed Parton Distributions.
- Measurement of multiplicity of charged and neutral pions in DIS and evidence of the universality of the fragmentation process. Isospin invariance seems to be violated when the leading pion carries most of the energy of the struck quark (exclusive limit).
- First evidence of a large nuclear medium effect in the unpolarized structure function $R = \sigma_L/\sigma_T$ at low Q^2 which can be related to the coupling with di-quark pairs or σ -mesons exchanged in the nucleus (HERMES effect ¹⁸).
- Preliminary analysis of nuclear attenuation on Kr and N .
- Preliminary analysis of exclusive two pion production.
- Preliminary analysis of single spin asymmetry π^0 production.
- Preliminary analysis of exclusive π^+ production.

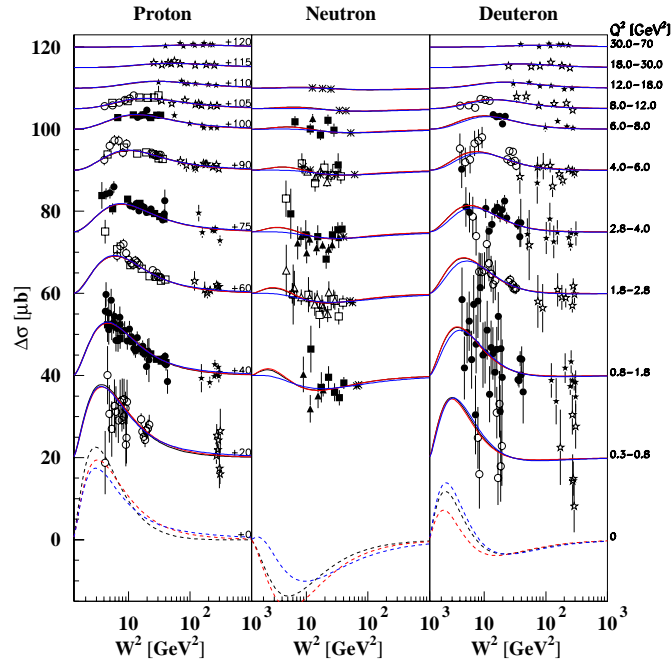


Figure 7: Spin-dependent cross section, for proton, neutron and deuteron at different Q^2 . Curves are Regge-inspired phenomenological descriptions. The lowest curves refer to the real photon ($Q^2=0$) extrapolation.

5 List of publications in 2000

1. P. Di Nezza, 14th Int. Spin Phys. Symp. (SPIN 2000), Osaka, Japan, Oct 16 - 21, 2000
2. D. Hasch, 35th Rencontres de Moriond, Les Arcs, France, Mar 18 - 25, 2000
3. V. Muccifora 38th Int. Winter Meet. on Nucl. Phys., Bormio, Italy, Jan 24 - 29, 2000
4. V. Muccifora MESON 2000 Work. Cracow, Poland, May 19-23, 2000
5. N. Bianchi LNF Spring School May 15-20, 2000 Lab. Naz. di Frascati, Frascati, Italy
6. E. Thomas 8th Int. Work. on DIS and QCD (DIS 2000) Liverpool, England Apr 25-30, 2000
7. P. Di Nezza 8th Int. Work. on DIS and QCD (DIS 2000) Liverpool, England Apr 25-30, 2000
8. H. Avakian 8th Int. Work. on DIS and QCD (DIS 2000) Liverpool, England Apr 25-30, 2000
9. E. De Sanctis, W.-D. Nowak, K. Oganessyan Phys. Lett. B 483 (2000) 69
10. V. Korotkov, W.-D. Nowak, K. Oganessyan hep-ph/0002268, DESY 99-176, (accepted by EP)
11. A.M. Kotzinian, K.A. Oganessyan, H. Avakian, E. De Sanctis Nucl. Phys. A 666-667 (2000) 290, hep-ph/9908466 (Proc. of NUCLEON '99)
12. N. Bianchi, P. Di Nezza, V. Muccifora, J.J. van Hunen, G. van der Steenhoven Int. Report.
13. A. Airapetian et al, Phys. Lett. B 494 (2000) 1-8. hep-ex/0008037, DESY-00-096

14. A. Airapetian et al, EPJC. (in press) hep-ex/0104004, DESY-01-037
15. A. Airapetian et al, Eur. Phys. Jour. C 17 (2000) 389-398. hep-ex/0004023, DESY-00-058
16. K. Ackerstaff et al, Eur. Phys. Jour. C 18 (2000) 303-316. hep-ex/0002016, DESY-99-199
17. K. Ackerstaff et al, Phys. Lett. B 475 (2000) 386-394. hep-ex/9910071, DESY-99-150
18. A. Airapetian et al, Phys. Rev. Lett. 84 (2000) 4047-4051. hep-ex/9910062, DESY-99-149
19. A. Airapetian et al, Phys. Rev. Lett. 84 (2000) 2584-2588. hep-ex/9907020, DESY-99-071
20. H. Avakian Future Transversity Measurements Brookhaven Nat. Lab., Upton, NY, USA, Sep 18 - 20, 2000
21. N. Bianchi Gordon Conf. on Photonuclear Reactions Jul 30 - Aug 4, 2000 - Tilton, USA
22. V. Muccifora Gordon Conf. on Photonuclear Reactions Jul 30 - Aug 4, 2000 - Tilton, USA
23. A. Fantoni, Hal Jackson APS Spring Meeting, Long Beach, USA, Apr 29 - May 2, 2000
24. N. Bianchi Work. on Elfe Physics Apr 27-29, 2000 - Valencia, Spain

References

1. K. Ackerstaff et al., Nucl. Instr. and Meth. **A 417** (1998) 230.
2. H. Avakian et al., NIM **A378** (1996) 155
3. H. Avakian et al., NIM **A417** (1998) 69
4. K. Ackerstaff et al., Phys. Lett. **B 404** (1997) 383.
5. A. Airapetian et al., Phys. Lett. **B 442** (1998) 484.
6. K. Ackerstaff et al., Phys. Lett. **B 444** (1998) 531.
7. K. Ackerstaff et al., Phys. Lett. **B 464** (1999) 123.
8. E.C.Aschenauer et al., Nucl. Instr. and Meth **A 440** (2000) 338.
9. T. Gehrman, W.J. Stirling, Phys. Rev **D 53** (1996) 6100.
10. M. Glück et al., Phys. Rev. **D 53** (1996) 4775.
11. T. Sjöstrand, Comp. Phys. Comm. **82** (1994) 74.
12. A. Airapetian et al., Phys. Rev. Lett. **84** (2000) 2584.
13. P. Mulders and R. Tangerman, Nucl. Phys. **B 461** (1996) 197.
14. J.C. Collins, Nucl. Phys. **B 396** (1993) 161.
15. A. Airapetian et al., Phys. Rev. Lett. **84** (2000) 4047.
16. A. Schäfer and O. Teryaev, hep-ph/9908412.
17. K.A. Oganessyan, H. Avakian, N. Bianchi and A.M. Kotzinian, hep-ph/9808368.
18. G. A. Miller, S. J. Brodsky and M. Karliner, Phys.Lett. **B481** (2000) 245.

LF-11: FIELD THEORY AND STATISTICAL MECHANICS IN LOW-DIMENSIONAL SYSTEMS

S. Bellucci, M. Benfatto, S. Di Matteo (Osp.) , J. Gonzalez (Osp.)
R. Gunnella (Ass.), C. Natoli (Resp.), N. Perkins (Osp.)

1 The project

This research program aims at the theoretical analysis of strongly correlated electron systems. These include the layered cuprates in their normal and superconducting state, the transition metal oxides, in particular colossal magnetoresistive manganites, and the fullerene clusters and lattices.

The enormous recent progress both in the art of sample preparation and in the measurement techniques has produced a wealth of high quality data on thermodynamic, transport and spectroscopic properties which often challenge the simple textbook interpretation. This is particularly true for materials showing evidence for strong electronic and magnetic correlation such as the materials mentioned above.

At the same time, new nonperturbative methods have been developed for dealing with strongly correlated systems, such as the Density Matrix Renormalization Group, the dynamical mean field theory or the extension of the Lanczos technique to finite frequencies and temperatures.

The main goal of the present proposal is on one side the application of these advanced theoretical methods to the "realistic" calculation of the response functions relative to particularly meaningful experiments that might illuminate the complicated interplay between electronic structure, magnetic and transport properties that often dominate the physical behaviour of such systems (eg manganites and cuprates) with the aim of disentangling their role in such a behaviour. In so doing we shall at the same time obtain a description of their ground state properties. On the other side, methods borrowed from field theory and statistical mechanics will be used to bear on the description of the essential physics of such systems (eg fullerene clusters and lattices).

We have in mind two possible areas of application:

1.1 Manganites, cuprates and transition metal oxides

Materials with an interesting combination of electric and magnetic properties attract now considerable attention, both from the basic point of view and as promising materials for applications. Such an interplay often permits a better understanding of both aspects, the origin of magnetism in different cases and the nature of electronic states and transport phenomena. Recently an upsurge of interest for these problems was caused by the observation of a phenomenon which was referred to as "colossal magnetoresistance" (CMR) in complex oxides of the type $La_{(1-x)}Ca_xMnO_3$. It turns out that in this class of compounds one encounters the whole wealth of interrelated phenomena such as insulator-metal transition, orbital (or Jahn-Teller) ordering, double exchange, lattice and magnetic polarons, charge ordering, and so on.

Actually the problem of the interplay of magnetic, structural and transport properties is an old one, which recent developments have put once again at the forefront of the present research activity on strongly correlated systems. The strong impetus to revisit such problems was given by the discovery of high Tc superconductors which are complex copper oxides displaying a close interrelation of electric and magnetic properties. In these systems the magnetic ordering is mostly of an antiferromagnetic type, whereas in CMR materials it is ferromagnetic. Arguments have been given (double exchange mechanism) in the case of doped $LaMnO_3$ to account for this observation, but then the question comes spontaneous: why the cuprates do not become ferromagnetic due to the same mechanism? One may argue that the copper spin in cuprates is 1/2, equal to the spin of an

oxygen hole, so that the formation of a Zhang-Rice singlet is favoured, due also to the coherence of the correct superposition of the 2p-orbitals of the four oxygens surrounding the copper atom with its 3d hole. This is just an example of how the study of the similarities and differences between the two class of material may provide insight in the understanding of both. Indeed disentangling the origin of high temperature superconductivity and colossal magnetoresistance in the transition metal oxides remains at the center of current activity in condensed matter physics.

1.2 Fullerene clusters and lattices

The fullerene clusters and lattices are the ground of interesting physical phenomena, which have mainly to do with their electronic properties. Some of them already stem from the particular features of the interaction in the graphite sheet. It has been shown that the electronic spectrum of the C_{60} and giant fullerenes can be understood from the frustration introduced by the pentagon rings in the honeycomb lattice. The unconventional screening properties of the interaction inside the clusters (which quite probably play an important role in the high- T_c superconductivity of the compounds) have their origin in the renormalization of the Coulomb interaction in the graphite sheet. Recent photoemission experiments have shown that the quasiparticle decay rate in graphite has a linear dependence on the frequency close to the Fermi energy. These measurements are consistent with the marginal Fermi liquid behavior of the interaction.

The purpose of our research is to apply these developments to the study of the electronic properties of the tubular fullerenes. The introduction of gauge fields may be very useful to explain the effect of dislocations in the lattice. In certain cases, these are known to produce metal/semiconductor junctions in a single nanotube. It would be interesting to have a field theoretical model for the combined effect of several such dislocations. On the other hand, the marginal behavior of the interaction may leave also imprints at the lower dimension of the nanotubes. These may inherit some of the electronic properties of graphite, especially for large radius of the tubule. The study of the crossover from the marginal Fermi liquid behavior to the regime of strong correlations in one dimension turns out to be an interesting matter of research.

2 Activity carried out in the year 2000

2.1 Manganites, cuprates and transition metal oxides

We have re-examined the low temperature ground state properties of the Antiferromagnetic Insulating Phase of V_2O_3 in the light of the recent experimental observations by L. Paolasini *et al*, (Phys. Rev. Lett.82, 4719 (1999)) based on Resonant X-ray Scattering at the V K-edge and non-resonant magnetic scattering. In 1978 Castellani, Natoli and Ranninger (CNR) (Phys. Rev. B 18, 4945 (1978)), under the assumption that there was only one magnetic electron in a doubly degenerate eg band, had explained the rather peculiar magnetic structure of V_2O_3 and predicted the existence of an orbital ordering (OO) concomitant with the spin structure. In this model the V atoms were thought to be in a state of spin $S=1/2$. However the experiments by Paolasini *et al*, while confirming the OO predicted by CNR, have also shown that V atoms carry a spin $S=1$. We have therefore derived the effective hamiltonian in the strong coupling limit of an Hubbard model with three degenerate t_{2g} states containing two electrons coupled to spin $S=1$. An axial trigonal distortion of the cubic states, as appropriate to V_2O_3 , has also been taken into account and shown to be important for a realistic assessment of the relative population of a_{1g} and e_g levels (in which the t_{2g} states are split by the trigonal field), in keeping with the findings of x-ray absorption spectra at the L edges of Vanadium. We find that there are still two degenerate orbital configurations for the two magnetic electrons coupled to spin $S=1$. We have derived and analyzed the phase diagram of the system as a function of the ratio of the intra-atomic exchange coupling

over the on site Coulomb repulsion J/U and the ratio of the two most relevant hopping parameters in the basal plane. We do find, as in the $S=1/2$ case, two regions of the parameters space where the stable configuration has the observed spin structure (that breaks the trigonal symmetry of the high temperature corund phase) and a ferro-orbital ordering throughout the crystal in one region (ie the same orbital state configuration for the two magnetic electrons), an antiferro orbital ordering in the other. However these two regions are rather small in the parameter space compared to the spin $S=1/2$ case, since nearly all phase space is occupied in equal parts by stable configurations with ferro or antiferro spin structure. The main results of our analysis point to a series of drawbacks of the new solution, which are summarized in the following:

a) A spin $S=1$ Heisenberg model with orbital degeneracy has problems in stabilizing the observed spin structure relative to competing configurations. In particular there is only a difference of 2 MeV (≈ 20 K) per atom between the ground state and an excited state which is very reminiscent of the paramagnetic insulating state, while experimentally the transition to this state occurs around 150 K.

b) Based on a magnetic crystal analysis of the structure factor we substantiate the classification of reflections given by Paolasini *et al* and show that the reflections with $h + k + l = 2n + 1$ and h odd are mostly pure orbital reflections. In particular we prove that the (111) reflection is mostly orbital in character. However neither of the two orbital configurations found with the real spin structure are capable of giving this type of reflections.

c) Using the results of a very recent observation of non-reciprocal x-ray giotropy by Goulon *et al* (PRL 85, 4385 (2000)) we point out that the magnetic space group of the AFI phase of V_2O_3 should be magneto-electric. There exists two such possible groups: $C_{2h}(C_s)$ and $C_{2h}(C_2)$. However the magnetic space group associated with the stable solutions found for the spin $S=1$ case do not have the magneto-electric symmetry. They are indeed invariant under time-reversal.

d) The $C_{2h}(C_s)$ group predicts for V_2O_3 a transverse magnetoelectric effect, which becomes a definite prediction for a future experiment.

As apparent from the above findings the resulting picture is contradictory. On one side there is experimental evidence of a strong intra-atomic exchange J that couples the two magnetic electrons to spin $S=1$, on the other the stable solutions with the observed spin structure do not have the correct magnetic symmetry to comply with Paolasini and Goulon's experiments. It seems that a small (≈ 30 %) component of $S=1/2$ wavefunction on a background of spin $S=1$ (in a correlated band approach) is necessary to stabilize the $S=1$ solution and to induce an orbital ordering compatible with observations. We have reexamined the experimental evidence of Orbital Ordering signal in $LaMnO_3$ and $La_{0.5}Sr_{1.5}MnO_4$ systems in the light of realistic "ab-initio" calculation based on multiple scattering theory and finite difference method. We found that the experimental signal at the forbidden reflection is due to the Jahn-Teller distortion present in the geometrical structure of both compounds ³⁾. At the same time, the geometrical structure of several amorphous systems containing copper has been analysed in details by multiple scattering analysis of the x-ray absorption spectra at the Cu K-edge. The local geometry has been determined with the aim to derive the electronic properties of the electronic ground state ^{4, 5)}.

2.2 Fullerene clusters and lattices

Focusing on the regime of strong correlations, the aim is to investigate the features that the Coulomb interaction may produce in the one-dimensional electron system. We have already shown that the long-range interaction does not give rise to the hybridization of the left and right chiralities present in the low-energy theory of the nanotubes ¹⁾. The phenomenological implications of this study are relevant for the fullerene nanostructures (metallic carbon nanotubules with a big transverse section).

3 Activity planned for the year 2001

3.1 Manganites, cuprates and transition metal oxides

We intend to pursue the study of V_2O_3 in three directions. First to calculate core level x-ray spectroscopies for correlated electron systems in order to better understand the implications of these spectroscopies in this case. A preliminary study has been published in Ref. ²⁾. Secondly to perform a correlated band calculation along the lines described in Ref. ²⁾ (resonating valence bond states). Thirdly, to introduce the coupling with the lattice which seems to be important in the monoclinic phase. It is worth mentioning that this problem has many similarities with the manganites problem. Moreover the development of x-ray spectroscopy for correlated systems will have an interesting fallout also in other fields, *eg* for the local structure determination of non crystallizable metallo-proteins relevant to the genome project. For this purpose we are developing a code to make geometrical and structural fits of the experimental x-ray Absorption Data. We have already moved in the direction of interdisciplinary applications by developing a code for photoelectron spectroscopies ⁶⁾.

3.2 Fullerene clusters and lattices

There have been recent attempts, relying on the use of bosonization methods, to interpret the experimental curves of the conductivity at low energy on the light of the Luttinger liquid behavior. We will apply renormalization group (RG) methods to ascertain the scaling behavior of the density of states near the Fermi level. We believe that the RG approach has to produce a more accurate low-energy description of the isolated single-walled nanotubes, since it does not require the ad hoc infrared regularization of the Coulomb interaction, needed to make sense of the bosonization approach. The RG approach predicts anyhow a sharp decrease of the quasiparticle weight at a given scale, which one may attribute to the effect of Coulomb blockade in the mesoscopic regime of the nanotube ¹⁾. Detailed estimates of this scale in terms of the parameters characterizing the nanotube as well as estimates of the scaling behavior of the conductivity are going to be worked out. This will allow to establish a comparison with the available data from scanning tunneling microscope measurements on isolated single-walled nanotubes.

References

1. S. Bellucci and J. Gonzalez, Eur. Phys. J. B **18**, 3 (2000).
2. M. Cuozzo, Y. Joly, K. Hlil and C.R. Natoli "Orbital ordering and metal-insulator transition in V_2O_3 " AIP Proc. of the Frascati Work. (Sept. 1999) on Theory and Comput. for Synchr. Rad. Spectroscopies, Vol **514**, (2000)
3. Y. Joly, M. Benfatto and C.R. Natoli "Orbital ordering and resonant diffraction in manganites" AIP Proc. of the Frascati Work. (Sept. 1999) on Theory and Comput. for Synchr. Rad. Spectroscopies, Vol **514**, (2000)
4. F. Rodriguez, R. Valiente, J.I. Espeso, M. Benfatto and S. Pascarelli, High Pressure Research **18**, 165 (2000)
5. C. Maurizio, F. D'Acapito, M. Benfatto, S. Mobilio, E. Cantaruzza, F. Gonella, Eur. Phys. Journal. **B14**, 211 (2000).
6. R. Gunnella, F. Solal, D. Sebilliau and C.R. Natoli, Comput. Phys. Commun. **132**, 252 (2000).

LF21: PHENOMENOLOGY OF ELEMENTARY PARTICLE INTERACTIONS AT COLLIDERS

R. Escribano (Bors. PD TMR), G. Isidori, H. Pichl (Bors. PD TMR), G. Pancheri (Resp.)

1 Summary of the project

The research topics investigated by this project can be divided into three main areas:

1. CP violation and rare decays;
2. Precision physics in hadronic processes at DAΦNE;
3. Quantum Chromodynamics and the rise of total cross-sections.

The first area, discussed in Section 2, concerns the possibility to perform new precision tests about the mechanism of quark-flavor mixing, within and beyond the Standard Model (SM). Other studies concerning precision physics in hadronic processes at DAΦNE will then follow in Sect. 3. An altogether different field of investigation, dedicated to reach into a much higher energy range, is the project related to the QCD description of hadronic and photonic total cross-section, which will be described in detail in Sect. 4.

2 CP violation and rare decays

2.1 Analysis of supersymmetric effects in rare K decays

In collaboration with A. Buras, G. Colangelo, A. Romanino and L. Silvestrini, G. Isidori has explored the connections between ϵ'/ϵ and the rare decays $K_L \rightarrow \pi^0 \nu \bar{\nu}$, $K_L \rightarrow \pi^0 e^+ e^-$, $K^+ \rightarrow \pi^+ \nu \bar{\nu}$ and $K_L \rightarrow \mu^+ \mu^-$, within generic supersymmetric models with non-trivial flavor structures (non-universal A terms).¹⁾ It has been found that the branching ratios of these modes could be substantially enhanced with respect to their SM expectations. It has also been shown that all modes carries a complementary information, so that a precise measurement of all of them would be extremely useful to shed light on the flavor structure of supersymmetric models. As shown in fig. 1, where we compare the information on the CKM unitarity triangle from B physics (and ϵ_K) and rare K decays, present data on rare K decays still allow sizable non-standard effects. On the other hand, when the experimental sensitivity will improve, new highly-nontrivial tests of the SM can be expected. The results of this analysis (and related works) have been presented by G. Isidori at ICHEP 2000²⁾ and RADCOR 2000.³⁾

The implications of these supersymmetric scenarios for the CP-violating asymmetries in $K \rightarrow 3\pi$ decays (one of the main goals of the ‘extended NA48 experiment’, recently approved at CERN, and of particular interest also for KLOE) have been investigated together with G. D’Ambrosio and G. Martinelli.⁴⁾ As a result, it has been shown that a slope asymmetry within the reach of the future experiments, i.e. at the level of 10^{-4} or above, can only be obtained under a considerable fine-tuning of both hadronic parameters and supersymmetric phases.

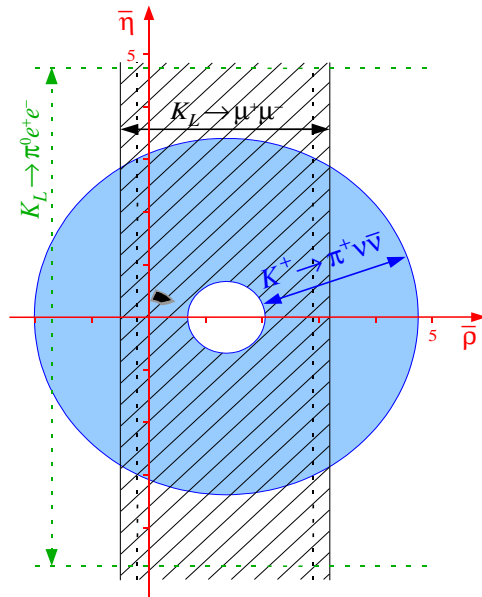


Figure 1: Constraints on the the CKM unitarity triangle (or $\bar{\rho} - \bar{\eta}$ plane) derived from rare K decays in 2001. The small dark region close to the origin correspond to the determination of $\bar{\rho}$ and $\bar{\eta}$ from B -physics and ϵ_K . The two vertical regions denote the theoretical uncertainty in the extraction of the bound from $K_L \rightarrow \mu^+ \mu^-$.

2.2 Isospin-breaking (IB) and final-state interactions (FSI) in ϵ'/ϵ

Stimulated by a recent claim of large FSI effects in ϵ'/ϵ , G. Isidori and his collaborators have critically re-examined this question, showing that at present it is not possible to draw precise model-independent conclusions about the size of this effect. ⁵⁾ With a similar motivation, in collaboration with G. Ecker, H. Neufeld, G. Muller and A. Pich, a systematic investigation of isospin-breaking effects in $K \rightarrow 2\pi$ decays has been started. As a result of this analysis, for the first time it has been possible to determine to the most general structure (including all anomalous dimensions) of the effective chiral Lagrangian of $O(G_F e^2 p^2)$, necessary to describe one-loop virtual-photon corrections in non-leptonic K decays. ⁶⁾ These and other topics in non-leptonic K decays have been discussed in a review talk at Chiral Dynamics 2000. ⁷⁾

2.3 $K \rightarrow \pi\pi\ell^+\ell^-$ decays

Weak decays of Kaons into pairs of pion and leptons have been the subject of the Ph.D. thesis of Hannes Pichl completed during the year 2000, ⁸⁾ under the supervision of G. Ecker from University of Vienna. This research activity on weak decays of the pseudoscalars K_L and K^+ into pairs of pions and leptons was started at the University of Vienna, Austria, where most of the analytical parts of the calculations had been done. However, the complete numerical analysis of the processes

considered and the comparison with recent experimental results as well as the preparation of the thesis and two derived papers took place in Frascati.

The theoretical setting for these studies was the framework of Chiral Perturbation Theory (CHPT), the effective field theory of low-energy physics of the pseudoscalar meson octet. Both decays mentioned above were interesting from a pure CHPT point of view, since they could provide possibilities of extracting experimentally combinations of so-called low-energy constants (LECs) appearing a priori unknown coupling constants in the next-to-leading-order effective weak Lagrangians.

The two papers that contain the results of the thesis in a very condensed form shall now be briefly described. The work, done in the second half of the year 2000 has since appeared as a preprint in Jan. 2001. ⁹⁾

The branching ratios of the measured decay $K_L \rightarrow \pi^+\pi^-e^+e^-$ and of the still unmeasured decay $K^+ \rightarrow \pi^+\pi^0e^+e^-$ have been calculated to next-to-leading order in CHPT. ¹⁰⁾ Taking advantage of recent experimental results two possible values of the combination $(N_{16}^r - N_{17})$ of weak low-energy couplings (LECs) from the $\mathcal{O}(p^4)$ chiral Lagrangian were derived. The obtained values were compared to the predictions of theoretical approaches to weak counterterm couplings to distinguish between the two values. Using the favoured value of the combination $(N_{16}^r - N_{17})$ and taking into account additional assumptions suggested by the considered models, the branching ratio of the second decay as a function of the unknown combination $(N_{14}^r + 2N_{15}^r)$ of weak low-energy couplings was obtained. Finally, using values of the individual LECs derived from a particular model, the branching ratio of the K^+ decay was also predicted.

Together with G. Ecker from Vienna, ⁹⁾ the theoretical analysis of the CP-violating asymmetry in the decay $K_L \rightarrow \pi^+\pi^-e^+e^-$ was updated, again relying on CHPT and on the most recent phenomenological information from KTeV. With the experimentally determined magnetic amplitude and branching ratio as input, the asymmetry was calculated with good accuracy. Additionally, the theoretical interpretation of the sign of the asymmetry was discussed within the CHPT framework.

3 Precision physics in hadronic processes at DAΦNE

3.1 QCD and meson interactions below 1 GeV

The research activity of R. Escribano, TMR post-doc with the EURPDAΦNE network, along the year 2000 has been devoted to the study of strong interactions at low energies in the framework of Quantum Chromodynamics (QCD) effective theories. More in particular, the phenomenology of the strong interactions among the pseudoscalar, scalar and vector mesons with masses of the order or below 1 GeV has been studied.

The research method is based on the use of the following tools: Chiral Perturbation Theory (ChPT) as the appropriate effective theory for describing the interactions among the lightest pseudoscalar mesons (π , K and η); Large- N_c expansion techniques for extending ChPT with the inclusion of the η' ; the Linear Sigma Model ($L\sigma M$) as a chiral model that incorporates in an explicit and systematic way the lightest scalar mesons together with their pseudoscalar counterparts; Vector Meson Dominance (VMD) as a phenomenological model for the interactions between the lightest vector and pseudoscalar mesons.

The research progress achieved along the year 2000 is summarized as follows :

Large- N_c , chiral approach to $M_{\eta'}$ at finite temperature ¹¹⁾:

We study the temperature dependence of the η and η' meson masses within the framework of $U(3)_L \times U(3)_R$ Chiral Perturbation Theory, up to next-to-leading order in a simultaneous expansion in momenta, quark masses and number of colours. We find that both masses decrease at low temperatures, but only very slightly. We analyze higher order corrections and argue that large- N_c suggests a discontinuous drop of $M_{\eta'}$ at the critical temperature of deconfinement T_c , consistent with a first order transition to a phase with approximate $U(1)_A$ symmetry.

The ratio $\phi \rightarrow K^+K^-/K^0\bar{K}^0$ ¹²⁾:

The ratio $\phi \rightarrow K^+K^-/K^0\bar{K}^0$ is discussed and its present experimental value is compared with theoretical expectations. A difference larger than two standard deviations is observed. We critically examine a number of mechanisms that could account for this discrepancy, which remains unexplained. Measurements at DAΦNE at the level of the per mille accuracy can clarify whether there exist any anomaly.

Chiral loops and $a_0(980)$ exchange in $\phi \rightarrow \pi^0\eta\gamma$ ^{13, 14)}:

The radiative $\phi \rightarrow \pi^0\eta\gamma$ decay is discussed emphasizing the effects of the $a_0(980)$ scalar resonance which dominates the high values of the $\pi^0\eta$ invariant mass spectrum. In its lowest part, the proposed amplitude coincides with the reliable and ChPT-inspired contribution coming from chiral loops. The $a_0(980)$ resonance is then incorporated exploiting the complementarity between ChPT and the $L\sigma M$ for this channel. The recently reported experimental invariant mass distribution and branching ratio can be satisfactorily accommodated in our framework. For the latter, a value of $B(\phi \rightarrow \pi^0\eta\gamma)$ in the range $(0.75-0.95) \times 10^{-4}$ is predicted.

3.2 Radiative corrections to the hadronic e^+e^- cross-section at DAΦNE

In collaboration with V. Khoze and N. Merenkov, a calculation of next to leading order radiative corrections to the above process has been under way ¹⁵⁾. This calculation is necessary in order to be able to extract, from data in e^+e^- annihilation into hadrons, relevant information for the theoretical estimate of the hadronic contribution to the vacuum polarization to the anomalous magnetic moment of the muon.

4 Quantum Chromodynamics and the rise of total cross-sections

This project is developed through collaborations between G. Pancheri and Rohini Godbole ¹⁶⁾, for what concerns strictly the Eikonal Minijet Model, Martin Block and Francis Halzen for the factorization picture which is extended up to cosmic ray energies ¹⁷⁾, A. Grau and Y.N. Srivastava ¹⁸⁾ for the studies of the effect of Soft Gluon Resummation on the taming of the rise of total cross-section.

The goal of this project is to obtain a QCD description of the initial decrease and the final increase of total cross-sections through soft gluon summation (via Bloch-Nordsieck Model) and QCD calculable jet x-sections, also known as mini-jets in this context. Thus, the physical picture includes multiple parton collisions and soft gluons dressing each collision.

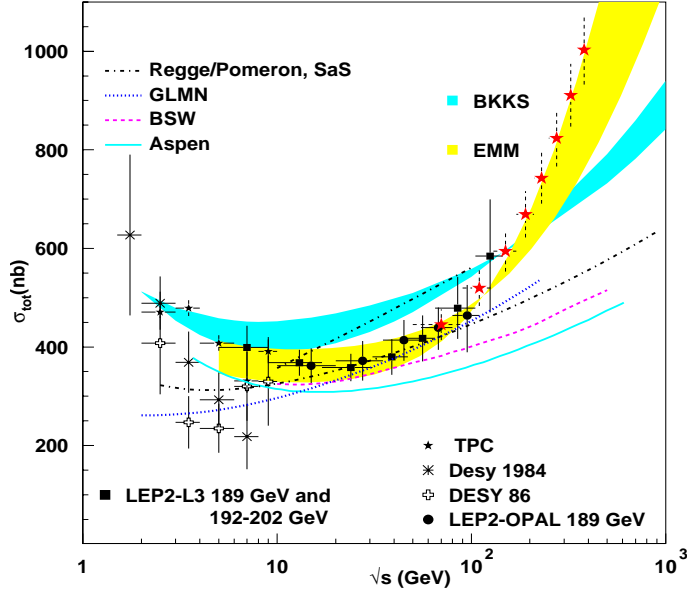


Figure 2: Photon photon total cross section data compared with various models. The stars at high photon-photon energies correspond to pseudo-data points extrapolated from EMM predictions

4.1 The Eikonal Minijet Model for protons and photons

In the Eikonal Minijet Model (EMM) the rise can be obtained using the QCD calculable contribution from the parton-parton cross-section, whose total yield increases with energy. For a unitary description, the jet cross-sections are embedded into the eikonal formalism, where the eikonal function contains both the energy and the impact parameter distribution in b -space. The simplest formulation with minijets to drive the rise, and hadronic form factors for the impact parameter distribution, can be applied to all the available x -sections. One finds that proton-antiproton high energy data can be reproduced by this model. However it is not possible to describe both the early rise, which in proton-antiproton scattering takes place around $10 \div 50 \text{ GeV}$, and the Tevatron data, with a single set of parameters.

Photo-production data can be described through the same simple eikonal minijet model, with the relevant parton densities for the jet cross-sections, scaling the non perturbative part with VMD and quark counting factors. A compilation of $\gamma\gamma$ data, including present LEP data has been done for future Linear Collider studies and is shown in fig.2, together with predictions from the EMM ^{16, 19)} and those from other models. The EMM describes quite well the rise at present energies, but the extrapolation to Linear Collider energies appears unrealistic and may need to be modified, as found in the proton case. A possible way to circumvent this problem is pursued through resummation of soft gluon emission from the initial state partons, a feature absent from most simple EMM.

4.2 Soft Gluon Summation and the impact parameter distribution of partons

A model for the impact parameter space distribution of parton in the hadrons has been developed and applied to the proton cross-sections in order to obtain a better description of total cross-section. The physical picture underlying this model is that the fast rise due to mini-jets and the increasing number of gluon-gluon collisions as the energy increases, can be reduced if one takes into account that soft gluons, emitted mostly by the initial state valence quarks, determine an acollinearity between the partons which reduces the overall parton-parton luminosity. This model can describe very well all available data for proton collisions. Work is in progress to extend this model to photon collisions¹⁸⁾.

5 Work Program for the year 2001

In addition to continue investigations along the lines just described, G. Isidori is planning to investigate the metastability of the Standard Model vacuum. If the Higgs mass m_H is as low as suggested by present experimental information, the Standard Model ground state might not be absolutely stable. It is planned to undertake a detailed analysis of the lower bounds on m_H imposed by the requirement that the electroweak vacuum be sufficiently long-lived.

As for the other participants, most of the activity previously described in hadronic physics will be continued into the year 2001. The work on QCD and total cross-sections, a long term project, will focus mainly on discussing the normalization of total cross-sections and the impact parameter distribution of partons in both in protons and photons.

References

1. A. J. Buras, G. Colangelo, G. Isidori, A. Romanino and L. Silvestrini, *Connections between ϵ'/ϵ and rare kaon decays in supersymmetry*, Nucl. Phys. B **566** (2000) 3.
2. G. Isidori, *Z penguins and rare B decays*, Talk presented at ICHEP 2000, Osaka, Japan, 27 Jul - 2 Aug 2000, [hep-ph/0009024].
3. G. Isidori, *Supersymmetric effects in rare semileptonic decays of B and K mesons*, invited talk at RADCOR 2000, Carmel, California, 11-15 Sep 2000 [hep-ph/0101121].
4. G. D'Ambrosio, G. Isidori and G. Martinelli, *Direct CP violation in $K \rightarrow 3\pi$ decays induced by SUSY chromomagnetic penguins*, Phys. Lett. B **480** (2000) 164.
5. A. J. Buras, M. Ciuchini, E. Franco, G. Isidori, G. Martinelli and L. Silvestrini, *Final state interactions and ϵ'/ϵ : a critical look*, Phys. Lett. B **480** (2000) 80.
6. G. Ecker, G. Isidori, G. Muller, H. Neufeld and A. Pich, *Electromagnetism in nonleptonic weak interactions*, Nucl. Phys. B **591** (2000) 419.
7. G. Isidori, *Weak decays of pseudo Goldstone bosons*, invited talk at Chiral Dynamics 2000, Newport News, USA, 17-22 July 2000 [hep-ph/0011017].

8. $K \rightarrow \pi\pi e^+e^-$ decays, low-energy constants and CP violation in Chiral Perturbation Theory. H. Pichl, Ph. D. thesis, University of Vienna, Dec. 2000.
9. *The CP-violating asymmetry in $K_L \rightarrow \pi^+\pi^-e^+e^-$.*
G. Ecker and H. Pichl, Phys. Lett. **B507**(2001) 193-199; hep-ph/0101097.
10. $K \rightarrow \pi\pi e^+e^-$ decays and chiral low-energy constants.
H. Pichl, Eur. Phys. J. **C20** (2001) 371-388; hep-ph/0010284.
11. R. Escribano, F. S. Ling and M. H. Tytgat, Phys. Rev. D **62** (2000) 056004 [hep-ph/0003052].
12. A. Bramon, R. Escribano, J. L. Lucio M. and G. Pancheri, *The ratio $\Phi \rightarrow K^+ K^- / K^0 \text{ anti-}K^0$* , Phys. Lett. B **486** (2000) 406 [hep-ph/0003273].
13. A. Bramon, R. Escribano, J. L. Lucio M., M. Napsuciale and G. Pancheri, *Chiral loops and $a_0(980)$ exchange in $\Phi \rightarrow \pi^0 \eta \gamma$* , Phys. Lett. B **494** (2000) 221 [hep-ph/0008188].
14. R. Escribano, *Chiral loop and $L\sigma M$ predictions for $\phi \rightarrow \pi^0 \eta \gamma$* , Proceedings of the Hadron Structure 2000 Conference, Stara Lesna, Slovak Republic, 2-8 Oct. 2000. [hep-ph/0012050].
15. V.A. Khoze, M.I. Konchatnij, N.P. Merenkoy, G. Pancheri, L. Trentadue, O.N. Shekhovzova, *Radiative Corrections to the Hadronic Cross-section Measurement at DAΦNE*, Eur.Phys.J.C18:481-490,2001, [hep-ph/0003313].
16. R. M. Godbole, G. Pancheri, *Hadronic Cross-sections in $\gamma\gamma$ processes and the Next Linear Collider*, Published in Eur.Phys.J.C19:129-136,2001 [hep-ph/0010104].
17. M.M. Block, F. Halzen, G. Pancheri, T. Stanev, *Breaking the Barriers : Uniting Accelerator and Cosmic Ray $p p$ Cross-sections*, [hep-ph/0003226].
18. R. M. Godbole, A. Grau, G. Pancheri, Y.N. Srivastava, *Total Cross-Sections*, Proceedings of Hadron Structure (HS 2000), Stara Lesna, Slovak Republic, 2-8 Oct 2000. [hep-ph/0104015].
19. R. M. Godbole, A. Grau, G.Pancheri, *Models for Photon-photon Total Cross-sections*, Proceedings of International Conference on the Structure and Interactions of the Photon (Photon 99), Freiburg, Germany, 23-27 May 1999. Published in Nucl.Phys.Proc.Suppl.82:246-251,2000

OG-21: GRAVITY THEORY AND PHENOMENOLOGY

D. Babusci, S. Bellucci (Resp.), T. Hambye (Ass.)

1 The project

There are groups from seven INFN units taking part in OG-21, i.e. LNF, Ferrara, Padova, Pisa, Roma 1, Roma 2 and Trieste.

According to General Relativity, the emission of gravitational waves is associated to a variety of physical processes that range from astrophysical phenomena, such as the evolution and coalescence of binary systems, gravitational collapse, stellar oscillations and instabilities, to cosmological processes that developed in the very early universe. Signals produced in these processes have different intensities, shapes, and characteristic frequencies; some of them are emitted in short bursts, some are continuous, some superimpose to form stochastic backgrounds with spectral properties that depend on the generating phenomenon.

In recent years, in addition to the resonant bars and to the prototypes of interferometric antennas developed since the early sixties, new detectors have been proposed which plan to explore different regions of the frequency spectrum, and new experiments will certainly be envisaged in the next future. The purpose of OG-21 is to determine the characteristic features of gravitational signals emitted by astrophysical sources, to study the spectral properties of stochastic backgrounds generated by astrophysical and cosmological processes, and to investigate which of these sources a given detector can possibly see.

The stochastic background of gravitational waves emerges as a result of processes occurring at early stages of the Universe's evolution. Owing to their cosmological origin, as shown by computing the decoupling time of the graviton from the rest of the Universe, stochastic gravitational waves yield information about the early Universe. Hence, observing their spectrum provides insight on fundamental physics at correspondingly high energies.

2 Activity carried out in the year 2000

The LNF group focussed on the possibility of detecting the stochastic background of gravitational waves, as well as the constraints given to string cosmology, inflationary models, scalar-tensor cosmology, topological defects, and first-order phase-transitions that might have occurred in the early stages of the Universe's expansion ¹⁾, and possibly quantum gravity theories. The relative contribution of gravitational waves and density perturbations to anisotropies in the cosmic microwave background needs to be understood in view of the satellite experiments (MAP and PLANCK) planned for the early 2000's.

In particular, the LNF group engaged in the study of quintessence and scalar-tensor theories, both in connection with possible measurements with laser interferometers and in the case of spherical detectors ²⁾. Our group elaborated in detail on the spectra predicted by quintessential theories ³⁾. We also worked out predictions for scalar gravitational waves originating from gravitational collapse, within the Brans-Dicke theory.

3 Activity planned for the year 2001

Our LNF group plans merging its activity with the group MI-12, working in the area of nonperturbative gravity theories. Our attention will be placed upon the fact that the weak and null energy conditions and the second law of thermodynamics are violated in wormhole solutions of Einstein's theory with classical, nonminimally coupled, scalar fields as material source. We want to study the relevance of possible ambiguities in the definitions of stress-energy tensor and energy density of a nonminimally coupled scalar.

References

1. T. Hambye, E. Ma and U. Sarkar, Phys. Rev. D **62**, 015010 (2000)
2. S. Bellucci, V. Faraoni and D. Babusci, SCALAR GRAVITATIONAL WAVES AND EINSTEIN FRAME, to be published in Phys.Lett.A
3. D. Babusci and M. Giovannini, Class. Quant. Grav. **17**, 2621 (2000)

PI-11: FERMIONIC SYSTEMS AND LATTICE

F. Palumbo (Resp.) and R. Scimia (Dott.)

1 Noncompact gauge fields on a lattice: SU(n) theories

One of the present problems of lattice gauge theories is how to increase the physical volume where the numerical simulations are performed. The physical size of the lattice is indeed a major limitation in the study of hadronic structure functions and light hadron spectroscopy, and in the evaluation of the ratio e'/ϵ .

A recent investigation showed that for SU(2) lattice gauge theory a noncompact regularization provides a physical volume larger than the Wilson theory with the same number of sites. It appears therefore interesting to repeat the simulation for the physically relevant SU(3) theory, but in its original formulation this regularization is directly applicable to U(n) theories for any n but to SU(n) theories for n=2 only.

We have then reconsidered this regularization. It makes use of auxiliary fields in order to enforce exact gauge invariance with noncompact fields. The form of the covariant derivative, for $n > 2$, is the same for U(n) and SU(n) theories. As a consequence the physical abelian field of the U(n) theory must become an additional auxiliary field in the SU(n) theory. This can be guaranteed at the quantum level by breaking explicitly the U(n) symmetry in such a way as to generate a divergent mass for this field. The terms of the lagrangian which realize this condition have been exhibited and their effect investigated. The regularization can now be used on essentially the same footing for every n.

We have also investigated the Ward identities of the effective action, confirming that the mass spectrum has the desired properties. Finally we have formulated the theory in the background gauge and written the BRS identities, showing that a perturbative treatment can be done in close analogy with the continuum, avoiding the cumbersome expansion of the link variables.

References

1. F. Palumbo and R. Scimia, Phys. Rev.D, submitted to.
2. G. Di Carlo, F. Palumbo and R. Scimia, Lattice 2001, Berlin.

PI-31: NUCLEAR THEORY

F. Palumbo (Resp.), M. Barbaro (Ass.), A. Molinari (Ass.)

1 Bosonization in Nuclear Physics

Effective bosons composite of nucleons are at the basis of the celebrated Interacting Boson Model of Arima and Iachello. They are analogous to the Cooper pairs of the theory of superconductivity. But the model has been developed so far only at the phenomenological level: In particular the parameters appearing in it have not been evaluated in terms of the fundamental nucleon-nucleon interaction, and the structure of the effective bosons is unknown.

To complete the theory we investigate an approach based on the Hubbard-Stratonovic transformation and the evaluation of the fermionic determinant by a saddle point expansion by a technique which does not violate the conservation of the number of particles. We are testing our approach on the pairing hamiltonian.

DOSIME2

E. Righi (Resp. Naz.), G. Trenta (Resp.), C. Catena (Ass.), D. Pomponi

1 Purpose of the experiment

Thyroid dose evaluation after ^{131}I administration to patients with metastasis iodine-capturing, and comparison with results of radiation protection multicompartiment model. The experiment was carried out in association with the Nuclear Medicine Unit of the II Medical Clinic of Roman University "La Sapienza" on thyroidectomized patients. The research was dealing also with the plasmatic and urinary content of ^{131}I at subsequent interval after treatment to evaluate the whole body and bone marrow dose. But at the other hand the dose was evaluated also with the biodosimetric method of micronucleus. During this experience was validated the MTT-test for the effectiveness of personal treatment and was verified the effectiveness of the 3AB-test as an index of personal radiosensitivity.

2 Results

The experimental result about the patients dose we obtained with the biodosimetric methods was very agreeing with the dose foreseen by the theoretical model. We intend use the validated methods either after accidental worker overexposure or before a radiotherapy treatment in view of evaluating the radiosensitivity of the patient.

3 Activity planned for 2001

With the foregoing results we deemed concluded the research project of DOSIME2 and we proposed a new project named INTRABIO. This Project at moment has the following objectives: International intercomparison for the MN-test, surviving evaluation of an oncological clone to different concentration of D_2O , study of particular cell proteins like p53 with the synchrotron infrared radiation, study of new *Ralstonia* bacteria for their biological properties and for the response of oncological clone to their presence.

4 List of publications

1. Catena C., Conti D., Trenta G., Righi E., Breuer F., Ventroni G., Mauro, G.A., Melacrinis F.F., Montesano T., Ronga G. - Micronucleus yield and MTT-test as indicators of damage in patient's lymphocytes after ^{131}I therapy. *The Journal of Nuclear Medicine* 41, 1522-1524, 2000.
2. Trenta G. Corso di radioprotezione per Medici Radiologi - Policlinico San Matteo - Pavia 15-16/3/00
3. Trenta G. - Seminario didattico INFN - Bologna Lezione su: Effetti biologici delle radiazioni 7/3/00
4. Trenta G. - A Possible Radiocancerogenesis Explanatory Model - 10 IRPA Congress Japan13-22 /5/00

5. Trenta G. - Lessons on nuclear emergencies cause - FARE Project of European Community Lituania and Slovacchia, 13-24/6/00
6. Righi E., Trenta G. - Lezioni al 140 corso avanzato di radioprotezione medica - 3-9/9/00.
7. Trenta G. - Lezione su Sorveglianza medica - Corso per neoassunti INFN, Padova 19-21/9/00
8. Trenta G. - Effetti biologici delle NIR - XVII Congresso AIRB, Catania 29-30/9/00
9. Trenta G. - La probabilit' causale- Relazione al III Convegno INAIL Cagliari 11-13/10/00
10. Trenta G. - Lezioni al corso europeo di radioprotezione, Saclay 7-9/11/00
11. Righi E., Trenta G. - Lezioni al Corso regionale su: Emergenza nucleare, Vercelli 14-17/11/00
12. Righi E., Trenta G. - Lezioni al seminario per Direttori INFN e al corso per collaboratori di prevenzione, LNF Frascati, Aprile 2000. (o 99?)
13. Righi E., Trenta G. - Lezioni al Master europeo per Esperti Qualificati, Pavia, Giugno 2000.
14. E. Righi, C. Catena, D. Conti, G. Trenta - Ipersuscettibilità e cancerogenesi. Modelli di riferimento per screening e monitoraggio genetico. Atti del Convegno su: Rischio ultravioletto , Cavalese 25-26 marzo 2000
15. F. Celani, A. Spallone, P. Marini, V. Di Stefano, M. Nkamura, A. Mancini, S. Pace, P. Tripodi, D. Di Gioacchino, C. Catena, G. D'Agostaro, R. Petraroli. P. Quercia, E. Righi, Trenta - High Hydrogen Loading of thin palladium wires through alkaline-earth carbonate precipitation on the cathodic surface: evidence for new phases in the Pd-H system. Unexpected problematics due to bacteria contamination in heavy water. 8th International conference on cold fusion, Lerici, May 21-26, 2000
16. F. Celani, A. Spallone, P. Marini, V. Di Stefano, M. Nkamura, A. Mancini, S. Pace, P. Tripodi, D. Di Gioacchino, C. Catena, G. D'Agostaro, R. Petraroli. P. Quercia, E. Righi, Trenta - Problems related to presence of new specific bacteria (genere Ralstonia and Streptotrophomonas) into D2O interesting with overloading of deuterium into Pd by electrolytic procedures. 2nd annual conference of the Japan Cold Fusion Society (JCF-2), October 21-22, 2000, Sapporo Japan.
17. G. Trenta - Probability of causation nel riconoscimento delle malattie a genesi multifattoriale: Probabilit' causale e radiazioni ionizzanti. Atti del III Convegno Nazionale di Medicina Legale Previdenziale, INAIL, S. Margherita di Pula (Cagliari) 11-13 ottobre 2000

FREEDOM

F. Celani (Resp.), A. Spallone (Ass.), G. D'Agostaro (Ass.), S. Pace (Ass.), D. Di Gioacchino
Collaboration with DOSIME (LNF-INFN), and EURESYS, ORIM Companies

1 Activity

The experimental task of FREEDOM (Fusion Research by Electrolytic Experiments of Deuterium On Metals) is to develop highly innovative and reproducible ($> 60\%$ success rate) techniques to maximise the value of Hydrogen (and later Deuterium) concentration in Palladium (the so called "overloading") through light water (H_2O) electrolysis ($H/Pd > 0.95$) with short waiting time for overloading (< 50 hours) and long > 4 hours). Obviously, the final target is to transfer the "method" to heavy water (D_2O) system.

The experimental activity performed, and milestones achieved, during year 2000 can be summarised as following:

- (a) several experiments to optimise the procedure of overloading H, changing the kind of electrolyte;
- (b) steps to minimise the input power of electrolysis: results very positive;
- (c) same procedure, developed as at a) and b), applied to heavy water not fully satisfactory: unexpected identification of bacteria (new species) living in (D_2O);
- (d) the bacteria, in proper conditions, produce H_2 and are able to "metabolise" heavy metals (Pb, Hg, Cd) and even U;
- (e) the two bacteria (genere *Ralstonia* and *Stenotrophomonas*) have been registered as new species at International data-banks (Japan and USA).

Because the kind of research is quite different from usual one performed at INFN and we understand that can be large scepticism about it, we will describe it in some details.

The lack of reproducibility observed in "Cold Fusion" experiments is mainly connected with the difficulty in obtaining loading atomic ratios (D/Pd) close to one. It has been shown in fact that such a high D/Pd ratio, which is considered as a necessary condition for the production of the so called "anomalous heat", is very difficult to be obtained and in particular to be maintained for reasonably long time, except few lucky occasions. In order to solve definitely such a serious problem our group has performed a systematic campaign of experiments, starting from simpler and more economic Pd-H system, aiming to find out a protocol capable to insure a fast and reproducible loading with thin Pd wires, up to a H/Pd ratio close to one.

The protocol, tested successfully in three different Laboratories (Pirelli-Labs, Milan-Italy; Stanford Research Institute International-USA; our Laboratory, in two completely different arrangements of the electrolytic cells), is based (in an acidic environment, pH about 5) on the addition of very small amount (typically $10^{-5}M$) of alkaline-earth ions (Strontium seems to be the most effective) to the re-distilled water used for the preparation of the electrolyte.

The use of re-distilled water was found to be a mandatory requirement: it has been found that the impurities normally yet present in the distilled and/or de-ionised water can negatively affect the loading process.

The protocol is based on the following physics-chemical principle: Strontium ions (as $SrCl_2$) are added to the re-distilled water in such an amount that no precipitation as $SrCO_3$ can occur in the bulk of the electrolyte with the carbonic ions normally dissolved (as H_2CO_3) in water.

Strontium carbonate is allowed to precipitate only on the cathodic surface, because of the local alkalization produced by the flowing of the electrolytic current: it is well known that the solubility of carbonates decreases strongly following to increase of the pH. In the cathodic process:



the OH^- ions formed on the cathode promote the precipitation of $SrCO_3$. The atomic Hydrogen adsorbed on the cathodic surface can either be absorbed into the Pd bulk:



or bubbled out as H_2 gas



The intrinsically catalytic surface of Pd, used as cathode, promotes generally the b) reaction, deleterious to (H,D) overloading purposes. By using our protocol, viceversa, because of the precipitation on the cathodic surface of a thin layer of $SrCO_3$, the catalytic properties are consistently reduced and the loading reaction a) turns to be predominant, thus allowing a fast achievement of H/Pd ratio =1. We have found that the addition of very small amounts of mercuric ions are also effective in maintaining the loading level over a large period of time. Hg, because its ability to form amalgams, is supposed to act as "anti-cracking agent" against Pd damage due to H,D absorption. When we tried to apply our protocol for D-Pd loading and H_2O was replaced by D_2O , the results in terms of D/Pd were consistently lower, and/or unstable, than those obtained with light water. The reasons of such an evident failure are essentially:

- - The amount of the impurities generally contained in the "as received" heavy water is too large. Foreign inorganic ions, galvanically deposited on the cathode, were found to hinder the formation of the proper $SrCO_3$ layer. Double distillation of D_2O , which is very difficult to be accomplished because of its hygroscopicity (no contact with the atmosphere is required), is a necessary but not sufficient pre-treatment.
- - Heavy water contains bacteria that were identified by us at ENEA-Casaccia. These bacteria belong to two new species, which were also found to form colonies on the cathodic surface. Therefore, several long treatments of the D_2O with $KMnO_4$ (1g/l) at pH of 1→7→13→7 under nitrogen at 90°C and at 25°C with vacuum, are previously required for a satisfactory sterilisation.

About those two new bacteria, we experienced that one of this, *Ralstonia* species, "metabolizes" several elements including the Hg used in our procedure. Thanks to specific studies, originally needed to understand the behaviour of this bacteria from the point of view of "Cold Fusion" (i.e. the effect of the elements added to electrolytic solution on H,D loading), we experimentally proved that they "absorb" almost any kind of heavy metals (Hg, Pb, Cd, Cr, Ni) included the Uranium, up to concentrations as large as several milli Moles. The beneficial effects of this new bacteria (originally living in heavy water) to polluted environments can be really impressive if all the test-tube experiments will show no side effects. The bacteria as been registered on June 2000, through the properly devoted International Scientific Institutions (DDBJ-Japan and NCBI-USA), with the name of *Ralstonia detusculanense*.

Aiming to eliminate wasting time and troublesome pre-treatments, needed to "kill" the bacteria and purify the heavy water from inorganic and organic pollutants, and taking into account that the main controlling parameter of the D-Pd loading seemed to be the ratio between the total amount of the impurities present in the electrolyte and the surface of the cathode, we realised that

the problem could be matched from a completely different point of view. In order to minimise the ratio between the amount of the impurities and the surface of the cathode, two different approaches could be taken into consideration:

- (1) build up a very thin cell, just around the electrodes (Pd surface about 1 cm²), thus containing a very small amount of electrolyte (i.e. 50cc) and consequently a negligible amount of impurities;
- (2) fill the cell currently used in our experiments, whose volume is about 1000 cc, with a new electrolyte prepared by mixing a majority part of suitable organic solvent (i.e. 950 cc) with a minority part (i.e. 50 cc) of heavy water.

In both cases, with respect to the 1000 cc of D₂O, normally used in our tests, the reduction to 50 cc is equivalent to a 20 times reduction of the impurities which could be deposited on the cathodic surface. The n.2 seemed to be extremely more attractive because of its simplicity (no need to build up a new and very delicate cell) and its flexibility (the ratio between the organic solvent and the heavy water can be varied over a large extent). As far as the choice of the organic solvent is concerned, the following requirements should be satisfied:

- - large miscibility with water,
- - very small amount of H₂O present as residual impurity (isotopic contamination of H in the D-Pd loading),
- - no (or negligible) acid properties (isotopic contamination for partial dissociation and production of H⁺ ions),
- - boiling point not too far from 100°C.

In relation to the above mentioned requirements, alcohol, keton, ester seem to be the most promising solvents.

2 Experimental results

If the hydro-organic electrolyte could be considered an elegant solution for the problem of the impurities, the proper precipitation of SrCO₃ on the surface of the cathode seemed difficult to be accomplished in the new ambient: how to control the concentration of carbonic ions? Taking into account that the actual concentration, the "activity", of the ions in the hydro-organic electrolyte could be remarkably higher than their nominal concentration (referred to both the components of the liquid phase), we realised that Strontium ions could be precipitated as SrSO₄ even though the solubility product of this compound is about 50 times higher than that of SrCO₃. In this case, the SrSO₄ precipitation in the hydro-organic ambient could be accomplished simply by controlling the amounts of Sr⁺⁺ and SO₄⁼ ions added to the electrolyte. After several tests we found that a suitable electrolyte could be prepared just by using 1000 cc of ethyl alcohol (95% concentration, i.e 50cc is water) and by adding to the hydro-alcoholic solution 20mg of SrCl₂, 1-2 cc of H₂SO₄ (0.01M) and 0.5-2 cc of HgCl₂ (0.01M). The electrolysis was started with the following conditions: Anode: Pt (wire, length 30cm, diameter 200μm); Cathode: Pd (wire, total length 30cm with 2 portions of 15cm, diameter 50μm); electrodes parallel (inter-distance 4cm); Current: 5mA.; Voltage: 20-50V; T=20°C. The loading rate of the cathode, after 1 day of "conditioning", was surprisingly high: in less than 20 minutes a H/PD ratio very close to one (R/R₀ = 1.20) is currently achieved. Our results have been completely reproduced at Pirelli Labs, Italy. Works are in progress for the application of the new protocol to a D₂O-organic solvent electrolyte.

3 List of Publications

1. High hydrogen loading of... LNF-00/006. (submitted to PL A).
2. High hydrogen... heavy water. Conference Proceedings (n.70) ICCF8, pg.181-190. Lericci, 21-26 May 2000. Editrice Compositori-Bologna. (Invited Paper).
3. New electrolytic procedure.. system. Conference Proceeding (n.70) ICCF8, pg. 191-198. Lericci, 21-26 May 2000. Editrice Compositori-Bologna.
4. Problems related to ...specific bacteria ... Japan Cold Fusion Society, Workshop n.2.(JCF2-19; pgg. 1-52). Sapporo, 21-22 October 2000. (Invited Paper).
5. Temperature coefficient of... Phys. Lett. **A 276** (2000), 122-126.
6. Invited Paper at LXXXVI Congresso Nazionale Societa' italiana di fisica", Sezione VI, Palermo, Ottobre 2000.

GEDI

A.Balerna, E.Bernieri (Resp.), M.Chiti (Tecn.), U.Denni (Tecn.)
A.Esposito, A.Frani (Tecn.)

1 Aim of the experiment

The aim of the GEDI (Gamma Emission in Deep Ice) experiment is the realisation of a portable gamma-ray spectrometer for "in situ" radioactivity measurements on glaciers and snowfields. This kind of measurements is very useful in a wide set of environmental and earth science researches, like glacial paleoclimatic studies and pollution monitoring in high altitude glaciers and snowfields or in remote areas, where sampling is difficult or impossible.

2 Activity 2000

During 2000 a first prototype has been realised and tested on the field during a glacial drilling on the Alps and at high altitude in Himalaya. The instrument is based on a standard scintillation detector made by a 100 mm \times 75 mm cylindrical NaI(Tl) crystal coupled with a photomultiplier and a preamplifier. The detector is housed in a stain-less steel waterproof box wrapped by flat electrical heaters. All the system is housed in an acrylic cylindrical box in order to be protected from water and mechanical shocks. Data acquisition is performed by using a Panasonic (Toughbook CF 27) portable computer - protected against water, dust and mechanical shocks - and a National Instruments DAQ Card (AI-16E-4). A stretching circuit has been developed to match the preamplifier output signal with the input requirements of the card. Power supply is based on a mixed system composed of a gel-lead battery and modular array of monocrystalline silicon photovoltaic cells developed for the experiment. The instrument has been tested during a glacial perforation performed in June by the glaciologist of the University of Milano and ENEA at Colle del Lys (Monte Rosa, Alps) at about 4100 m a.s.l. The detector worked well up to a depth of about 25 m in the ice. But unforeseen technical problems during the drilling prevented to reach the interesting ice layer related to Chernobyl year (1986) where we expected to detect "in situ" the Cs-137 gamma-emission, already detected analysing ice cores in laboratory in the past. A second very useful test was performed at very high altitude in September, during a scientific-mountaineering expedition directed to Cho-Oyu (8201 m a.s.l. Northern Himalaya, Tibet). A set of radioactivity measurements was performed in the snow at different altitudes, ranging between 5700 and 6400 m a.s.l., in very harsh environmental conditions. The measurements showed the efficiency of the whole system and gave many indications about some minor improvements to be realised. During one of these measurements the presence in the snow of a small quantity of Cs-137 was detected. The origin of this artificial radioactive contaminant remains at the moment unknown.

3 Activity 2001

During 2001 we planned to improve the electronics and the acquisition system in order to obtain a lighter instrument easy to employ in a systematic programs of measurements on glaciers and snowfields, in collaboration with other scientific institutions which showed a great interest for this new instrumental tool.

ICMAG2

F. Celani (Resp.), D. Di Gioacchino, U. Gambardella, S. Pace (Ass.), A.M. Testa (Ass.)

1 Program and Results

Determination of the critical current, by magnetic measurements and separation of the hysteretic superconducting contributions from the normal losses, on High Temperature Superconductors (HTS): Bi2223/Ag (tape shaped) and YBCO123(melted). It is the continuation, and evolution, of experiments started at LNF since April 1987 with YBCO material specially developed at INFN (International Patent on "Ozone Annealing of Perovskite Superconductors" obtained on 15 January 1988 from F. Celani, S. Pace, N. Sparvieri and R. Messi; see, for further details, experiments HTSCPIR and ICMAG at previous Annual Reports of LNF-INFN).

1.1 Goals

The HTS tapes as $\text{Bi}_2\text{Sr}_2\text{Ca}_2\text{Cu}_3\text{O}_x/\text{Ag}$ (usually called "Bi2223/Ag") or/and semi-fused $\text{Y}_1\text{Ba}_2\text{Cu}_3\text{O}_7$ (usually called "YBCO123") samples, are important in several scientific and technological applications, for instance (as specific interest of our Institute) to develop HTS magnets. For these reasons it is essential to know the AC losses in respect to pinning processes that sustain the superconducting current. Measures of the AC higher harmonic of the magnetic susceptibility (HHMS) under DC magnetic field, together with electric transport measures on HTS samples, can define the above-mentioned quantities. Moreover, comparison of these experimental results with computer simulations on the magnetic field diffusion in HTS samples (previously developed in the past years) are possible tests for the theoretical models that try to explain the observed experimental behaviours.

1.2 Outline

- (a) Determination of the magnetic and thermal behaviours of the critical current (I_c) in YBCO and Bi2223/Ag tapes with AC seven harmonic susceptibility measurements at low DC magnetic field (100G) near the superconducting critical temperature (T_c) with an home-made susceptometer at liquid nitrogen temperature (LN2).
- (b) Experimental facility of liquid Helium (LHe) flux-cryostat with DC magnetic field up to 7 Tesla for HHMS measurements.
- (c) Realisation (in progress) of a sensitive, non-metallic, probe for the seven (real and imaginary) harmonics of AC magnetic susceptibility. A sample-holder temperature insert from 4K to 300K for liquid He-flux cryostat will be assembled.
- (d) Numerical analysis of the non-linear magnetic field diffusion equation of the fluxons in the HTS samples. The frameworks are several: critical state models; temperature activation losses (flux creep motions); free flux-flow motion; normal electric losses. Hysteretic loops are calculated with experimental sinusoidal boundary conditions. The Fourier coefficients of the magnetic loops are proportional to the HHMS.

- (e) Comparison between the HHMS measurements and the numerical models "produce" values of some superconducting parameters as pinning potential (U_p) and critical current (J_c).
- (f) Measure of hysteretic cycles in high magnetic field on Bi2223/Ag tapes with VMS (Vibrating Sample Magnetometer) apparatus of the University of Salerno. These measurements give information on the critical current under applied high magnetic field at low temperature.

1.3 Results

A non-magnetic, home-made, variable temperature and magnetic field susceptometer ($77K < T < 300K$) has been used for HHSM versus frequency and amplitude of the applied magnetic field of melted YBCO samples (produced by Prof. Donglu Shi, Univ. of Cincinnati USA, "MAGLEV Project"). With the support of the numerical analysis have been defined the critical current and pinning potential values in the ranges near T_c . Measurements with BSCCO/Ag monofilamentary tapes (Nordic Superconductor Technologies) with the previous apparatus are in progress. Measurement using LHe flux-cryostat with the non-metallic AC HHMS probe are also in progress.

The numerical analysis of the magnetic diffusion equation in HTS samples has been published. VMS measures on BiSCCO/Ag monofilamentary tapes by Nordic Superconductor Technologies for different low temperatures have been done. Moreover, a parallel activity to reconfirm the increasing of the superconducting properties (T_c , J_c) of the HTSC samples by the electrolytic hydrogen loading at room temperature have been done. This last experimental activity was originally developed by our group at LNF, since 1993, in the framework of loading Hydrogen and Deuterium both inside Pd and several superconducting materials (YBCO, BSCCO): experiments D2O, FREE and FREEDOM (see previous Activity Reports of LNF-INFN for further details).

2 List of Publications

1. Third harmonic susceptibility..." Phys. B **284 – 288**, 895-896(2000).
2. Field and frequency dependencies of..." Philosophical Magazine B, 2000, Vol. 80, No 5, 997-2001;
3. Increasing of superconducting pinning potential..." Physica C: Superconductivity, Vol 341-348 (1-4) (2000) pp.1127-1128;
4. Frequency, amplitude of magnetic field..." Physica C: Superconductivity, Vol 341-348 (1-4) (2000) pp.1101-1102;
5. Room temperature oxidation of sintered YBCO using μs pulsed electrolysis" Physica C: Superconductivity, Vol 341-348 (1-4) (2000) pp.1135-1136.

MIVEDE

M. Pallotta (Resp.), M. Caponero (Ass.), A. Paolozzi (Ass.), F. Felli (Ass.)

1 Aim of the experiment

The aim of MIVEDE (MICrostrip VERtex DETector) is to apply optical fiber sensing techniques for permanent and real-time monitoring of both the geometrical shape and the position of particle detectors used in high energy physics experiments. The necessity of such monitoring is quite evident for high spatial resolution vertex detectors, which are usually required to be supported by very light (ideally *massless*) mechanical holding structures. Since the stability of such structures can become very critical, both displacements and deformations of the hold detector can happen because of thermal and mechanical perturbations (uncontrolled thermal gradients, long-term mechanical settling-down, residual strain relaxing, etc.). The inspection technique proposed by MIVEDE allows for a continuous metrological survey of the detector during the run of the experiment, with obvious and unrivalled advantages in case of vertex detectors whose signal coincidences has to be used as a trigger. Moreover, the availability of the technique proposed by MIVEDE can allow for lowering the stiffness requirement of detector holding structures if avoiding scattering is a must. MIVEDE proposes to use optical fiber sensors because of their immunity from electromagnetic disturbance, low mass and high resolution; among optical fiber sensors Fiber Bragg Grating type sensors are proposed as favorite because of their unrivalled long term stability

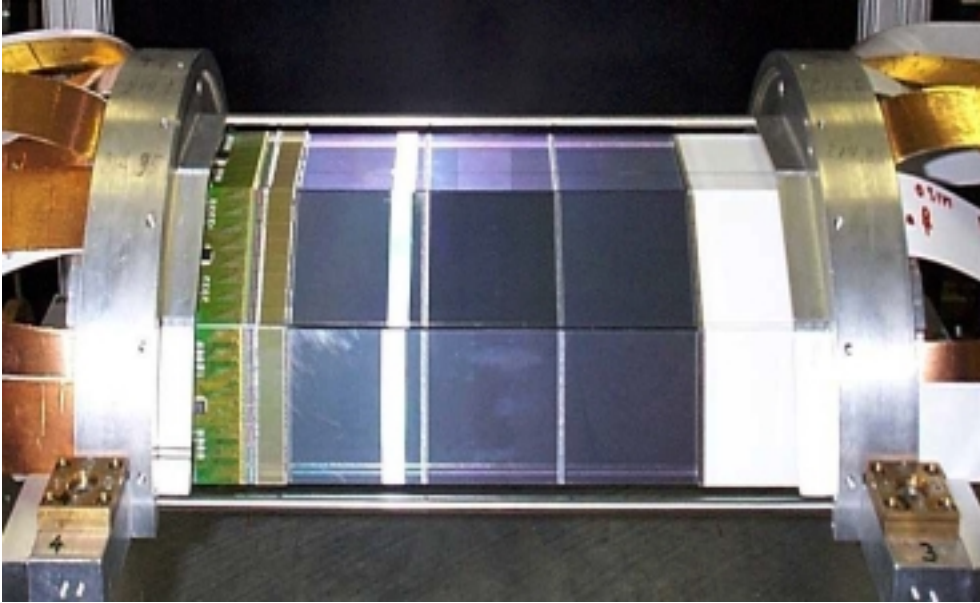


Figure 1: *FINUDA* Vertex detector. Hatched rectangles show the planned position of fiber sensors on the steel connection bar and on the microstrip detector. Instrumented steel bars and microstrip have not yet been mounted in the actual vertex detector.

2 Activity 2000

In 2000 the work of MIVEDE has been devoted to verify the feasibility of the proposed technique in the set-up of the FINUDA experiment, selected as a representative test case. The FINUDA vertex detector holding frame is a very *light* mechanical structure which houses two microstrip layers among which the target is arranged. MIVEDE has planned to monitor the deformations of both the vertex detector holding frame and the microstrip plates. As a first step, gluing tests of dummy optical fibers and dummy microstrips have been performed. Glueing test have been characterised by measurements worked out by in-fiber Michelson Interferometry and Speckle Shearographic Interferometry. Results have shown that an adequate structural bonding is obtained by use of glue normally used for microstrip construction. Afterwards, detection of the deformation field experienced by the whole surface of the microstrips in run conditions, due to thermal stress produced by heat dissipation of on-board electronics, have been performed by use of Speckle Interferometry. The identification of minimum sensors to be placed along microstrip edges for efficient deformation monitoring has been performed by software simulation.

3 Activity planned for 2001

In 2001 sensors will be attached to the holding frame of the vertex detectors and to the edges of a full functional microstrip plate. Position of sensors for best monitoring will be identified by experimental measurements and software simulation performed during the previous year. Extensive experimental tests will be performed for validating data obtained by the sensors attached to both the holding frame and the microstrip plate; Electronic Shearography is used as a reference measurement technique.

MUST

S. Dabagov, A. Marcelli (Resp.), M. Matzuritsky (Ass.),
A. Soldatov (Ass.), A. Raco (Tecn.)

1 Activity

This research project is based on the INFN Patent UE N. 97830282.6-220 (submitted also to Japan Nr. 339424/97 and U.S.A. Nr. 09/063482) that describe the idea of a novel type of diffractor for e.m. radiation, i.e. x-rays, γ -rays and neutrons based on the Bragg geometry and it is performed in cooperation with scientists of the Rostov University (CSI).

A typical device designed with the pseudo-spherical stepped geometry proposed in our research, focus with high resolution and high throughput, a beam of e.m. radiation allowing a significant gain (proportional to the number of steps) respect to a comparable, in terms of size, device having the same crystal resolution. Main goals of this experiment is to realise and test compact and efficient diffractors and to measure the gain respect to the conventional ones based on single crystal in cylindrical or spherical geometry, in order to demonstrate the advantage for scientific but also for technological and/or industrial applications (see Fig.1). After the preliminary construction and test in 1999 of the first multisteped prototypes with cylindrical geometry and low resolution crystals (gypsum and mica), we designed and test during the year new prototypes with cylindrical geometry and high resolution crystals (LiF). Although technical manufacture difficulties and not easy availability of large perfect high resolution crystals delayed the construction of the first multisteped spherical prototypes, planned in the first months of 2000, the project is substantially in time.

In 2001 following the results achieved on both the cylindrical and spherical prototypes manufactured for conventional sources and commercial apparata we will work on designing and manufacturing a new large prototype with more steps and large spherical crystal surface for SR experiments. (Additional information are available at the URL: <http://www.projectx.aaanet.ru/left1.htm>)

References

1. M.I. Matzuritsky *et al.* Tech. Phys. Lett.**26**, 502 (2000).

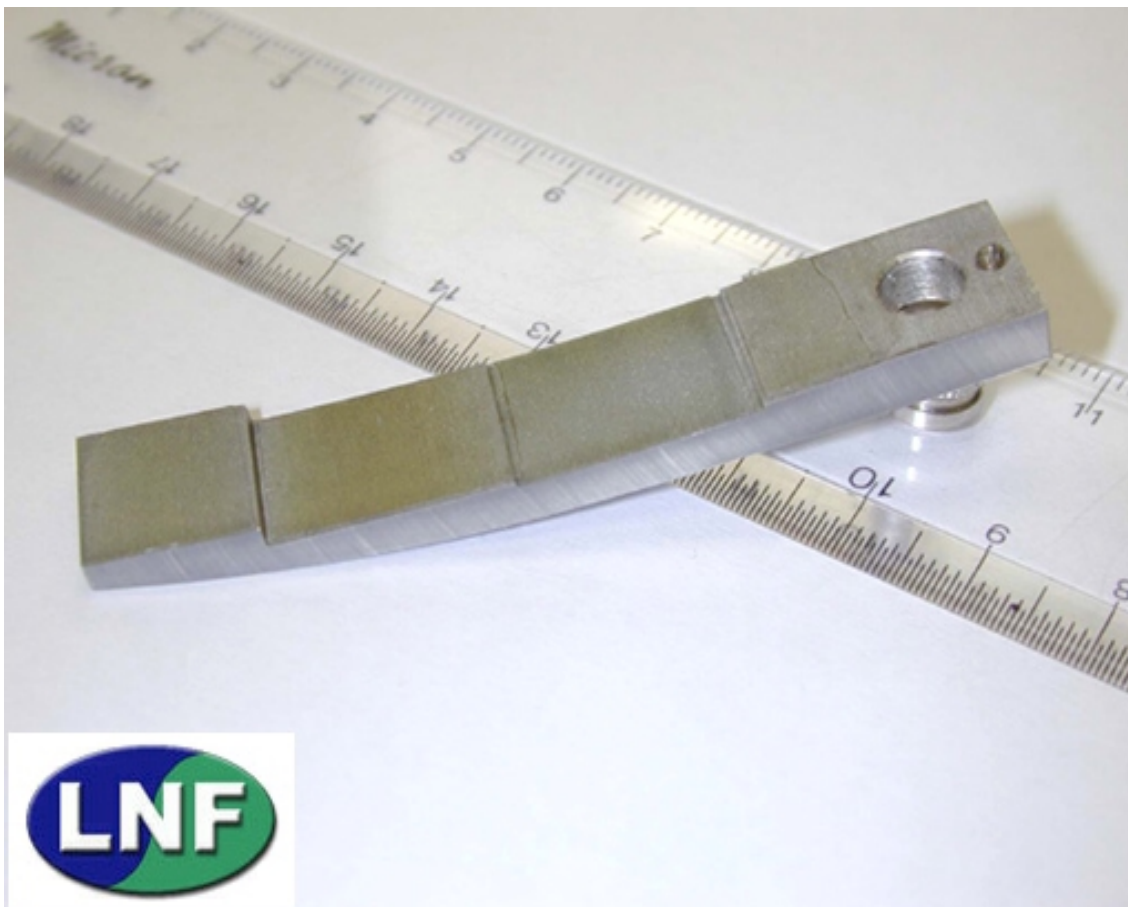


Figure 1: A photo of an asymmetric 4 steps crystal cylindrical diffractor manufactured for a commercial microanalyser (CAMEBAX). The holder is made with an aluminium alloy while the crystals glued are four thin oriented quartz (10-11) crystals.

NEMO5

M. Cordelli, A. Martini, L. Trasatti (Resp.)

1 Activity

In the framework of an European effort toward the construction of a kilometer cube detector for neutrino astronomy, the NEMO project has studied in detail the best possible sites in the Mediterranean sea, and produced several instruments to study the marine depths. During the year 2000 the group has participated in the ANTARES effort and has been preparing for the Catania Test Site.

The experiment includes INFN groups from Bari, Bologna, Cagliari, Catania, Genova, LNF, LNS, Messina and Roma 1.

The LNF group has built the prototype of an instrument to measure with great accuracy the water transparency using measurements performed at several distances from the source (NERONE). The instruments will be tested in marine waters before the end of 2001.

At the same time the group has developed several prototypes using the PIC microcontroller system, that will be used for the Catania test site slow controls.

OBD

A. Ferrari, M. Pelliccioni (Resp.), T. Rancati

1 Activity during 2000

Calculations of atmospheric showers initiated by galactic component of the cosmic rays were carried out using the Monte Carlo transport code FLUKA. The spectra of secondary particles resulting from interactions of primary cosmic rays with the nuclei in the atmosphere have been determined. The simulations have been performed at solar minimum and solar maximum activity, for several values of the vertical geomagnetic cut-off. The calculated fluence rates of secondary particles have been converted to effective dose rate and to ambient dose equivalent rate by means of appropriate sets of conversion coefficients. Although calculations are associated with large uncertainties, which comes from different sources (primary spectra, superposition model, etc.), it was found a generally satisfactory agreement between the results of calculations and experimental data. Simple equations have been proposed to calculate the radiation exposure at aircraft altitudes.

2 Program for 2001

In 2001 it will be investigated the dependence of the doses on solar activity for intermediate levels of solar modulation. In addition it will be studied the characteristics of the radiation field at aviation altitudes in order to design a dosimeter (quality factor, tissue equivalent materials, etc.)

References

1. M. Pelliccioni, Napoli 17/3/00, Voli ad alta quota, problemi di sorveglianza e protezione, Lecture at Univ. Federico II, Facoltà di Medicina e Chirurgia.
2. M. Pelliccioni, Helsinki, 5/9/2000, A simple method applicable to the individual estimates of cosmic radiation doses for air crew, European Workshop on Individual Monitoring of External Radiation, 4-6/9/2000.
3. M. Pelliccioni, Villa Olmo (Como), 16/11/2000, Dosimetria dei raggi cosmici, Lecture at School "La radioattività naturale nel nuovo assetto normativo".
4. M. Pelliccioni, Palermo 1/12/2000, La radioprotezione nella navigazione aerea e il D.Lgs. 241/2000, Giornata di Studio AIFM.
5. A. Ferrari, M. Pelliccioni and T. Rancati, Calculation of radiation environment caused by galactic cosmic rays for determining air crew exposure, *Radiat. Prot. Dos.* **93**, 101-114 (2001).

PIAP-2

A. La Monaca (Resp.), G. Cappuccio, E. Costa, G. Di Persio, B. Martino,
G. Patria, A. Rubini, P. Soffitta, N. Zema

1 Introduction

The PIAP2 experiment was closed at the end of 2000 after an activity of four years. The experiment, supported by G5 INFN, planned to realize a second generation X-ray polarimeter for detecting linearly polarized X-rays emitted from compact astronomic sources such as: binary neutron stars, black holes, gamma ray bursts and their X-ray afterglow sources. The polarimeter was built using: I) the already pre-existent PIAP equipment, developed by the same authors¹⁾, and II) two new micro-tube plates systems, aimed to multiply the ultraviolet photons created by the photoelectron charge. In Fig. 1 we report a region of capillary plate, 1.2 mm in diameter, imaged on the CCD system. The dimension of each micro-channel is about $100\mu\text{m}$.

2 2000 Activities

The first preliminary tests done on the polarimeter showed undesirable electric discharges that damaged the coating of capillary plates. For preventing these effects, we have designed and built a new holder for the micro-tube plates made with metallic and Teflon rings. The capillary plates coating was restored by ISM (CNR).

In the summer 2000, the polarimeter was tested again by our group using a mixture of Argon and Benzene at a pressure of 300 mbar and at room temperature. PIAP-2 successfully registered X-ray polarized events.

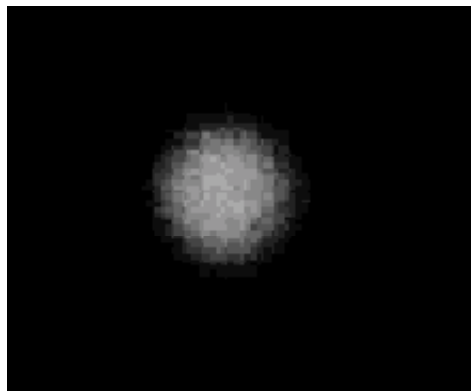


Figure 1: *Region of capillary plate, 1.2 mm in diameter, imaged on the CCD system. The dimension of each micro-channel is about $100\mu\text{m}$.*

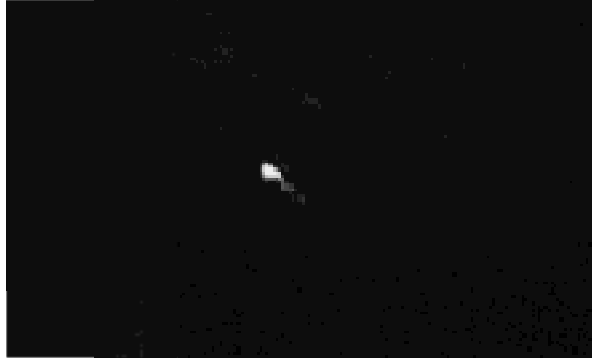


Figure 2: *Images of photoelectrons produced in Argon and Benzene by an X-ray event (^{55}Fe source, energy 5.9 keV). It is possible to recognize the beginning of the track (bottom point) with the Auger electron (starting on the right) followed by a much larger energy loss by the photoelectron (top left) at the end of the track (maximum length 1.4 mm).*

An example is shown in Fig. 2 where the light track of a photoelectron produced in the gaseous mixture by an X-ray event is imaged (^{55}Fe source, energy 5.9 keV). It is possible to recognize the beginning of the track (bottom point) with the Auger electron (starting on the right) followed by a photoelectron much larger energy loss at the end of the track (top left). The total track length is about 1.4 mm.

The initial direction of the light track of photoelectron carries memory of the polarization direction. The undesired electric discharges, with their large production of ultraviolet light, were less present but never completely eliminated. To overcome such a difficulty for the next year we plan to use instead of capillary plates the gaseous electron multiplier technique (GEM), which has the advantage to have no wire or strip planes.

3 Future plans

Due to the interest shown by the Italian Space Agency (ASI) for the PIAP-2 project during next year a collaboration between INFN CNR and ASI will become operative. In the agreement framework we plan to move and to install the polarimeter at the Institute for Space Astrophysics (IAS-CNR) to do new tests of the instrument performances for future space missions. In such contest we will experiment two fundamental problems: a) how the electron diffusion in the drift region perturbs the photoelectron track and b) how a gaseous mixture with heavy molecules can improve the modulation factor of the polarization.

References

1. A. La Monaca *et al.*, Nucl. Instr. and Meth. **A416**, 267, (1998).

PLAMIC

E. Bernieri (Resp.)

1 Aim of the experiment

The aim of the PLAMIC experiment is the realisation of an optical beam line for soft X-ray. The beam line will be utilised for X-ray microscopy on biological samples and to perform diagnostic applications on X-ray sources. This line can be used either with capillary plasma either with synchrotron radiation sources. The optics of the beam line is based on x-ray zone plates which act as lenses and monochromators to obtain magnified images of the source (or of the sample) at selected wavelengths.

2 Activity 2000

During 2000 many measurements with the capillary plasma source already built at the Physics Dept. of the University of L'Aquila (CODICE-X experiment) have been carried out. The measurements were performed to characterise in detail the x-ray emission in the "water window" energy range (200eV-500eV) which is interesting for all biological applications and at lower energies - between 50 eV and 70 eV. In particular we measured the flux and the geometrical characteristics of the beam, as a function of the source-detector distance and as a function of the pressure of the Ar gas inside the source, by using a stand-alone gold grating (1000 l/mm) a PIN diode and x-ray films. We report here some reference data: The integrated X-ray flux is about 4×10^{13} ph/cm² at a distance of 40 cm from the source, 0.4 Torr of gas pressure and 50 ns of pulse length. In the energy range 50eV-70eV the source size (S) is about 1.2 mm and the source angular divergence (A) is about 12 mrad. In the water window we measured: S=0.2 mm and A= 2 mrad. These data have been utilised to select the zone plates necessary to optimise the match between the source and the optical system. Our optical system utilises two different zone plates. A condenser zone plate (CZP) that monochromatises and focuses the x-ray beam on the sample, and a micro zone plate (MZP) that produces a magnified image of the sample (or of the source) on the detector (a CCD camera). Two kind of CZP has been chosen: a first one made by e-beam technique (CZP1: diameter: 0.92 mm, number of zones: 920, outer zone dimension: 250 nm) and the other one made holographically at the Gottingen University (CZP2: diameter: 9 mm, number of zones: 41890, outer zone dimension: 53.7 nm). CZP1, with a depth of focus of 0.08 mm, is suitable for thick samples. CZP2, with a depth of focus of 0.004 mm, has been chosen to obtain high flux on thin samples. As MZP a zone plate with the following characteristics has been chosen: diameter: 0.1 mm, number of zones: 475, outer zone dimension: 0.05 mm. This latter parameter determines the ultimate resolution obtainable with this optical configuration. On the basis of the optical requirements of the system a complete design of the apparatus, in particular concerning mechanics and micro-stages characteristics has been realised.

3 Activity 2001

During 2001 we plan to obtain and to test CZP1 and MZP ordered to the Fastec Company. The CCD camera and all the mechanical components will be bought. At the same time other measurement with the plasma source will be carried out - by using other gases and a multilayer monochromator - in order to further optimise the X-ray beam characteristics.

POLYX

G. Cappuccio (Resp.), S. Dabagov, A. Marcelli, A. Raco (Tecn.)
A. Pifferi, C. Gramaccioni (Tecn.), M. Kumakhov, R. Fedorchuk

1 Experiment aims

The main aim of POLYX (polycapillary optics in X-ray applications), funded by INFN - Gruppo V, is to study and to utilize polycapillary optics in X-ray applications using both conventional sources (X-ray tubes) and synchrotron radiation (SR). Polycapillary lenses allow the increase of the radiation density in the focal spot position. Polycapillary semi-lenses allow quasiparallel X-ray beams from divergent sources or convergent beams from quasiparallel sources (SR) to be obtained. Finally straight polycapillaries (pillars) match parallel beams with X-ray detectors, monochromators, etc.

2 2000 Activities

In order to propagate and transfer X-ray beams, glass polycapillary optics must work in total external reflection regime, i.e., the grazing incidence angle of the impinging radiation must be less than 4 mrad for Cu wavelength. During 2000 year, co-working with Institute for Roentgen Optics (Moscow) and Istituto di Strutturistica Chimica (CNR) an original alignment procedure was set up using a four circles diffractometer. After the alignment the X-ray focal image was viewed on a fluorescent screen and registered on a film. The density gain was measured to be $\sim 30\%$ ^{1, 2}). Moreover, for the first time, a theoretical explanation was also given for the reduction of the divergence value at the output of a polycapillary lens ³).

During 2000 our group gave oral presentations on the first results obtained by means of the polycapillary optics in the following conferences and meetings:

- EPDIC -7 - The 7th European Powder Diffraction Conference, Barcelona, May 20-23, 2000
- SPIE'00 - The Annual SPIE Meeting, San Diego, July 29 - August 3, 2000
- XXX Congresso Nazionale AIC, Martina Franca, September 19-22, 2000

3 2001 Program

Polycapillary optics will be installed and tested on the high-resolution diffraction station that will be operative on the X-ray beam-line at "DAΦ-Light Laboratory" (LNF, Frascati). This station will utilize both a Cu tube and SR as X-ray sources. At the output of the X-ray tube a polycapillary semi-lens, held up by a "Gimbal mount", will be aligned for obtaining a parallel beam to be used for thin solid film diffraction measurements; while a full lens will be installed for micro-diffraction experiments. Polycapillary optics will also be used in connection with synchrotron radiation mainly to condense the beam.

References

1. G. Cappuccio, S. Dabagov, Preprint INFN - LNF - 00 / 003 (P), 1-11, 2000
2. G. Cappuccio, S. Dabagov, Proceedings of SPIE 4155, 40, 2000.
3. G. Cappuccio, S. Dabagov, Proceedings of SPIE 4138, 88, 2000.

SFERA

F. Tazzioli (Resp.), C. Vicario
collaboration with Univ. Roma 2, Univ. Milano and Univ. Roma 1.

1 Activity

The SFERA experiment comprises two programs. The first one is situated at Milan INFN and University section and is concerned with the study of ferroelectric cathodes for the generation of electron beams by voltage pulse excitation. The year 2000 program has been completed and an application to ECR ion sources has been devised. Details can be found in the Milan activity report.

The second program, which is carried on at Frascati LNF, has the goal of studying and developing robust photo-cathodes for linear accelerators. The experiment uses an apparatus consisting of a medium power Nd-Yag mode-locked laser, a vacuum chamber containing the diode for the emission measurements and an RF streak camera with picosecond resolution for the measurement of the temporal distribution of emitted electrons.

In 2000 we have set up a crystal for the generation of the fourth harmonic of the laser (266 nm) to extend the spectrum of analysis. We have also set the streak camera operating. Ferroelectric PLZT ceramics, besides emitting by voltage excitation, are also photo-emitters and were studied in the first phase of the experiment.

They have shown a photo-emission efficiency not adequate to the goal requirements. Therefore in 2000, after completing a measurement campaign on such ceramics, we started a collaboration with the Department of Chemical Science and Technology of University of Roma 2 for the study and development of photocathodes made of synthetic CVD diamond films on metallic substrates. Measurements have shown that such cathodes have an interesting emission efficiency at 266 nm and moreover they can work in moderate vacuum environment. In 2001 the study of such diamond film cathodes is further pursued.

References

1. Polycrystalline diamond and Nd-doped diamond photoemitters., I. Boscolo *et al.*, Optics Communications **187** 179-184 (2001).
2. Measurement of the temporal response of ferroelectric photocathodes- M. Castellano et al., Proc. XX Linac Conference, Monterey 2000, 169-171.
3. Effects of prepoling and polarization on p hotoemission from ferroelectric ceramics.- I. Boscolo *et al.* - Journal of Applied Physics, **89**, 1367-1370 2 Jan 2001.

SIEYE2

S.Bartalucci, G.Mazzenga (Tecn.), M.Ricci (Resp.)

Participant Institutions:

ITALY: INFN LNF, Firenze, Roma2, Trieste;
RUSSIA: MePhi, IBMP, RKK"Energiya" (Moscow)
SWEDEN: KTH (Stockholm)

1 Introduction

The SIEYE2 experiment has been carried out on the MIR Space Station to study, using a silicon strip segmented detector, the biophysical effects related to the radiation environment inside the Station (altitude 400 Km , inclination 51.5°) with particular attention to the phenomenon of "Light Flashes" (LF) ¹⁾. A prototype of the detector (SIEYE1) was placed on the Station MIR in October 1995 obtaining, during its two years in operation, 25 measurement sessions with 6 different astronauts, and recording more than 50 LF's. Following the success of this mission, a new detector (SIEYE2) has been developed and built in order to have a more accurate analysis of the radiation flux (in particular for high Z particles) in the zone of the South Atlantic Anomaly (SAA) and in the subpolar zones. The equipment of SIEYE2 provides the opportunity for a simultaneous definition of the particle trajectory and its arrival time, an estimation of its energy and the recognition of its charge. A complete description of the experiment is given in ²⁾, ³⁾ and ⁴⁾. SIEYE2 was delivered on board of the Space Station MIR in October 1997, and several acquisition sessions (since February 1998) have taken place with different astronauts until the reentry of MIR in March 2001 and its subsequent destruction in the Earth atmosphere.

The SIEYE2 experiment makes use of silicon strip detectors to measure the coincidence between the passage of an ionizing particle and the occurrence of a LF. The astronaut wears a helmet which holds on its side the detector box; a joystick, connected to the same detector box, and controlled by the acquisition PC, is used for LF acquisition. The system can be seen as a completely software controlled solid state instrument. Its main characteristics are: small dimensions, portability, low power consumption, user friendly interface, real time data analysis.

The detector is compact (max dim. 264 mm) and with a low mass (less than 5.5 Kg); it measures particle energy losses from 0.25 to more than 250 MeV and determines the particle trajectory with an angular accuracy of 3 degrees.

Final analysis of SIEYE2 data is in progress, while a brand new project, called ALTEA is under development to install on board the International Space Station a larger telescope with the concomitant use of electroencephalography and visual stimulation, to directly correlate LF and particle crossing the head with brain activity.

2 Activity of the LNF group

The LNF group has taken the responsibility of the design, test and construction of all the mechanical structures and interfaces of both SIEYE1 and SIEYE2 detectors contributing also to the integration of the mechanical support for the DAQ. It participates in the beam test activity (performed at GSI-Darmstadt and TSL-Uppsala). In view of the new ALTEA experiment, the LNF

group, with the support of the Service of Development and Construction of Detectors, has the responsibility of the design, test and construction of the complete structure and assembly of the qualification model for ground testing and calibrations.

References

1. G. Horneck: "Radiobiological experiments in space: a review", Nucl. Tracks Radiat. Meas., 20, 185 (1992).
2. A. Galper et al., "Sileye on MIR – First active detector for the study of light flashes in space", Proceeding of the Sixth European Symposium on Life Sciences Research in Space 17-21 June, Trondheim, Norway, (1996).
3. A. Morselli, et al.: "Cosmic ray studies on the MIR space station", Proc. XXIV ICRC, Durban 1997 Vol.5, (1997).
4. G.Furano et al.: "Measurement of Nuclear Mass Distribution of Primary and Recoil Heavy Ions inside MIR Space Station with SilEye Silicon Detector", Proc. XXVI ICRC, Salt Lake City vol.5 p128 (1999).

CTF3

D. Alesini, C.Biscari, R.Boni, M.Boscolo, A.Clozza,
G.Delle Monache, G.Di Pirro, A.Drago, A.Gallo, A.Ghigo (Resp.),
F.Marcellini, G.Mazzitelli, C.Milardi, L.Pellegrino, M.A.Preger,
C.Sanelli, F.Sannibale, M.Serio, F.Sgamma, A.Stecchi, A.Stella, M.Zobov,

1 Activity

The next generation of high-energy e^+e^- machines after LEP will be linear colliders. The Compact Linear Collider (CLIC) has the potential to achieve a MultiTeV collision energy. A special feature of CLIC as compared to other schemes presently being studied is the high frequency of accelerating cavities, 30 GHz, and the high accelerating gradient of 150 MV/m.

CLIC is based on a two beam scheme: a drive beam running parallel to the main beam, whose bunch structure carries a 30 GHz component. The RF power is extracted from the drive beam in Power Extraction and Transfer Structures (PETS) and transferred to the main beam.

The main goals of the CLIC Test Facility (CTF3) are to test this new RF power generation scheme and to produce 30 GHz RF power at the nominal peak power and pulse length, such that all 30 GHz components for CLIC can be tested at nominal parameters.

The facility will be built in the existing infrastructure of the LPI complex and make maximum use of equipment which have become available after the end of LEP operation. The existing RF power plant from LIL at 3 GHz will be used. The project is a collaboration between CERN, INFN Frascati, IN2P3/LAL at Orsay and SLAC. The layout of CTF3 in its nominal phase is shown in Fig. 1.

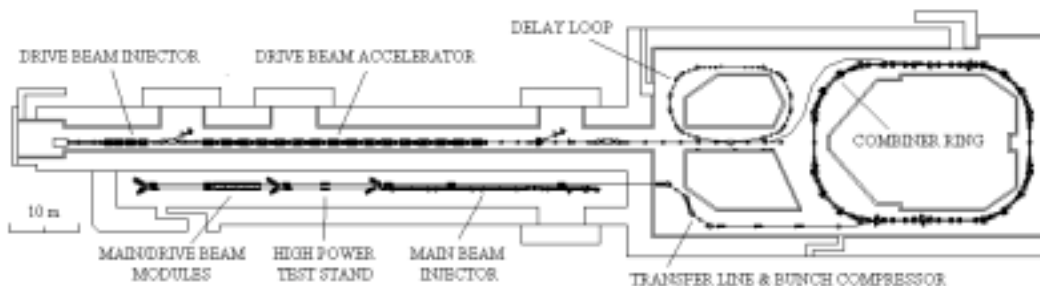


Figure 1: *Layout of the CLIC Test Facility.*

The Accelerator Division activity has been devoted mainly to studying and projecting the delay loop, combiner ring and transfer lines in between in which the long train of bunches coming from the linac are compressed by a factor ten. The compressed pulse has the temporal structure needed to produce the 30 GHz RF power in the PETS. The optical design of the transfer line and rings has been completed and layout prepared ¹⁾. The beam dynamic studies including the impedance budget are well advanced; the parameters of the injection RF deflectors and combiner ring extraction kicker have been fixed ²⁾. The Accelerator Division activity on the CTF3 project for the year 2001 will be on:

- the CTF3 Nominal Phase Design Report completion;
- the rings parameter optimisation;

- the study and realization of the low impedance vacuum chamber prototypes;
- the project of the RF deflectors;
- the collaboration to the CTF3 preliminary phase commissioning.
- a closed-cycle and liquid helium cryostats.

References

1. C. Biscari *et al.*: "CTF3: Design of Driving Beam Combiner Ring", presented at EPAC2000, 26-30 June 2000, Wien, Austria, Frascati Report LNF-00/021(P).
2. A. Gallo *et al.*: "Studies on the RF Deflectors for CTF3", presented at EPAC2000, 26-30 June 2000, Wien, Austria, Frascati Report LNF-00/021(P).

DAΦNE-LIGHT

D. Bettega (Osp.), E. Burattini (Resp.), P. Calvani (Ass.), G. Cappuccio (Ass.),
G. Cinque, S. Dabagov (Ass.), C. Iliescu (Ass.), A. Grilli (Tecn.),
A. Marcelli, C. Mencuccini (Ass.), R.M. Montekali (Ass.), F. Monti (Ass.),
A. Mottana (Ass.), E. Pace, M. Piacentini (Osp.),
A. Raco (Tecn.), L. Tallone (Guest)

1 Activity

DAΦNE is a double storage ring with a non-conventional layout, which exhibits interesting and unique characteristics as synchrotron radiation source useful for research and technological applications in an energy range that span from the far infrared to the soft x-ray range. The DAΦNE spectral distribution is shown in Fig.1.

In the Synchrotron Light Laboratory - DAΦNE-Light - several experimental apparatus connected to three separate beamlines are installed. The first one, called DXR-1, is a beamline that collects about 15 mrad of the radiation emitted by one of the multipole wiggler installed in the storage ring, having a critical energy of 310 eV. This beamline, equipped with a double crystal monochromator, will be used for absorption and fluorescence spectroscopy, diffraction experiments and LIGA processes. In fact the final part of the wiggler beamline is installed inside a "clean room" - A 100 class - where a x-ray stepper K.SUSS, shown in Fig. 2, will be used for microlithography processes particularly devoted to biomedical devices.

The second beamline, called DXR-2, is a branch line achieved by means of a 2 degree grazing incidence mirror which divides the DXR-1 beam in two parts as shown in Fig. 3, where the layout of the DAΦNE-Light Laboratory is reported.

The experiments planned at this beamline will be performed in a dedicated experimental area where photons in the spectral range between 1 eV and 800 eV will be selected by suitable monochromator. The first planned experiment concerns the determination of biological effects induced by the B-band of UV radiation on cultures of human cells. A dedicated laboratory where in situ post-irradiation treatment on cell cultures will be performed is under way. The third beamline, called SINBAD, is an infrared beamline, which collects photons emitted from a bending magnet. Indeed, the unique characteristics of this ring, namely high current ($I > 1$ A), make it a powerful tool for applications in the IR range. The expected gain in brilliance of this SR source is about two orders of magnitude higher than an intense thermal source like a black body at 2000 K in the medium and far IR, as shown in Fig. 4, where the ratio between the brilliances is shown. The optical system installed allows preserving the high brilliance and intensity of the photon beam. Moreover, it has been designed to match several dedicated equipments:

- a Bruker Equinox interferometer modified for vacuum operation, covering the range 10-12000 cm^{-1} with a resolution of 0.5 cm^{-1} , equipped for both transmittance and reflectance measurements;
- a Bruker microscope working in the range 400-6000 cm^{-1} , equipped with computer-controlled sample stage;
- a closed-cycle and liquid helium cryostats.

Unique experiments in biophysics, solid state physics and material science will be possible. During the year 2000 the DAΦNE-Light group completed the installation of the synchrotron radiation beamlines both in the DAΦNE hall and in the laboratory. In December 2000 both the x-ray and the UV beamlines have been connected to the storage ring and on 11th of December, for the first time, the two x-ray beams have been observed.

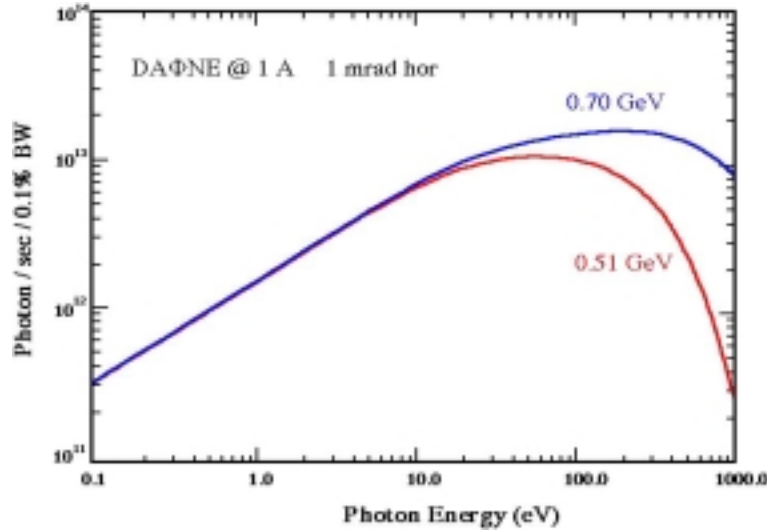


Figure 1: *The spectral distribution of DAΦNE bending magnet at two different electron energies for 1 mrad hor. and at 1 A of circulating current.*

In Fig. 5 the viewports installed at the end of the two beamlines are shown. The two beams are visible by means of the light emitted by the phosphors excited by synchrotron radiation. The safety systems of the two beamlines, according to the protocol fixed by the Radiation Protection Service and the remote control of the beamlines have been completed, in cooperation with the Electronics and Controls Service of the LNF.

During the year 2001 the DAΦNE-Light program will proceed with the alignment of the three beamlines and with the tests on the optical system installed on the lines. The start up of the experimental activity on the three beamlines is planned for the final fraction of the year. In Fig. 6 and in Fig. 7 respectively, the two X-ray beamlines and the IR beamline into their respective tunnels are shown. To perform the LIGA research activity the Laboratory is also equipped with a SEM with an ELPHY III tool that allows electron beam lithographic processes. The system, with a proper SW and HW, allows making sensors or microdevices and may be used in the technology of the x-ray mask production. In cooperation with the ENEA the electron beam lithography has been used to write a color-center channel 15 mm long and 140 micron wide on the surface of an optically polished LiF crystal. This research program is devoted to the investigation of devices able to guide and amplifying the light.

2 List of publications

1. G. Cappuccio *et al.*, Talk at the VII European Powder Diffraction Conference (20-23 May 2000, Barcelona, Spain).
2. S. Dabagov, Talk at the Annual SPIE Meeting (July 29 - August 3, 2000, San Diego, USA).
3. S. Dabagov, Talk at the Annual SPIE Meeting (July 29 - August 3, 2000, San Diego, USA).
4. S. Dabagov, Talk at the HERCULES Euroconference (April 6-9, Grenoble, France).



Figure 2: *The Karl SUSS x-ray stepper.*

5. S. Dabagov, Talk at the International Conference on Synchrotron Radiation Instrumentation 2000 (August 21-25, Berlin, Germany).
6. A. Marcelli, Invited Talk at the 5th International School and Symposium on Synchrotron Radiation in Natural Science (12-17 June 2000, Ustron-Jaszowiec, Poland).
7. A. Marcelli, Invited Talk at the 5th International School and Symposium on Synchrotron Radiation in Natural Science (12-17 June 2000, Ustron-Jaszowiec, Poland).
8. A. Marcelli, Talk at the International Meeting Advances on Micas (Problems, methods, applications in geodynamics)(2-3 November 2000, Roma, Italy).
9. R.M. Montereali, Talk at the LXXXVI Congresso Nazionale SIF (6-11 Ottobre 2000, Palermo, Italy).
10. J. Abdallah Jr. *et al.*, Quant. Electr. **30**, 694 (2000).
11. M.F. Brigattiet *al.*, Clays and Clay Miner. **48**, 272 (2000).
12. E. Burattini *et al.*, Proc. Near Infrared Spectroscopy 9th Int. Conference, Ed. A.M.C. Davies and R. Giangiacomo, p. 165 (2000).
13. G. Cappuccio and S.B. Dabagov, Proc. SPIE **4138**, 88 (2000).
14. G. Cappuccio and S.B. Dabagov, SPIE Selected Papers **4155**, 40 (2000).
15. G. Cinque *et al.*, Biophysical J. **79**, 1706 (2000).
16. G. Cinque *et al.* Photosynthesis Res. **64**, 233 (2000).
17. G. Cinque *et al.*, Proc. Near Infrared Spectroscopy 9th Int. Conference, Ed. A.M.C. Davies and R. Giangiacomo., p. 483 (2000).

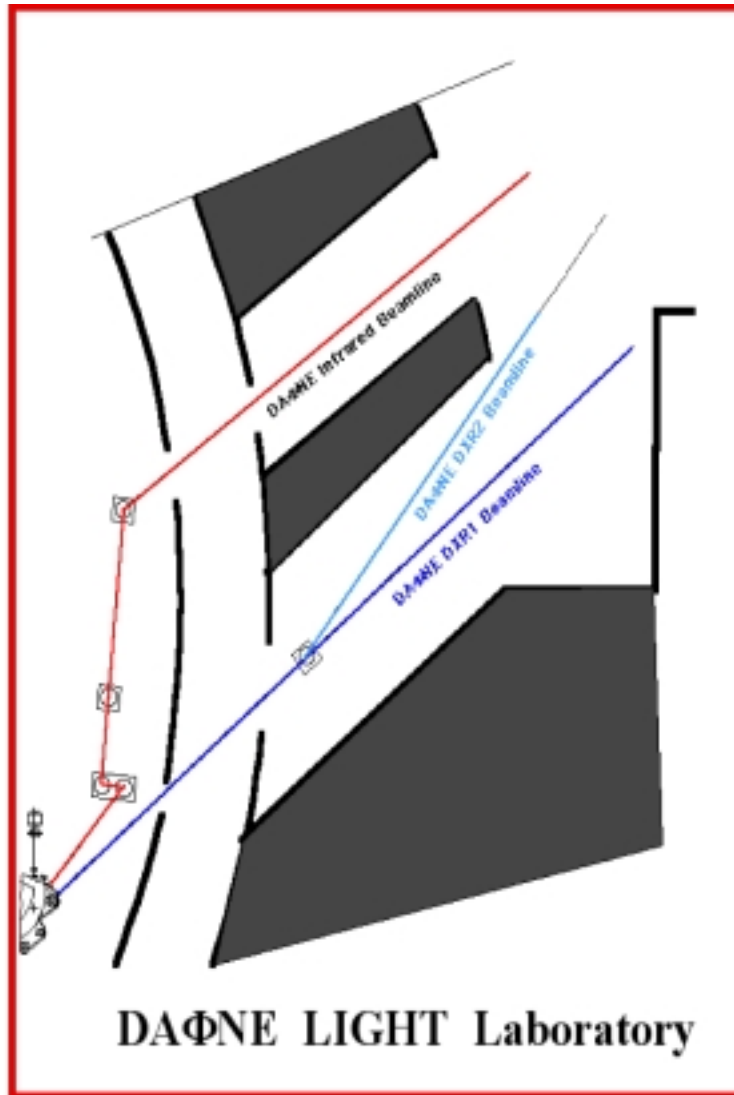


Figure 3: *Schematic layout of the three beamlines.*

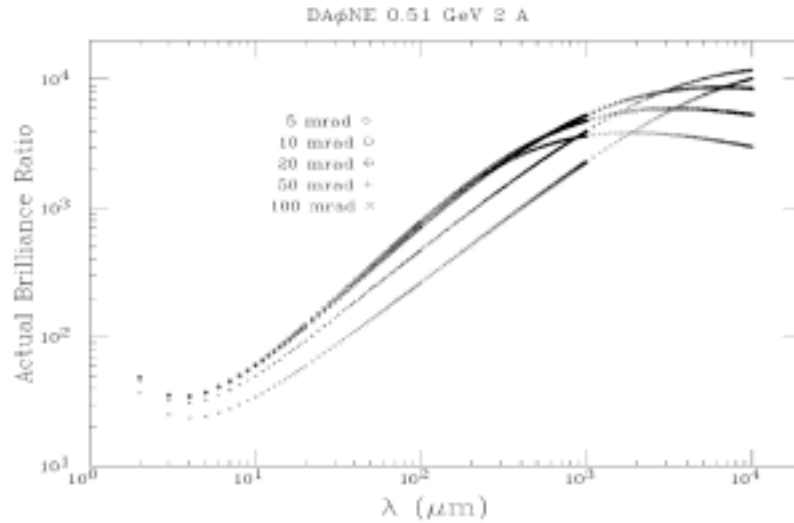


Figure 4: Ratio between the brilliance of the SINBAD IR beam and that of a black body at 2000 K at different horizontal collection angles. The simulations have been performed integrating SR over the full vertical emission angle at 0.51 GeV and with 2 A of circulating current.

18. R. Croce *et al.*, Photosynthesis Res. **64**, 221 (2000).
19. S.B. Dabagov *et al.*, Appl. Opt. **39**, 3338 (2000).
20. S.B. Dabagov *et al.*, Proc. SPIE **4138**, 79 (2000).
21. S.B. Dabagov, SPIE Selected Papers **4155**, 73 (2000).
22. S.B. Dabagov *et al.*, SPIE Selected Papers **4155**, 86 (2000).
23. S.B. Dabagov *et al.*, SPIE Selected Papers **4155**, 93 (2000).
24. G. Dalba *et al.*, Phys. Chem. Glasses **41**(5) (2000).
25. V.N. Makhov *et al.*, Synchr. Rad. News **13**, 20 (2000).
26. A.N. Mansour *et al.*, J. Synch. Radiat. **8**, 809 (2001).
27. M.I. Mazuritsky *et al.*, Tech. Phys. Lett. **26**, 502 (2000).
28. A. Marcelli *et al.*, J. Appl. Cryst. **33**, 234 (2000).
29. A. Marcelli, *et al.*, SPIE 99 vol. **3775**, pp. 7-12 (2000).
30. V.A. Murashova *et al.*, SPIE Selected Papers **4155**, 28 (2000).
31. F.B. Rosmej *et al.*, J. Quant. Spectr. Rad. Trans. **65**, 477 (2000).
32. Ziyu Wu *et al.*, J. Synch. Radiat. **8**, 215 (2001).



Figure 5: *The two visible spots shown in the photo are the light emitted by the phosphorus excited by the two SR X-ray beams striking the two viewports*

33. Ziyu Wu *et al.*, *J. Synch. Radiat.* **8**, 934 (2001).

34. Ziyu Wu *et al.*, *J. Phys. Cond. Matter.* **12**, 6971 (2000).



Figure 6: The soft X-ray beamline (on the left) and the UV beamline (on the right) inside the laboratory are shown.



Figure 7: Final elements of the IR beamline.

GILDA

A. Balerna, F. Campolungo (Tecn.), S. Mobilio (Resp.)
V. Sciarra (Tecn.), V. Tullio (Tecn.)

1 Introduction

GILDA (General Purpose Italian BeamLine for Diffraction and Absorption), is the Italian CRG beamline, built to provide the Italian scientific community with an easy access to the European Synchrotron Radiation Facility to perform experiments with a high energy and brilliance X-ray photon beam, which, up to now, is not available in Italy. GILDA is funded by the three Italian public research Institutes: Consiglio Nazionale delle Ricerche (CNR), Istituto Nazionale per la Fisica della Materia (INFN) and Istituto Nazionale di Fisica Nucleare (INFN). The main scientific goal of GILDA is the study of local structural properties. To this purpose the beamline was designed and realized by the GILDA group to provide a focussed X-ray beam of high intensity in a wide spectral range. Experimental stations for X-ray Absorption Spectroscopy and Anomalous X-ray Scattering were realized. X-ray Absorption Spectroscopy (XAS), both in the extended region (EXAFS) and in the edge and near edge region (Xanes and multiple scattering region) as well as Anomalous X-ray Scattering are powerful experimental techniques to study the local structure: both give a quantitative description of the local structure that is distances, coordination numbers, kind of atoms surrounding an absorbing center up to the third-fourth coordination shell.

2 Activity on the GILDA beamline during 2000

During 2000 a big effort was dedicated to the commissioning of the second mirror, that vertically focuses the beam in the different experimental apparatus along the beam line. During 2000, following a procedure developed by the ESRF optics group, test measurements has been performed on the mirror with the X-ray in order to assess the proper working of the piezo actuators in the operating conditions and in order to accurately check the actual possibility to curve the mirror at the desired radii of curvature to focus the beam. In order to renew the control hardware of the beamline and of the instrumentation, largely no more on the market, and in order to use the standard card used by the ESRF beamlines, the hardware controlling the monochromator has been changed with cards currently in use at ESRF. Big part of the technical and computer updates were performed by the LNF technicians.

2.1 Absorption Hutch

For the first time high accuracy EXAFS spectra at very high energies (60-80 keV) has been measured by using the 3rd harmonic transmission of the monochromator. In particular the EXAFS spectrum at the K edge of gold ($E=80725$ eV) has been measured: at our knowledge it is the spectrum at the highest energy ever collected in the world. The excellent quality of the spectrum allows to schedule experiments requiring high energy when the beamline is in the standard configuration (i.e. with the Si(311) as crystal monochromator). A new oven for high temperature has been successfully tested on the beamline and used by an Italian experiment (08-01-246). It is based on a graphite-stripheather and can be used between RT and up to 2000 K. A preparation system consisting in an evaporation stage and oven for thermal treatments up to 1300 K has been designed for the REFLEXAFS chamber and is now under construction. The first tests on the beamline are scheduled for May 2001. Concerning the 13 element fluorescence detector, a new

method for isolating the fluorescence signal of interest from the spurious signals (due to elastic, scattering, to Compton scattering and fluorescence from other atoms) is under study: instead of a raw integration between two limits, the fluorescence spectrum will be fitted with mathematical functions modeling the various contributions. Moreover also the correction of the raw data for the detector response due to dead time is under study. Finally, the software of the EXAFS hutch (vacuum operations + motor motions) has been completed and now is fully operative in the client-server philosophy.

2.2 Diffraction hutch

The angle dispersed set-up, based on 2D Imaging Plate (IP) detector, was installed in the GILDA diffraction hutch in 1999 and became fully operative at the beginning of 2000. The low noise and wide dynamical range of IP detector coupled with the high flux of the beam, allows to achieve very good signal to noise ratio on weak scatterers and/or diluted polycrystalline materials ($\leq 1\%$ in weight) in short collection time (a full diffraction pattern is recorded in less than a minute in these conditions). The instrument has been specifically designed to perform time resolved XRD experiments to follow in-situ structural modifications.

3 Beamtime use during 2000 and scientific outcomes

During 2000 15 public and 36 Italian experiments were performed on GILDA: 37 were of X-ray Absorption and 14 were of X-ray diffraction. Results to be mentioned during 2000 were obtained on the Co segregation in CoCu granular alloys and its influence on the magnetoresistance, on the structural origin of the oxygen doping mechanism in artificially layered superconducting superlattices, on the comparison between the beta-decay electron spectrum and the X-ray absorption spectrum of Re, on the Cu-Pd/pumice supported catalysts.

4 2001-GILDA Forseen Activity

Tests on the second mirror will be completed and the intervention on the beamline will be scheduled in order to optimize the vertical focusing of the beam. The hardware of the optical hutch and of the absorption hutch will be implemented in the new standard. The beamline and instruments control software will be implemented under LABVIEW. An high temperature oven for the X-ray absorption hutch will be designed, realized and installed. The REFLEXAFS apparatus will be commissioned and implemented.

References

1. F. Boscherini, G. Capellini, L. Di Gaspare, F. Rosei, N. Motta, S. Mobilio, Appl. Phys. Lett. **76**, 682 (2000).
2. C. Maurizio, F. D' Acapito, M. Benfatto, S. Mobilio, F. Gonella, Eur. Phys. J. B **14**, 211 (2000).
3. F. D' Acapito, G. Battaglin, F. Caccavale, E. Cattaruzza, F. Gonella, P. Mazzoldi, S. Mobilio, J.R. Regnard, J. Appl. Phys. **87**, 1819 (2000).
4. A.Longo, A. Balerna, F. Deganello, L.F. Liotta, C. Meneghini, A. Martorana, A. M.Venezia, Studies on Surface Science and Catalysis D **130**, 3207 (2000).

TTF-TESLA

L. Cacciotti (Tecn.), M. Castellano (Resp.), G. Di Pirro, M. Ferrario,
G. Fuga (Tecn), R. Sorchetti (Tecn), F. Tazzioli, V. Verzilov
In collaboration with INFN-Mi (LASA) and INFN-Roma2

1 Activity

The construction of the TTF (TESLA Test Facility) linac was established as an international collaboration aimed at the development of the technologies required for a Superconducting Linear Collider (TESLA).

The main goals of TTF where the demonstration of a higher accelerating gradient for 1.3 GHz superconducting cavities, the design of a suitable and cost effective cryostat and all ancillary RF components, the production and acceleration in a series of such cavities of an electron beam with the characteristics required by the Linear Collider.

The quality of an electron beam produced by a superconducting accelerator appeared soon very promising for the production of coherent radiation through the Self Amplified Spontaneous Emission (SASE) Free Electron Laser (FEL) process. So, while the TESLA project was completed with the association of a X-ray SASE FEL, a phase II of TTF was foreseen to demonstrate the feasibility of the project and to establish an user facility producing coherent radiation in the soft X-ray range.

At the end of year 2000 all the TTF goals have been achieved. The accelerating gradient of the cavities, produced in a standard way by different industries, well exceeded the 15 MV/m that was the first aim. Now gradients in excess of 25 MV/m are routinely obtained, and even better performances are expected in the near future. The planned cryostat cost reduction has been reached, and a full TESLA beam has been successfully produced and accelerated at 300 MeV.

The demonstration of the SASE effect at a wavelength as short as 90 nm has also been obtained.

The main contribution of LNF has been in the electron beam diagnostics. Starting from the experience gained in the home construction of the small LISA accelerator, we have, for the first time, introduced the use of Optical Transition Radiation as the standard diagnostics tool on a rather large machine. The peculiar properties of this radiation allow the measurement of a large amount of beam parameters, as beam profiles, energy, energy spread, angular divergence and transverse emittance. A complete set of analysis tools has been provided for the accelerator commissioning and operation.

Some example of the beam measurements are shown in the following pictures 1,2,3.

2 Activity for 2001

The work to reduce the beam emittance at the undulator will continue. An improved laser photon diagnostics will be installed.

3 Publications

1. N. Baboi *et al.*, Superconducting Superstructure for the TESLA Collider: New Results; LINAC 2000.
2. M. Ferrario *et al.*, Low Emittance Photo-injector, invited talk at the High Energy Photon Colliders Workshop, Hamburg, 2000, to be published on NIM A.



Figure 1: *OTR picture of the beam selected by the pepper-pot slit.*

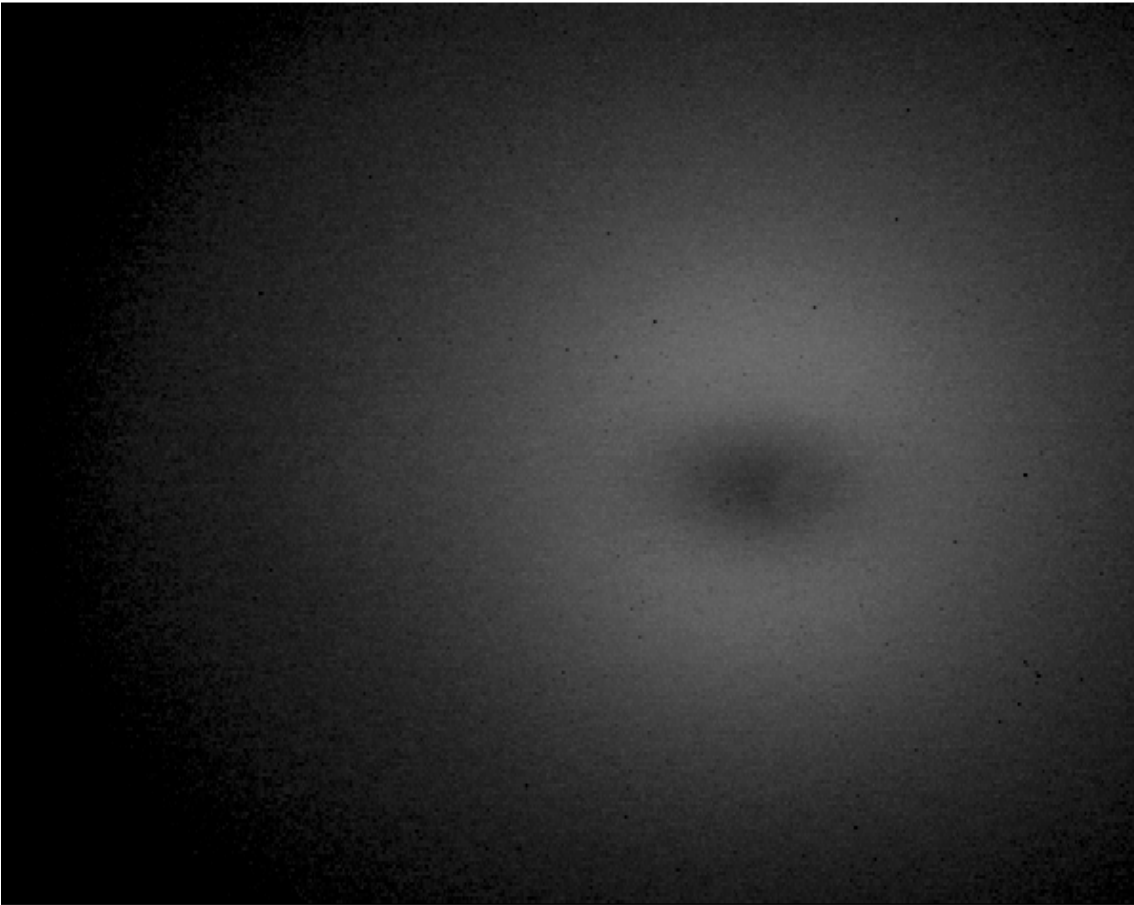


Figure 2: *OTR angular distribution and its vertical profile with a fitting function from which energy and angular spread can be obtained.*

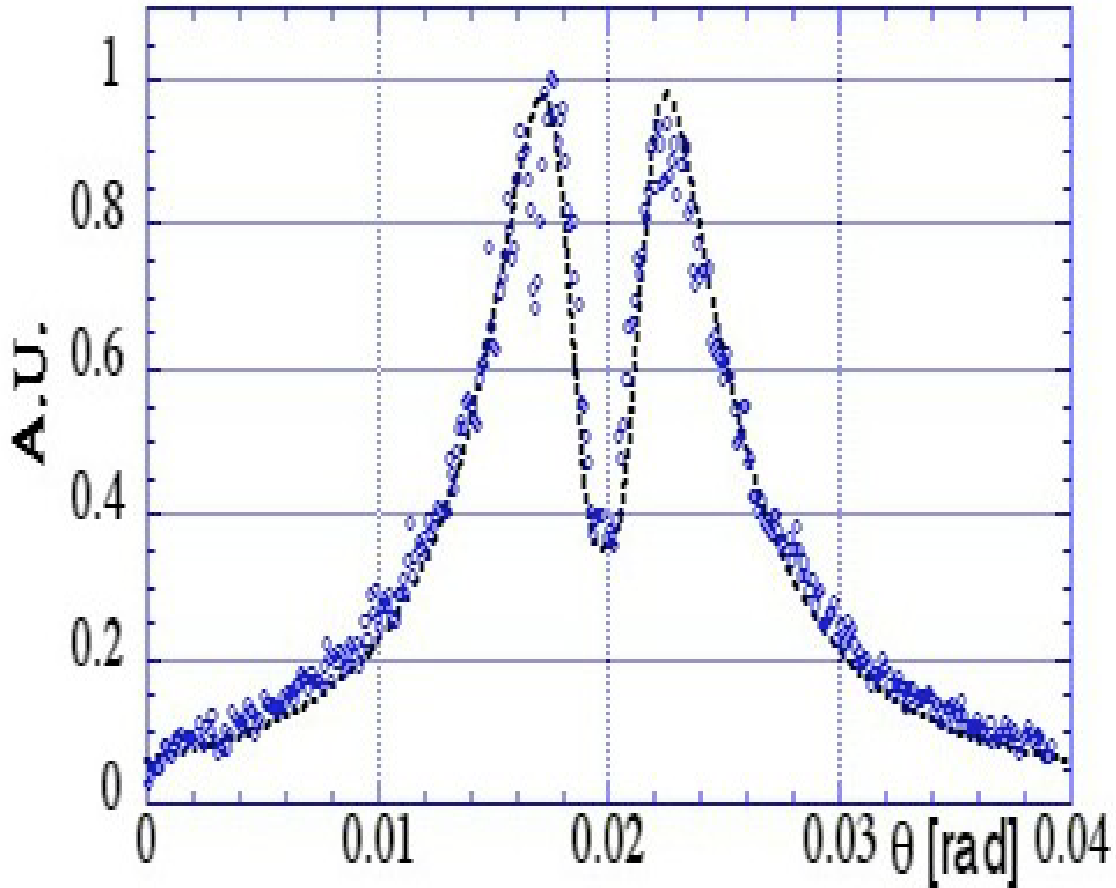


Figure 3: *OTR angular distribution and its vertical profile with a fitting function from which energy and angular spread can be obtained.*

3. D. Edwards *et al.*, The Flat Beam Experiment at the FNAL Photoinjector LINAC 2000.
4. J. P. Carneiro *et al.*, Emittance Measurement at the A0 Photo-injector LINAC 2000.
5. M. Ferrario *et al.*, New design study and related experimental program for the LCLS RF photoinjector EPAC 2000.
6. L. Serafini *et al.* Velocity bunching in photo-injectors, LNF-00/036, presented at 20th ICFA Beam Dynamics Workshop on "Physics of, and Science with, the X-ray Free Electron Laser, Arcidosso, Settembre 2000.
7. M. Ferrario *et al.*, Adiabatic Plasma Buncher IEEE Transactions on Plasma Science 28, August 2000.
8. J. Andruszkov *et al.*, First Observation of Self-Amplified Spontaneous Emission in a Free-Electron Laser at 109 nm Wavelength, Phys. Rev. Letts, **85**, 3825 (2000).
9. M. Castellano *et al.*, Bunch Length Measurements at TTF Using Coherent Diffraction Radiation Presented at the EPAC2000 Conference - Austria 2000.

10. L. Catani *et al.*, A Distributed Multiplatform Control System with LabVIEW Proceedings of PCaPAC 2000 - Desy (Amburg) October 2000.

YEAR 2000 FRASCATI INTERNAL REPORTS

Available at [/www.lnf.infn.it/](http://www.lnf.infn.it/)

1 Frascati Reports

- LNF-00/001 (P)
T. Hambye, G.O. Kohler, E.A. Paschos, P.H. Soldan
Analyzing ϵ'/ϵ in the $1/N_c$ Expansion
Proc. of the 3rd Inter. Conf. on B Physics and CP Violation, Taipei, Taiwan, December 3 - 7, 1999
- LNF-00/002 (P)
T. Hambye, E. Ma, U. Sarkar:
Leptogenesis from R Parity Nonconservation
Phys. Rev. Lett.
- LNF-00/003 (P)
Giorgio Cappuccio, Sultan B. Dabagov
Capillary Optics as an x-ray Condensing Lens: An Alignment Procedure,
Submitted to SPIE Selected Papers Kumakhov Optics and Application
- LNF-00/004 (P)
M. Ferrario, J. E. Clendenin, D. T. Palmer, J. B. Rosenzweig, L. Serafini
Homdyn Study for the LCLS RF Photo-Injector
2nd ICFA Advanced Accelerator Workshop on The Physics of High, Brightness Beam, UCLA Faculty Center, Los Angeles, CA, November 9-12, 1999
- LNF-00/005 (P)
R. Escribano, F.S. Ling, M.H.G. Tytgat
Large N_c , Chiral Approach to M_η , at Finite Temperature
Phys. Rev. D
- LNF-00/006 (P)
F. Celani, A. Spallone, P. Marini, V. di Stefano, M. Nakamura, S. Pace, A. Vecchione, A. Mancini, P. Tripodi, D. Di Gioacchino
High Hydrogen Loading of thin Palladium Wires Through Alkaline Earth Carbonate Precipitation on the Cathodic Surface - Evidence of a New Phase in the PD-H System
Phys. Lett. A
- LNF-00/007 (P)
C. Chen, M. Ferrario
Space Charge Effects in Rectilinear Motion: Emittance Compensation, Pulse Lengthening, and Halo Formation (Working Group n.1 Summary)
Presented at the 2nd ICFA Advanced Accelerator Workshop on The Physics of High Brightness Beams UCLA Faculty Center, Los Angeles, CA, November 9-12, 1999
- LNF-00/008 (P)
S. Bellucci, A. Galajinsly

Consistent Batalin–Fradkin quantization of Infinitely Reducible First Class Constraints
Submitted to Physics Letters

- LNF-00/009 (P) S. Bellucci, E. Ivanov
N=(4,4), 2D Supergravity in SU(2) x SU(2) Harmonic Superspace
Submitted to Nucl. Phys. B
- LNF-00/010 (IR)
S. Tomassini
Analisi Termostutturale del Sistema Clessidra-Straws dell'Eperimento FINUDA
- LNF-00/011 (IR)
B. Dulach, S. Tomassini
Calibrazione del Robot per l'Installazione del Vertice di FINUDA
- LNF-00/012 (P)
M. Ferrario, T.C. Katsouleas, L. Serafini, I. Ben Zvi
Adiabatic Plasma Buncher
Submitted to IEEE Transactions on Plasma Science
- LNF-00/013 (P) A. Bramon, R. Escribano, J.L. Lucio M., G. Pancheri
The ratio $\Phi \rightarrow K^+ K^- / \bar{K}^0 K^0$
Submitted to Physics Letters B
- LNF-00/014 (P)
S. Bellucci, E. Ivanov, S. Krivonos
Superworldvolume Dynamics of Superbranes from Nonlinear Realizations
Submitted to Physics Letters B
- LNF-00/015 (P)
V.A. Khoze, M.I. Konchatnij, N.P. Merenkov, G. Pancheri, L. Trentadue, O.N. Shekhovzova
Radiative Corrections to the Hadronic Cross-Section Measurement at DAΦNE
Physical Journal C
- LNF-00/016 (P)
G. Eker G. Isidori, G. Müller, H. Nefeld, A. Pich
Electromagnetism in Nonleptonic Weak Interactions
Submitted Nucl. Phys. B
- LNF-00/017 (P)
Thomas Hambye, Ernest Ma, Utpal Sarkar
Leptogenesis from Neutralino Decay with Nonholomorphic R-parity Violation
Nucl. Phys. B
- LNF-00/018 (P)
A. Spallone, F. Celani, P. Marini, V. di Stefano
A Reproducible Method to Achieve Very High (Over 1:1) H/Pd Loading Ratio Using Thin Wires in Acidic Solution with Addition of Very Low Concentration Impurities
Presented at the "IV Workshop on Anomalies in Hydrogen/Deuterium Loaded Metals" 22-24 October, Asti (Italy)
- LNF-00/019 (P)
A. Bramon, E. Escribano, J.L. Lucio M, M. Napsuciale, G. Pancheri
Chiral Loops and $a_0(980)$ Exchange in $\phi \rightarrow \pi^0 \eta \gamma$
Submitted to Phys. Letts. B

- LNF-00/020 (P)
T. Hambye, P.H. Soldan
 $1/N_c$ and ϵ'/ϵ
Nucl. Phys. Proc. Supp.
- LNF-00/021 (P)
DAΦNE Team
DAΦNE Machine Project 7th European Particle Accelerator Conference (EPAC 2000)
Austria Center Vienna, 26 to 30 June 2000
- LNF-00/022 (P)
F. Celani, A. Spallone, P. Marini, V. Di Stefano, M. Nakamura, A. Mancini, S. Pace, P. Tripodi, D. Di Gioacchino, C. Catena, G. D'Agotaro, R. Petraroli, P. Quercia, E. Righi, G. Trenta
High Hydrogen Loading into Thin Palladium wires Through Precipitate of Alkaline-Earth Carbonate on the Surface of Cathode: Evidence of New Phases in the Pd-H System and Unexpected Problems due to Bacteria Contamination in the Heavy Water
Invited paper to Inter. Conf. on Cold Fusion 8 (ICCF8), May 21-26 (2000) Lerici (Italy)
- LNF-00/023 (P)
P. Astone, M. Bassan, P. Bonifazi, P. Carelli, E. Coccia, S.D'Antonio, V. Fafone, G. Federici, A. Marini, G. Mazzitelli, Y. Minenkov, I. Modena, G. Modestino, A. Moleti, G. V. Pallottino, V. Pampaloni, G. Pizzella, L. Quintieri, F. Ronga, R. Terenzi, M. Visco, L. Votano
Energetic Cosmic Rays Observed by the Resonant Gravitational Wave Detector NAUTILUS
Submitted to Phys. Letters. B
- LNF-00/024 (P)
Rohini M. Godbole, G. Pancheri
Hadronic Cross-Sections in $\gamma\gamma$ Processes and the Next Linear Collider
- LNF-00/025 (P)
G. Modestino, G. Pizzella
Algorithms for Search of Correlation Between GRBs and Gravitational Wave Data
Submitted to Astronomy and Astrophysics
- LNF-00/026 (P)
Hannes Pichl
 $K \rightarrow \pi\pi e^+e^-$ Decays and Chiral Low-Energy Constants
The European Physical Journal C
- LNF-00/027 (P)
R.M. Godbole, A. Grau, G. Pancheri
Total Photonic and Hadronic Cross-sections
Presented at the Photon2000 Conference, Ambleside, U.K., 26-31 August 2000
- LNF-00/028 (P)
M. Castellano, L. Catani, A. Cianchi, G. Orlandi, M. Geitz, V.A. Verzilov
Measurements of Coherent Diffraction Radiation and its Application for Bunch Length Diagnostics in Particle Accelerators
Submitted to Physical Review E
- LNF-00/029 (P)
S.B. Dabagov, A. Marcelli

X-ray Scattering in Capillary Waveguides
Submitted to Physical Review Letters

- LNF-00/031 (P)
A. Bramon, R. Escribano, M.D. Scadron: Radiative $VP\gamma$ Transitions and η - η' Mixing
Submitted to Physics Letters B
- LNF-00/032 (P)
R. Escribano: Chiral loop and $L\sigma M$ predictions for $\phi \rightarrow \pi^0\eta\gamma$
Talk given at the "Hadron Structure'2000 Conference", Stara Lesna, High Tatras Mountains, Slovakia, 2-7 October 2000
- LNF-00/033 (P)
L. Benussi, M. Bertani, S. Bianco, F.L. Fabbri, P. Gianotti, M. Giardoni, V. Lucherini, E. Pace, L. Passamonti, F. Pompili, N. Qaiser, S. Sarwar, V. Tomassini
Charge Clustering in a Cylindrical Drift Cell
- LNF-00/030 (IR)
M. Agnello, M. Bertani, E. Botta, D. Calvo, P. Cerello, F. De Mori, G. D'Erasmus, A. Feliciello, A. Filippi, V. Filippini, P. Gianotti, G. Gómez, S. Marcello, O. Morra, A. Panzarasa, G. Tagliente, L. Venturelli
Performances of the FINUDA Drift Chambers in a Cosmic Ray Test
- LNF-00/034 (P)
J. Lhotka, R. Kuzel, G. Cappuccio, V. Valvoda
Thickness Determination of thin Polycrystalline Film by Grazing Incidence X-ray Diffraction
Thin Solid Film
- LNF-00/035 (P) M. Ferrario
Low Emittance Photo-Injectors
Invited talk given at the Inter. Workshop on "High Energy Photon Colliders" DESY, Hamburg, June 2000, to be published on Nucl. Instr. and Meth. A
- LNF-00/036 (P)
L. Serafini, M. Ferrario
Velocity Bunching in Photo-Injectors
Presented at the: 20th ICFA Beam Dynamics Workshop on "Physics of, and Science with, the X-ray Free-Electron Laser" Arcidosso (Italy), Settembre 10-15, 2000
- LNF-00/037 (P)
F.L. Fabbri
Results on Charmed Meson Spectroscopy from FOCUS
ICHEP 2000, Osaka Japan
- LNF-00/038 (P)
S. Sarwar, S. Bianco (FOCUS Collaboration)
Preliminary Results on Charmed Meson Spectroscopy
DPF 2000 Cleveland, Ohio (USA), August 2000
- LNF-00/039 (P)
S. Bianco (FOCUS Collaboration)
New Results on Charm Mixing and CP Violation
Nucl. Phys. B

- LNF-00/040 (P)
S. Bellucci, E. Ivanov, S. Krivonos
N=2 N=4 Supersymmetric Born-Infeld Theories from Nonlinear Realizations
Submitted to Phys. Lett. B

2 Frascati Series

1. Volume XVII (Special Issue)
Les Rencontres de Physique de la Valle d'Aoste - Results and Perspectives in Particle Physics,
Ed. M. Greco, La Thuile, Aosta Valley, February 27 - March 4, 2000
2. Pre-Prints
Advances on Micas (Problems, methods, applications in Geodynamics) Accademia dei Lincei,
Curatori (A. Mottana, A. Marcelli), Roma 2-3 Novembre 2000", "2000
3. Volume XIX
XX Physics Collision Conference, Ed G. Barreira, Lisbon June 29 July 1st. 2000
4. Volume XX
Heavy Quarks at Fixed Target, Eds. I. Bediaga, J. Miranda, A. Reis, Rio de Janeiro, Brasil,
October 9-12, 2000
5. Volume XXI
IX International Conference on Calorimetry in High Energy Physics, Eds. B. Aubert, J.
Colas, P. Nedelec, , L. Poggioli, Annecy Le Vieux Cedex, France, October 9-14, 2000

Glossary

These are the acronyms used in each status report to describe personnel qualifications other than Staff Physicist:

Ass.	Associated Scientist
Osp.	Guest Scientist
Bors	Fellowship holder
Tecn.	Technician
Resp.	Local Spokesperson
Resp.Naz.	National Spokesperson
Ass.Ric.	Research Associate
Bors. PD	Post-Doc Fellow
Dott.	Graduate Student
Laur.	Undergraduate Student
art.23	Term Contract (Scientist)
art.15	Term Contract (Technician)